Non-glycosidic analogues of alpha-galactosylceramide: Design, synthesis and biological activity

Roser Borràs Tudurí

Non-glycosidic analogues of alpha-galactosylceramide: Design, synthesis and biological activity.

Tesi doctoral

Memoria presentada per Roser Borràs Tudurí per optar al títol de doctor per la Universitat de Barcelona

Aquesta Tesi ha estat realitzada en el Programa de Doctorat en Química Orgànica de la Universitat de Barcelona, al les instal·lacions de l'Institut de Química Avançada de Catalunya (IQAC-CSIC)

Doctoranda:
Roser Borràs Tudurí

Director:
Dr. Amadeu Llebaria Soldevila
Investigador científic
Dpt. Química Biomèdica (IQAC-CSIC)

Tutor:
Dr. Angel Manuel Montaña Pedrero
Professor Titular
Dpt. Química Orgànica

Juny 2018

The present doctoral thesis has been carried out at the Institute for Advanced Chemistry of Catalonia (IQAC), which belongs to the Spanish National Research Council (CSIC).

This work was supported by the grant from Ministry of Economy, Industry and Competitiveness (CTQ2014-57020-R and CTQ2011-29549-C02-01) and pre-doctoral FPU Spanish research and teaching fellowship from the Ministry of Education, Culture and Sport (FPU2013-01783).

All reported data exposed in this Doctoral Thesis has been the object of Spanish patent application (Patent application number: P201731348)

Als que han lluitat i al final no han pogut vèncer.

A les que heu lluitat i heu vençut.

A la meva família.

INDEX

ACRONIMS AND ABREVATIONS

αGalCer	Alpha-Galactosylceramide
Å	Angstroms
ACN	Acetonitrile
AcOEt	Ethyl acetate
atm	atmospheres
APC	Antigen Presenting Cell
β_2m	β_2-microglobulin
BSA	Bovine Serum Albumin
Cl	Chloride
CSA	10-Camphorsulfonic acid
CTL	Cytotoxic T Lymphocyte
DBU	1,8-Diazabicyclo[5.4.0]undec-7-ene
DC	Dendritic Cell
DCM	Dichloromethane
DIPEA	*N,N*-Diisopropyulethylamine
DMAP	*N,N*-Dimethylaminopyridine
DMF	Dimethylformamide
EDC	1-ethyl-3-(3-dimethylamnopropyl)carbodiimide
Eq	Equivalents
H-Bond	Hydrogen bonds
HCl	Chloridric acid
HOBT	1-Hydroxybenzotiazole
IFN-γ	Interferon-γ
IL	Interleukin

iNKT cell	invariant Natural Killer T cell
K	Kelvin degrees
Kcal	Kilocalories
MΦ	Macrophage
M	Molar
MeOH	Methanol
MD	Molecular Dynamics
MHC	Major Histocompatibility Complex
mp	Melting Point
min.	Minutes
mmol	Milimols
MS	Mass Spectroscopy
Ms	Mesylate group
µg	Micrograms
µs	Microsecond
NaH	Sodium hydride
NHS	N-hydroxysuccinimide
NK cell	Natural Killer cell
NKT cell	Natural Killer T cell
NMR	Nuclear Magnetic Resonance
Ns	Nanoseconds
o.n.	overnight
OPD	o-Phenylenediamine
PAMP	Pathogen-associated molecular pattern
PBMCs	Peripheral Blood Mononuclear cells
PBS	Phosphate Buffer Solution

PEG	Polyethylene glycol
PRP	Pattern-recognition receptor
Psi	pounds-force per square inch / pressure unit
pTSA	para-Toluenesulfonic acid
RMSD	Root-mean-square deviation
r.t.	Room temperature
SAR	Structure-Activity Relationship
Seg	Seconds
TBAF	Tetrabutylammonium fluoride
TBDPS	Tert-butyldiphenylsilyl
tBuOLi	Lithium tert-butoxide
TCR	T cell receptor
TEA	Triethylamine
Tf	Triflate group
THF	Tetrahydrofuran
TLC	Thin Layer Cromatography
T_H	T Helper

1. INTRODUCTION

Human health is one of the most important focuses of interest in science. Many research projects have their major objective in understanding a disease, its cure or its prevention. One of the most complex systems in mammalians is Immune System, comprising the organs, cells and proteins involved in defense response to repel external disease-causing organisms (pathogens) and toxins, or against internal own cells that are abnormally transformed or dysfunctional, such as cancerous cells. Immunity protection is due to two cooperative defense systems, the nonspecific, innate immunity and the specific, acquired or adaptive immunity. Innate protective mechanisms repel invaders equally, while the adaptive immune responses are customized to particular types of molecules or pathogens. Both systems work together to prevent dangerous organisms or cells to proliferate within the body and help to eliminate them. Immune system is composed by different cells with specific roles. In general, they are characterized by targeting a restricted type of pathogen, so its role is limited to a subtype of threat. Some of the most known Immune System cells are T lymphocytes (T cells), B cells, Natural Killer cells (NK cells), Dendritic cells (DC) and Macropheges (MΦ). However, over the last decades a new type of cells has rise as important cells, combining typical surface markers of NK and T cells, known as Natural Killer T cells (NKT cells). They are believed to be involved in several immune response pathways and could be implicated in several different diseases[1-3]. Therefore this diverse implication put NKT cells in a top research position, producing hundreds of papers each year about their implication in a disease, new possible agonists or their mechanisms of action.

Given the complex nature of this subject, it is beyond the scope of this thesis to provide an in-depth review of all aspects of NKT immunology. Rather, the purpose of this introduction is to provide a general overview of immunology and a closer look to NKT cells and their challenge as therapeutic target using specific antigens.

1.1. Immune System

The Immune System refers to a collection of cells, tissues and organs that function together to keep the host in a homeostatic state and protect the body against foreign threats, such as microbes, viruses, parasites, fungi, tumor cells or toxins. It is an amazingly complex system that can recognize and remember millions of different enemies and produce secretions and orchestrate an army of cells to match up with and wipe out each one of them[4].

The secret of a successful result is a dynamic and complex communication network between all involved parts - cells, tissues and organs. When immune cells are alarmed, they undergo tactical changes and begin to release powerful chemicals which act like "neurotransmitters" of Immune System communications and regulate cell growth, behavior or point them to trouble spots. When the Immune System targets a wrong

threat, however, it can lead to a torrent of diseases known as *autoimmune disease*. To avoid this, discriminate self from non-self components is one of the first issues to be solved to ensure a correct system function and equilibrium.

Establishing different and effective defense barriers is crucial to control invaders and to direct response properly. To this end, immune response is historically divided into innate and adaptive responses[4]. The first one refers to a non-specific and rapid response - it could refer to the first try to solve a problem or to kill an invader in a non-specific manner. On the other hand, adaptive response takes longer to be released but it is specifically directed to a target, this specificity is associated to the ability of immune system to remember a pathogen and a proper response against it from a previous encounter, or what is called the *memory* of immune system. All this precise complexity is reflected in all types of cells, tissues, organs and molecules that compose Immune System, each one designed to take part in a specific role or process and to live in an equilibrated balance to maintain a homeostatic state between successive infection events.

1.1.1. Self and Non-self discrimination

How can Immune System recognize cells from its own host? Or how can differentiate them from bacteria? Or what is even more complicated, how can it localize self cells invaded by viruses or microbes inside them? All these questions are regulated by what is known as *self-tolerance*[5,6], *pathogen-associated molecular pattern* (PAMP) recognition and specialized antigen-presenting proteins called *Major Histocompatibility Complexes* (MHC).

Self tolerance is the ability of immune system to differentiate foreign pathogens from host cells and to not attack healthy tissues or organs rather than damaged ones. It is thought that the innate immunity has a major role in these decisions although it is antigen non-specific. To avoid self-damage, innate immune system has evolved to recognize highly conserved structure present in large groups of microorganisms rather than every single antigen a pathogen could generate; these structures are referred to as pathogen-associated molecular patterns and have some features in common[7]:

- First: PAMPs are exclusively produced by microbial pathogens and not by their hosts.
- Second: They are usually essential for the survival or pathogenicity of microorganisms.
- Third: They are usually invariant structures shared by entire bacteria pathogens.

Innate immune system has several *pattern-recognition receptors* (PRR) able to detect these characteristic molecules and releasing the first immune response[6,8].

On the other hand, adaptive immunity has developed a complex mechanism by which cells bearing antigen-receptors which recognize auto-antigens during their mature process undergo programmed cell death before being released to circulation [5,9,10], maintaining adaptive immunity silent against self-antigens. In a similar mechanism, cells of this system are able to generate specific receptors able to recognize specific antigens presented by *Antigen Presenting Cells* (APCs) through their MHC proteins. MHCs are cell membrane proteins able to detect and express peptide Ag to other immune cells to guide their response against specific threat. To reinforce specificity and self-tolerance, adaptive immunity used to require cross-recognition, meaning that not only antigen (Ag)-MHC recognition is needed, but also other co-receptors recognition is under demand. Theses co-receptors are generated by APCs during Ag recognition and expressed at cell membrane to adaptive cells[10].

Any failure over these mechanisms would cause tissue or self-cell damage triggering an autoimmune disease such as type I diabetes or rheumatoid arthritis, an hyperreactivity against harmless antigens causing allergy or an ineffective or silent response causing immunodeficiency such as viral or bacterial infection or tumor cell progression causing cancer[4].

1.1.2. Immune System army: organization and lines of defense

The Immune System gathers a huge arsenal of cells; some impulsive and aggressive cells that act without premeditation – phagocytes; others more tactically addressed and trained against specific threats – lymphocytes. For a successful result, it is critical a perfect organization of all cells and enroll them in specific function so all them can play a complementary role. To work effectively, most immune cells need the cooperation of their comrades, sometimes communicating by direct physical contact, others by releasing chemical messengers[11].

Immune System has several classifications depending on the principal feature is analyzed. 1) If the path of the pathogen is what we look at, three lines of defense can be identified: physical, chemical and microbiological barriers; innate immunity and adaptive immunity[12]; 2) If the killing agent is the main objective, two classes emerge: *humoral immunity* or *cellular immunity*[12,13]; 3) If we look at the nature of the response, this one can be divided into natural or acquired. All these categories, although different, are not mutually exclusive.

Nonetheless, talking about innate and adaptive immune system is the most commonly used classification and it is the way in which Immune System is usually presented and explained in most papers or books and it will be the one used in this theses.

1.1.2.1. The innate immunity

Usually, innate immunity includes skin and all other physical and anatomical barriers and it represents the first line of defense to an introducing pathogen. It is an antigen-independent (non-specific) defense mechanism that is used by the host immediately or within hours of encountering an antigen. The primary function of innate immunity is the recruitment of immune cells to site of infection and inflammation through the production of a *cytokines* (small proteins involved in cell-cell communication). Cytokine production leads to the release of antibodies and other proteins and glycoproteins which activate the complement system, a biochemical cascade that function to identify and opsonize (coat) foreign antigens and microbes, rendering them susceptible to be attacked. The major soldiers of innate immunity are leukocytes (neutrophiles and monocytes, which become macrophages after antigen encounter and maturation), Natural Killer cells and dendritic cells (DCs). The first ones are phagocytic cells while the second ones are expert microbe assassins. DCs are specialized in antigen recognition and exposure to effectors immune cells. They are characterized by their expression of PAMP receptors (also known as PRR), able to recognize small structural characteristic molecules from microbes or viruses, and also expression of MHCs able to present specific Ag to other immune cells[11,12].

1.1.2.2. The adaptive immunity

Despite innate immunity, some viruses, microbes and other threats have learned to evade it. To fight against those threats immune system has developed a second line of defense composed by two different strategically organized cell families[14]. B cells (so called because they mature in the **b**one marrow) are able to secret proteins called *antibodies,* which bind specifically to extracellular microbes or pathogens and eliminate them. T lymphocytes, also called T cells (which mature in **T**hymus) are able to detect and fight against pathogens that have learned to live inside cells, being undetectable by antibodies. T cells can be divided into two subtypes depending on their main function, T Helper cells (T_H) and cytotoxic T lymphocytes (CTLs). Their functions will be further explained in 1.1.2.3 Cells of Immune System.

Adaptive immunity is a delayed response. Contrary to innate immunity, always ready to fight within hours after infection, adaptive immunity takes longer to initiate (**Figure 1.1**). Response goes through several steps:

1) Recognition: Cells encounter the antigen in its appropriate context
2) Proliferation: Cells increase in number to generate a broad army of specialized soldiers
3) Differentiation and activation: some cells become effectors and others will remind as memory cells
4) Antigen elimination: cells fight and destroy the threat

5) Contraction: after the battle, immune system has to return to a basal sate, known as homeostasis.
6) Memory: some survivor cells will live longer to ensure immune system remembers what pathogen it may have encountered.

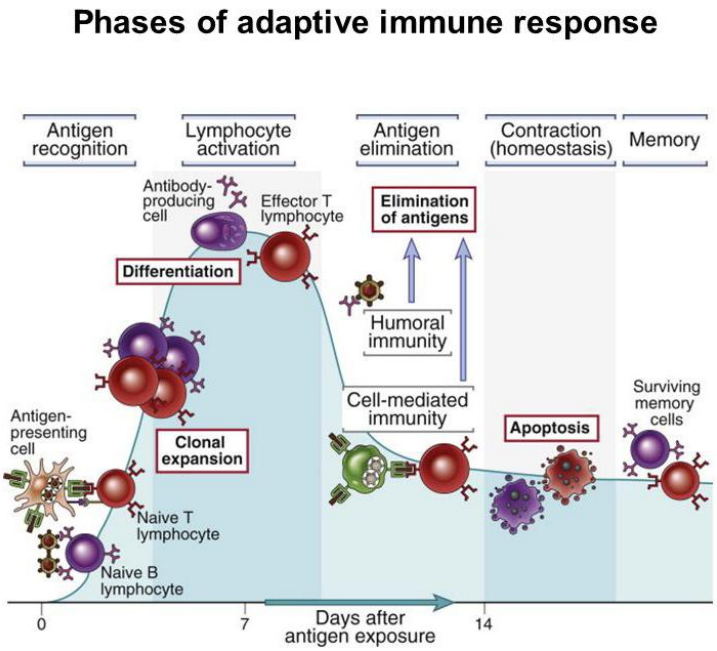

***Figure 1.1**: Steps of adaptive immune response. Kinetics is approximate.*

Adaptive immunity is selective to the encountered antigen, releasing an appropriate response to each threat. After that, some B cells and T cells live longer waiting for antigen to return. These cells are called *memory cells* due to their ability to rapidly recognize same antigen when it appears for a second time. Memory cells respond more rapidly than naïve (inexperienced) cells.

1.1.2.3. Cells of Immune System

Some of the most important cells of Immune System have already been introduced. Let's take a closer look to their characteristics and how they work (**Figure 1.2**).

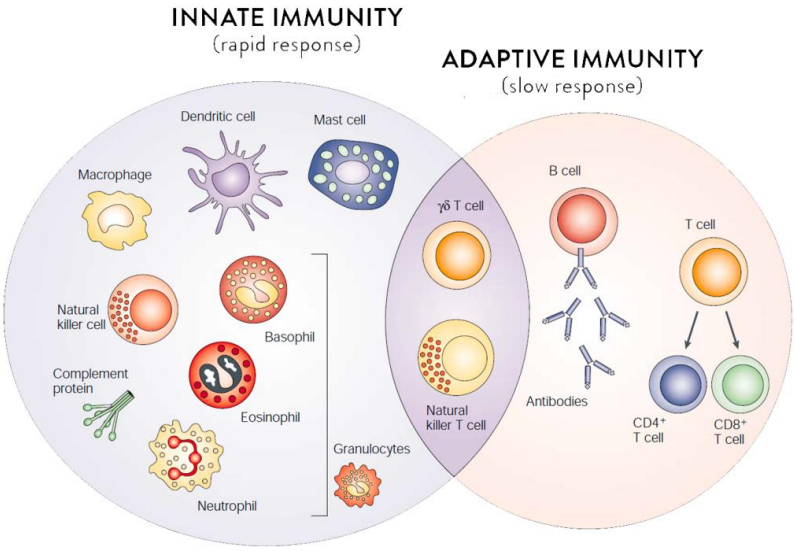

Figure 1.2: *Immune System cells classified by its role in innate or adaptive immunity (adapted from Dranoff, G. 2004, Nat. Rev. Cancer[15]).*

Cells of Innate immunity[9,11]:

Dendritic cells (DCs): Their main function is capturing, digesting and displaying antigens to other immune cells acting as Antigen Presenting Cells. DCs recognize and express antigens by MHCs. Furthermore, DCs are able to regulate costimulatory molecules secretion of pro-inflammatory cytokines which will modulate the immune response.

Leukocytes: Macrophages and neutrophiles are phagocytizing cells capable to kill microbes and digest them into small peptides and other molecules. Macrophages can also capture antigens and display them through MHCs, being the second most important APCs.

Natural Killer cells (NK): Ultra-specialized killing cells. They are classified as cytotoxic cells which are able to kill microbe-infected and malignant cells. NK cells do not require specific antigen recognition and they usually act before adaptive immunity response or in cooperation. NK cells act after co-stimulation of cell surface receptor recognition (through PRRs) and pro-inflammatory cytokine signals. They have been involve in tumor cell control by immune system and are believed to play a crucial role in tumor recognition and suppression.

Cells of Adaptive immunity[14]:

B cells: Their main role is antibody production against specific pathogens and antigen recognition by surface cell receptors, activation of antigen internalizing process and re-expression on the MHC molecules of B cells to T cells. B cells are also able to kill and eliminate threats with specificity thanks to their ability to generate specific antibodies after antigen encountering. This kind of immunity is also known as humoral immunity.

T cells: Their main characteristic is their membrane cell receptors (T cell receptor – TCR), which are the result of different gene rearrangements generating a wide diversity of similar TCRs but with different antigen specificity; these receptors are APC-dependent in the way that antigen presentation by MHC proteins is required for its detection and identification. This kind of response is also known as cellular immunity. After naïve T cell stimulation, they become specialized T cells able to release a specific response and they can be divided into two effectors sub-types depending on their main function: T Helper cells (T_H) and Cytotoxic T Lymphocytes (CTLs). The activation of both cell types provides the control of intracellular infections that cannot be achieved by the innate system.

T_H cells: As their name indicates, these cells help others to do their tasks such as B cell antibody production or NK cell activation and direction to desired threat. Depending on the nature of this response this mature T cells can be divided into T_H1 or T_H2 cells. They only differentiate from each other by cytokines they produce (**Table 1.1**). T_H1 cells produce Interleukin 2 (IL-2) and Interferon-γ (IFN-γ), cytokines related with pro-inflammatory response. On the other hand, T_H2 cells produce Interleukin 4, 5, 6 and 10, more associated with anti-inflammatory and regulatory responses. Each cytokine profile T_H1 or T_H2 has suppressor effects on the other subtype. Recently, other T_H subtypes have been reported such as T_H17.

CTLs: These are directly cytotoxic to antigen bearing cells. They act similar to NK cells, introducing cytoplasmatic granules into target cells causing cell apoptosis.

Cell subtype	Cytokine	Major role
T_H1	IL-2	T cell proliferation induction; CTLs division stimulation and cytotoxicity.
	IFN-γ	Macrophage activation to kill intracellular pathogens and NK cytotoxicity induction.
T_H2	IL-4	B cell isotype class-switching induction, favoring antibody production. Positive feedback to induce further T_H2 responses.
	IL-5	Innate system cells (eosinophils) growth promotion.

Table 1.1: *Summary of most important and commonly cited cytokines produced by T_H cells*

Among all these cells appears a new family that combines typical properties of NK and T cells, called *Natural Killer T (NKT) cells*.

1.2. Natural Killer T cells: A frontier cell class

In the 90s, a conjunction of several works about a rare T lymphocytes type ended up with the discovery of Natural Killer T cells[16-18]. The most remarkable features of this new subset of lymphocytes were the combination of surface markers of both NK cells (NK1.1 in mouse and CD161 in human) and T lymphocytes (typical TCRs). In parallel of surface markers, NKT cells have the ability to act either in innate response with similar abilities as NK cells and in adaptive immunity like T lymphocytes, generating specific responses against stimulus, secreting a wide range of cytokines like T_H cells and even memory cells leaving NKT cells at the interface of innate and adaptive immunity[19].

NKT cells were initially found in mice but human analogues were early identified. There is a highly conserved evolution between species as it can be observed from their surface proteins[17]. Different NKT cells subtype had been identified and they mainly differ from each other by their TCR sequence, some surface markers and their ability or not to produce some kind or cytokines: NKT type I (also known as **invariant Natural Killer T** cells or **iNKT** cells), NKT type II and NKT17 are the most popular ones. Among these three subtypes, iNKT cells are the most studied ones and its stimulation with synthetic molecules will be the main focus of this thesis.

NKT cells differ from conventional T lymphocytes by their activation mode. Adaptive immunity has evolved to generate specific response to invaders through the body with a complex mechanism involving pathogen processing, antigen recognition and presentation. In this way, as it was previously mentioned, some cells (APCs) have the ability to detect specific antigens and “show” them to lymphocytes by surface proteins called Major Histocompatibility complexes or MHC. These proteins are able to present peptide-antigens to TCRs of T cells and then activate them. By contrast, NKT cells do not recognize antigens through MHC presentation however they do recognize antigens in a CD1d-dependent manner, reason for being so called CD1d-restricted T lymphocytes. CD1d is a member of the CD1 protein family[20], which are antigen-presenting molecules that present lipid antigens to T cells. Similar to the structure of MHC class I, the CD1 heavy chain associates with β2 microglobulin to form a heterodimer that is expressed on the cell surface of the antigen-presenting cell. However, in contrast to MHC molecules, CD1 proteins have a deep hydrophobic antigen binding pocket that is well suited to binding lipid antigens. This antigen presenting protein recognizes and presents glycolipids instead of peptides, another hallmark of NKT cells and an enormous challenge as endogenous ligand has not been identified yet (both features are further discussed later, 1.2.1 *invariant* NKT: CD1d-

restricted cells and 1.3 NKT cells antigens: from αGalCer to new analogues respectively).

Upon CD1d-antigen recognition, NKT cells undergo a rapidly and massive cytokine release triggering a strong immune response. Both T_H1 and T_H2 cytokines can be released by NKT cells, what confers them a versatile role in immunity however its regulation is not well understood. NKT cell population differs between mice and human; while their abundance is notorious in mice being around 50% of total lymphocytes in liver and 1 to 3% in blood, in human decreases down to less than 1% in liver and having a low presence in blood. Although this difference becomes crucial at time to explore therapeutic application of NKT cells, NKT cells have been largely related with lots of diseases and deeply studied as potential immunotherapeutic tool[1-3].

All along last two decades, NKT cells have been studied as possible modulators of the immune system capable of restoring the response to a normal state capable of dealing with the disease that threatens the organism. Its ability to produce both T_H1 and T_H2 responses has led to the study of a wide range of different diseases ranging from autoimmune to cancerous disease, even infectious ones. Good examples are studies on type 1 Diabetes[21], Multiple Sclerosis[22,23], Asthma[24] or other autoimmune disease[25] as well as studies on infections[26]. Cancer immunotherapy with NKT cells has caught the main focus of studies with copious research articles published each year about it and generating some interesting pre-clinical and clinical trials[27]. One recent pre-clinical work deserved to be highlighted; Dr. Briones' Lab published encouraging results of Lymphoma B treatment using NKT cells as therapeutic target. In their work, a "lymphoma vaccine" was proposed using digested cancerous cells as a cancer antigen and combining them with a mixture of DCs loading CD1d antigen. This vaccine not only eradicates lymphoma at 100% of efficacy but also generates specific resistance to same malignance but not other cancer lines[28]. These findings could shed some light on NKT cells immunotherapy and taking into account that up to now most studies did not incorporate "disease antigen", this could make the difference.

Another widely researched application has been to target NKT cells as vaccination enhancers[29]. This approach consists in combining vaccine antibodies with NKT antigen either as a mixture of compounds or chemically linked. The aim of these studies was to take advantage of NKT cells' ability to shake Immune System and direct this warning to activate the lymphocytes that are simultaneously stimulated by vaccine antibody to generate memory cells.

Using NKT cells as immunotherapeutic tool has been an enormous challenge as dealing with T_H 1/T_H2 response polarization has not been as easy as it could seem. Although NKT cells can produce both types of cytokines, each disease requires a specific profile.

In some cases, a pro-inflammatory (T_H1) response would be necessary to shake immune cells and point them to the threat, for example to treat cancer; however other illness would required a regulatory or anti-inflammatory (T_H2) effect, such as in autoimmune disease therapies. Notice that each type of response has a suppressive effect on the other one, being a huge limitation in therapies if both types of cytokines are simultaneously secreted. Up to date, many efforts were reported seeking synthetic compounds capable of modulating NKT response with selectivity in cytokine production. Most of these researches run in either poor selectivity, low potency or compound instability *in vivo* due to metabolic degradation. Another challenge is the identification of the endogenous antigen, as it could reveal some important clues in the modulation of the response, ligand-protein(s) interactions or the physiological mechanism involved in activity hitherto unknown and its role in NKT cell related diseases.

1.2.1. *invariant* Natural Killer T cells: CD1d-restricted cells

NKT cells relevance in Immune System is well accepted however it is not so clear their modulation. As it was mentioned before, there are several NKT cells subtypes and the most studied subtype is *invariant* NKT (iNKT) which name refers to its particular TCR and, as it indicates, it is invariant, always the same rearrangement. TCR repertoire and diversity is one of the characteristics of T cells and it allows these lymphocytes to detect every antigen but iNKT do not present such diversity and they are strictly restricted to antigens presented by APCs through CD1d proteins. These invariant TCRs have typical structure of αβTCRs with Variable (V), Joining (J) and Constant (C) domains and its sequence showed a high conserved evolution differing only on a few amino-acid residues. In mice iNKT-TCR presents a highly constant alpha chain Vα14-Jα18 combined with Vβ8, 7 or 2 beta chains while in human presents its homologous sequence Vα24-Jα18 combined with Vβ11 (see **Table 1.2** for iNKT properties summary). This unique combination points to a highly specific antigen recognition however many efforts have been reported for self-antigen identification without success.

Characteristics	Mouse	Human
TCR α chain	Vα14-Jα18	Vα24-Jα18
TCR β chain	Vβ8, 7 and 2	Vβ11
Co-receptor expression	CD4 DN	CD4, DN, CD8αα
Frequency	1-3% in spleen, ≤50% in liver	0.001-1% in blood, 1% in liver
Cognate antigen	Microbial and self-glycolipids, phospholipids	
Localization	Liver, thymus, spleen, lung, bone marrow and fatty tissue	
NK markers	NK1.1	CD161

Table 1.2: *Comparative of mice and human iNKT cells (adapted from Chandra, S. et al, 2015, Advances in Immunol.[17])*

1. INTRODUCTION

At mid-90s Kirin Brewery Co., a famous beer Japanese company that opened a pharmaceutical branch, was carrying out a screening of anti-tumor activity of marine sponge *Agelas Mauritianus* components resulting in the discovery of a novel compound able to stimulate anti-tumor activity and with promising potency[30,31]. Structural determination revealed an alpha-Galactose linked to a ceramide skeleton known as Agelasphin-9b (**1**)[32]. Some years later, a synthetic analogue called KRN7000 and also known as α-Galactosylceramide (**2**) (αGalCer, from now this abbreviation will exclusively refer to synthetic analogue) was published[33] and some years later it was revealed its the anti-tumor activity occurred via iNKT cell activation[34,35]. Deeper studies of immunologic properties of αGalCer (**2**) revealed its huge potency in terms of cytokine production without selection between T_H1 and T_H2 responses. After αGalCer (**2**) stimulation, a rapid and profuse release of cytokines was determined with high levels of IFN-γ and IL-4, which as it was previously indicated, results in antagonistic effects. Other studies also point other drawbacks for developing **2** as anticancer drug such as NKT cell anergy after stimulation[36,37]. This promising but not ideal activity promoted the αGalCer (**2**) analogues research as a boisterous field producing thousands of compounds and describing the activity as NKT cell activators for hundreds of them. Bearing in mind αGalCer (**2**) structure, many efforts were focused on endogenous ligand determination. An initial proposal by Michael B. Brenner group[38] was a β-glucosylceramide (**3**) as a self-antigen however same group reported a retraction of their previous work[39,40] pointing to small trace impurities of alpha-analogue (**4**) as the authentic responsible of activity. Although several groups are still working on it, looking among self-glycolipids and phospholipids as candidates, NKT cell self-antigen(s) structure remind still a mystery (**Figure 1.3**).

Despite NKT the cell ability for producing a wide range of cytokines is conferring to these cells interesting roles at the frontier or innate and adaptive immunity, with potential implication in several diseases, the control of their potency modulation or the cytokine production has not been achieved. The prototypical synthetic glycolipid (αGalCer (**2**)) shows huge potency as NKT cell activator; however, several drawbacks were identified as it has been deeply studied:

- No discrimination between T_H1 or T_H2 cytokine production, with antagonistic effects in immune cells
- Unresponsiveness state after stimulation with αGalCer (**2**)
- Metabolic degradation of glycosidic bond by glycosidases reducing its half-live *in vivo*, and therefore its bioavailability

All together, the exploration of new NKT stimulants is an interesting challenge and many groups have put their interest on it, looking for a better antigen able to selectively produce one type of T_H response, not shake cells until stun them or improving compound half-life.

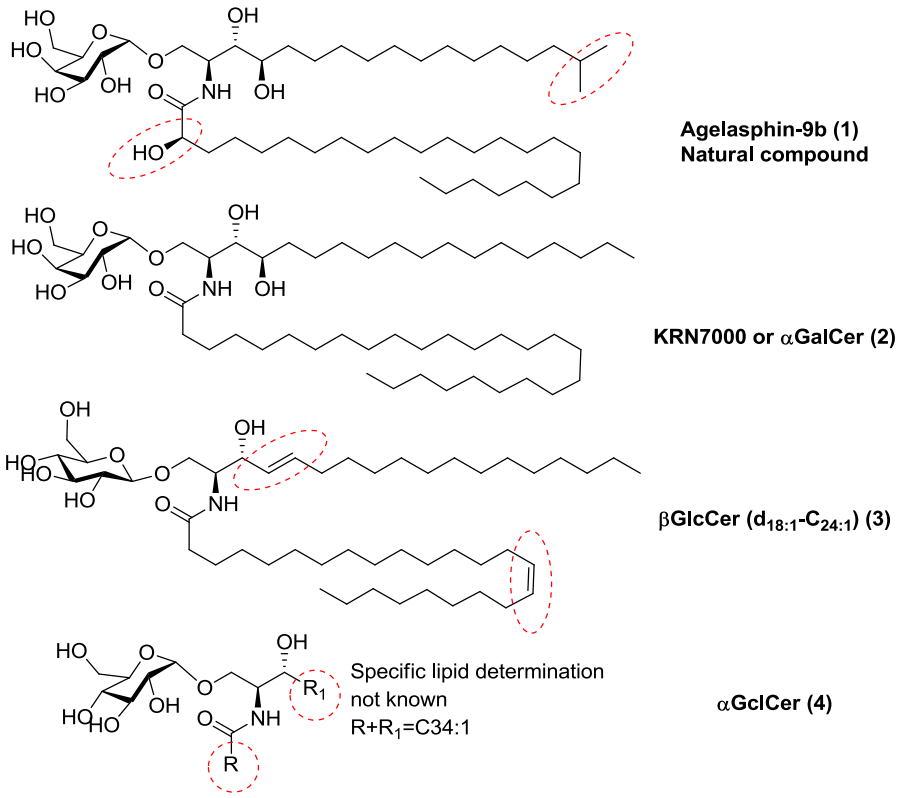

Figure 1.3: *NKT cells antigens. Structural differences of compounds against αGalCer (**2**) are indicated in red-dashed circles.*

1.3. NKT cell antigens: from αGalCer to new analogues

Since the discovery of αGalCer (**2**), many efforts have been focused in developing new analogues[41] with better properties, whether physicochemical or biological. Even though that large library of compounds, the critical factors for biological activity or the ways it can be modulated remains today uncertain.

In 2005 several crystal structures of CD1d-Ag were published[42-45], providing some light on the structural interaction of antigens and receptors. During the following years, crystal structure release has proliferated notoriously, including some ternary structures of both human and mice TCR-Ag-CD1d complexes[46-48]. This information prompted the rational design of new αGalCer analogues.

1.3.1. TCR-Ag-CD1d complex: a cell – cell communication mechanism

CD1d is an antigen presenting protein expressed by APCs such as DCs and B cells with a close related MHC-structure and commonly described as non-classical MHC type I or MHC type I-like protein because its similar structure of this subtype of receptors. CD1d is composed by three α-domains coupled to β_2-microblobulin (β_2m) protein. Both α1 and α2 chains have an α-helix at the top which are exposed to TCR and create a hydrophobic cavity where lipid tails falls into (**Figure 1.4**). Acyl chain falls into A' pocket

while sphingoid base occupies F' pocket (called C' in human protein). The sugar ring is exposed at the top lying onto both α-helixes.

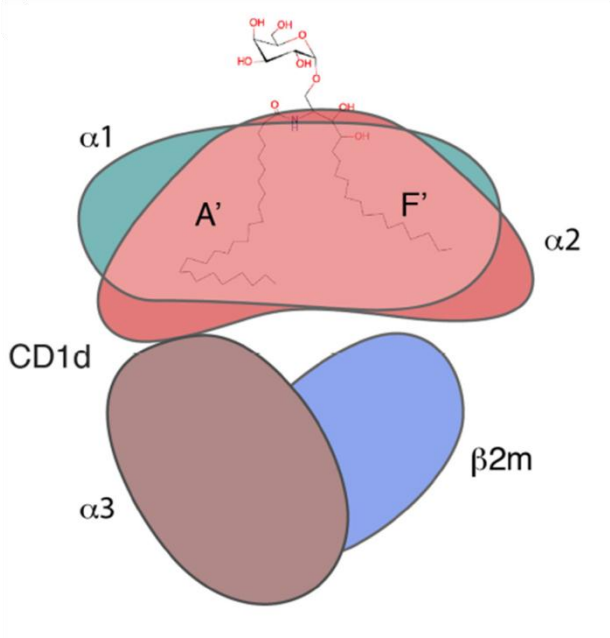

Figure 1.4: *Cartoon of αGalCer (**2**) recognition by CD1d. The α1- α2 domain (green, salmon shading) from the two major pockets A' and F' of CD1d that bind the lipid backbone, while the carbohydrate epitope is exposed. The α3-domain (brown) non-covalently binds β_2-microblobulin (β_2m, blue) and together supports the α1- α2 domain (adapted from Zajonc, DM and Girardi E., 2015, Front. Immunol.[49])*

As it was previously mentioned, TCRs are composed by two chains (α and β) with three domains (variable- joining-constant domains - V-J-C). Variable domains are those ones most relevant for binding interpretation since make contact with CD1d presenting protein and the glycolipid antigens. Contrary to common TCR-MHC contacts, which are lineal, NKT-TCRs interact with the antigen only by the α-chain while the β-chain only contacts with CD1d. This restriction forces TCR to bind slightly twisted (**Figure 1.5**).

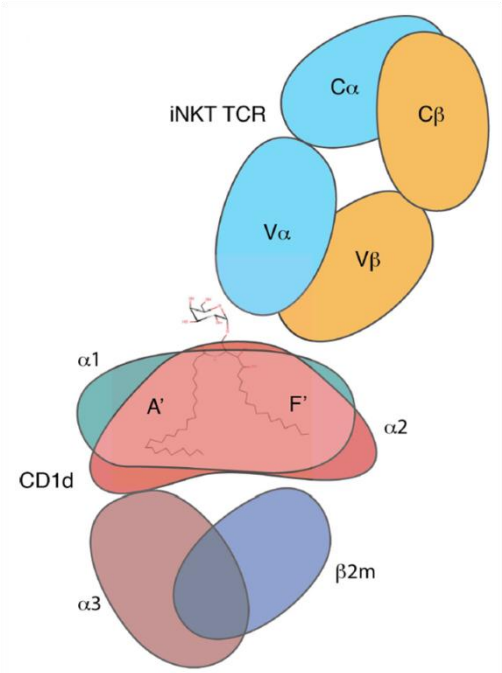

Figure 1.5: *Cartoon of the CD1d-aGalCer-TCR ternary complex (adapted from Zajonc, DM and Girardi E., 2015, Front. Immunol.[49])*

Thanks to crystal structures, it was proposed an H-Bond network as main glycolipid-protein interactions responsible of activity or susceptible to modulate it (**Figure 1.6**). Lipid tails fall into hydrophobic cavities of CD1d and mostly interact without H-Bonds. The polar part of the ceramide skeleton is involved in several H-Bonds: Both hydroxyl groups of phytosphingosine base interact with $Asp80_{CD1d}$ while nitrogen of amide participates in a network of H-Bonds named as **OTAN** network in some papers because of initial letter of atoms and Amino Acids implicated. Thus **N**H of Amide interacts with Oxygen of **T**hr156$_{mCD1d}$ (**T**hr154$_{hCD1d}$) which at same time interacts with **A**sp153$_{CD1d}$ (Asp151$_{hCD1d}$) connected with 2'-**O**H of Galactose head. This 2'OH also interacts with TCR through an H-Bond with $Gly96_{TCR}$. Other hydroxyl substituents in the sugar are assumed to be important: 3'-OH interacts with Asp153$_{mCD1d}$ (Asp151$_{hCD1d}$); 4'-OH interacts with Asn30$_{mTCR}$ (Ser30$_{hTCR}$) either directly or through water-mediated H-bonds. In contrast, the 6'-OH of the sugar ring is exposed to the water and it has been widely modified without losing activity as it will be later introduced.

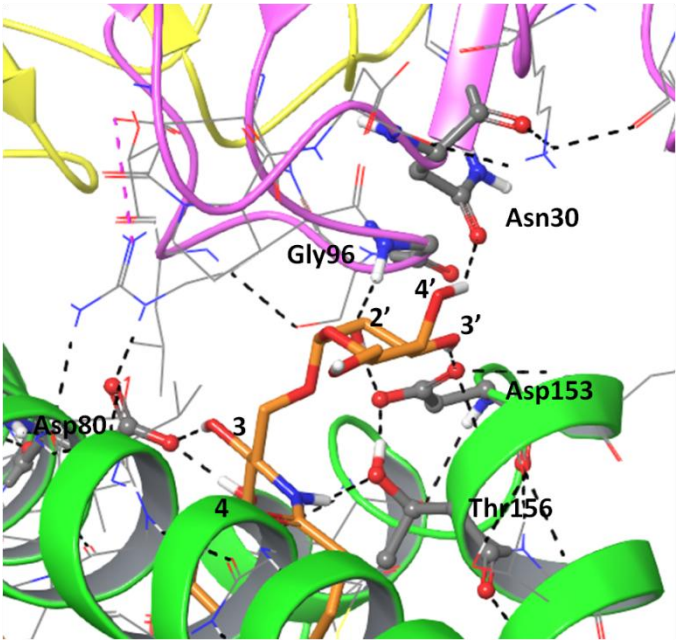

Figure 1.6: *Representation of αGalCer (**2**) interactions with mCD1d and mTCR. CD1d is colored in green ribbons, αTCR in pink and βTCR in yellow. H-Bonds are colored in black.*

All these molecular interactions are considered structural hotspots for the activation of iNKT cells and most groups used them to carry out their rational designs of new analogues seeking a greater cytokine selectivity or modulation of potency to avoid cellular anergy, generating hundreds of compounds throughout all these decades.

1.3.2. Structure-Activity relationship of αGalCer analogues

Analyzing the interactions mentioned above together with αGalCer (**2**) structure four principal moieties can be recognized as potentially modifiable to achieve that NKT cell activity modulation (**Figure 1.7**): (I) the modification of the length or substitutions on lipid tails; (II) the modification of polar part of ceramide skeleton; (III) the nature or configuration of the glycosidic bond and (IV) The sugar ring substitution or modification.

Establishing Structure-Activity Relationship (SAR) has not been trivial due to controversial activities of some compounds supposed to have one profile and turn out to be the other. The fact that NKT cells are able to produce both IFN-γ and IL-4 makes sometimes difficult to specify a single type of response, and this is commonly rationalized comparing the production of both cytokines by the new analogue with those induced by **2** and then determining the relative increases or decreases for each cytokine. It is worthy to mention that αGalCer (**2**) produces between 10 to 25 times more IFN-γ than IL-4 when tested *in vitro* with mice cells (in some cases even higher differences are reported). Although both IFN-γ and IL-4 cytokines are produced after stimulation, the relative cytokine increases or decreases of the analogue compared to that obtained with **2** as standard compound define the relative response bias or

polarization. Up to date, no compound has shown a total polarization towards a T_H1 or T_H2 response. Another consideration to be mentioned is related to the kinetics of cytokine production. For example, while IL-4 is rapidly produced during the first hours after compound stimulation, IFN-γ can take longer to reach its maximum value; this is widely used to correlate a high stability of the ternary complex with T_H1 profile and less stable complexes with T_H2 responses. Finally, it should be pointed that the extensive use of αGalCer **2** as reference compound can result in misleading conceptions in NKT biology, being only acceptable as an approximation owing to the lack of knowledge of the structure and real effects of the endogenous glycolipid antigen(s), this precluding a realistic assessment of the compound activity in NKT immune response.

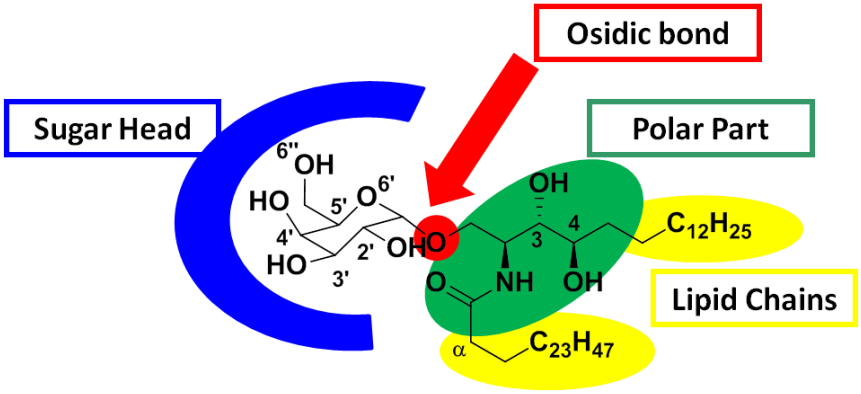

Figure 1.7: *αGalCer (**2**) parts susceptible of being modified*

There are many examples of new analogues in the literature[41]; it is not the purpose of this thesis to present a complete review but some selected examples for each group will be used to illustrate the discussion.

(I) Modifications in the lipid tails

Both lipid tails had been modified to skew the response towards T_H1 or T_H2 cytokine production. The most commonly mentioned analogue with lipid chain modification is OCH (**5**)[50](**Figure 1.8**); it is also an alpha-galactose linked to a ceramide backbone, however its phytosphingosine chain was truncated to C9 replacing the natural C18 sphingoid chain, and its acyl fatty acid was reduced in two carbons. This compound was the first one able to polarized cytokine profile towards T_H2 profile, with a comparable potency to αGalCer (**2**) in mice, unfortunately its potency decrease notoriously when tested in human cells. This difference in activity is not well understood, however polarized response is justified in terms of ternary complex stability. Due to a reduction of lipid chain, compound affinity for CD1d decreases, making complex less stable and thus production of IFN-γ decreases (remember that maximum IL-4 is produced rapidly after TCR recognition while maximum IFN-γ is detected a while after). Similar results were obtained when acyl chain was reduced

from C26 to C8 leaving phytosphingosine chain as natural; this compound is known as C8:0 or also PBS-25 (**6**)[51].

In **Figure 1.8** there are some examples and their activities are summarized in **Table 1.3** and represented in **Graph 1.1**.

Other modifications have been introduced at this part. It is the case of introduction of aromatic moieties at the end of the acyl chain (**7**)[52] and phytosphingosine chain[53,54] with a polarization to T_H1 profile; however a minimum length is required to stabilize this response, shorter sphingoid chains such as C6 (**8**) triggers a T_H2 response similar to OCH ones[55]. Introduction of some amide bonds in de middle of the chains (**9**) switching towards T_H2 response[56] (**Figure 1.8** and **Table 1.3**).

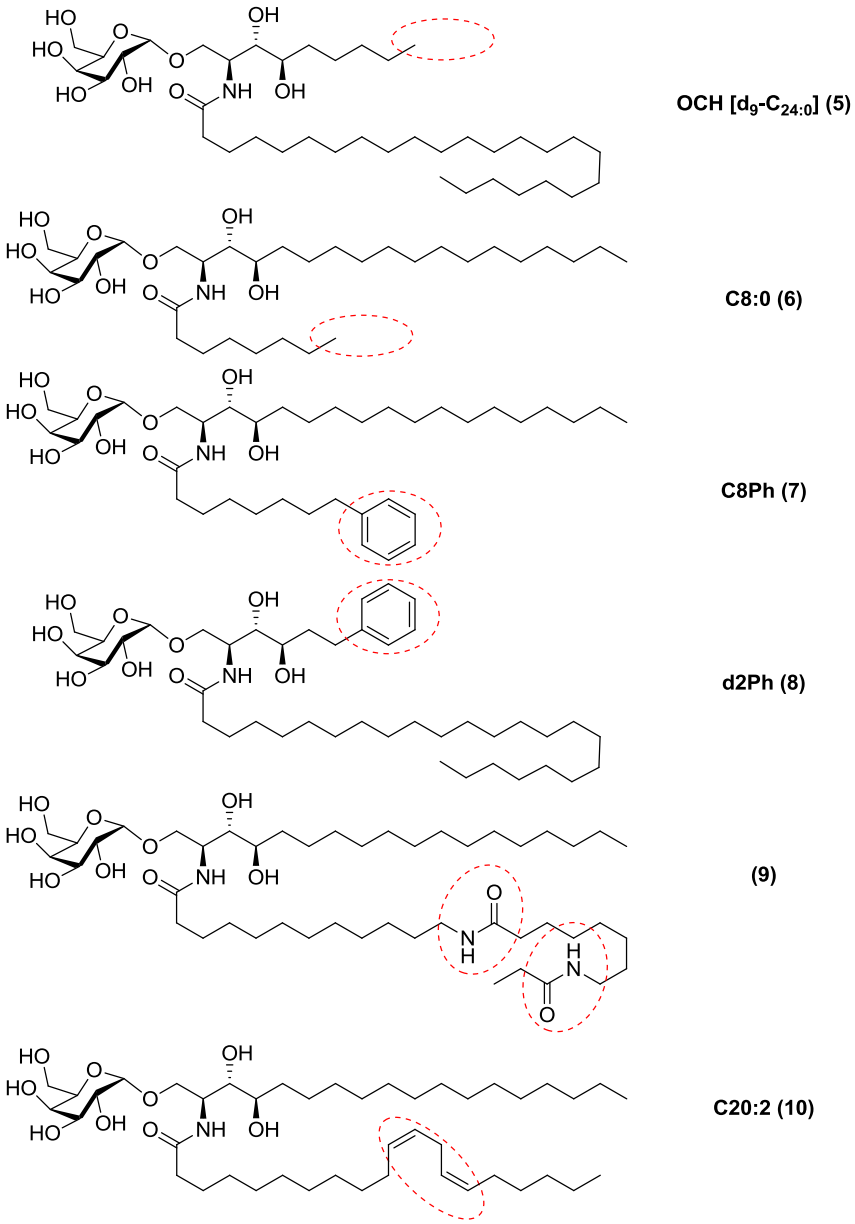

Figure 1.8: Examples αGalCer analogues with truncated or modified lipid tails

Compound	% IFN-γ (T_H1)	% IL-4 (T_H2)	Ratio IFN-γ/IL-4	Specie
2 – αGalCer	100	100	1	m
	100	100	1	h
5	38,6	966,67	0,04	m
	60,9	95,1	0,64	h
6	84,4	392,2	0,21	m
	71,6	81,2	0,86	h
7	372,3	162,9	2,28	m
8	49,9	164,8	0,27	m
9	43,5	182,1	0,24	m
10	5,3	112,5	0,05	m

Table 1.3: *Summary of biological properties of truncated or modified lipid tails analogues. Ratios are obtained from % IFN-γ/% IL-4*

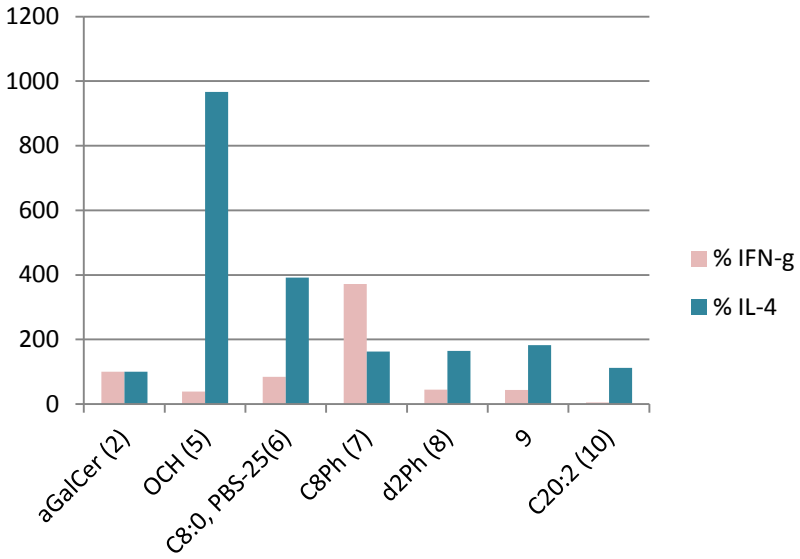

Graph 1.1: *Comparison of cytokine response of analogues **5**-**10** with αGalCer (**2**) in vitro with mouse cells*

What seems to be quite accepted is the direct implication of lipid chains in response polarization, relating T_H1 response with compounds capable of promoting a more stable TCR-Ag-CD1d interaction as well as linking T_H2 type with those that destabilize that interaction. Long lipid chains fill in hydrophobic pockets of CD1d and thus stabilize complex formation and subsequent TCR-Ag-CD1d interaction producing longer interactions and then T_H1; on the other hand, short lipid chains analogues form less stable CD1d-Ag complex and therefore TCR-Ag-CD1d complex has lower half live triggering T_H2 response.

This hypothesis is widely accepted although it not always explains some activities. It is the case of C20:2 (**10**), despite its long lipid chains this compound produces a strong T_H2 polarized response in mice[57]. Authors propose other biological considerations to explain this activity, but to date the actual reasons are not well delineated.

(II) Modification in the polar part of ceramide skeleton

Some groups focus their attention on modulating H-Bonds implicated either in CD1d-Ag binding or TCR-Ag-CD1d recognition. As it was previously mentioned, both amide group and the hydroxyls of the sphingoid chain are involved in polar interactions. The amide group accepts some modifications without dramatically decreasing activity. Replacement by triazole combined with long acyl chain (**11**)[58] presents a notably increase of IL-4 cytokine production while IFN-g is reduced. When the NH of amide is replaced by an oxygen (forming an ester link)in compound (**12**) a weaker activity biased T_H2 profile and the ether analogue (**13**) is totally inactive[59] (see **Figure 1.9, Table 1.4** and **Graph 1.2** for details), highlighting the importance of NH group ability to form H-Bond with Thr156 ($Thr154_{hCD1d}$). Recently, replacement with carbamate, thioamide (**14**)[60] or ureido (**15**)[61] group seems to induce a polarized T_H1 response. On the contrary, similar analogues with sulfonamide linker (**16**)[62] or α,α'-difluoro-α-GalCer (**17**)[63] show a T_H2 biased response. Tashiro et al.[61] postulated pK_a values of NH group as a main reason of this variability; therefore, the more basic H of linking group, the more T_H1 response and the more acid H the more T_H2 profile. Thus, pK_a value of NH group seems to play an important role in response modulation (see **Table 1.4** for summary of activities).

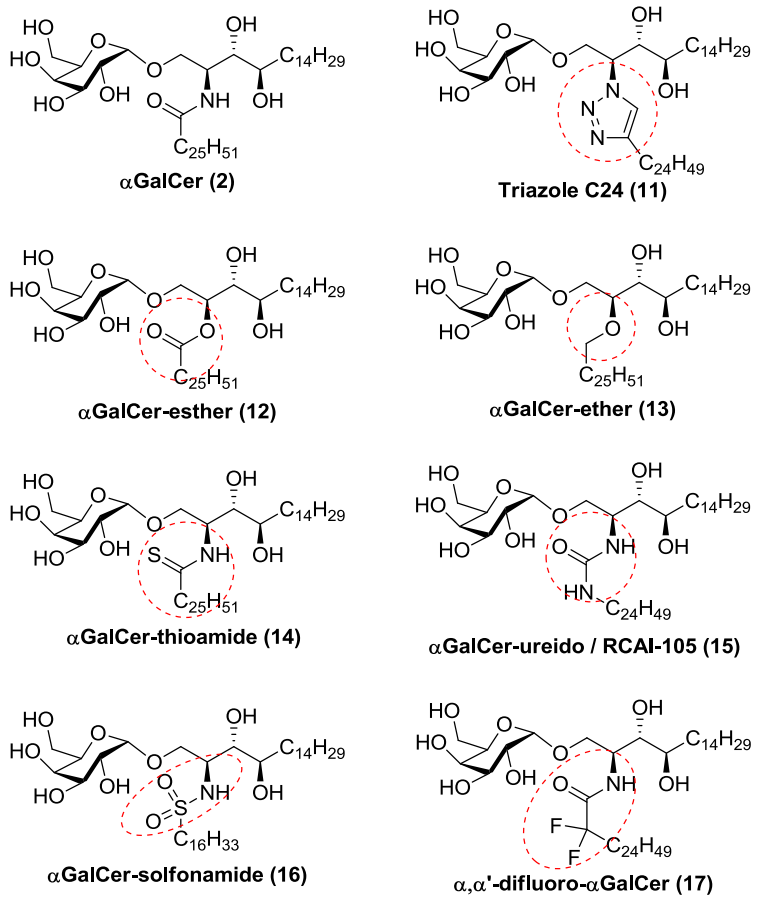

Figure 1.9: *Amide group modified analogues of αGalCer (**2**)*

Compound	% IFN-γ (T_H1)	% IL-4 (T_H2)	Ratio IFN-γ/IL-4	Specie
2 – αGalCer	100	100	1	m
11	29,68	134,82	0,22	m
12	14,7	68,75	0,21	m
13	0	0	Inactive	m
14	90,32	43,48	2,08	m
15	196,77	78,46	2,51	m
16	2,67	125	0,021	m
17	52	96,43	0,54	m

Table 1.4: *Summary of biological properties of amide group modified. Ratios are obtained from % IFN-γ/% IL-4*

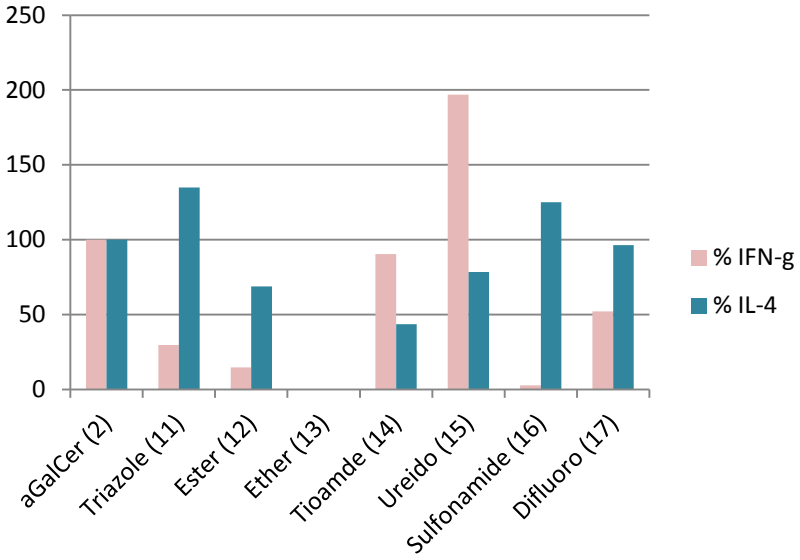

Graph 1.2: *Comparison of cytokine response of analogues **11**-**17** with αGalCer (**2**) in vitro with mouse cells*

The other polar moiety contained in the ceramide skeleton and susceptible to modification comprise the hydroxyl substituents in the sphingoid base. Several groups have synthesized and evaluated the activity of deoxy analogues (**Figure 1.10**), epimers or diastereomers of αGalCer (**2**). The 3-deoxy (**18**) and 4-deoxy (**19**) analogues of **2** showed similar but weaker cytokine profile as reference however a slightly decrease of IFN-γ was observed[64-66]. In relative amounts, **18** and **19** favor towards T_H2 response respect to αGalCer (**2**); even so, in absolute amounts both compounds still produce bigger amounts of IFN-γ than IL-4 (notice that αGalCer (**2**) produces around 10 to 25 times more IFN-γ than IL-4). When both hydroxyls are removed, the 3,4-deoxy analogue (**20**) results in inactive (**Table 1.5** and **Graph 1.3**). Thus at least one hydroxyl is needed to ensure a correct binding mode to be recognized by TCR, as it is demonstrated by non detected signal while measuring affinity constants of this compound[67].

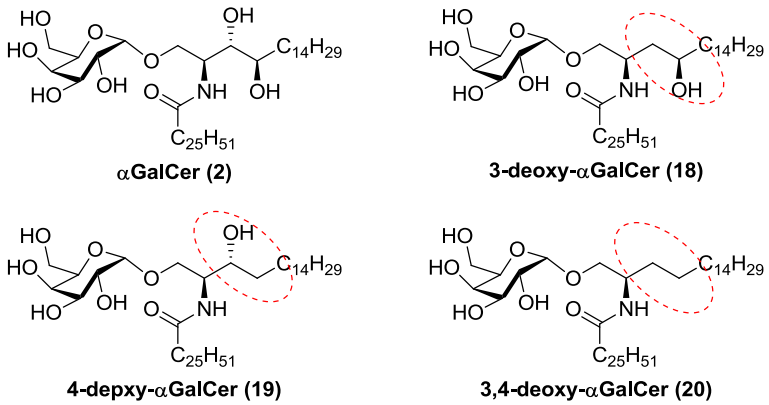

Figure 1.10: *Deoxy-analogues of αGalCer (**2**)*

This bioactivity is reasoned from the H-Bond of OHs with $Asp80_{CD1d}$; it seems crucial for a correct compound disposition that at least one OH interacts with CD1d. Beak et al. point to a compensatory effect of 4-OH when 3-OH is missing supported by docking studies[64]. Absolute configuration of both hydroxyls was also studied by Trappeniers et al.[68] and Park et al.[69] concluding that, although no drastically decrease of activity was observed among diastereomers, natural phytosphingosine configuration was the most potent one, the C2 configuration being critical. Substitution of one hydroxyl by an amino group in both possible configuration results in a drastic decrease of activity[70]. All this research in analogues reinforces the idea that the hydroxyl groups play an important role in both CD1d recognition and glycolipid orientation for a productive TCR interaction.

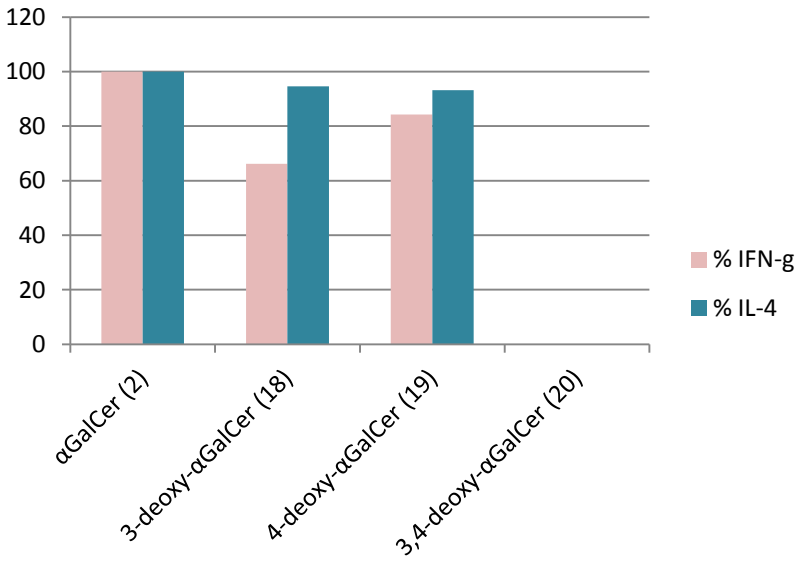

Graph 1.3: *Comparison of cytokine response of analogues **18**-**20** with αGalCer (**2**) in vitro with mouse cells*

Compound	% IFN-γ (T_H1)	% IL-4 (T_H2)	Ratio IFN-γ/IL-4	Specie
2 – αGalCer	100	100	1	m
18	66,2	94,6	0,70	m
19	84,3	93,2	0,90	m
20	0	0	Inactive	m

Table 1.5: *Summary of biological properties of hydroxyls 3 and 4 modified analogues. Ratios are obtained from % IFN-γ/% IL-4*

(III) Modifications on glycosidic bond

Metabolic instability of glycosidic bond *in vivo* is evident, for this reason some analogues exploring this substitution had been reported (**Figure 1.11** and **Table 1.6**). α-C-GalCer (**21**) exhibits a potent T_H1 activity leading to a promising anti-malaria and anti-tumor antigen with better selectivity than αGalCer (**2**) in mice[71]. Increase of half-life of compound *in vivo* was pointed as main reason of IFN-γ increment. Despite of these promising results, α-C-GalCer (**21**) failed to stimulate human iNKT cells[72], at least in a significant manner. It was proposed the loss of H-Bond interaction of oxygen of glycosidic bond with $Thr154_{mCD1d}$ ($Thr156_{hCD1d}$) and its decrease of affinity as main causes of activity alteration however real significance of this contradictory behavior reminds uncertain. Analogues with unsaturated acyl chains of **21** have been also tested showing notable increase of activity (structure not shown); this results support the idea of sugar orientation failure of saturated analogue **21** as a main reason for poor NKT cell stimulation[72].

When the glycosidic oxygen is replaced by sulfur (α-S-GalCer (**22**)), the resulting derivative was inactive in mice[73] and active in human assays with similar profile but lower levels of activity to those of αGalCer (**2**)[74].

Compound	% IFN-γ (T_H1)	% IL-4 (T_H2)	Ratio IFN-γ/IL-4	Specie
2 – αGalCer	100	100	1	m
	100	100	1	h
21	89,2	7,8	11,6	m
	0	0	Inactive	h
22	0	0	Inactive	m
	53,3	53,8	0,99	h

Table 1.6: *Summary of activities of analogues with glycosidic bond modifications*

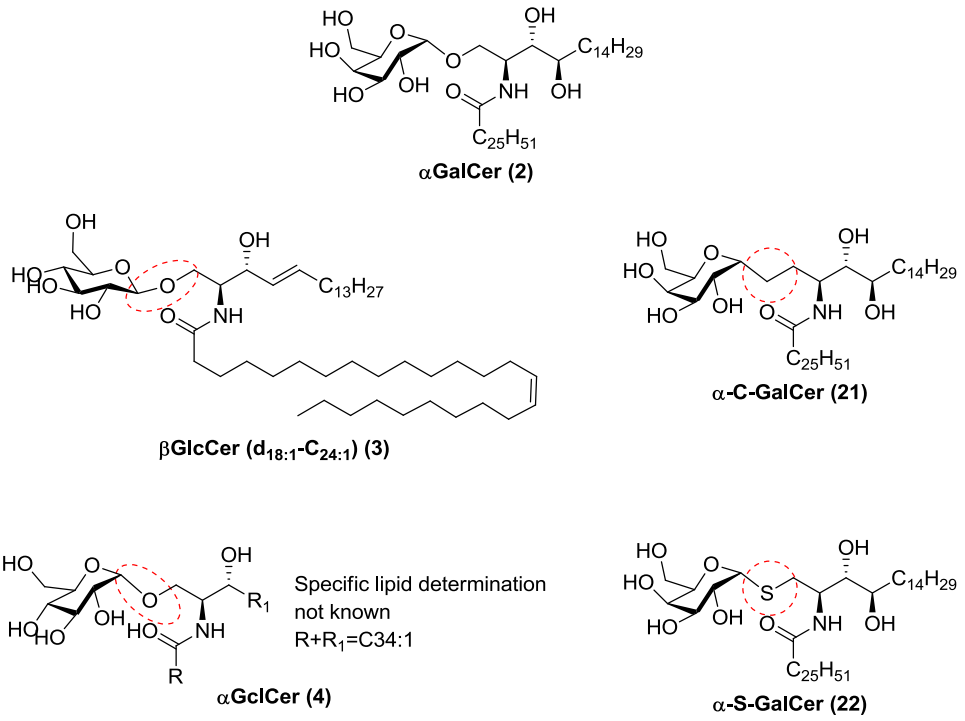

Figure 1.11: *Examples of modifications at the glycosidic bond of αGalCer (**2**)*

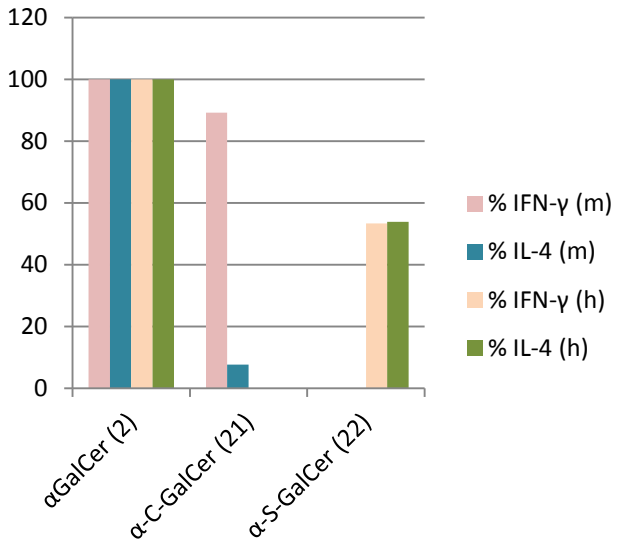

Graph 1.4: *Comparison of cytokine responses of analogues **21** and **22** with αGalCer (**2**) in vitro with mouse cells and human cells*

As it was mentioned above, alpha or beta configuration of sugar link has essential relevance as switching alpha (**2 and 4**) to beta (**3**) triggers an inactive compound.

No clear hypothesis has been proposed about the involvement of this part in the activity; however some implication in sugar head orientation and its interaction with TCR are present.

(IV) Modification on the sugar ring:

Probably this is the most thoroughly examined part in αGalCer analogues. Hundreds of compounds had been synthesized exploring whether one or other hydroxyl is necessary or not for activity or which one can be replaced by other polar or bulky groups or if its configuration could influence the structural recognition and the biological activities. Another strategy was to replace the sugar head by other chemical structures able to mimic sugar configurations and therefore galactose interactions with the proteins, but avoiding the presence of metabolically labile glycosidic bond.

Modifications at 2'-OH of galactose moiety such as 2'-(H, F, NH_2 or OMe)-galactose analogues (**23, 24, 25 and 26** respectively, **Figure 1.12**) were reported inactive[50,75,76], pointing this hydroxyl as essential for the activity. About 3'-OH, it seems also very critical; most modifications reported showed a dramatic loss of activity[77] while only 3'-sulfatide-derivative **27** showed equivalent potency as (**2**)[54,78]; this hydroxyl is also considered crucial for NKT activation. Hydroxyl at position 4' has been somewhat modified since it seems to accept better and more widely the variations. Thus, modifications with small groups such as 4'-OMe, 4'-H or 4'-OCH_2CHOH-galactose analogues[77] seem to slightly polarize the response towards IL-4 production while larger groups such as benzoate (**31**) or phenylethylether (**32**) were described as T_H1 polarizing analogues (notice that when relative cytokine production is compared, the ratio of % IFN-γ versus % IL-4 results less than 1; however when absolute values are considered, IFN-γ production is still higher, see *Absolute Ratio* in **Table 1.7**), however 3-phenylpropyl ether (**33**) seems to exhibit a marked increase of IL-4 production, polarizing response towards T_H2[79] (**Graph 1.5** and **Table 1.7**). The authors suggest some π-π interactions as main reason for this gain of potency.

Another widely modified group is 6'-OH which accepts very different substitutions without losing activity or even increasing it in some particular cases. At this position had been attached a wide variety of moieties from aromatic groups to PEGs for example[41,80]. Group of S. V. Calenbergh described a series of derivative with aril-ureido or aril-carbamate with promising results, some of them were also crystallized showing a feasible pocket were aromatic moieties can fit[48,81], an example of this series is NU-α-GalCer (**37**) (**Figure 1.12, Table 1.7** and **Graph 1.5**).

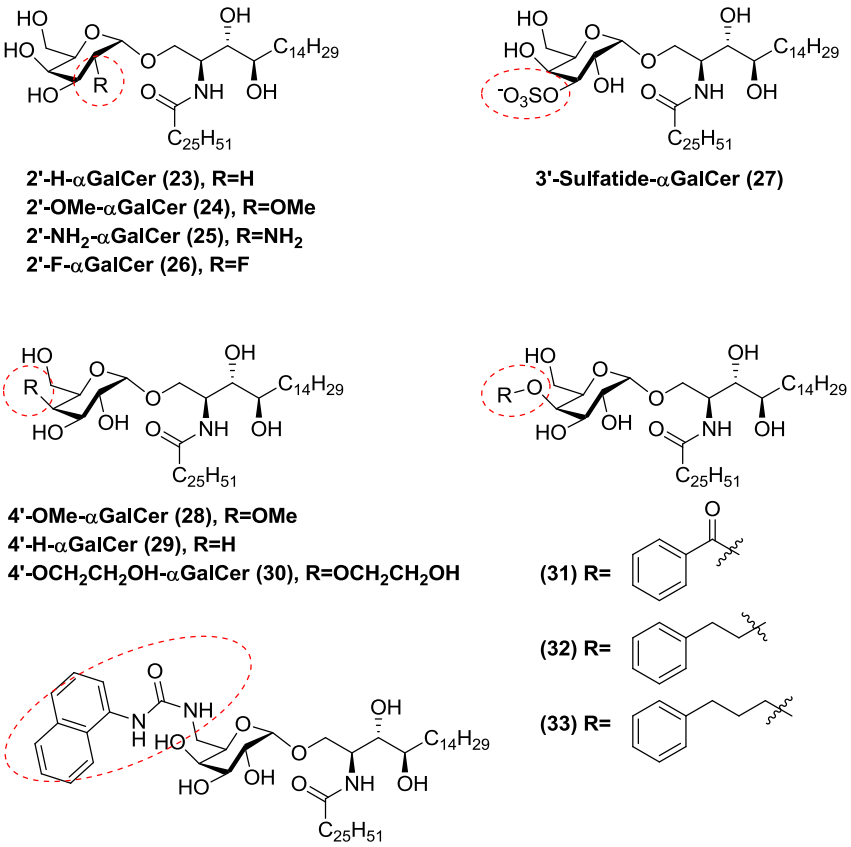

Figure 1.12: *Examples of αGalCer (**2**) derivatives with modified or substituted hydroxyls of galactose-head.*

Compound	% IFN-γ (T_H1)	% IL-4 (T_H2)	Ratio IFN-γ/IL-4[a]	Absolute Ratio[b]	Specie
2 – αGalCer	100	100	1	1,3 – 6,7 53,00	m
27	53,6	17,9	2,998	10,3	m
28	17,4	33,3	0,52	27,7	m
29	10,9	29,2	0,37	19,8	m
30	13,0	29,2	0,45	23,7	m
31	100	47,1	2,12	2,9	m
32	183,4	211,8	0,87	1,2	m
33	183,4	370,6	0,49	0,7	m
34	67,6	54,3	1,25	8,3	m

Table 1.7: *Summary of activities of galactose modified derivatives of αGalCer (**2**); a) Relative ratio calculated from relative response (%); b) Ratio IFN-γ/IL-4 calculated from absolute values of cytokines produced by the ligands.*

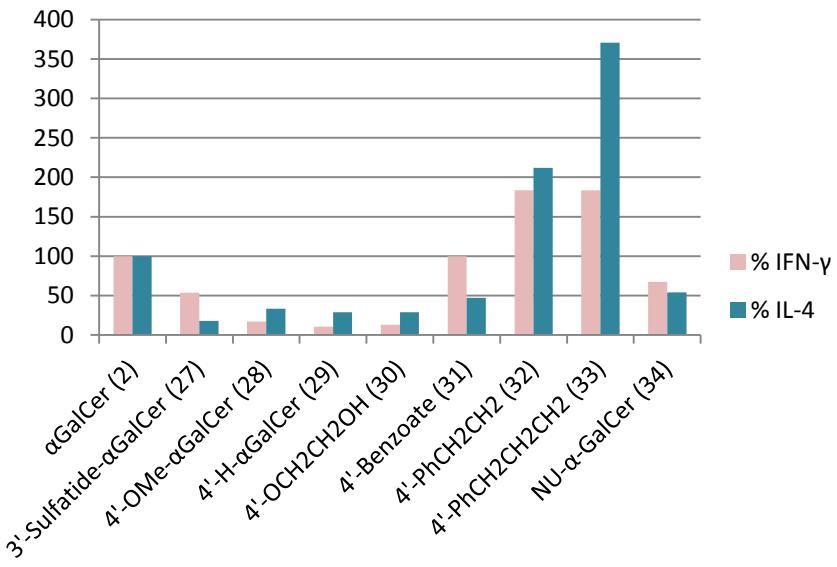

Graph 1.5: *Comparison of cytokine response of analogues **27** to **34** with αGalCer (**2**) in vitro with mouse cells*

Substitution of galactose by other sugars did not result in any improvement of activity but the study revealed the relevance of alpha-link as essential[82,83]. Glucose derivatives were thought to be perfect candidate as self-antigen but despite its good activity in mice, it had weaker potency in human. This difference in activity is commonly explained by the presence on $Trp153_{hCD1d}$ instead of $Gly155_{mCD1d}$ directly orientated to 4'-OH of sugar head. The equatorial configuration of 4'-OH in glucose could destabilize glycolipid interaction with CD1d in human protein.

Finally, replacement of galactose head group by other non-glycosidic sugar-mimetic moieties was also widely explored. In this list there are many different structures, from simply using a carba-sugar (RCAI 56 – **35**)[84,85] (where the oxygen of the ring is replaced by a methylene group) to more drastic ones such as threitol (ThrCer, (**36**)[86] or glycerol (GlyCer, (**37**)[87]) derivatives. The first one showed a biased activity towards T_H1 response and the authors suggest a positive hydrophobic interaction between the methylene group and a $Pro28_{TCR}$. Truncated polyols have different behavior depending on number of hydroxyls groups present; ThrCer was a weaker agonist albeit it was able to improve some of the drawbacks of αGalCer such as iNKT anergy while the glycerol substituted GlyCer has been reported to activate human iNKT cells but not murine iNKT cells, suggesting a different minimal H-Bond requirement between murine and human receptors (see **Figure 1.13** and **Table 1.7** for structures and activities)[87].

Our research group has focused efforts in non glycosidic derivatives. Taking advantage of our strong background on ceramide chemistry as well as aminocyclitol synthesis, a series of aminocyclitol-ceramide derivatives were synthesized and evaluated as NKT activators in collaboration with the Rossjohn and Godfrey groups. These analogues are non-glycosidic sugar-mimetic ceramides with different lipid skeletons some of which

showed an interesting cytokine profile and a similar binding mode as αGalCer in mice. HS44 (**38**)[88,89], HS161 (**39**)[90] and HS138 (**40**)[88,91] are some examples with different structures and activities. They have the same phytoceramide lipid backbone present in αGalCer (**2**) but different aminocyclitol configuration; HS161 (**39**) has a galacto-like structure, HS44 (38) has inositol configuration and HS138 (**40**) presents a galacto-like configuration with an extra axial-OH at position 6 of the ring. Three analogues presenting a few structural differences however they had different biological profile; while HS161 (**39**) bias the response towards IFN-γ increase (its effects were notably higher *in vivo***)**, HS44 showed controversial results (it bias response towards T_H2 although in a weaker manner *in vitro* and a potent T_H1 *in vivo*) and HS138 (**40**) is inactive (see **Figure 1.13** and **Table 1.7** for structures and activities).

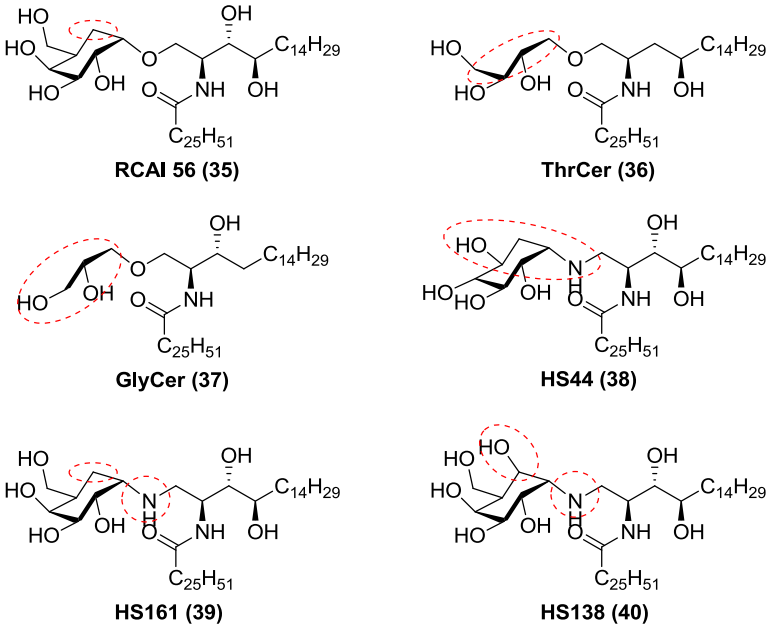

Figure 1.13: Examples of non-glycosidic derivatives

Compound	% IFN-γ (T_H1)	% IL-4 (T_H2)	Ratio IFN-γ/IL-4[a]	Absolute Ratio[b]	Species
2 – αGalCer	100	100	1	27,0-45,2 1,9-8,7	m
35	1000	47,1	21,3	961,5	m
36	60,4	11,6	5,2	9,85	m
37	No data	No data	-	-	-
38	6,5 78	68 3,6	0,1 21,5	0,91 187,2	m *in vitro* m *in vivo*
39	22,2 171,4	55,6 15,2	0,4 11,3	10,8 34,3	m *in vitro* m *in vivo*
40	0	0	In active	Inactive	m

Table 1.8: Summary of activities of non-glycosidic derivatives of αGalCer (**2**)*; a) Relative ratio calculated from relative responses (%); b) Ratio IFN-γ/IL-4 calculated from absolute values of cytokines produced by the ligands.*

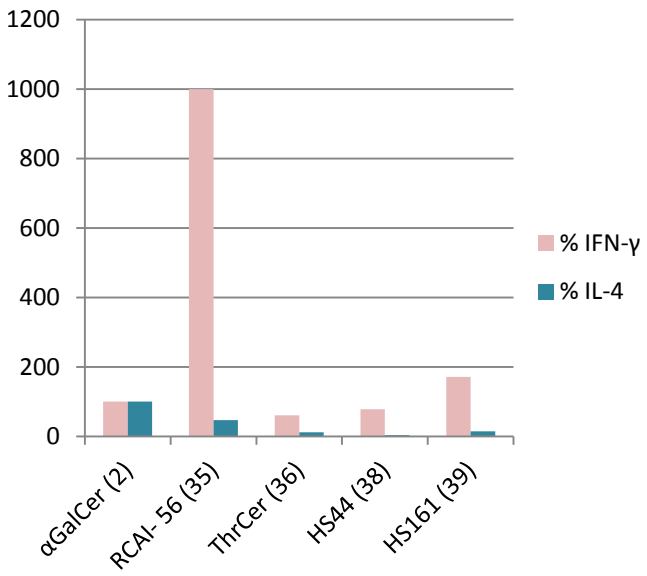

Graph 1.6: *Comparison of cytokine response of analogues **35** to **39** with αGalCer (**2**).In vivo data are shown for aminocyclitol derivatives*

Figure 1.14 tries to summarize current hypothesis of modifications accepted on αGalCer (**2**) to maintain activity as NKT antigens. Some features are considered crucial while others seem to have some relevance in either potency or selectivity modulation.

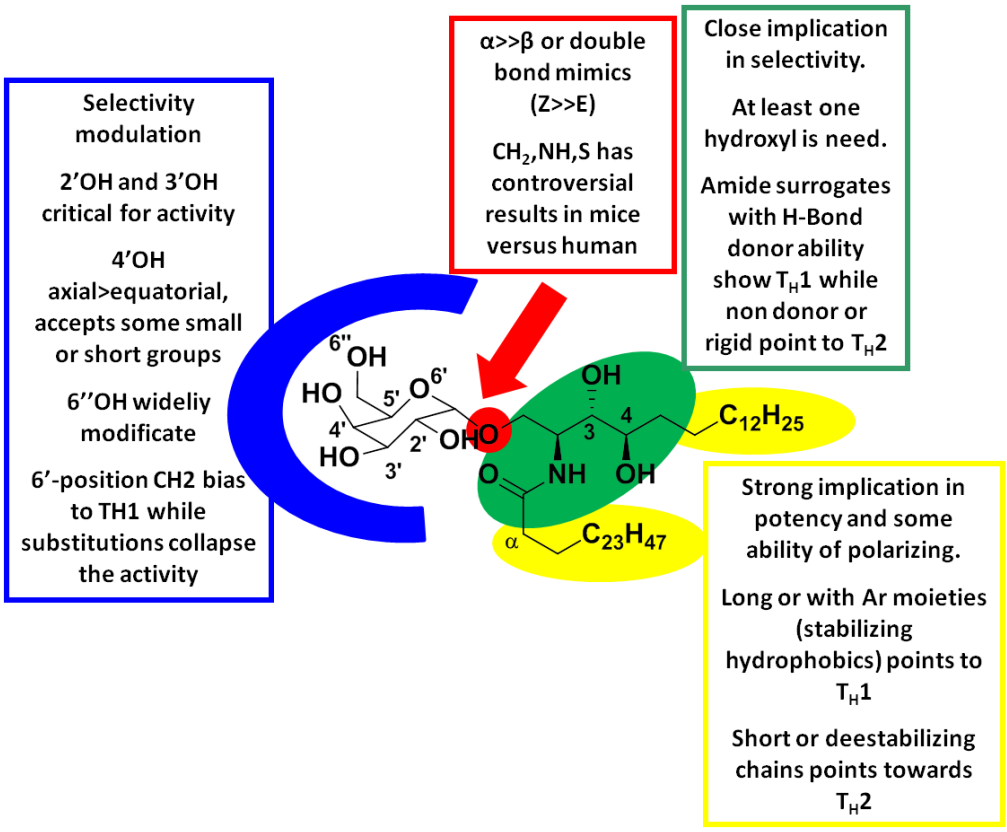

Figure 1.14: *Summary of modification impact on ligand activities as iNKT cell activators*

Among compounds synthesized and tested as NKT activators, no compound shows a completely T_H polarized activity; some of them had been clinically tested as antigens in

different disease treatments, with special emphasis in cancer with promising results but to date these efforts have not resulted in a clinically useful therapy. The pharmacophore structure is not fully understood and an ideal candidate reminds elusive. On the other hand, the majority of active αGalCer – derivatives proposed in literature are glycolipids and hence metabolic degradation problems can still being present. Another consideration that cannot be omitted is the difference between compound activity when tested in mice or human cells. An appropriate administration method for treatments should be explored to use NKT as immunotherapeutic tool and more information about how to implement it is under demand by clinicians. The lack of knowledge on the natural endogenous antigens is also an important factor that can influence the clinical failures. For all these reasons, NKT antigen research remains an interesting field for immunologists, biologists, computational scientists and chemists.

BIBLIOGRAPHIC REFERENCES:

1. Bendelac, A., Savage, P.B. & Teyton, L. The biology of NKT cells. *Annu Rev Immunol* **25**, 297-336 (2007).
2. Taniguchi, M., Harada, M., Kojo, S., Nakayama, T. & Wakao, H. The regulatory role of Valpha14 NKT cells in innate and acquired immune response. *Annu Rev Immunol* **21**, 483-513 (2003).
3. Subleski, J.J., Jiang, Q., Weiss, J.M. & Wiltrout, R.H. The split personality of NKT cells in malignancy, autoimmune and allergic disorders. *Immunotherapy* **3**, 1167-1184 (2011).
4. Warrington, R., Watson, W., Kim, H.L. & Antonetti, F.R. An introduction to immunology and immunopathology. *Allergy, Asthma & Clinical Immunology* **7**, S1 (2011).
5. Hogquist, K.A., Baldwin, T.A. & Jameson, S.C. Central tolerance: learning self-control in the thymus. *Nat Rev Immunol* **5**, 772-782 (2005).
6. Raulet, D.H. & Vance, R.E. Self-tolerance of natural killer cells. *Nat Rev Immunol* **6**, 520-531 (2006).
7. Medzhitov, R. & Janeway, C. Innate Immunity. *New England Journal of Medicine* **343**, 338-344 (2000).
8. Coers, J. Self and non-self discrimination of intracellular membranes by the innate immune system. *PLoS Pathog* **9**, e1003538 (2013).
9. Parkin, J. & Cohen, B. An overview of the immune system. *The Lancet* **357**, 1777-1789.
10. Parijs, L.V. & Abbas, A.K. Homeostasis and Self-Tolerance in the Immune System: Turning Lymphocytes off. *Science* **280**, 243 (1998).
11. Chaplin, D.D. Overview of the Immune Response. *The Journal of allergy and clinical immunology* **125**, S3-23 (2010).
12. Turvey, S.E. & Broide, D.H. Innate immunity. *Journal of Allergy and Clinical Immunology* **125**, S24-S32 (2010).
13. Beutler, B. Innate immunity: an overview. *Mol Immunol* **40**, 845-859 (2004).
14. Bonilla, F.A. & Oettgen, H.C. Adaptive immunity. *Journal of Allergy and Clinical Immunology* **125**, S33-S40 (2010).
15. Dranoff, G. Cytokines in cancer pathogenesis and cancer therapy. *Nat Rev Cancer* **4**, 11-22 (2004).
16. MacDonald, H.R. NKT cells: In the beginning…. *European Journal of Immunology* **37**, S111-S115 (2007).
17. Chandra, S. & Kronenberg, M. Chapter Three - Activation and Function of iNKT and MAIT Cells. in *Advances in Immunology*, Vol. 127 (ed. Alt, F.W.) 145-201 (Academic Press, 2015).
18. Albert Bendelac, M.N.R., Se-Ho Park, and & Roark, J.H. MOUSE CD1-SPECIFIC NK1 T CELLS: Development, Specificity, and Function. *Annual Review of Immunology* **15**, 535-562 (1997).
19. Cerundolo, V. & Kronenberg, M. The role of invariant NKT cells at the interface of innate and adaptive immunity. *Seminars in Immunology* **22**, 59-60 (2010).
20. Barral, D.C. & Brenner, M.B. CD1 antigen presentation: how it works. *Nat Rev Immunol* **7**, 929-941 (2007).
21. Fletcher, M.T. & Baxter, A.G. Clinical application of NKT cell biology in type I (autoimmune) diabetes mellitus. *Immunol Cell Biol* **87**, 315-323 (2009).
22. O'Keeffe, J., Podbielska, M. & Hogan, E.L. Invariant natural killer T cells and their ligands: focus on multiple sclerosis. *Immunology* **145**, 468-475 (2015).
23. Van Kaer, L., Wu, L. & Parekh, V.V. Natural killer T cells in multiple sclerosis and its animal model, experimental autoimmune encephalomyelitis. *Immunology* **146**, 1-10 (2015).

24. Matangkasombut, P., Pichavant, M., Dekruyff, R.H. & Umetsu, D.T. Natural killer T cells and the regulation of asthma. *Mucosal Immunol* **2**, 383-392 (2009).
25. Simoni, Y., Diana, J., Ghazarian, L., Beaudoin, L. & Lehuen, A. Therapeutic manipulation of natural killer (NK) T cells in autoimmunity: are we close to reality? *Clin Exp Immunol* **171**, 8-19 (2013).
26. Slauenwhite, D. & Johnston, B. Regulation of NKT Cell Localization in Homeostasis and Infection. *Front Immunol* **6**, 255 (2015).
27. Nair, S. & Dhodapkar, M.V. Natural Killer T Cells in Cancer Immunotherapy. *Front Immunol* **8**, 1178 (2017).
28. Escribà-Garcia, L., Alvarez-Fernández, C., Tellez-Gabriel, M., Sierra, J. & Briones, J. Dendritic cells combined with tumor cells and α-galactosylceramide induce a potent, therapeutic and NK-cell dependent antitumor immunity in B cell lymphoma. *Journal of Translational Medicine* **15**, 115 (2017).
29. Cerundolo, V., Silk, J.D., Masri, S.H. & Salio, M. Harnessing invariant NKT cells in vaccination strategies. *Nat Rev Immunol* **9**, 28-38 (2009).
30. Natori, T., Koezuka, Y. & Higa, T. Agelasphins, novel α-galactosylceramides from the marine sponge Agelas mauritianus. *Tetrahedron Letters* **34**, 5591-5592 (1993).
31. Natori, T., Morita, M., Akimoto, K. & Koezuka, Y. Agelasphins, novel antitumor and immunostimulatory cerebrosides from the marine sponge Agelas mauritianus. *Tetrahedron* **50**, 2771-2784 (1994).
32. Akimoto, K., Natori, T. & Morita, M. Synthesis and stereochemistry of agelasphin-9b. *Tetrahedron Letters* **34**, 5593-5596 (1993).
33. Morita, M.*, et al.* Structure-activity relationship of alpha-galactosylceramides against B16-bearing mice. *J Med Chem* **38**, 2176-2187 (1995).
34. Kobayashi, E., Motoki, K., Uchida, T., Fukushima, H. & Koezuka, Y. KRN7000, A Novel Immunomodulator, and Its Antitumor Activities. *Oncology Research Featuring Preclinical and Clinical Cancer Therapeutics* **7**, 529-534 (1995).
35. Kawano, T.*, et al.* CD1d-Restricted and TCR-Mediated Activation of Vα14 NKT Cells by Glycosylceramides. *Science* **278**, 1626 (1997).
36. Parekh, V.V.*, et al.* Glycolipid antigen induces long-term natural killer T cell anergy in mice. *J Clin Invest* **115**, 2572-2583 (2005).
37. Sullivan, B.A. & Kronenberg, M. Activation or anergy: NKT cells are stunned by alpha-galactosylceramide. *J Clin Invest* **115**, 2328-2329 (2005).
38. Brennan, P.J.*, et al.* Invariant natural killer T cells recognize lipid self antigen induced by microbial danger signals. *Nat Immunol* **12**, 1202-1211 (2011).
39. Brennan, P.J.*, et al.* Structural determination of lipid antigens captured at the CD1d-T-cell receptor interface. *Proc Natl Acad Sci U S A* **114**, 8348-8353 (2017).
40. Brennan, P.J.*, et al.* Activation of iNKT cells by a distinct constituent of the endogenous glucosylceramide fraction. *Proc Natl Acad Sci U S A* **111**, 13433-13438 (2014).
41. Laurent, X.*, et al.* Switching invariant natural killer T (iNKT) cell response from anticancerous to anti-inflammatory effect: molecular bases. *J Med Chem* **57**, 5489-5508 (2014).
42. Zajonc, D.M.*, et al.* Structure and function of a potent agonist for the semi-invariant natural killer T cell receptor. *Nat Immunol* **6**, 810-818 (2005).
43. Zajonc, D.M.*, et al.* Structural basis for CD1d presentation of a sulfatide derived from myelin and its implications for autoimmunity. *J Exp Med* **202**, 1517-1526 (2005).
44. Giabbai, B.*, et al.* Crystal structure of mouse CD1d bound to the self ligand phosphatidylcholine: a molecular basis for NKT cell activation. *J Immunol* **175**, 977-984 (2005).
45. Koch, M.*, et al.* The crystal structure of human CD1d with and without alpha-galactosylceramide. *Nat Immunol* **6**, 819-826 (2005).

46. Borg, N.A*., et al.* CD1d-lipid-antigen recognition by the semi-invariant NKT T-cell receptor. *Nature* **448**, 44-49 (2007).
47. Pellicci, D.G*., et al.* Differential recognition of CD1d-alpha-galactosyl ceramide by the V beta 8.2 and V beta 7 semi-invariant NKT T cell receptors. *Immunity* **31**, 47-59 (2009).
48. Aspeslagh, S*., et al.* Galactose-modified iNKT cell agonists stabilized by an induced fit of CD1d prevent tumour metastasis. *EMBO J* **30**, 2294-2305 (2011).
49. Zajonc, D.M. & Girardi, E. Recognition of Microbial Glycolipids by Natural Killer T Cells. *Front Immunol* **6**, 400 (2015).
50. Miyamoto, K., Miyake, S. & Yamamura, T. A synthetic glycolipid prevents autoimmune encephalomyelitis by inducing TH2 bias of natural killer T cells. *Nature* **413**, 531-534 (2001).
51. Goff, R.D*., et al.* Effects of lipid chain lengths in alpha-galactosylceramides on cytokine release by natural killer T cells. *J Am Chem Soc* **126**, 13602-13603 (2004).
52. Fujio, M*., et al.* Structure-based discovery of glycolipids for CD1d-mediated NKT cell activation: tuning the adjuvant versus immunosuppression activity. *J Am Chem Soc* **128**, 9022-9023 (2006).
53. Park, J.J*., et al.* Syntheses and biological activities of KRN7000 analogues having aromatic residues in the acyl and backbone chains with varying stereochemistry. *Bioorg Med Chem Lett* **20**, 814-818 (2010).
54. Chang, Y.J*., et al.* Potent immune-modulating and anticancer effects of NKT cell stimulatory glycolipids. *Proc Natl Acad Sci U S A* **104**, 10299-10304 (2007).
55. Toba, T*., et al.* Minimum structure requirement of immunomodulatory glycolipids for predominant Th2 cytokine induction and the discovery of non-linear phytosphingosine analogs. *Bioorg Med Chem Lett* **17**, 2781-2784 (2007).
56. Inuki, S*., et al.* Isolated Polar Amino Acid Residues Modulate Lipid Binding in the Large Hydrophobic Cavity of CD1d. *ACS Chem Biol* **11**, 3132-3139 (2016).
57. Yu, K.O*., et al.* Modulation of CD1d-restricted NKT cell responses by using N-acyl variants of alpha-galactosylceramides. *Proc Natl Acad Sci U S A* **102**, 3383-3388 (2005).
58. Lee, T*., et al.* Synthesis and evaluation of 1,2,3-triazole containing analogues of the immunostimulant alpha-GalCer. *J Med Chem* **50**, 585-589 (2007).
59. Shiozaki, M*., et al.* Synthesis and biological activity of ester and ether analogues of alpha-galactosylceramide (KRN7000). *Carbohydr Res* **345**, 1663-1684 (2010).
60. Wojno, J*., et al.* Amide analogues of CD1d agonists modulate iNKT-cell-mediated cytokine production. *ACS Chem Biol* **7**, 847-855 (2012).
61. Tashiro, T., Shigeura, T., Watarai, H., Taniguchi, M. & Mori, K. RCAI-84, 91, and 105-108, ureido and thioureido analogs of KRN7000: their synthesis and bioactivity for mouse lymphocytes to produce Th1-biased cytokines. *Bioorg Med Chem* **20**, 4540-4548 (2012).
62. Tashiro, T*., et al.* RCAI-17, 22, 24-26, 29, 31, 34-36, 38-40, and 88, the analogs of KRN7000 with a sulfonamide linkage: their synthesis and bioactivity for mouse natural killer T cells to produce Th2-biased cytokines. *Bioorg Med Chem* **16**, 8896-8906 (2008).
63. Leung, L*., et al.* The synthesis and in vivo evaluation of 2',2'-difluoro KRN7000. *ChemMedChem* **4**, 329-334 (2009).
64. Baek, D.J*., et al.* The 3-Deoxy Analogue of alpha-GalCer: Disclosing the Role of the 4-Hydroxyl Group for CD1d-Mediated NKT Cell Activation. *ACS Med Chem Lett* **2**, 544-548 (2011).
65. Lacone, V*., et al.* Focus on the controversial activation of human iNKT cells by 4-deoxy analogue of KRN7000. *J Med Chem* **52**, 4960-4963 (2009).
66. Ndonye, R.M*., et al.* Synthesis and evaluation of sphinganine analogues of KRN7000 and OCH. *J Org Chem* **70**, 10260-10270 (2005).

67. Sidobre, S.*, et al.* The T cell antigen receptor expressed by Valpha14i NKT cells has a unique mode of glycosphingolipid antigen recognition. *Proc Natl Acad Sci U S A* **101**, 12254-12259 (2004).
68. Trappeniers, M.*, et al.* Synthesis and in vitro evaluation of alpha-GalCer epimers. *ChemMedChem* **3**, 1061-1070 (2008).
69. Park, J.J.*, et al.* Synthesis of all stereoisomers of KRN7000, the CD1d-binding NKT cell ligand. *Bioorg Med Chem Lett* **18**, 3906-3909 (2008).
70. Trappeniers, M.*, et al.* Synthesis and evaluation of amino-modified alpha-GalCer analogues. *Org Lett* **12**, 2928-2931 (2010).
71. Fujii, S.*, et al.* Glycolipid alpha-C-galactosylceramide is a distinct inducer of dendritic cell function during innate and adaptive immune responses of mice. *Proc Natl Acad Sci U S A* **103**, 11252-11257 (2006).
72. Li, X., Chen, G., Garcia-Navarro, R., Franck, R.W. & Tsuji, M. Identification of C-glycoside analogues that display a potent biological activity against murine and human invariant natural killer T cells. *Immunology* **127**, 216-225 (2009).
73. Blauvelt, M.L.*, et al.* Alpha-S-GalCer: synthesis and evaluation for iNKT cell stimulation. *Bioorg Med Chem Lett* **18**, 6374-6376 (2008).
74. Hogan, A.E.*, et al.* Activation of human invariant natural killer T cells with a thioglycoside analogue of alpha-galactosylceramide. *Clin Immunol* **140**, 196-207 (2011).
75. Balducci, M.*, et al.* Impact of dose and volume on the tolerance of central nervous system. *Rays* **30**, 189-195 (2005).
76. Barbieri, L.*, et al.* Immunomodulatory α-Galactoglycosphingolipids: Synthesis of a 2'-O-Methyl-α-Gal-GSL and Evaluation of Its Immunostimulating Capacity. *European Journal of Organic Chemistry* **2004**, 468-473 (2004).
77. Xia, C.*, et al.* The roles of 3' and 4' hydroxy groups in alpha-galactosylceramide stimulation of invariant natural killer T cells. *ChemMedChem* **4**, 1810-1815 (2009).
78. Xing, G.W.*, et al.* Synthesis and human NKT cell stimulating properties of 3-O-sulfo-alpha/beta-galactosylceramides. *Bioorg Med Chem* **13**, 2907-2916 (2005).
79. Zhang, W.*, et al.* Introduction of aromatic group on 4'-OH of alpha-GalCer manipulated NKT cell cytokine production. *Bioorg Med Chem* **19**, 2767-2776 (2011).
80. Banchet-Cadeddu, A.*, et al.* The stimulating adventure of KRN 7000. *Org Biomol Chem* **9**, 3080-3104 (2011).
81. Aspeslagh, S.*, et al.* Enhanced TCR footprint by a novel glycolipid increases NKT-dependent tumor protection. *J Immunol* **191**, 2916-2925 (2013).
82. Motoki, K.*, et al.* Immunostimulatory and Antitumor Activities of Monoglycosylceramides Having Various Sugar Moieties. *Biological & Pharmaceutical Bulletin* **18**, 1487-1491 (1995).
83. Uchimura, A.*, et al.* Immunostimulatory activities of monoglycosylated alpha-D-pyranosylceramides. *Bioorg Med Chem* **5**, 2245-2249 (1997).
84. Tashiro, T.*, et al.* RCAI-37, 56, 59, 60, 92, 101, and 102, cyclitol and carbasugar analogs of KRN7000: their synthesis and bioactivity for mouse lymphocytes to produce Th1-biased cytokines. *Bioorg Med Chem* **17**, 6360-6373 (2009).
85. Tashiro, T.*, et al.* Induction of Th1-biased cytokine production by alpha-carba-GalCer, a neoglycolipid ligand for NKT cells. *Int Immunol* **22**, 319-328 (2010).
86. Jukes, J.P.*, et al.* Non-glycosidic compounds can stimulate both human and mouse iNKT cells. *Eur J Immunol* **46**, 1224-1234 (2016).
87. Silk, J.D.*, et al.* Cutting edge: nonglycosidic CD1d lipid ligands activate human and murine invariant NKT cells. *J Immunol* **180**, 6452-6456 (2008).
88. Harrak, Y.*, et al.* Aminocyclitol-Substituted Phytoceramides and their Effects on iNKT Cell Stimulation. *ChemMedChem* **4**, 1608-1613 (2009).

89. Kerzerho, J.*, et al.* Structural and Functional Characterization of a Novel Nonglycosidic Type I NKT Agonist with Immunomodulatory Properties. *The Journal of Immunology* **188**, 2254 (2012).
90. Harrak, Y., Barra, C.M., Delgado, A., Castaño, A.R. & Llebaria, A. Galacto-Configured Aminocyclitol Phytoceramides Are Potent in Vivo Invariant Natural Killer T Cell Stimulators. *Journal of the American Chemical Society* **133**, 12079-12084 (2011).
91. Patel, O.*, et al.* NKT TCR Recognition of CD1d-α-C-Galactosylceramide. *The Journal of Immunology* **187**, 4705 (2011).

BIOLOGICAL GLOSSARY

Antibody	molecules (also called immunoglobulins) produced by B cells in response to antigens. When an antibody attaches to an antigen, it helps the body destroy or inactivate it
Antigen (Ag)	small peptide or other biochemical structure capable to generate immune response
Antigen Presenting Cells (APCs)	cells capable to recognize, process and express antigens to other immune cells through specific receptors
Autoimmune disease	disease resulting when immune system mistakenly attacks the host's own tissues with pathogenic consequences and tissue damage. Self-tolerance failure leads to autoimmune disease.
Autoimmunity	refers merely to aberrant immune responses against self-antigens and does not necessary causes an autoimmune disease
Adjuvant	is a pharmacological or immunological agent that modifies the effect of other agents. In immunology are added to vaccines to stimulate immune System's response to target the antigen, but do not provide immunity themselves.
Cellular Immunity	is the immune response directly mediated by cells. It is carried out by NK cells, T cells or other phagocyting cells.
Cytokine	chemical substances secreted by immune cells to communicate with one to another.
Immune response	is the coordinated reaction of the immune system against infections (and other foreign substances)
Immune system	is the collection of cells, tissues and molecules that functions to defend us against infectious microbes.
Immunity	refers to protection against infection.
Inflammation	is the process by which the cells of Immune System are recruited to sites of infection and injury and activated to get rid of the infectious agent and dead tissues.
Humoral Immunity	is the immune response mediated by antibodies or any other small molecules like cytokines or chemokines or complement system (not discussed in this thesis)
Major Histocompatibility Complexes	cell surface proteins essential for immune system to recognize foreign antigens. Its main function is to bind to antigens and display them on cell surface for recognition by T cells
Memory cells	group of T cells and B cells that have been exposed to antigens and can then respond more readily when same threat appears again

Natural Killer T Cells (NKT)	T cell expressing a CD1d-restricted, lipid-specific T cell receptor combining a canonical Vα14-Jα18 α chain with a variable Vβ8, -7, or -2 β chain in mouse or Vα24-Jα18/Vβ11 in human. At same time they express NK surface markers (NK1.1 in mouse and CD161 in human).
Pathogen-associated molecular pattern (PAMP)	molecules associated whit groups of pathogens. These molecules can be referred to as small molecular motifs conserved within a class of microbes.
Pattern recognition receptors (PRR)	cell surface receptors able to detect molecules typical for pathogens (PAMPs).
Self-tolerance	mechanism by which lymphocytes that happen to express receptors for self antigens are killed or shut off when they recognize these antigens.
Vaccine	preparations that stimulate an immune response generating memory against a specific antigen creating resistance to an infection. They did not cause disease.

2. GENERAL OBJECTIVES

2. GENERAL OBJECTIVES

As it was previously introduced in the preceding section, NKT cells have a challenging role in immunity. However their effective modulation has not been properly reached, which is precluding its implementation as an operative therapeutic tool. The complexity of Strucutre-Acitivity Relationship of glycolipids in APC-NKT cells context demands more data and more compounds in order to put some light on the crucial interactions of ternary complex as well as their implication in the NKT cell activity. Up to now, the prototypical antigen αGalCer (**2**) is still being the most potent compound as well as the most tested in a wide range of disease treatments. Although this glycolipid has been deeply studied, it presents some drawbacks limiting it beyond Phase I Clinical trials:

1) αGalCer (**2**) is not able to modulate cytokine response; upon NKT cells activation with this antigen, rapid and copious amounts of cytokines are released without discrimination between T_H1 and T_H2 types.
2) This poor selectivity may reduce its efficacy when it is tested in any disease model as both cytokine types have suppressive effects against the other.
3) αGalCer (**2**) has showed such potency that unresponsiveness cell state has been detected in mice after NKT cell activation.
4) αGalCer (**2**) possesses some moieties susceptible to metabolic degradation by enzymes (glycosidic bond by glycosidases and amide bond by amidases).
5) αGalCer (**2**) has a complex synthesis, specially for alpha-glycosidic linkage.

Another mystery around CD1d-TCR complex and interaction mode is the identification of the endogenous ligand of this system. Many questions arise: Is this ligand as potent as αGalCer (**2**)? Or, on the contrary, is it less potent but with more sustained activity? All together, αGalCer derivatives research is a fruitful and challenging field that caught the attention of many scientific groups either chemist or biologists.

As it was mentioned in the Introduction, our group had previously worked on amiocyclitol derivatives as NKT activators with promising results and gathering a strong background in the field of NKT cells and antigens. In parallel, Dr. Anna Alcaide carried out her PhD thesis on sphingolipid derivatives as inhibitors of sphingolipid metabolism enzymes such as mammalian enzyme Glucolsyceramide Synthase and Sphingomyelin Synthase, and fungal enzymes Inosytolphosphosyl ceramide Synthase[1]. Despite this different biological context, the close similarity of sphingolipid backbone of her compounds with αGalCer (**2**) was not overlooked (**Figure 2.1**).

2. GENERAL OBJECTIVES

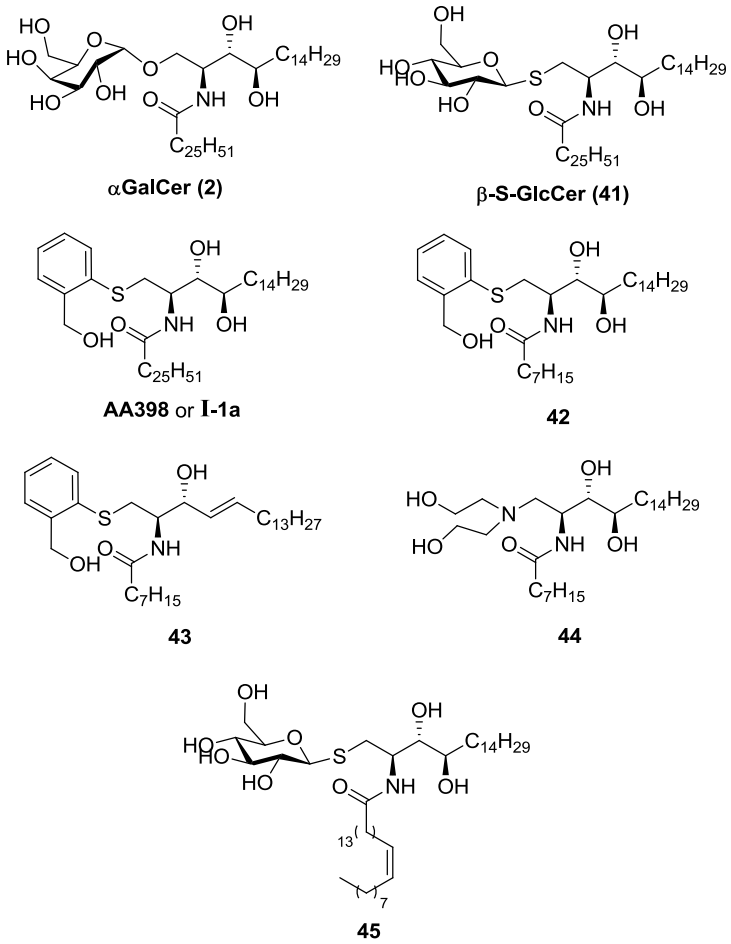

Figure 2.1: some examples of Alcaide's compounds tested as NKT cells activators

Analyzing the structural features in common of Alcaide's compounds with αGalCer (**2**), some compounds were selected and tested as NKT cells activators, finding out one interesting candidate. Among the tested compounds were some β-thiosugar-ceramides however they were not the best tested compounds. Surprisingly, it was a hydroxymethylphenylthio-ceramide derivative the most potent tested compound (**Figure 2.2**). It presented among 15% of cytokine production referred to αGalCer *in vitro* and promising activity *in vivo* (data not published). This compound presents same lipid-backbone as αGalCer (**2**) with an aromatic head instead of sugar or sugar-mimetic moiety. This type of derivatives was structurally innovative, conferring to this compound an extremely high interest as a new feasible family of NKT stimulators with a challenging structure-activity relationship to be explored.

2. GENERAL OBJECTIVES

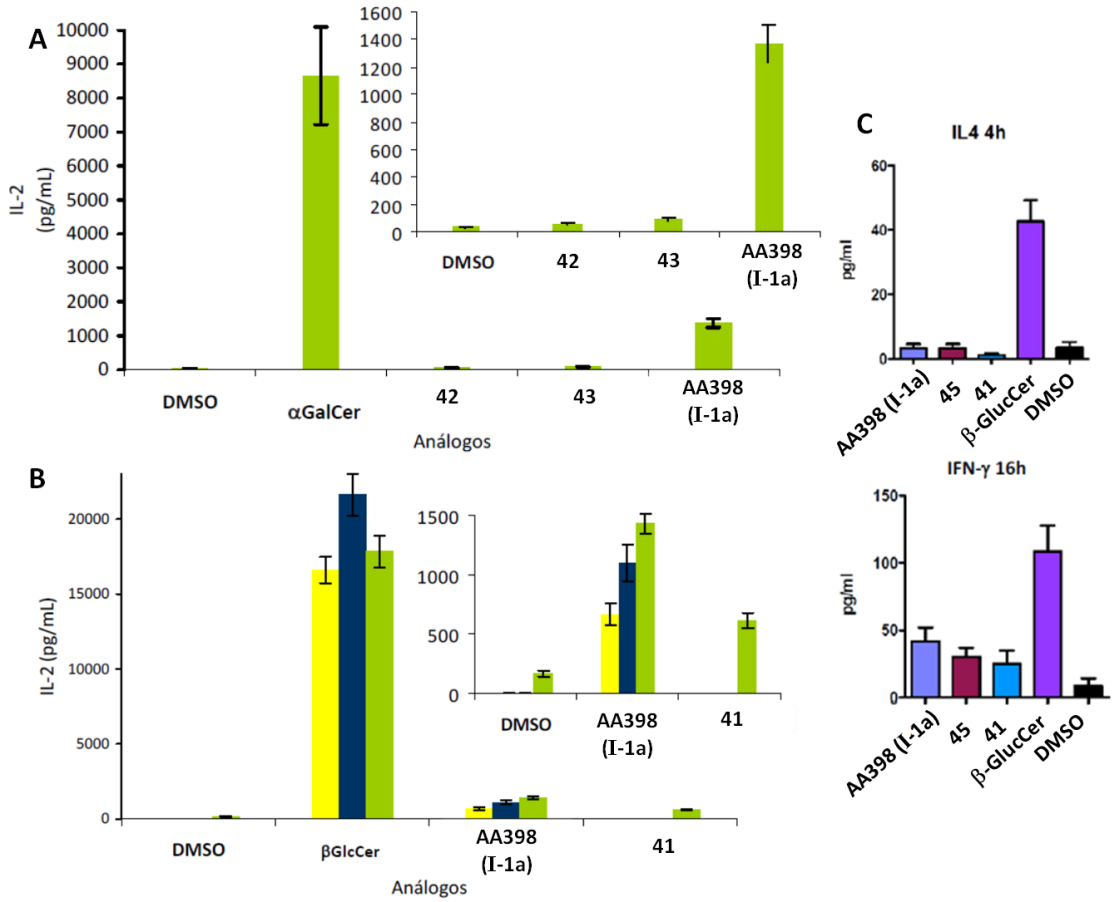

Figure 2.1: A) and B) represents in vitro activity; C) represents cytokine production in vivo (pictures taken from Dr. Alcaide's Thesis).

Bearing in mind all considerations mentioned above, the **main general goal** of this thesis is:

> **The design, synthesis and biological evaluation of new aromatic-ceramide derivatives mimicking alpha-galactosylceramide as NKT cell activators.**

Taking into account the main objective, this PhD thesis was focused on four specific objectives:

1) Design of small family of compounds based on Dr Alcaide's compound AA398. This objective will involve two specific goals:
    a) Establishing a docking model able to point promising active compounds
    b) Design of small family based on generated docking model

    For this aim, computational software will be used to carry out docking studies to generate a computational model of the proteins-antigen complex which will be used to select which compounds will be our target ones for synthetic stage.

Taking advantage of crystal structure available at PDB web site, docking studies will be carried out on real structures.

2) Synthesis of the new aromatic-ceramide families.

Incorporating aromatic groups as glycoside surrogates in ceramide scaffolds towards biological mimetics of glycolipids, has not been largely explored, so new synthetic methodology is likely needed to be developed.

3) Biological activity screening of the aromatic analogues as potential NKT cells activators either in mice and human cells in vitro.

The novel structure of this non-glycosidic-ceramide derivatives give them a challenging opportunity to become ground-breaking NKT cells activators if their activity is extended to whole family, not only to one compound.

BIBLIOGRAPHY:

1. Alcaide, A. & Llebaria, A. Aziridine ring opening for the synthesis of sphingolipid analogues: inhibitors of sphingolipid-metabolizing enzymes. *J Org Chem* **79**, 2993-3029 (2014).

3. RESULTS AND DISCUSSION

3.1. CHAPTER 1: Computational design of new aromatic-ceramide analogues of αGalCer

An initial objective of this thesis was to propose a new family of aromatic-ceramide analogues of αGalCer (**2**) based on the expansion of the previously discovered analogue **I-1a**. When the present doctoral thesis started, few computational studies on the CD1d-Ag-TCR complex had been reported. Hénon et al. studied the influence of lipid chains in Ag-CD1d interactions and its impact on sugar ring orientation by short (10 ns) Molecular Dynamics (MD) simulation[1]; αGalCer (**2**) and three other ligands were analyzed, concluding that ring orientation results from a set of H-Bond mediated by hydroxyls 2' and 3' of galactose ring with Asp153 of CD1d as well as interaction with Thr156 by NH of amide group. Another study from Nadas et al. reported the impact of sugar ring modifications on the ternary complex CD1d-Ag-TCR interactions[2]. In this study, a combination of MD and molecular docking were carried out on a library of 49 ligands. The authors conclude that modifications on hydroxyl 4' were more acceptable than those ones on hydroxyls 2' and 3' of sugar ring. Finally, a third publication from Laurent et al. presented longer (240 ns) MD simulation of αGalCer (**2**) and seven other ligands exploring the relation of complex stability with T_H2 polarizing response. Authors were able to correlate a set of T_H2 biased antigens with a destabilizing effect of sugar conformation on H-Bond network[3]. With these antecedents it was proposed to study a virtual library using molecular docking and MD tools which could help to identify potentially active ligands which would be more attractive to be synthesized as promising NKT cell modulators.

It is worthy to describe the general structure of the CD1d-Ag-TCR ternary system. CD1d is the presenting protein composed by 3 structural domains (α1-α3 chains) that generate two hydrophobic pockets, A' and F' (C' in human proteins) in which the lipid tails of the glycolipid fall in. The TCR is composed by two chains, α and β, however only the α chain interacts with the ligand while the β one interacts exclusively with CD1d. Crystal structures released allowed a better understanding of how αGalCer (**2**) or its analogues interact with both proteins and point to the idea of some minimal features required on glycolipid antigens (**Figure 3.1**). In this sense, the structure of CD1d-αGalCer-TCR ternary complex suggested that: (1) lipid chains of a minimum length were required to be recognized by CD1d, (2) the amide moiety of ceramide participates into a hydrogen-bond (H-Bonds, from now on) net known as OTAN[1], (3) phytosphingosine hydroxyls were needed to maintain both interactions with Asp80 of CD1d, (4) the alpha-configuration of the glycosidic bond was strongly preferred to the beta one, (5) hydroxyls 2' and 3' of the galactose ring interacts with Asp153 of CD1d while only the 2' makes contact with Gly96 of TCR and (6) 4' should be preferentially in axial configuration to be able to interact with Asn30 of TCR.

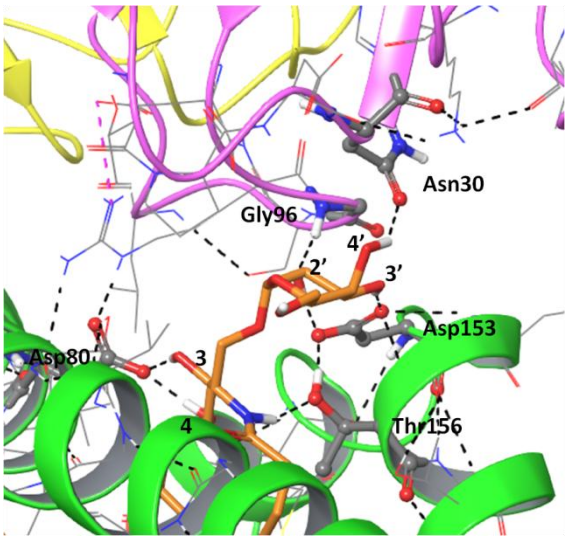

Figure 3.1: *Crystal structure of the CD1d- αGalCer-TCR complex from mouse (PDB code 3HE6). H-Bond interactions of αGalCer (**2**) with mCD1d (green ribbons) and mTCR (pink and yellow ribbons) are colored in black dashed lines. See **Table 3.1** for interactions list.*

Some CD1d-Ag-TCR crystal structures with αGalCer (**2**) analogues had been reported. Among all them two structures were of our interest: one of our reported aminocyclitol (HS44, **38**)[4] and NU-α-GalCer (**34**)[5] for its aromatic substituent at 6" position (**Figure 3.2**). Superimposing all three ligands directly to its crystal structure it could be appreciated they had similar binding mode; lipid tails adopted nearly the same disposition into hydrophobic cavities (**Figure 3.2**) while the ring were disposed in a similar manner in all three cases. Hydroxyls 2' and 3' of all three ligands interact with same residues ($Asp153_{CD1d}$) **(Figure 3.3).** Two main differences of these two derivatives: HS44 (**38**) had equatorial hydroxyl 4' and NU-α-GalCer (**34**) incorporates a naphthylureido substituent at position 6", which seemed to occupy some cavity of CD1d.

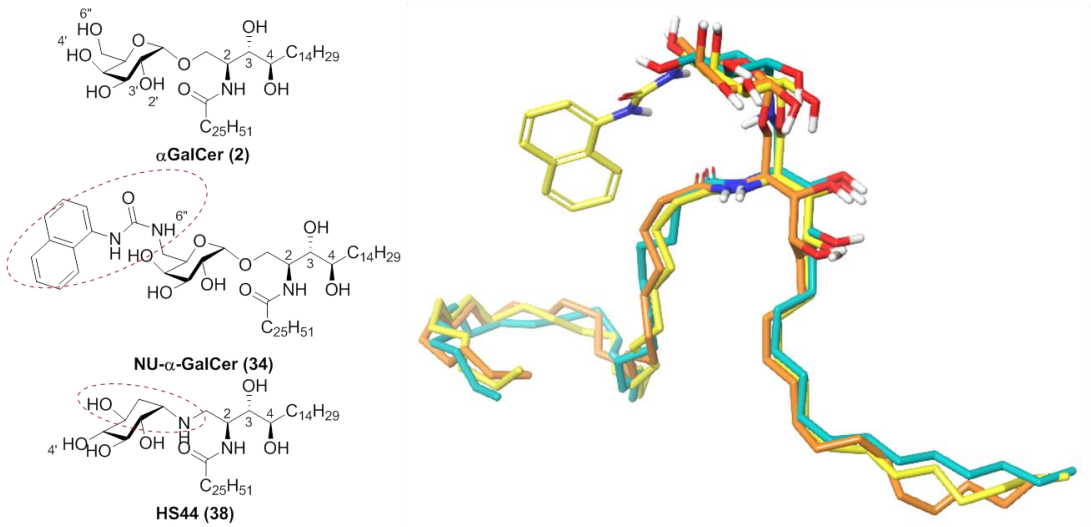

Figure 3.2: *Chemical structure and structures superimposing of αGalCer (**2**) (in orange, from 3HE6), NU-α-GalCer (**34**) (in yellow, from 3QUZ) and HS44 (**38**) (in blue, from 3RTQ)*

Comparisons of the ligand-protein interactions of the three antigens confirmed that both analogues mimic the H-Bond network interactions of αGalCer (**2**), what could explain the strong activity of both compounds (**Figure 3.3**). As it was mentioned in introduction, **34** was reported as a strong T_H1 polarizing antigen *in vitro*[5] and authors pointed to a favorable stabilizing interaction of the naphthyl group inside a CD1d grove as a possible reason. On the other hand **38** was initially reported as a T_H2 polarizing antigen after *in vitro*[6] evaluation however deeper studies *in vivo* together with its crystal structure evaluation point to a strong T_H1 polarizing compound with the same binding mode as αGalCer (**2**)[4].

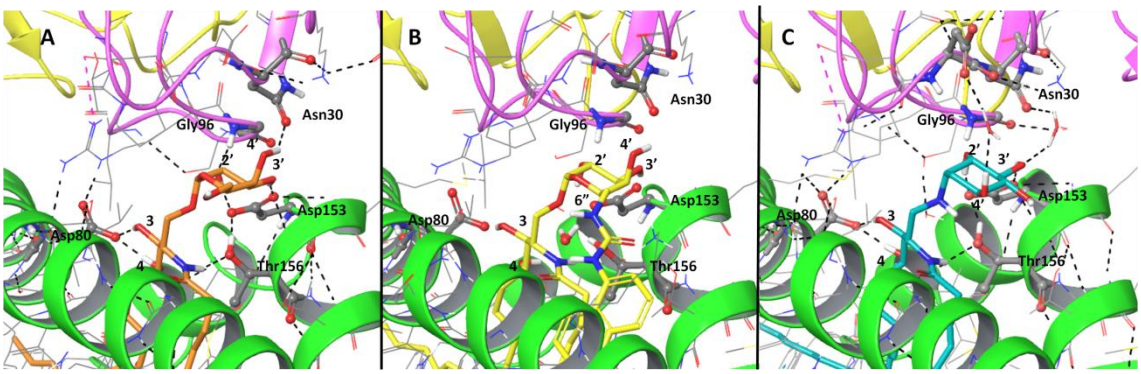

Figure 3.3: *crystal structures of αGalCer (**2**) (in orange, from 3HE6), Nu-α-GalCer (**34**) (in yellow, from 3QUZ) and HS44 (**38**) (in blue, from 3RTQ)*

Despite those minimum ligand structural features required for the activity, the complex diversity of the biological results reported in the literature made it difficult to establish a real SAR or to build a pharmacophore purely based on the glycolipid structure. As a brief summary of what was exposed in Introduction; reported results for αGalCer (**2**) were not always comparable; how a compound was considered T_H1 or T_H2 polarizing was not always explained under same criteria. Moreover, the same compound could be reported to have different response profiles or even showed opposite effects when tested with mice or human cells. All together, the generation of more biological data, with consistent and equivalent results among groups and with higher reproducibility is necessary for a better understanding of how these ligands could modulate NKT cell response and how their interaction with proteins affects cytokine response. Weaknesses in the basic knowledge of NKT cell biology also contribute to the difficulties in assay standardization.

Despite those diverse results, some Ag-proteins interactions were considered essential for activity retention based in the glycolipid structure-activity relationships; it was the case of $Asp80_{CD1d}$, $Thr156_{CD1d}$, $Asp153_{CD1d}$, $Gly96_{\alpha TCR}$ and $Asn30_{\alpha TCR}$ (**Figure 3.1** and **Table 3.1**). This hypothesis was based on reported glycosidic or glyco-mimetic ligands and their activities (**Figure 3.4**); hence, the 2'-desoxy derivative 2'-H-αGalCer (**23**) was totally inactive while the sulfate ester 3'-Sulfatide-αGalCer (**27**)[7,8] was notably less active than αGalCer (**2**) but slightly polarizing towards T_H1. Removal of 4' hydroxyl in 4'-H-αGalCer (**29**)[9] strongly decreased activity with T_H2 bias and introduction of an

aromatic *O*-benzoate substituent at this position reinforce NKT cell activation although with controversial polarizing effects[10].

Protein	AA	Interacting part	αGalCer (2)	Relevance
CD1d	Asp80	Side chain	3-OH	At least one
CD1d	Asp80	Side chain	4-OH	
CD1d	Thr156	Side chain	NH amide	Essential
CD1d	Asp153	Side chain	2'-OH	Essential
CD1d	Asp153	Side chain	3'-OH	Strong positive impact
αTCR	Gly96	NH	2'-OH	Essential
αTCR	Asn30	Side chain	4'-OH	Modifiable

Table 3.1: *key Ag-protein interactions based on αGalCer (**2**) structure*

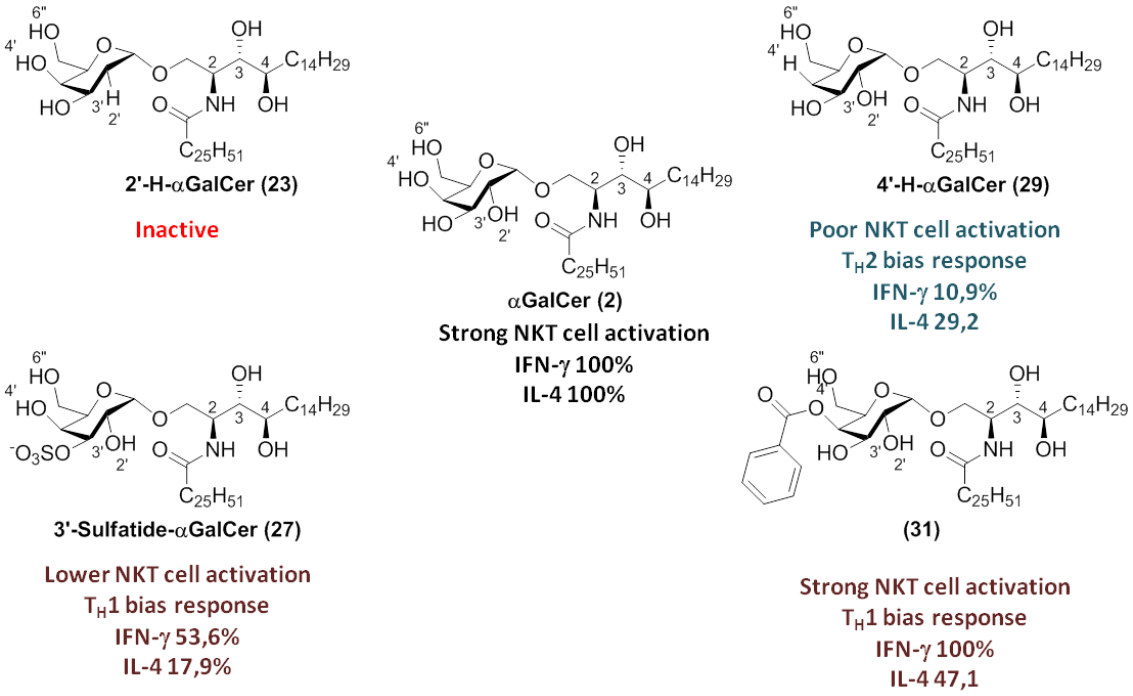

Figure 3.4: *Representative modification on sugar ring and their influence on activity response in terms of cytokine production relative to αGalCer (**2**)*

Another widely accepted structure-activity relationship is the stability of ternary complex and its implication in TFN-γ versus IL-4 production. As production of IL-4 is almost immediate after compound stimulation while production of IFN-γ takes longer, those ligands able to stabilize ternary complex and therefore having a more sustainable interaction in time are assumed to be T_H1 polarizing compounds. On the contrary, those ligands with less stable complex interaction would induce a T_H2 biased response.

As it was briefly presented in the preceding section, our *hit* compound **I-1a** showed weak but promising activity as NKT cell activator (around 15% compared to **2**) with T_H1 biased response. Bearing in mind which interactions were considered essential and comparing referenced ligands with our *hit* compound **I-1a** (**Figure 3.5**), some initial

ideas emerged: On one hand, our compound shares the same ceramide skeleton as **2** so similar binding affinity to CD1d could be expected; on the other hand, its new aromatic-head group has only one polar substituent (hydroxymethyl group) which could not establish as many interactions as αGalCer (**2**). Thus, the lower activity of **I-1a** seemed in line with the impossibility to satisfy at the same time similar interactions of those established by the 2' and 3' hydroxyl of αGalCer (**2**) which were considered essential for the activity.

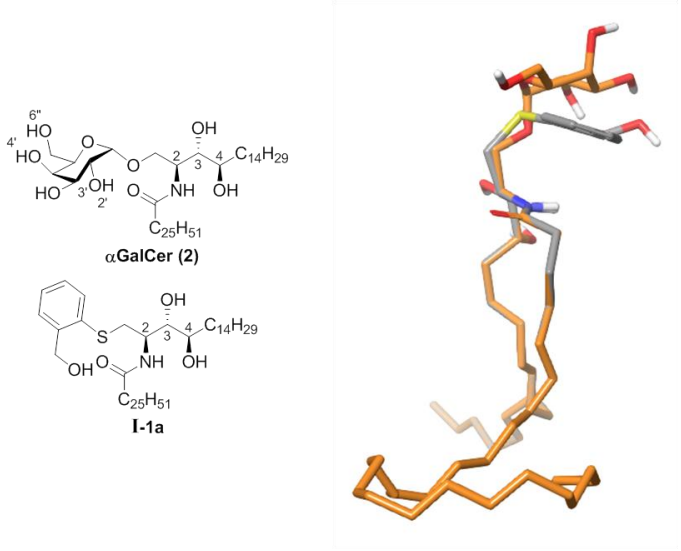

Figure 3.5: *Comparison of* αGalCer (**2**) *(orange) and our "hit" compound (grey) (on the left) and initial 3D model built based on* ***2*** *skeleton (on the right).*

All together, seeking compounds able to mimic the H-Bond interactions mentioned above would allow us to discriminate which could be the better target compounds to be synthesized. Additionally, those compounds with potentially stabilizing interactions could be also interesting as T_H1 polarizing candidates (that could be ligands with new interactions or showing theoretically good affinity), in accordance to the residence time in the ternary complex.

3.1.1. Virtual library selection

Bearing in mind all the above considerations, our starting idea was to build a virtual library of ligands that would keep the same phytoceramide skeleton as αGalCer (**2**) and varying the aromatic moiety. Thus, our ligand design was based on the innovative structure of previously discovered analogue **I-1a**, with four main structural elements of diversity (**Figure 3.6**): 1) linking atom (X); 2) ring type (Y); 3) *ortho* substituent modification (R) and 4) introduction of new substituents (R'). Each element could have its particular implication either in binding contacts or compound orientation.

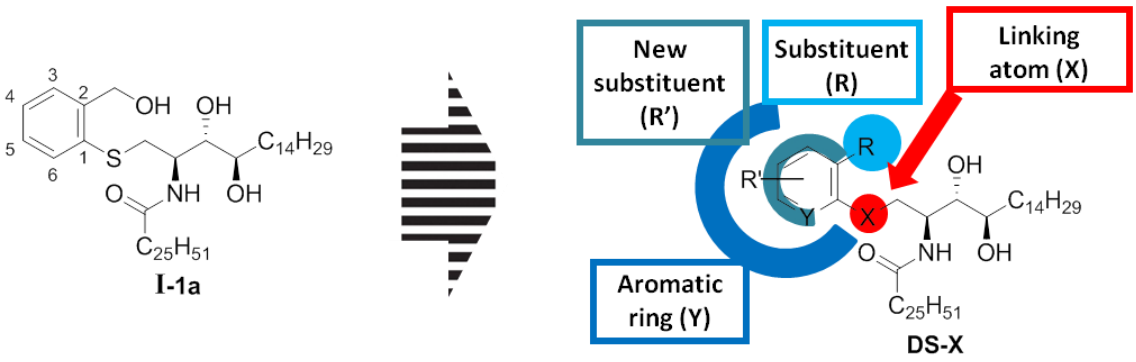

Figure 3.6: *Structural points that could accept modification*

1) Linking atom (X): substitution of sulfur by oxygen would provide a variety of commercially available precursors and it is a common modification in drug design as sulfur and oxygen are considered isosteres. Another consideration was the different stability of glycolipids versus thio-glycolipids, being the second ones more stable due to resistance against hydrolases; in this sense, exploring phenolic ether-like compounds compared with phenylthioether-like could result in different activities, as it occurs with αGalCer (**2**) and α-*S*-GalCer (**22**). In addition, thioethers are metabolically or chemically oxidizable, and can lead to sulfoxides and sulfones.
2) Ring type (Y): replacement of the phenyl ring by its bioisostere pyridine could modify some physical properties such as solubility, and the introduction of a heteroatom could allow new H-Bond interactions with the proteins.
3) Substituent modification (R): It is known that there are a minimum number of H-Bonds required for the activity. As our starting compound has only one hydroxyl on the aromatic moiety, the replacement by a more functionalized group, like an amide group, appears as a good approximation to increase H-bonding capacity of the ligands.
4) Introduction of additional substituents on the aromatic ring (R'): This was foreseen as a way to increase the H-bonding capacity in order to enhance binding to CD1d (as previously exploited in sugar compounds like Nu-α-GalCer (**34**) or similar) and also achieve new interactions with TCR. In this sense, introduction of second aromatic ring could play a similar role as the naphthyl group of **34**, or introduction of aminoacid-like moieties could expand H-Bond capacity with the TCR recognition protein. To this purpose, functionalization at position 4 was selected as candidate to explore new optimal interactions.

Taking into account the above considerations, a virtual collection of about 50 ligands was proposed. **Figure 3.7** shows some of the selected ligands (*see ANNEX 1 for full list*).

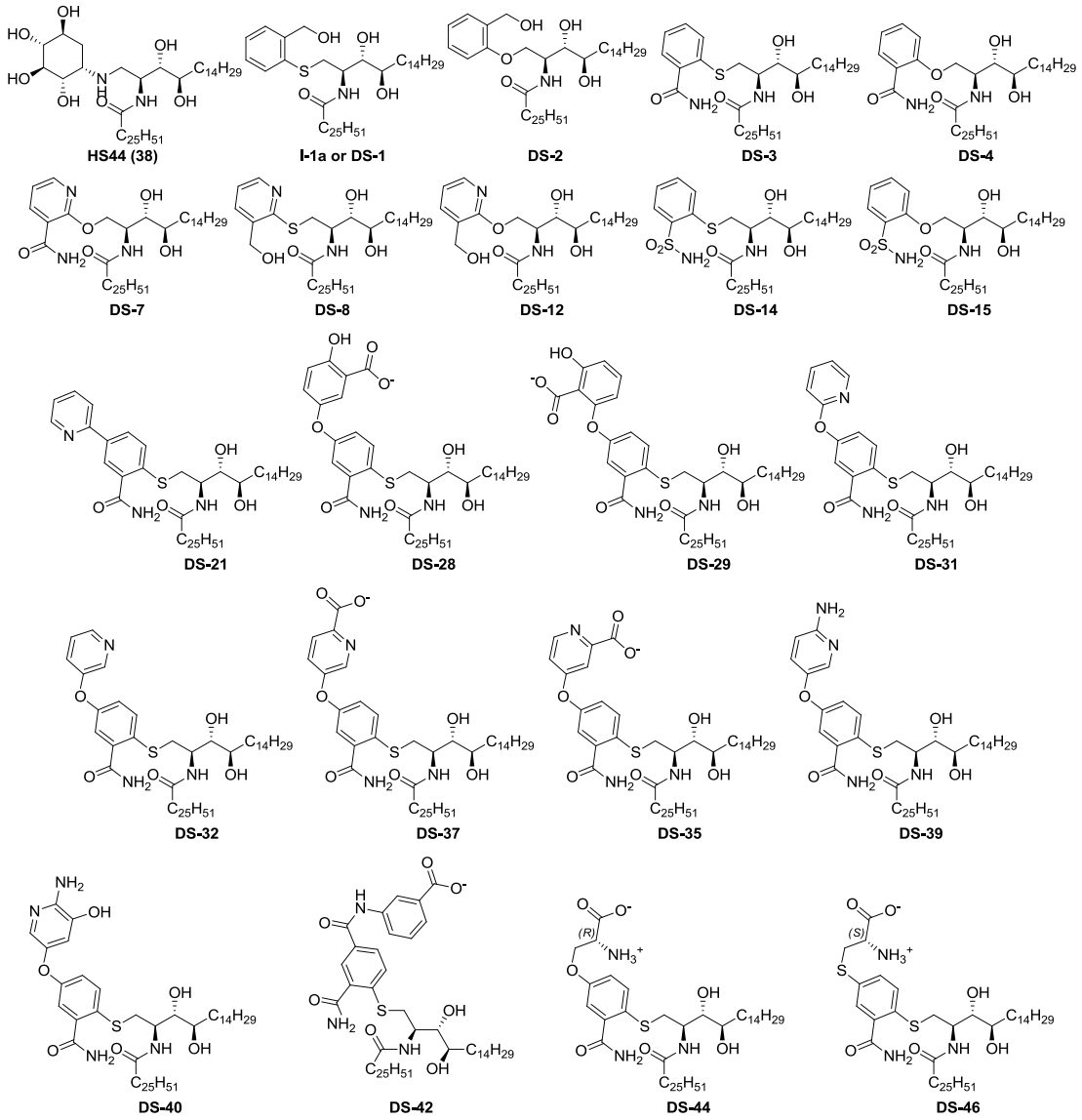

Figure 3.7: *Some examples of ligands selected for computational screening*

3.1.2. Docking screening of selected ligands

At the beginning of the present doctoral thesis, a collaborative work resulted in a published crystal structure of one of our aminocyclitols (mCD1d-HS44-mTCR, PDB entry 3RTQ[4]) so this structure was taken to set up our studies (from now on, all amino acid numbering will refer exclusively to murine sequence unless otherwise specified). Therefore, the PDB protein structure 3RTQ was considered as rigid receptor and HS44 (**38**) was used as positive control for our docking studies. The program Glide[11] from the Schrödinger Suite 2014[12] was used to carry out the docking experiments.

Considering all exposed at the beginning of this chapter, the docking studies were started seeking for ligands capable to establish at least some of the essential interactions. Initial computational jobs were launched considering full ligand, however, these jobs failed due to a too large number of degrees of freedom in the long lipid

chains. Therefore, truncate version of ligands were used for docking, assuming that our ligands would have similar binding mode as αGalCer (**2**) as they share same ceramide skeleton To this end, virtual ligands were truncated up to only 4 carbons at acyl chain and 7 carbons on phytosphingosine (shown in **Figure 3.8**) in order to reduced CPU-time-demand in computational studies.

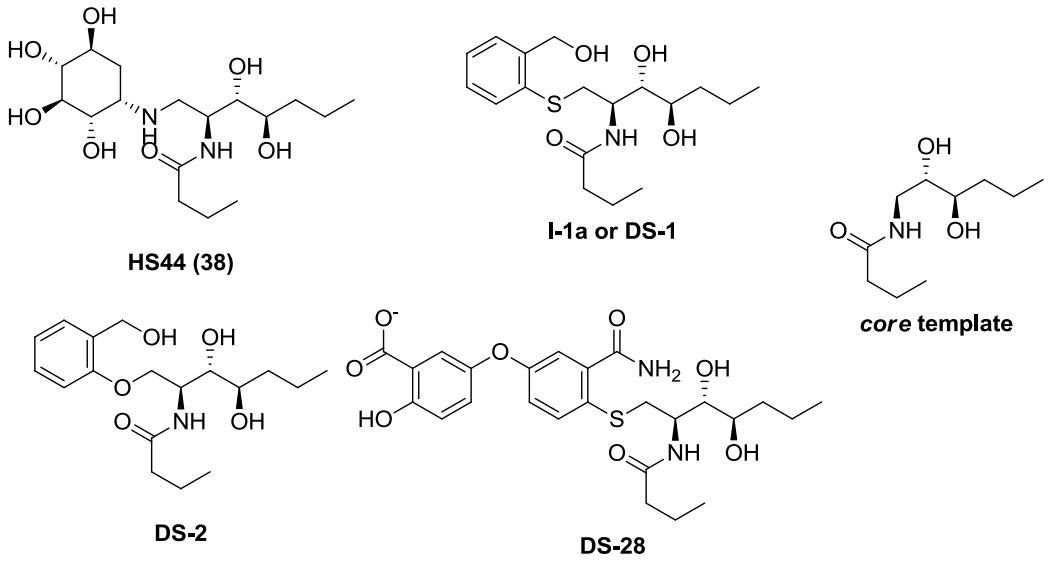

Figure 3.8: *Example of truncated ligands used for docking studies and core template of docking studies*

This approximation required imposing positional restrains to the remaining atoms of ceramide moiety to avoid them to fall into CD1d cavities or out of the binding site, to that purpose ceramide skeleton was "fixed" as template (*core* template) and free flexibility to the aromatic moiety was allowed. After two initial jobs and different final poses, it was clear that final results depend on initial pose. In order to improve sampling, a set of 10 iterative jobs was planned (each job starting from the final pose obtained in the immediately preceding calculation).

Analyzing the obtained results, our positive control HS44 (**38**) showed consistent results both in docking scores and poses, which maintained H-bond interactions with $Asp153_{CD1d}$ and $Gly96_{\alpha TCR}$, in good agreement with the bound ligand conformation observed in the crystal structure. In general, our library reached similar punctuation in each job (around ±0,5 Kcal/mol from media) what made not possible to differentiate any results based only on scoring. In light of this, a second criteria was taken in consideration: the ligand ability to establish or not some of the assumed essential interactions. Our *hit* compound **DS-1** (or **I-1a**) showed promising poses in which some of essential H-Bonds were satisfied (**Figure 3.9**) however some other completely different poses were obtained in which the hydroxymethyl group was orientated to the opposite site and did not show interaction with $Asp153_{CD1d}$, $Gly96_{\alpha TCR}$ or $Asn30_{\alpha TCR}$.

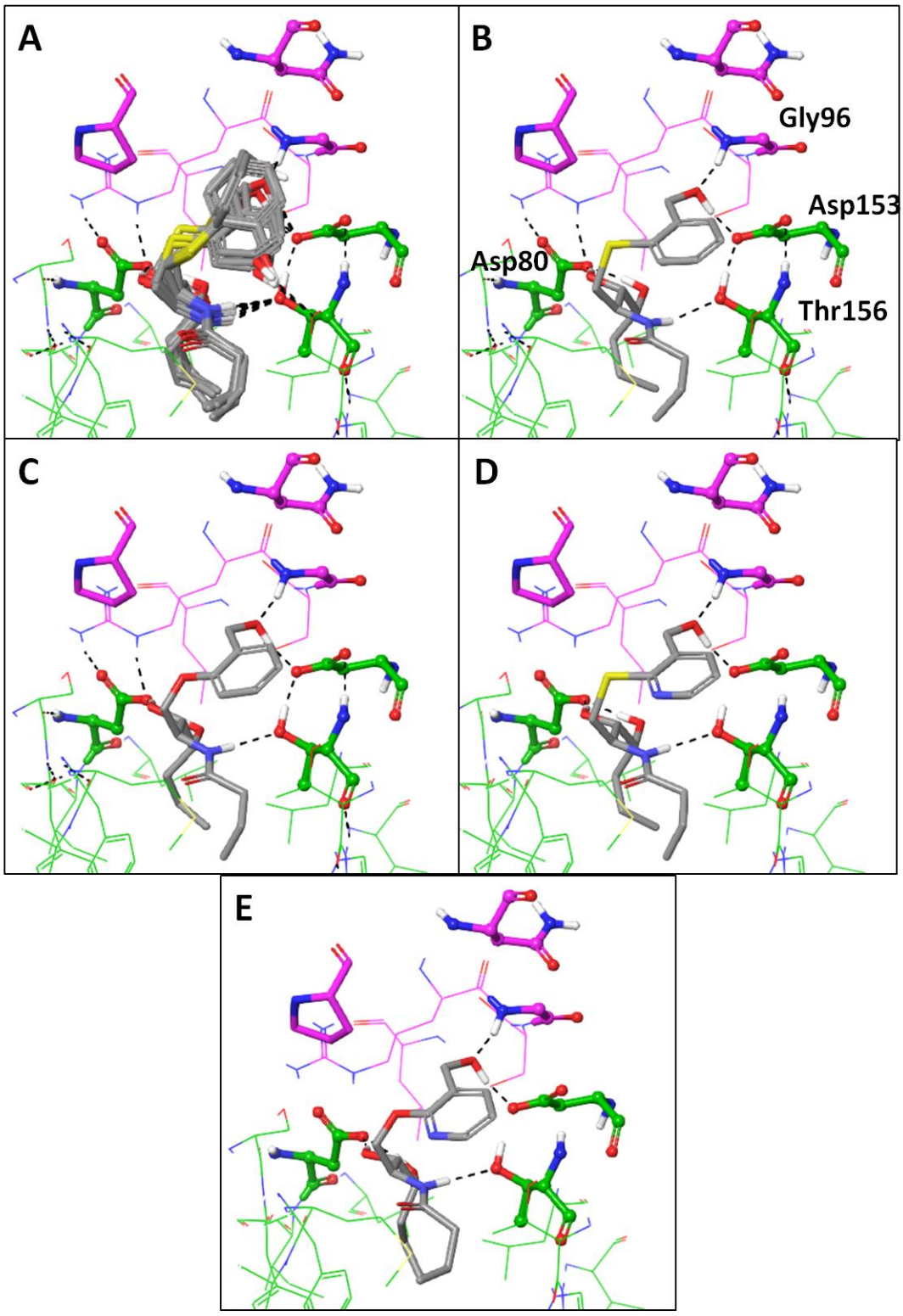

Figure 3.9: *A) Superposition of 10 poses obtained after iterative docking jobs. B)* ***DS-1*** *(or* ***I-1a****), C)* ***DS-2****, D)* ***DS-8*** *and E)* ***DS-12*** *are representative images of the best poses. CD1d carbons are colored in green while TCR α-chain carbons are colored in pink. H-Bond interactions are colored in black dashed lines.*

Similar results were obtained when comparing ligands with the same 2-hydroxymethyl substituent but having different linking atom (sulfur or oxygen) or different ring (phenyl or pyridine ring); comparable scores and similar interactions with $Asp153_{CD1d}$

and $Gly96_{\alpha TCR}$ were obtained indicative of potentially similar biological profiles (**Figure 3.9**).

On the other hand, replacement of hydroxymethyl group by and amide yield compounds that were less likely to maintain the H-Bond interactions with $Asp153_{CD1d}$, only the sulfur linked **DS-3** leaded to some poses displaying interactions with $Asp153_{CD1d}$ and $Gly96_{\alpha TCR}$. Amides **DS-4** (with oxygen as X) and **DS-7** (pyridine ring with N in position 6 and oxygen as X) apparently could only keep the interacted with $Gly96_{\alpha TCR}$; a new interaction was observed with $Asp94_{\alpha TCR}$ which might also contribute to raise NKT cell interaction however this interaction had never been described in any reported ligand (**Figure 3.10**). Comparing these results with ligands having a hydroxymethyl group revealed some different behavior; while the hydroxymethyl substituted compounds showed similar poses despite of minimal structural changes, the interactions were not conserved in the amide derivatives pointing to more pronounced effects of ring heteroatoms and C-X bond distances in this group (*see ANNEX 2 for tables and images*).

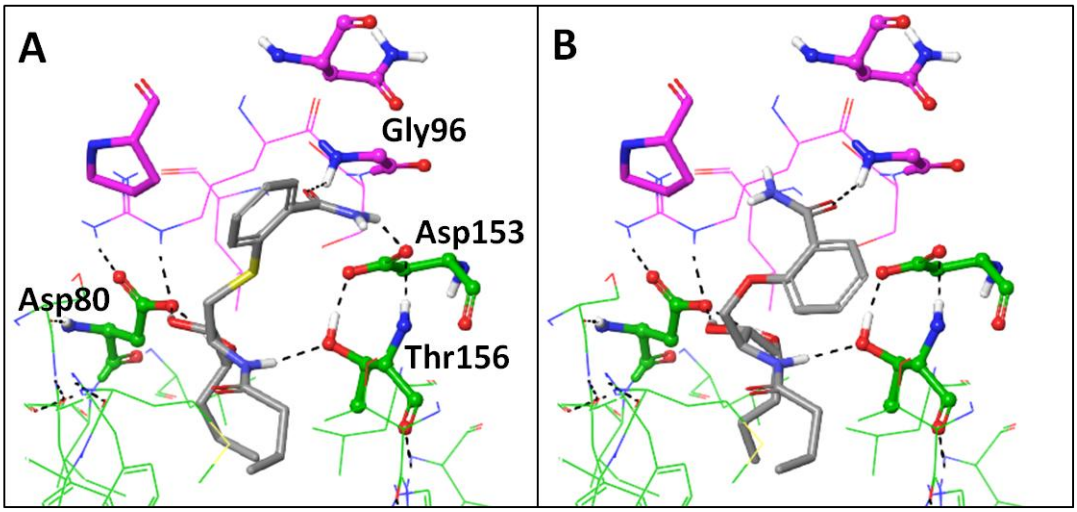

Figure 3.10: *Representative image of best pose of A)* ***DS-3*** *and B)* ***DS-4****. CD1d carbons are colored in green while TCR α-chain carbons are colored in pink. H-Bond interactions are colored in black dashed lines.*

Another studied substituent was a sulfonamide with sulfur (**DS-14**) or oxygen (**DS-15**) as linking atoms X (**Figure 3.11**). Ligand **DS-14** turned out to be one of the better scored ligand and, more important, being able to interact simultaneously with $Asp153_{CD1d}$, $Gly96_{\alpha TCR}$ and $Asn30_{\alpha TCR}$, being the ligand which showed a higher number of interactions under docking screening. On the contrary, **DS-15** did not interact with $Asn30_{\alpha TCR}$ and received a significantly lower score (*ANNEX 2*). Even so, **DS-15** could be also considered a good candidate having a similar scoring to **DS-1**. This differences could be attributed to different lengths of the C-X bonds (being X the linking atom: ~1,8 Å for C-S, 1,4-1,5 Å for C-N and 1,4-1,45 Å for C-O). However, these effects observed both in amide and sulfonamide containing ligands might be of little

significance considering that during the docking process the protein is considered rigid, making impossible any adaptation of the protein to the presence of the ligand, which could reduce the differences observed.

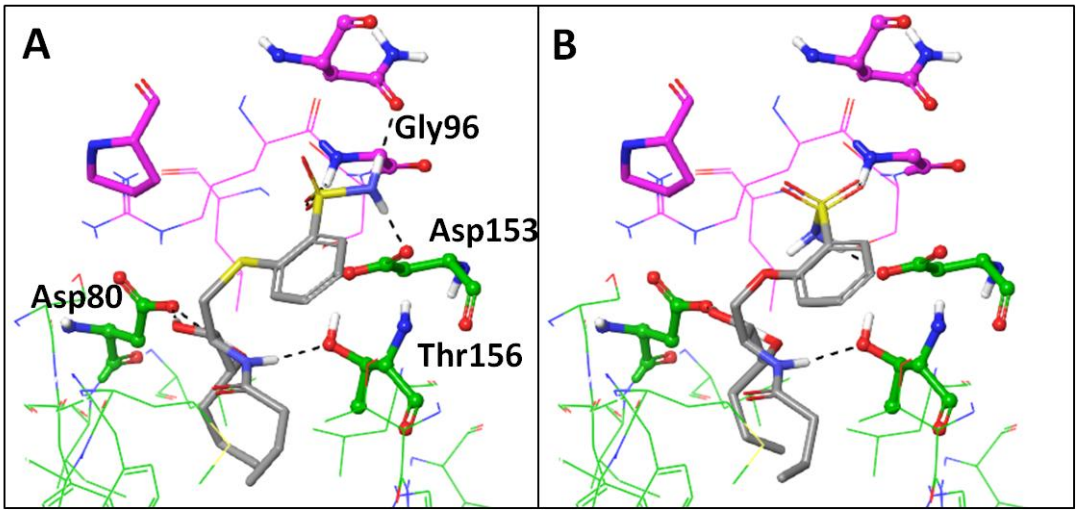

Figure 3.11: *Representative image of best pose of A)* ***DS-14*** *and B)* ***DS-15****. CD1d carbons are colored in green while TCR α-chain carbons are colored in pink. H-Bond interactions are colored in black dashed lines.*

In general, disubstituted aromatic ligands seem to show some ability to interact with one or more residues of the so-called essential, suggesting a stronger binding potential for those that have a more functionalized substituent in the aromatic ring and which have sulfur as linking atom.

The addition of an extra substitution in ligands was proposed to reach a similar number of interactions to αGalCer (**2**) and other reported glycolipid derivatives. In this sense, Nu-α-GalCer (**34**) and its binding mode was taken as a source of inspiration. The new ligands having two aryl groups were designed looking for stabilizing distal interactions with CD1d in a similar way as Nu-α-GalCer (**34**). Introduction of 4-phenyl or 4-pyridinyl substituent in the aromatic ring of **DS-3** (for example **DS-21**) did not change much the docking scores however interactions with Asp153 and Gly96 were less frequently reached. Phenyl or pyridine substituent did not bind in a similar manner as the naphtyl moiety of **34**, as could be expected due to conformational restrictions of these ligands. (*See* ***DS-21*** *in ANNEX 2 as representative example)*.

When a bridging oxygen atom is added as spacer between the aromatic groups, more flexible ligands were obtained and interactions with $Asp153_{CD1d}$, $Gly96_{\alpha TCR}$ or $Asn30_{\alpha TCR}$ were partially restored compared to bis-aryl derivatives. Some of these diphenyl ether ligands retained the ability of amide group to interact simultaneously with $Asp153_{CD1d}$ and $Gly96_{\alpha TCR}$ while new interactions with αTCR were reached (for example **DS-28**, **DS-31** or **DS-37** in **Figure 3.12**); as it was the case of H-Bonds of $Asp29_{\alpha TCR}$ with ether oxygen and of $Lys68_{\alpha TCR}$ and $Lys71_{\alpha TCR}$ as well as salt bridge interactions when ligands

had carboxylic acids in the second ring. On the other hand, a new interaction which was previously reported as positive was an H-Bond with $Gln52_{\alpha TCR}$[13] and it was reached by some of these ligands in some of the obtained poses. In general, the phenyl ether analogues were able to establish some of the defined essential interactions although showed some fluctuation between them; furthermore new not described interactions were reached, but their real impact in biology was uncertain (**Figure 3.12** and **Table 3.2**).

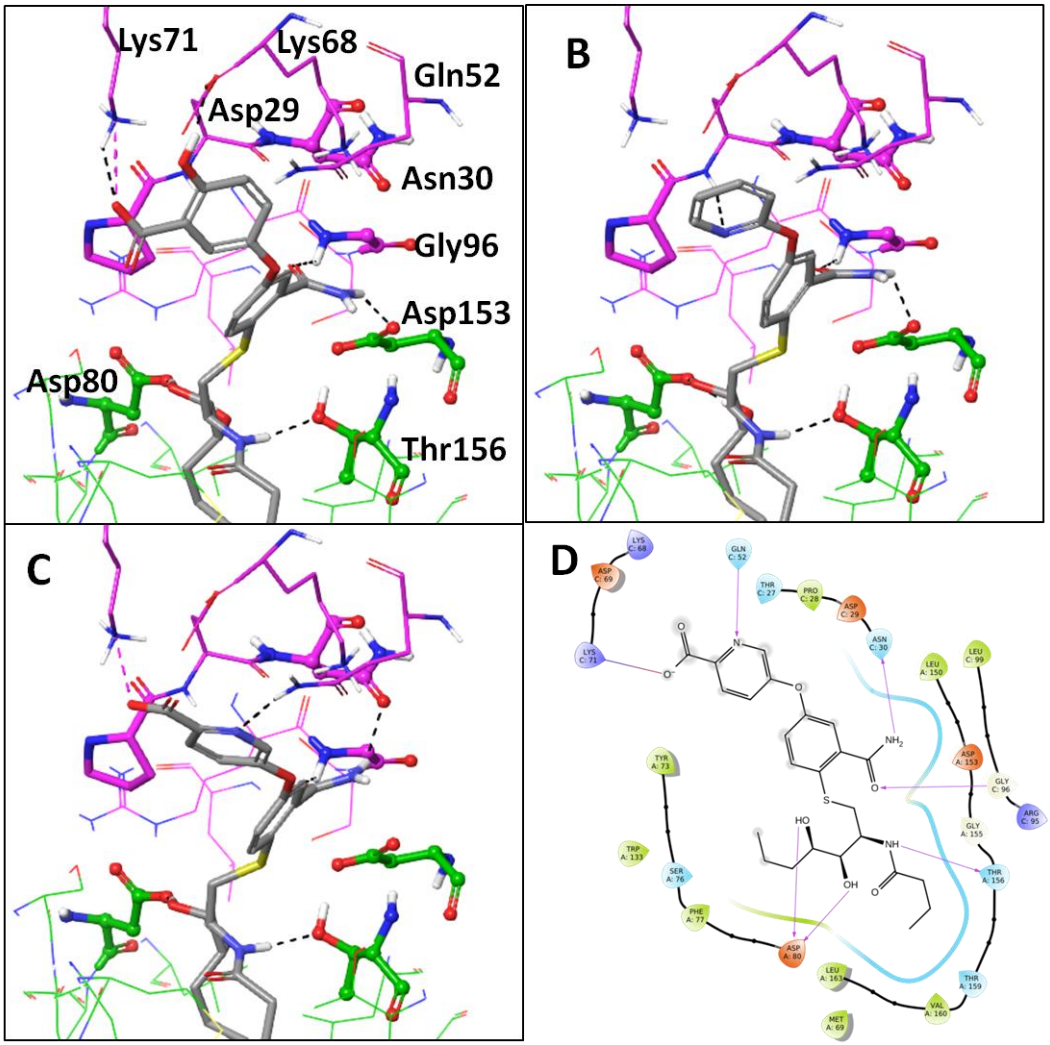

Figure 3.12: *A)* ***DS-28****, B)* ***DS-31*** *and C)* ***DS-37*** *show best docking posed for representative ligands. D) shows 2D diagram of* ***DS-37*** *interactions*

	Interactions
DS-28	$Asp153_{CD1d}$, $Gly96_{\alpha TCR}$, $Lys68_{\alpha TCR}$, $Lys71_{\alpha TCR}$ salt
DS-31	$Asp153_{CD1d}$, $Gly96_{\alpha TCR}$, $Asp29_{\alpha TCR}$
DS-37	$Gly96_{\alpha TCR}$, $Asn30_{\alpha TCR}$, $Gln52_{\alpha TCR}$, $Lys71_{\alpha TCR}$ salt

Table 3.2: *Summary of interactions reached by phenyl ether analogues*

A similar effect was observed when a more flexible aminoacid moiety, such as Ser (**DS-44**) or Cys (**DS-46**), was introduced instead of the second aromatic ring (*ANNEX 2*). However, taking in consideration the larger heterogeneity of binding poses obtained

for each of these more complex ligands, it was difficult to anticipate what could be the effect on the stability of the CD1d-Ag-TCR complex and their biological activity.

To summarize all the results mentioned until now, our *hit* compound **DS-1** showed a binding mode able to interact with the key residues described in αGalCer (**2**) SAR studies. Replacement of the sulfur atom by oxygen or the phenyl by pyridine in **DS-1** did not predict a big impact in scores or binding modes. The replacement of **DS-1** hydroxymethyl by a carboxamide group aiming to improve H-Bonding properties of our ligands resulted in ambiguous results; while the thioether **DS-3** showed a promising binding mode, the analogues with oxygen or pyridine were devoid of the positive interactions. When an extra aryl functionalization is added to **DS-3** in position 4, the H-Bond pattern of the amide group was less frequently achieved, pointing to somehow destabilizing effects of second substituent. When *O*-phenyl ether moieties where incorporated at position 4 of phenyl ring, some new interactions were reached without an important decrease of the key H bonds; however how important are the individual protein-ligand interactions in modulating NKT cell response should be experimentally corroborated.

3.1.3. Flexible docking studies of 10 ligands

Until now, all docking experiments were carried out with rigid receptors and sampling only conformations of the aromatic head of the ligand. Taking into account the structural differences between HS44 (**38**) and the compounds of our virtual library added to limitations of disregarding any conformational change for the protein in response to the binding of the ligands, what is known as Induced Fit, it was raised the question if some missing interactions were simply due to the lack of conformational adjustment of the protein moiety. To solve this problem, there are computational docking methodologies that can account for some degree of receptor flexibility. The Induced Fit Docking (IFD) protocol implemented in the Schrödinger Suite[14] was used; considering the higher computational cost of IFD, this protocol was only applied to a subset of 10 compounds of our virtual library.

Several considerations were taken for compound selection: range of docking scores, diversity of binding modes and structural diversity (see the list in **Table 3.3**).

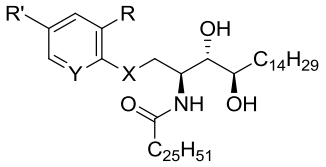

	X	Y	R	R'
I-1a or DS-1	S	CH	CH_2OH	-
DS-3	S	CH	$CONH_2$	-
DS-14	S	CH	SO_2NH_2	-
DS-15	O	CH	SO_2NH_2	
DS-21	S	CH	$CONH_2$	2Pyr
DS-28	S	CH	$CONH_2$	O-[(3-COO^-,4-OH)-Ph]
DS-29	S	CH	$CONH_2$	O-[(2-COO^-,3-OH)-Ph]
DS-32	S	CH	$CONH_2$	O-3Pyr
DS-39	S	CH	$CONH_2$	O-[(4 -NH_2)-3Pyr]
DS-46	S	CH	$CONH_2$	S-(S)Cys

Table 3.3: *List of ligands selected for Induced Fit docking studies (see also* ***Figure 3.6*** *for drawn structures)*

All 10 ligands were launched under same conditions, starting from the best initial poses or at least those ones considered more optimal to satisfy H-Bond interactions reported as essential ($Asp80_{CD1d}$, $Thr156_{CD1d}$, $Asp153_{CD1d}$, $Asn30_{\alpha TCR}$, and $Gly96_{\alpha TCR}$). Again, the ceramide skeleton was considered as core template to orientate ligands in an appropriate mode and aromatic ring was left without restrictions. The residues with atoms in a sphere of 5 Å around each ligand were considered flexible.

With these settings, our study ended up with 55 results for our 10 ligands. Surprisingly, one ligand (**DS-28**) did not reach any solution and among the rest only reached a few ones. Only two ligands reached 17 and 19 results (**DS-15** and **DS-29** respectively). The calculations outcomes were rather unexpected since the best docking candidate (**DS-14**) ended up as one of the less attractive ligands since it lost some of the essential interactions (**Table 3.4**).

	Initial score	Final score	Pose classification*	H-Bond interactions (ligand-proteins)**
I-1a or DS-1	-6,492	-5,840	b(1), r (2)	$Asp80_{CD1d}$ x2, $Thr156_{CD1d}$
DS-3	-6,259	-5,828	b(2), r(1)	$Asp80_{CD1d}$ x2, $Thr156_{CD1d}$, $Thr156_{CD1d}$
DS-14	-8,566	-7,495	b(4), r(3)	$Asp80_{CD1d}$ x2, $Thr156_{CD1d}$, $Asp153_{CD1d}$
DS-15	-5,676	-5,456	g(15), r(2), b(2)	$Asp80_{CD1d}$ x2, $Thr156_{CD1d}$, $Asp153_{CD1d}$, $Gly96_{\alpha TCR}$, $Arg95_{\alpha TCR}$
DS-21	-6,023	-5,997	g (2), r (1), b (1)	$Asp80_{CD1d}$ x2, $Thr156_{CD1d}$
DS-28	-8,327			No results
DS-29	-8,331	-6,812	g(6), r(7), b(4)	$Asp80_{CD1d}$ x2, $Thr156_{CD1d}$, $Asp153_{CD1d}$, $Asn30_{\alpha TCR}$, $Lys68_{\alpha TCR}$, $Gln52_{\alpha TCR}$,
DS-32	-7,312	-6,812	b(1), r(1)	$Asp80_{CD1d}$ x2, $Thr156_{CD1d}$, $Asp153_{CD1d}$, $Asp29_{\alpha TCR}$, $Lys71_{\alpha TCR}$ π-cat., $Gln52_{\alpha TCR}$,
DS-39	-7,587	-8,528	b(1)	$Asp80_{CD1d}$ x2, $Thr156_{CD1d}$, $Thr159_{CD1d}$, $Lys65_{CD1d}$
DS-46	-7,841	-7,512	b(1)	$Asp80_{CD1d}$ x2, $Thr156_{CD1d}$, $Asp29_{\alpha TCR}$ x2, $Asp29_{\alpha TCR}$ sb, $Lys71_{\alpha TCR}$ sb
HS44 (38)	-8,045	-7,298	g(4)	$Asp80_{CD1d}$ x2, $Thr156_{CD1d}$, $Asp153_{CD1d}$ x2, $Gly96_{\alpha TCR}$

Table 3.4: *Report of results obtained from Induced Fit docking studies. Average of all results is indicated both in Initial score (average of 10 docking studies) and Final score (average of all results obtained). H-Bond interactions listed of the best pose. *g=good, b=bad, r=regular for pose classification. NR=no results. ** π-cat.= pi-cation interactions, sb= salt bridge*

Again, Induced Fit docking scores could not be only considered due to their unreliable accuracy as energetic value. For that reason, ligand ability to establish some of the essential interactions was another criteria considered to evaluate this results.

A detailed examination of each pose demonstrated that our positive control HS44 (**38**) showed minimal fluctuation of ligand and nearby residues in obtained results. Concerning the aromatic derivatives, our *hit* candidate **DS-1**, which showed good docking poses able to interact with $Asp153_{CD1d}$ and $Gly96_{\alpha TCR}$, lost all interactions mediated by aromatic ring or its substituent despite apparently low protein residue fluctuation. Only the ceramide skeleton H-Bond network remained. Similar results were obtained by **DS-3**; although promising binding mode was revealed by docking studies, the flexibility of surrounding residues disturbed the initial potential binding mode (**Figure 3.13**, **Table 3.4**). The other disubstituted aryl compound analyzed by this technique was the promising sulfonamide **DS-14**. This ligand had showed the best H-Bond network of all studies compounds with simultaneous interaction with all essential residues and it had reached good marks in docking studies; in this case, seven results were obtained in with two different binding modes. One pose in which only essential interactions mediated by polar part of ceramide skeleton were maintained while sulfonamide moiety interacted with $Asp29_{\alpha TCR}$. In the other pose sulfonamide moiety was able to establish one H-Bond with Asp153 as well as those interactions

with Asp80 and Thr156 from polar part of ceramide. In light of these results, some kind of destabilizing interactions could be present to force ligand to a different orientation losing some of the putative essential interactions for NKT cell activity, although IDF was not able to predict such effects and therefore this hypothesis should be object of study under other more flexible simulations (**Figure 3.13**, **Table 3.4**). The sulfonamide analogue with oxygen (**DS-15**) showed consistent results with highly stable poses displaying an interesting binding mode (interactions with $Asp153_{CD1d}$ and potentially with $Gly96_{\alpha TCR}$ or $Asn30_{\alpha TCR}$) despite moderate scoring. While in initial "protein frozen" docking studies seemed to stand out the thioether **DS-14** in front of its oxygen analogue **DS-15**, Induced Fit docking results pointed to an opposite order (**Figure 3.13**, **Table 3.4**).

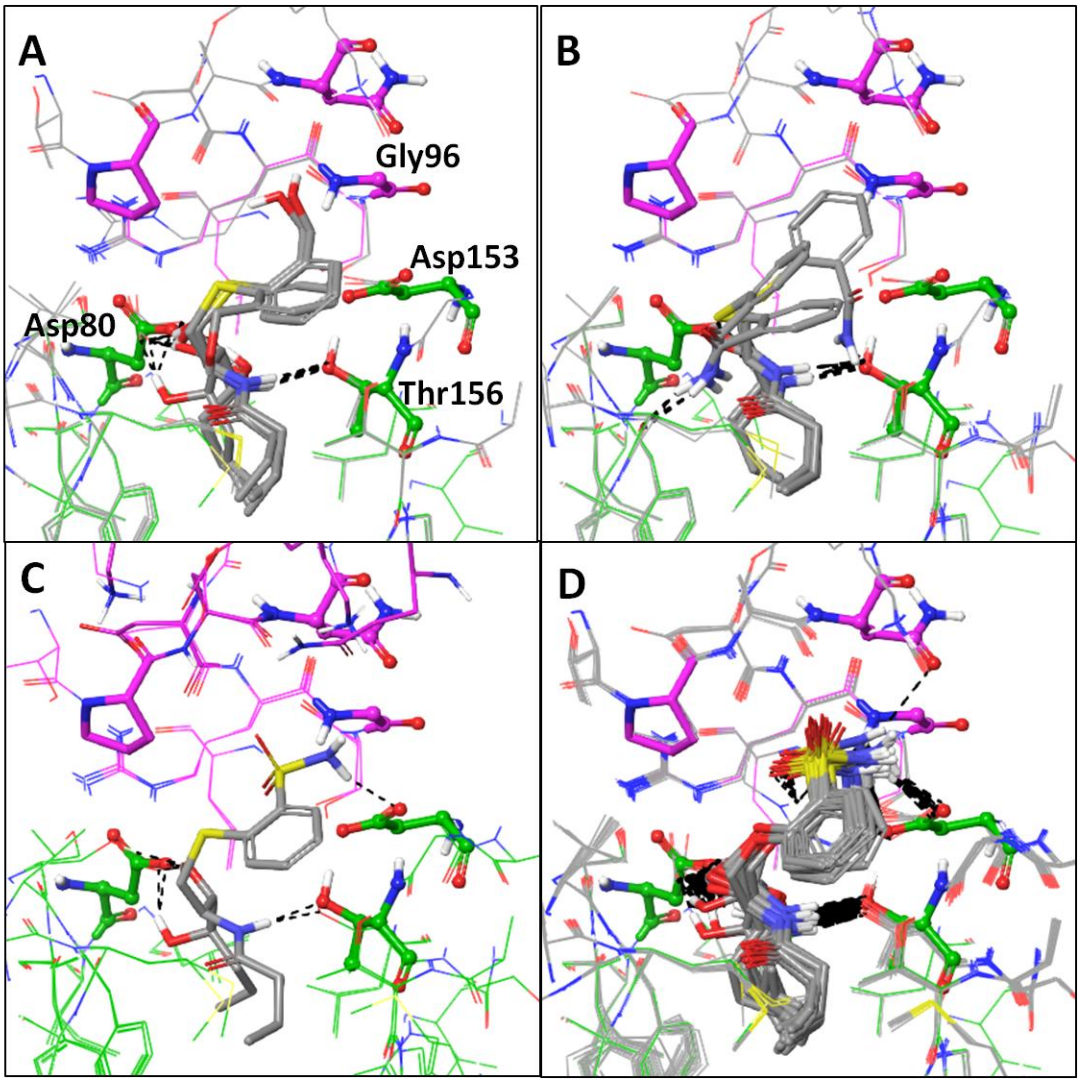

Figure 3.13: *Superimposing Induced Fit docking results for A)* ***DS-1****, B)* ***DS-3****, C)* ***DS-14*** *and D)* ***DS-15****. Crystal structure is colored as following: CD1d carbons are colored in green while TCR α-chain carbons are colored in pink. H-Bond interactions are colored in black dashed lines and salt bridge in purple dashed lines.*

As it was mentioned in the preceding section, trisubstituted ligands showed less frequent formation of essential interactions, pointing to some detrimental effects of the extra substituent. The protein flexible studies allowed **DS-21** orientating better than rigid docking, although only in two of the four results and scoring was not high (**Table 3.4**, **Figure 3.14**); hence, the fluctuation of closer residues would induce a more effective binding mode for this ligand.

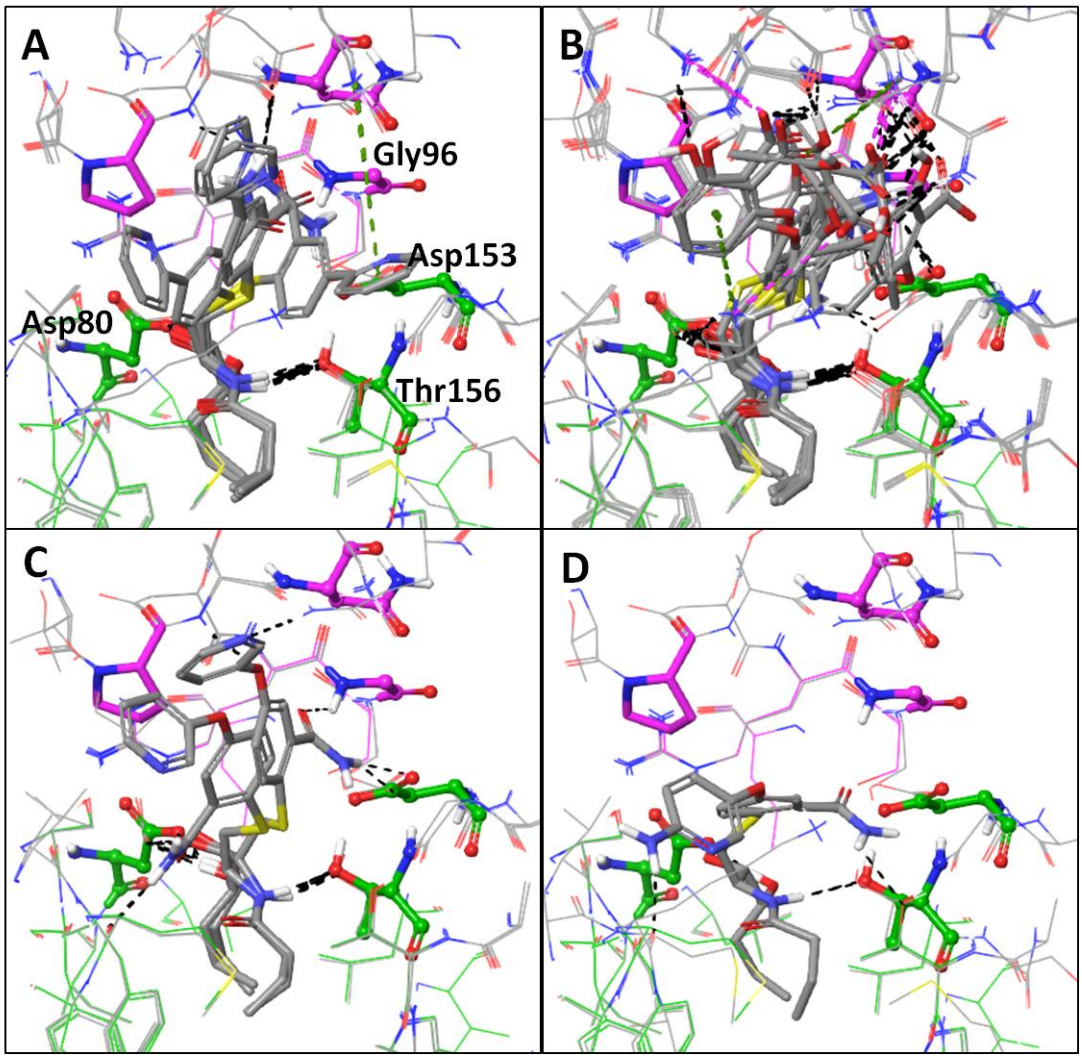

Figure 3.14: *Superimposition of Induced Fit docking results for A)* ***DS-21****, B)* ***DS-29*****, C)* ***DS-32*** *and D)* ***DS-39****. *some of best poses were selected for simplification. Crystal structure is colored as following: CD1d carbons are colored in green while TCR α-chain carbons are colored in pink. H-Bond interactions are colored in black dashed lines and salt bridge in purple dashed lines.*

Phenyl ether ligands showed a diversity of results. The carboxamide *S*-derivative **DS-28** was one of most promising candidates after first docking screening, showing good ability to interact with both CD1d and TCR proteins; however Induced Fit studies end up without clear results. Other three 4-(phenylether)thiophenyl-ceramide ligands were studied (**DS-29**, **DS-32** and **DS-39**). **DS-29** was one with most variable poses in the docking computations and the Induce Fit docking pointed to a similar tendency: many different poses with high scores (**Table 3.4**, **Figure 3.14-B**). Ligands **DS-32** and **DS-39**,

which had previously showed potential ability to establish some of essential interactions, did not showed good binding mode neither higher energy scoring (lower values were obtained) when residues were allowed to fluctuate. Interactions with Lys68 or Lys 71 of TCR were also observed as well as Gln52 also mention in docking studies. All together, the Induced Fit Docking studies do not clearly establish that trisubstituted ligands could lead to improved binding modes.

Finally, it is worth noting that when second substituent was an aminoacid as in **DS-46**, the residue flexible docking triggers a total perturbation of the initial protein frozen binding studies. Initial docking pose for this ligand was able to interact with $Asp153_{CD1d}$ and $Asn30_{\alpha TCR}$ simultaneously; in sharp contrast, Induced Fit docking result was totally unexpected, resulting in an orientation where all the interesting interactions were lost (**Figure 3.15**, **Table 3.4**).

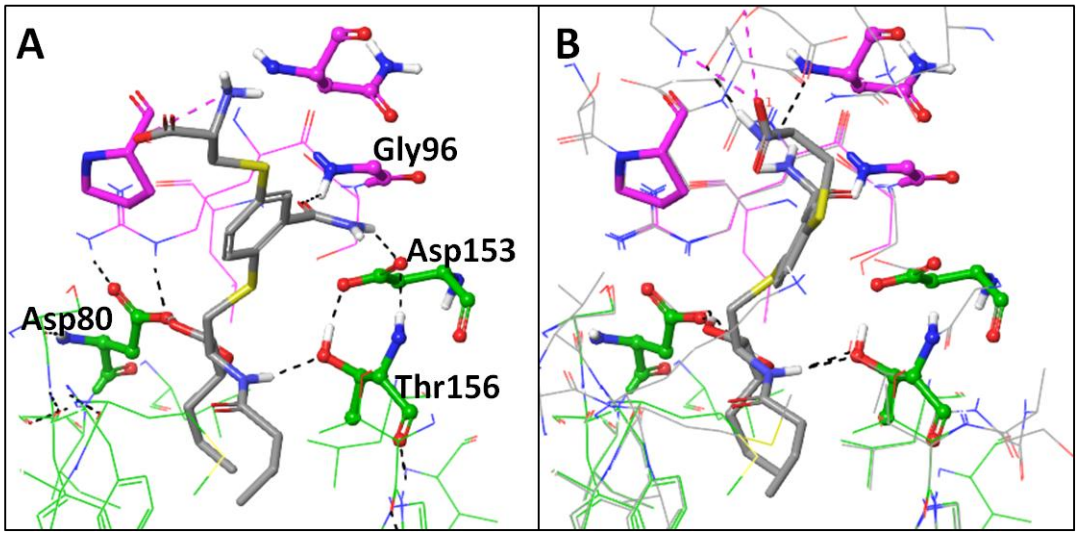

Figure 3.15: *Comparison of poses of **DS-46** reached after A) Docking studies and B) Induced Fit docking studies. CD1d carbons are colored in green while TCR α-chain carbons are colored in pink. H-Bond interactions are colored in black dashed lines and salt bridge in purple dashed lines.*

As a general conclusion, disubstituted ligands showed less attractive binding mode to CD1d-TCR than previous docking studies although it was not clear how the residue fluctuation influenced on the initially selected promising poses to reach a set of less attractive ones. Trisubstituted ligands showed diversity of results without delineating a clear tendency and interactions with other residues of TCR were observed but no clear trend of their structural impact emerged from all the collected computational data. No significant protein residue fluctuations were observed.

3.1.4. Short Molecular Dynamic Simulations

The preceding studies revealed information on ligands ability to form or not desired interactions with specific residues but no information of how they influence protein-protein interactions or complex stability were obtained. At this point, no clear

tendency among all ligands could be establish, therefore Molecular Dynamics (MD) Simulations were proposed to monitor how proteins tolerate these new aromatic-ceramide ligands and to further assess the new ligands impact on protein structure and protein-protein interactions. The same 10 ligands studied under Induced Fit protocols were used; however complete ligands were considered (meaning full C26 acyl chain as well as all phytosphingosine carbons). The best poses obtained for each ligand were selected as starting point to run 20 ns Molecular Dynamics Simulations (300K, periodic boundary conditions, NPT ensemble) in explicit water, using the program Desmond[15]. Two main considerations were analyzed from MD simulations: ternary complex stability in terms of root-mean-square deviation (RMSD) and H-Bond capacity of ligands all along simulation. In this sense, interactions with key residues interactions ($Asp80_{CD1d}$, $Thr156_{CD1d}$, $Asp153_{CD1d}$, $Asn30_{\alpha TCR}$, and $Gly96_{\alpha TCR}$) were monitored.

The results showed that ternary complex structure was mostly stable in all cases with RMSDs between 2,0 to 3,0 Å relative to the starting structures with exception of **DS-29** and **DS-39** that showed a higher RMSD (4,2 and 4,1 Å respectively) suggesting that both ligands could have a destabilizing tendency (**Figure 3.16**).

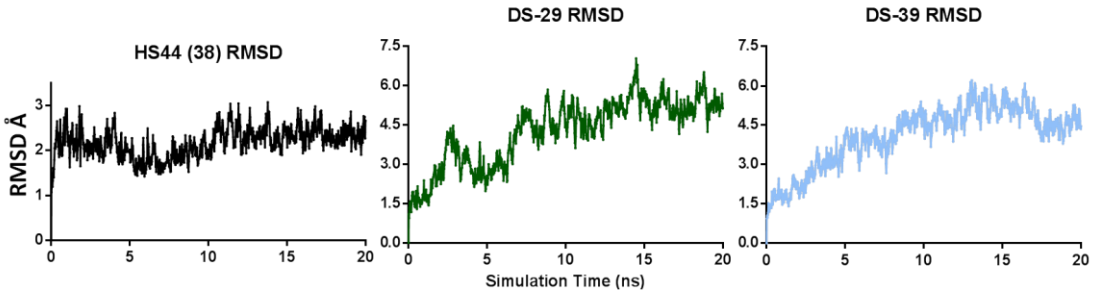

Figure 3.16: *RMDS of HS44 (**38**), **DS-29** and **DS-39** that illustrates ligand destabilizing effect to ternary complex*

Analysis of H-Bond interactions, MD simulation for HS44 (**38**) did not show ligand interaction with $Gly96_{\alpha TCR}$, something quite unexpected as this ligand did form H-Bond interactions with this residue when docked (see *ANNEX 4* for details) and in crystal structure; on the other hand, interactions with $Asn30_{\alpha TCR}$ (not observed in docking studies) was mostly stable all simulation. All together, aminocyclitol moiety showed stable interactions with 3 of 4 of essential residues all along simulation. On the other hand, interactions with CD1d ($Asp80_{CD1d}$, $Thr156_{CD1d}$, $Asp153_{CD1d}$) were conserved all along the simulation, as expected.

All disubstituted ligands (**DS-1**, **DS-3**, **DS-14** and **DS-15**) showed conserved interactions with Asp80 and Thr156 of CD1d in a similar frequency as HS44 (**38**) with only one exception; **DS-14** interaction with Thr156 was drastically reduced after the first part of simulation (**Figure 3.17** and *ANNEX 4*). All four ligands showed conserved interaction with Asp153 although only one H-Bond was observed for our new ligands versus two H-Bonds formed by HS44. This tendency was expected as our ligands are much less

functionalized. As it was mentioned, HS44 (**38**) did not showed H-Bond formation with $Gly96_{\alpha TCR}$ nor **DS-1** and **DS-14** while ligands **DS-3** and **DS-15** remarkably presented a frequent interaction with this residue. Conversely, only **DS-14** showed H-Bond formation with $Asn30_{\alpha TCR}$ stable nearly all simulation similar to HS44 (**38**). As it was deduced from Induced Fit docking results, **DS-14** could be considered the poorest candidate among studied disubstituted ligands because of the loss of important interactions. As it could be expected, interactions mediated by "*head*" group of new aromatic ligands, particularly decreased due to low level of functionality of our ligands compared with the glycolipid scaffold. Overall, these results point to this group of ligands as promising candidates.

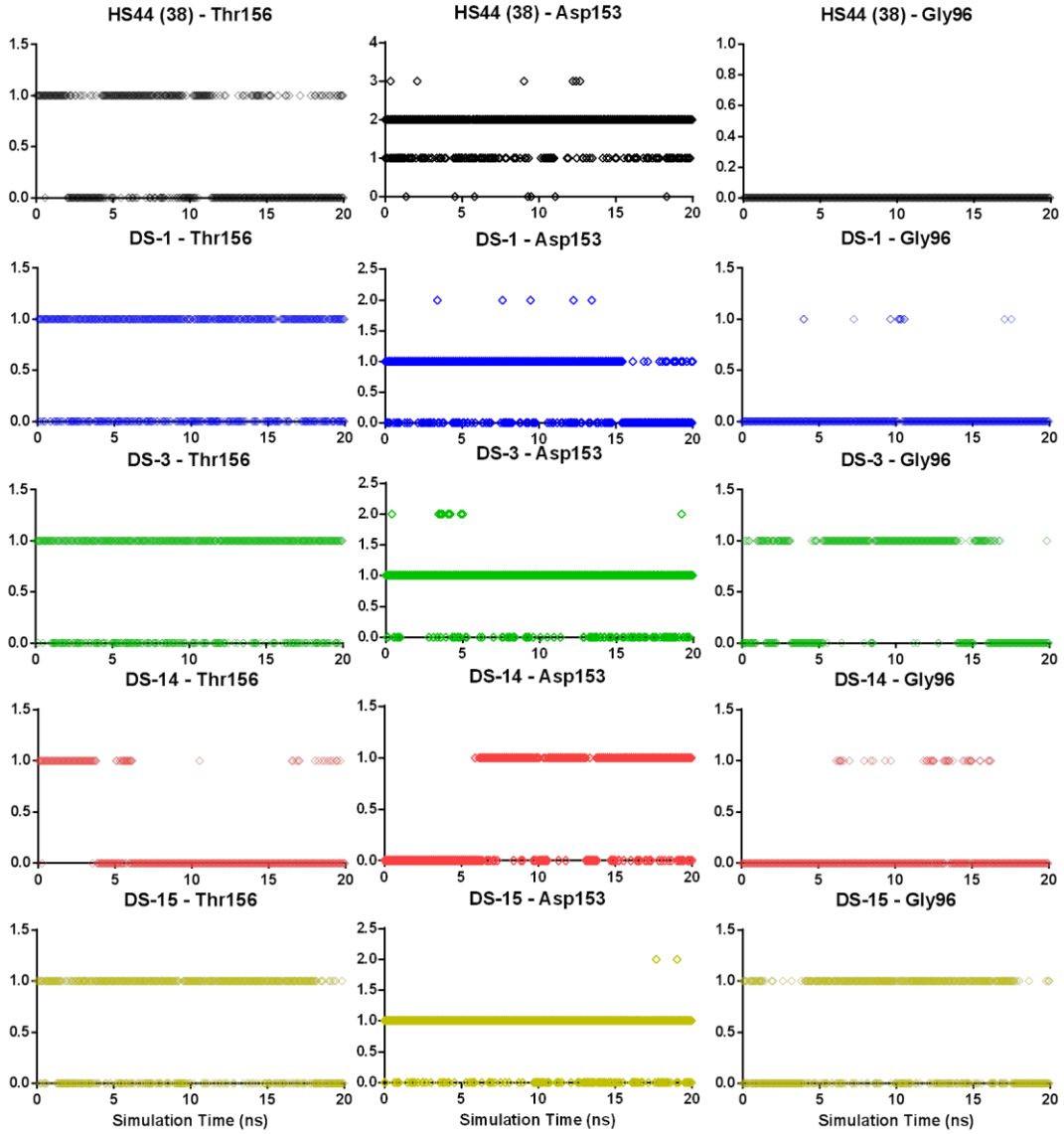

Figure 3.17: *Dependence of number of H-Bond interactions of indicated ligands with simulation time. HS44 (**38**) is colored in black, **DS-1** in blue, **DS-3** in green, **DS-14** in red and **DS-15** in yellow*

Trisubstituted ligands had shown controversial results when they were studied with docking tools, showing a diversity of results not having a structural tendency. MD

simulation showed a kind of destabilizing tendency among two of them (**DS-29** and **DS-39**) as mentioned. These ligands not only exhibit infrequent interactions with αTCR residues (Gly96 and Asn30), but also suffered from a marked decrease of H-Bond network interactions with CD1d residues (Asp80, Thr156 and Asp153) (**Figure 3.18** and *ANNEX 4*). **DS-21** was the only trisubstituted ligand able to maintain interactions with Asp153 however forcing the loss of contacts with Thr156.

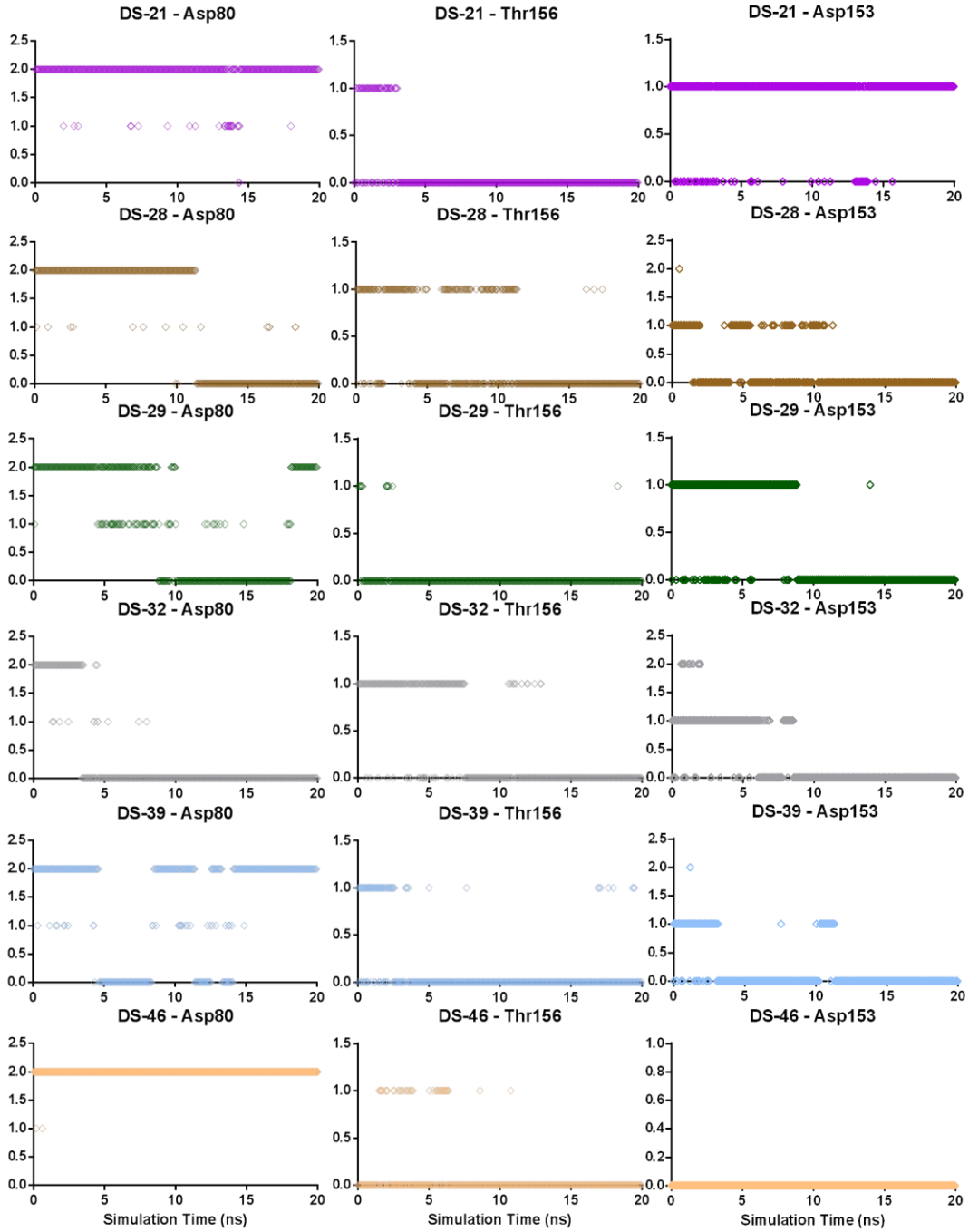

Figure 3.18: *Dependence of number of H-Bond interactions of indicated ligands with simulation time.* ***DS-21*** *is colored in lilac,* ***DS-28*** *in brown,* ***DS-29*** *in dark green,* ***DS-32*** *in grey,* ***DS-39*** *in light blue and* ***DS-46*** *in light orange*

These results were in line with those previously obtained, evidencing a negative effect of this extra-substitution. Occasionally, other interactions were observed however how would modulate the protein stability and cell response were not known.

Hence, after MD simulations of small group of ligands some general conclusions emerged: disubstituted aromatic ligands showed an interaction profile more similar to that one reported as optimal for NKT cell activity in the glycolipid series, while trisubstituted aromatic ligands analyzed showed an extensive H-Bond network perturbation, establishing new interaction modes, not previously described and, therefore, of uncertain impact in biological responses.

3.1.5. Summary of results and final remarks

Rigid docking experiments point to interesting H-Bond ability of disubstituted ligands, while only some of trisubstituted ones were able to establish some of the essential interactions. Among all ligands**, DS-14** was the best candidate not only because of having a good score but also for its ability to simultaneously interact with $Asp153_{CD1d}$, $Asn30_{\alpha TCR}$, and $Gly96_{\alpha TCR}$. Induced Fit calculations suggested a better binding mode for disubstituted ligands while trisubstituted ligands showed more diverse results and somewhat unfavorable binding mode losing the ability of the carboxamide group to interact with $Asp153_{CD1d}$, $Asn30_{\alpha TCR}$, or $Gly96_{\alpha TCR}$ in most cases. Taking into account that both Docking and Induced Fit Docking consider rigid receptors, MD simulations were carried out to determine a more accurate impact of our virtual ligands onto ternary complex structure. The preliminary computational studies of a set of compounds define monocyclic ligands as priority compounds, due to their good ability to interact with both CD1d and TCR in a similar manner as experimentally reported active ligands such as HS44 (**38**) or αGalCer (**2**). The lack of biological information of the aromatic head phytoceramide compounds impedes to establish structure-activity relationships. Therefore, our initial hypothesis considering the essential interactions ($Asp80_{CD1d}$, $Thr156_{CD1d}$, $Asp153_{CD1d}$, $Asn30_{\alpha TCR}$, and $Gly96_{\alpha TCR}$) remains at this point to be validated by experimental data of this new type of ligands; only the biological activity of one of new ligands (**DS-1**) was available at the time of computational studies were done.

3.2. CHAPTER 2: Synthesis of new aromatic-ceramide analogues of αGalCer

Glycoceramide derivatives had been extensively studied in several biological contexts[16] such as structural (as main components of cell membrane) or bioactive signaling molecules that have a crucial role in cell growth, cell regulation, intracellular trafficking and inflammation. Among all these complex roles, involvement of glycolipids in inflammation processes was of interest to us, more specifically in APC-NKT cell context. As it was exposed in the Introduction, an extensive work was made on glycolipid derivative seeking for NKT cell modulators since agelasphin, the first chemical structure of a potent NKT cell antigen was revealed and the synthetic derivative KNR7000 better known as αGalCer (**2**)[17,18] (**Figure 3.19**) achieved a fundamental role in the development of NKT cell biology. Our group had a chemical background in sphingolipids, ceramides and glycoceramides or chemical analogues of them; taking advantage of this expertise, new structures were synthesized exploring several biological applications. In this context, Anna Alcaide investigated new ceramide derivatives and some of them were tested as NKT cell activators, emerging a promising candidate among all them: AA398 (from now on **I-1a**), an aromatic-ceramide analogue of αGalCer (**2**) with an unprecedented structure that, surprisingly, was active in the stimulation of NKT cells and, unwrapped a new class of non glycosidic antigens, delineating a new landmark in the field (**Figure 3.19**).

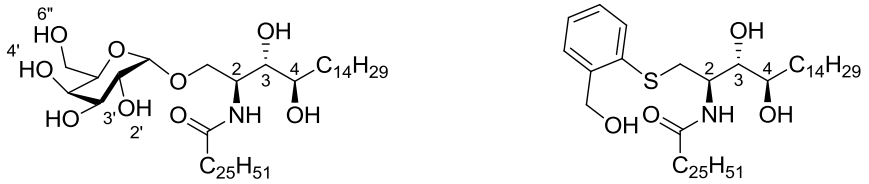

Figure 3.19: *Chemical structure of αGalCer (**2**) and **I-1a***

With all this in mind, the **main objective** of the present doctoral thesis was to synthesize new aromatic-ceramide family based on previously found **I-1a**. As it was stated in the preceding chapter, a rational design based on computational studies was tackled although a system to precisely define the molecule candidates was not fully reached. After all, ligands with three aryl substituents showed ambiguous computational results suggesting a destabilization of the protein complex while for disubstituted aryl ligands the calculations predict a set of promising interactions with the receptors.

Considering these results, a proposal for a first family was based on the following considerations:

1) Ceramide skeleton of phytosphingosine with acyl C26 side chain would be maintained to guarantee effective CD1d recognition and antigen exposure to NKT cells receptors.
2) For this first family design, a single aromatic ring would be selected.
3) Only one substituent would be included in position 2 of the ring apart from the heteroatom (O, S or NH) bridge to the ceramide.
4) Commercial availability of aromatic precursors was preferred to ensure a large family to complete SAR studies.

Taking into account all the considerations above mentioned, three main modifications were proposed (**Figure 3.20**): the ring substituent (R) could be replaced by other groups with higher functionality able to increase H-Bonding capacity of new compounds, for example introducing ester, acid or amide groups (this last one was also explored in the preceding section with some H-Bonding properties improvement); linking atom (X) could be replaced by other heteroatoms such oxygen or nitrogen; phenyl ring (Y) could be replaced by an isostere such as pyridine. Mostly all these considerations were explored among some of the proposed virtual ligands analyzed in the computational studies with promising results compared to our *hit* compound **I-1a**.

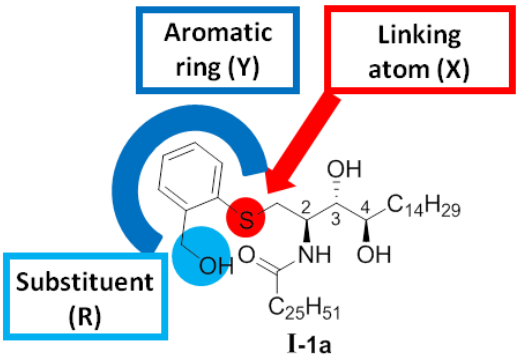

Figure 3.20: *Structure of* ***I-1a*** *and which parts were proposed as modifying*

All together, exploring commercial availability of synthetic precursors and the modifications mentioned above, the following scaffolds were selected as first candidates to be incorporated (**Figure 3.21**):

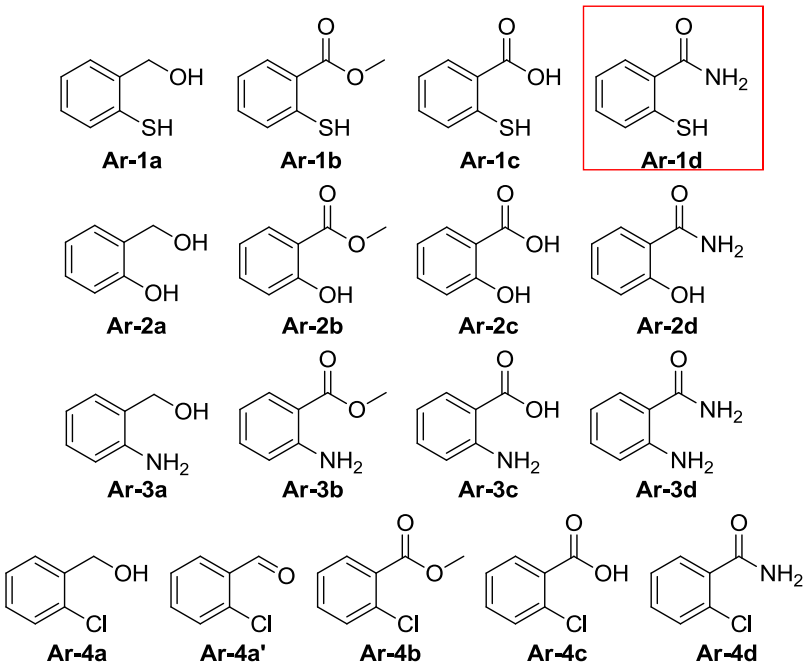

Figure 3.21: *Aromatic scaffolds selected for our first ceramide family design; only 2-mercaptobenzamide* ***Ar-1d*** *was not commercially available*

To obtain the sulfur derivatives, only 2-mercaptobenzamide was not commercially available, and should be synthesized. The ether derivatives need aromatic phenolic scaffolds **Ar-2a-d** that were accessible as well as aniline-like ones **Ar-3a-d**. To obtain the pyridine derivatives, the chloropyridine precursors **Ar-4** were selected due to synthetic strategies as will be later introduced. The combination of the proposed aromatic moieties with αGalCer (**2**) ceramide skeleton ended up with a collection of 20 compounds (**Figure 3.22**).

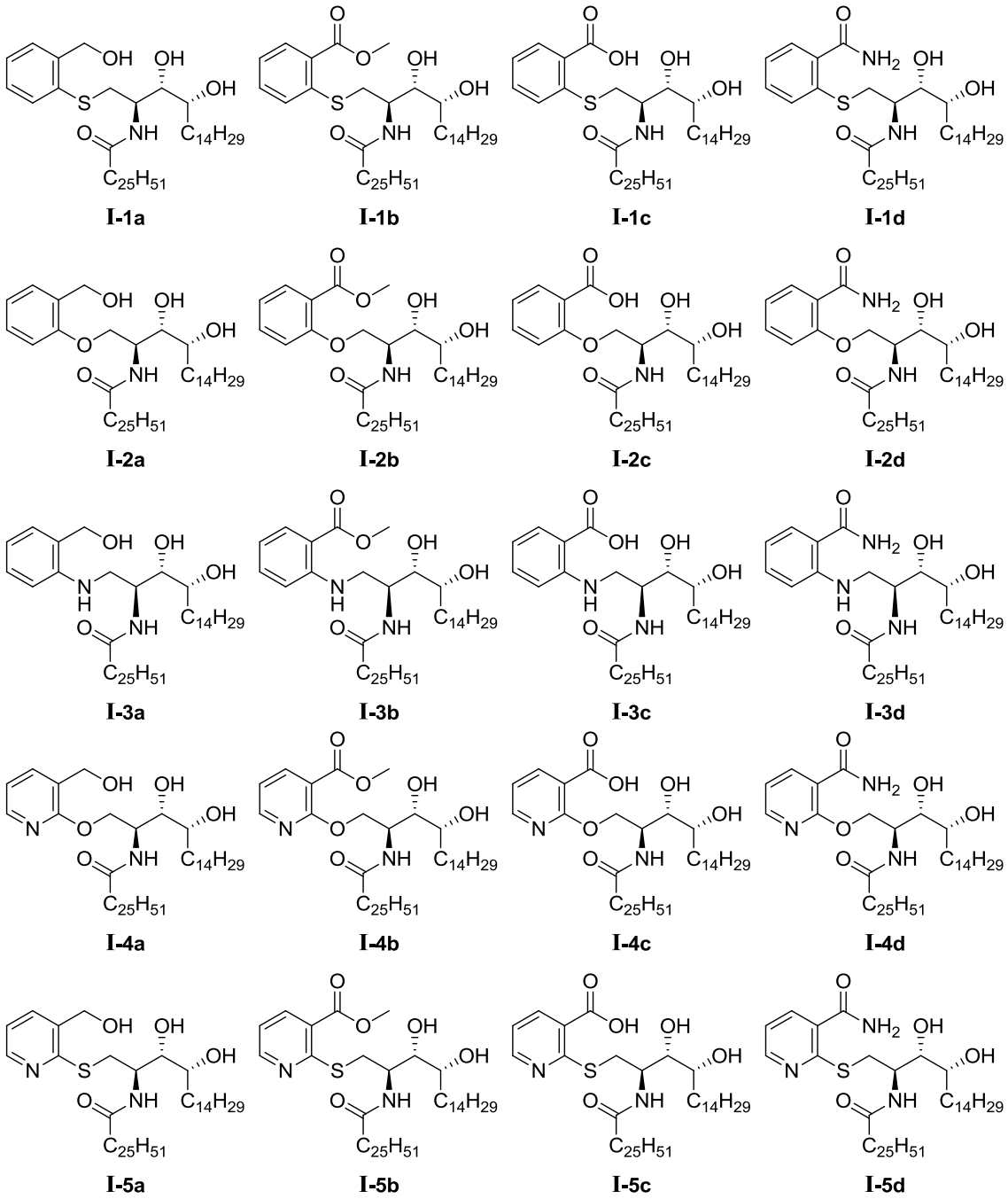

Figure 3.22: *First family of target compounds. Numbering referring to aromatic ring derivative (**1**: thiophenols, **2**: phenols, **3**: anilines, **4**: 2-O-linked-pyridines, **5**: 2-S-linked-pyridines) and small letter to substituent in position 2 (**a**: CH_2OH, **b**: COOMe, **c**: COOH, **d**: $CONH_2$). Roman numbers will refer to synthetic step, being **I** as target compound.*

The synthetic strategy to obtain the compounds was based on a methodology explored in our group, involving aziridine-ring-opening reactions to obtain the phenyl derivatives, while the pyridine compounds were planned to be obtained via aromatic nucleophilic substitution (**Scheme 3.1**). Our initial strategy was based on acylaziridine **G** ring opening reaction following Alcaide's procedure of **I-1a** obtaining (route *1*, **Scheme 3.1**); the use of more activated nosylaziridine (**H**, Scheme 3.1, – (*2*)) was

considered as alternative pathway to the route involving the acylaziridine intermediate, which was predicted could have some lack of reactivity based in previous experience in the group (route *2*, **Scheme 3.1**); the synthesis of 2-*O*-linked-pyridine derivatives was designed by *O*-arylation of primary hydroxyl in the azido-alcohol **D**, in turn obtained as an intermediate in the sphingoaziridines synthesis (route *3*, **Scheme 3.1**); finally, 2-*S*-linked-pyridine compounds would need to previously install a sulfur nucleophile at C-1 in sphingosine chain, able to attack desired chloropyridine (route *4*, **Scheme 3.1**).

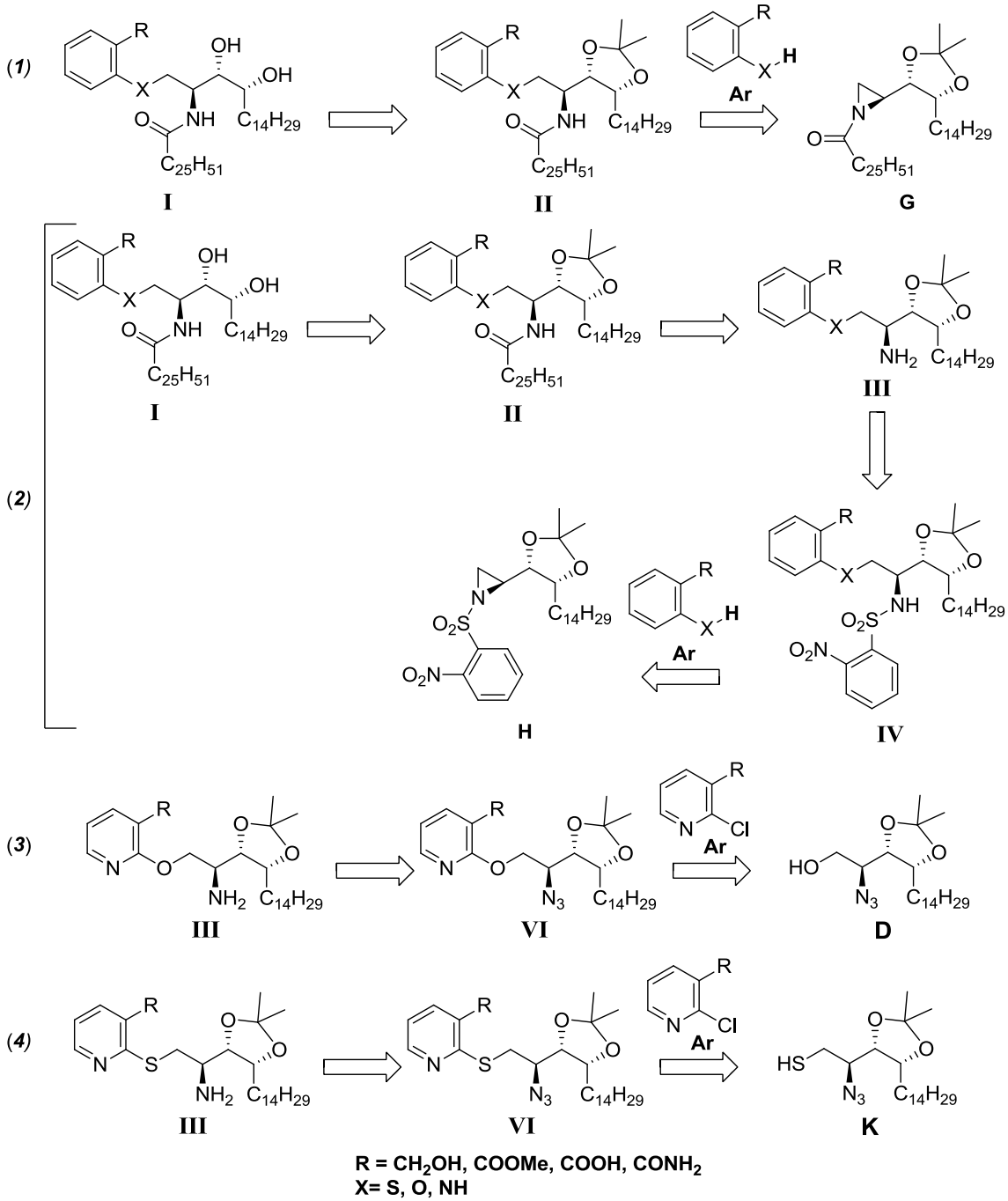

Scheme 3.1: *Retrosynthetic analysis of aromatic target compounds: 1) acylaziridine ring opening reaction; 2) nosylaziridine ring opening reaction; 3 and 4) aromatic nucleophilic substitution*

All together, several specific objectives emerged for this synthetic Chapter:

I) Exploring proposed synthetic strategies to incorporate aromatic moieties to ceramide skeletons.
II) Synthesis of non commercial aromatic moieties.
III) Synthesis of the library of target compounds, in quantities and purities for biological screening.

3.2.1. Synthesis of reactive pytosphingosine derivatives as key intermediates

As it was previously mentioned in the Introduction, our group has extensive experience in the synthesis of aminocylitol-ceramide derivatives[6,19,20] as well as on phytosphingosine and sphingosine derivatives[21,22]. Following known procedures previously described in the literature[23-25], the desired key intermediate **D** was obtained from phytosphingosine hydrochloride as illustrated in **Scheme 3.2**. This methodology is a well-establish route used in our group with excellent yields.

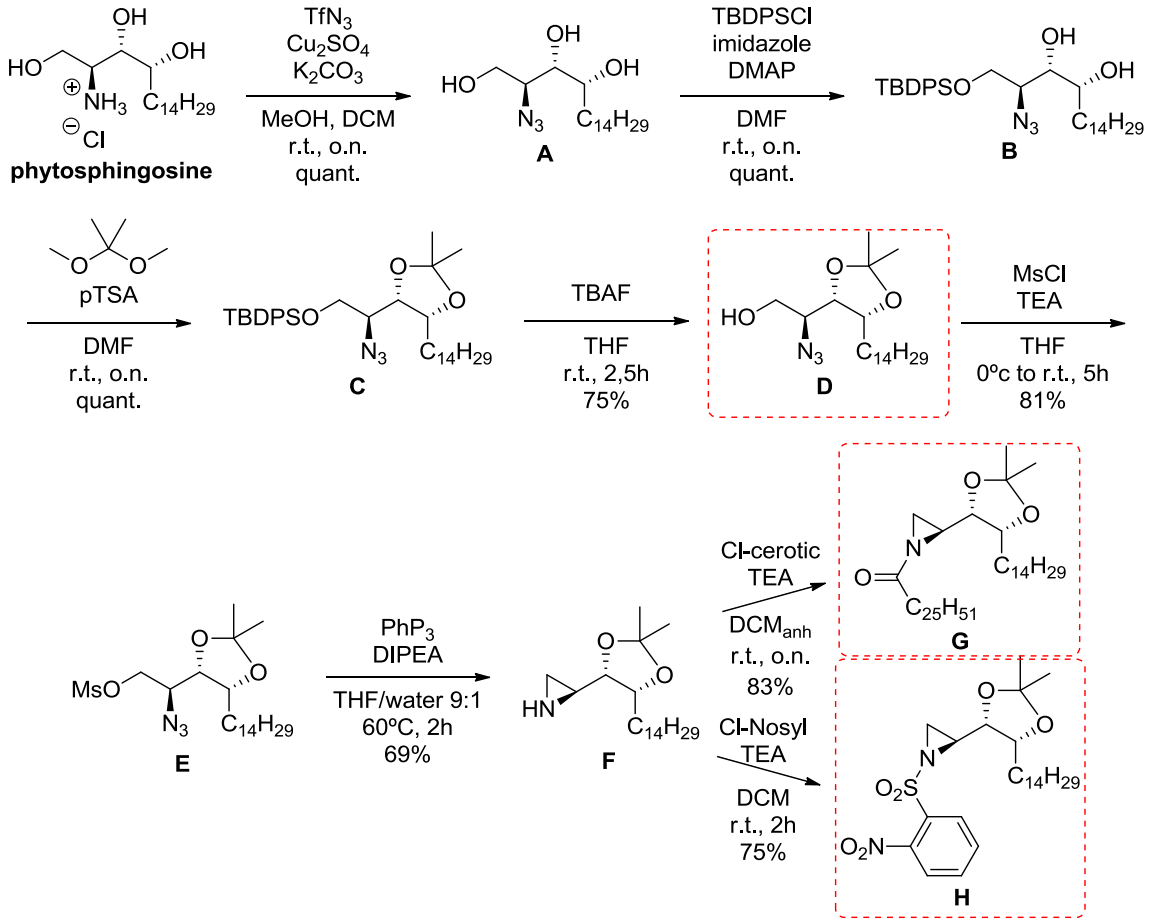

Scheme 3.2: *Synthetic route of key intermediate **D**, **G** and **H** needed for target compound obtaining.*

The final steps to reach the desired aziridines from azido-alcohol **D** were carried out following new procedures developed in our group[6,20-22]. During the present doctoral thesis some procedures were improved in order to facilitate reactions handlings.

Thus, starting from commercial **phytosphingosine hydrochloride**, the 2-amino group was transformed to azide (**A**)[23] followed by primary alcohol protection with TBDPSi protecting group[24] to give azido-diol **B** in quantitative yield. Both secondary hydroxyl groups were protected as an acetal with dimethoxypropane[25] to give the fully protected intermediate **C**. Primary alcohol deprotection with conventional TBAF conditions afforded key intermediate azido-alcohol[25] **D** with excellent conversion. Primary alcohol mesylation gave intermediate **E** which was used without further purifications. Azide reduction under Staudinger conditions[20] and *in-situ* intramolecular cyclization gave aziridine **F**. Acylation with acyl chloride derivatives of cerotic acid afforded acyl-aziridine **G**[26] with and overall yield of 35% after 7 steps, while NH-functionalization with 2-Nitrobenzenesulfonyl chloride[20] gave nosylaziridine **H** with an overall yield of 32% after 7 steps.

Some key considerations were established during present thesis:

- When azido-alcohol **D** is used in mesylation step, TBDPS traces coming from preceding deprotection were well tolerated. However when it is used as key intermediate the TBDPS derived trace compounds had to be totally removed because aromatic nucleophilic substitution reactions are affected, decreasing conversion.

- The intermediate mesylate **E** was usually used as stock intermediate during aziridines obtaining; this compound was usually frozen until needed however when some stocks of this intermediate were checked prior to be used, product degradation was observed. Product purification and impurity isolation lead us to identify cyclic byproduct **BP-1**, which could come from acetal removal due to acid traces from MsCl and *in-situ* intramolecular attack of 4-hydroxyl to C1 position and mesylate[27].

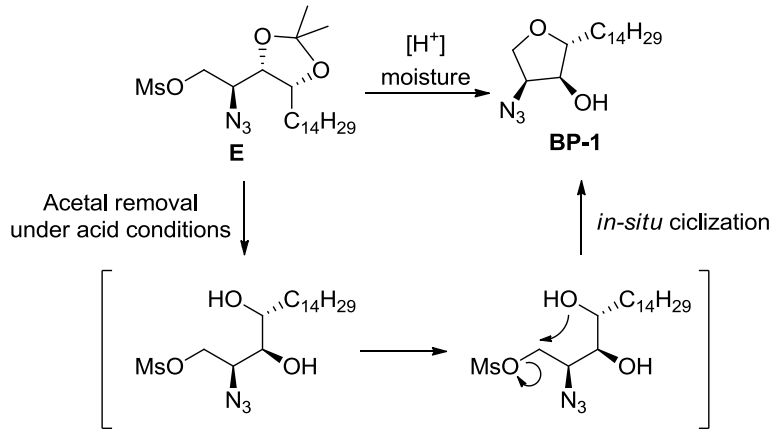

Scheme 3.3: *Proposed mechanism of cyclic by-product from mesylate* ***E*** *degradation*

Finally, in order to obtain 2-*S*-pyridine derivatives via aromatic nucleophilic substitution of 2-chloropyridines, a new key intermediate incorporating a sulfur atom was synthesized. To that purpose, we took advantage of the intermediate mesylate **E**, which was subjected to mesyl group displacement with potassium thioacetate under basic conditions to yield desired compound **J** in good yields.

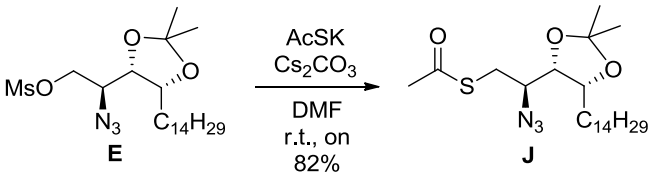

Scheme 3.4: *Synthesis of key intermediate* ***J***

As general overview, the desired key intermediates **D**, **G**, **H** and **J** were obtained with excellent yields starting from commercial phytosphingosine hydrochloride.

3.2.2. Synthesis of Arylthioceramide derivatives (I-1)

First target attempted compounds were the analogues of our *hit* compound **I-1a** (**Figure 3.23**). Thus, replacement of hydroxymethyl substituent on phenyl ring by an ester, acid or amide group leaded to compounds **I-1b**, **I-1c** and **I-1d** respectively.

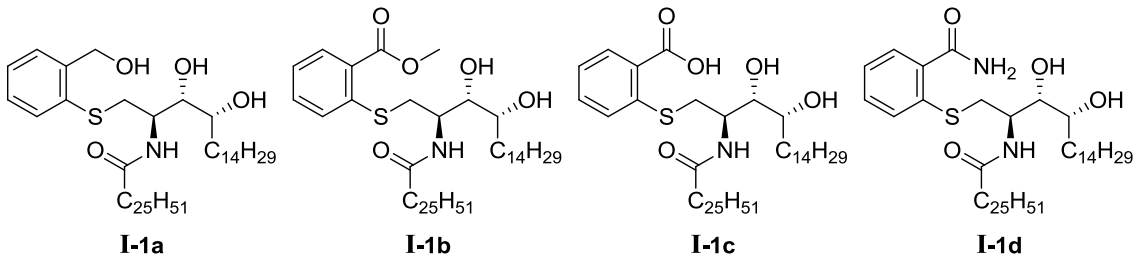

Figure 3.23: *Thiophenol-like derivatives, analogues of* ***I-1a***

During a preceding doctoral thesis, Anna Alcaide set up a microwave protocol to incorporate different nucleophiles to phytosphingosine skeleton via aziridine ring

opening reactions[21,26] (**Scheme 3.5**). Most of the tested nucleophiles were aliphatic thiols or amines, thiosugars or aminocyclitols. However, some thiophenols were incorporated using this methodology, among them there was **I-1a**. This compound was synthesized from acyl-aziridine **G** under microwave irradiation at 150W, 120ºC and 100 psi in ACN and using DBU as organic base. This methodology was taken as our starting strategy to obtain desired analogues **I-1**.

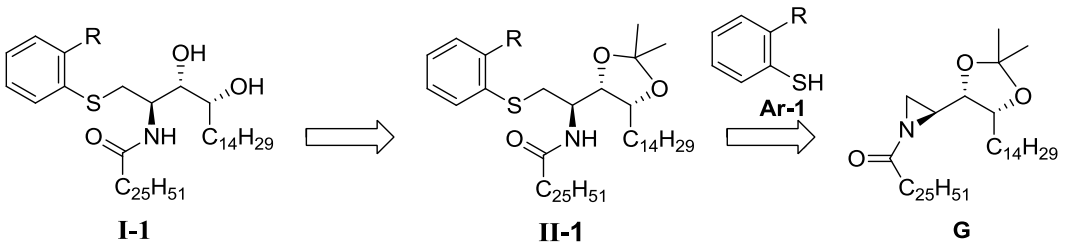

Scheme 3.5: *Retrosynthesis of thiophenol analogues type* ***I-1***

The corresponding thiophenols, 2-mercaptobenzylalcohol (**Ar-1a**), methyl 2-mercaptobenzoate (**Ar-1b**) and 2-mercaptobenzoic acid (**Ar-1c**) were commercial products, while 2-mercatobenzamide (**Ar-1d**) was not accessible so it had to be synthesized in our lab.

3.2.2.1. Synthesis of 2-mercaptobenzamide (Ar-1d)

The desired amide **Ar-1d** synthesis was initially planned through key disulfide intermediate **Ar-5**, which would be obtained from its diacid precursor **Ar-6**, easily obtainable form commercially available 2-mercaptobenzoic acid (**Ar-7**) (**Scheme 3.6**).

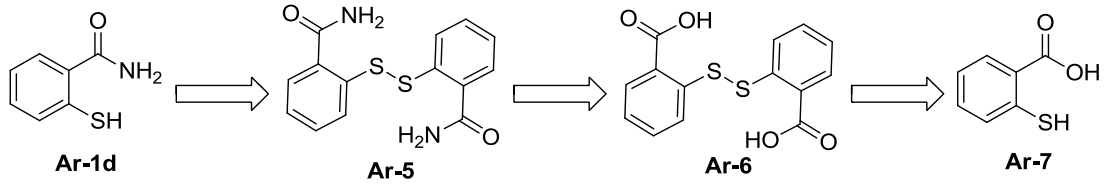

Scheme 3.6: *Retrosynthetic strategy of* ***Ar-1*** *obtaining*

Following this plan, the synthesis of **Ar-1d** was tackled from commercial available 2-mercaptobenzoic acid **Ar-7** (**Scheme 3.7**). Thiol protection was achieved by disulfide bond formation under mild conditions using iodine in quantitative yield[28]. The conversion of the acid group into the amide was first attempted using EDC, HOBT methodology, however the desired product was not detected neither in crude analysis by ^{1}H-NMR nor subsequent column purification.

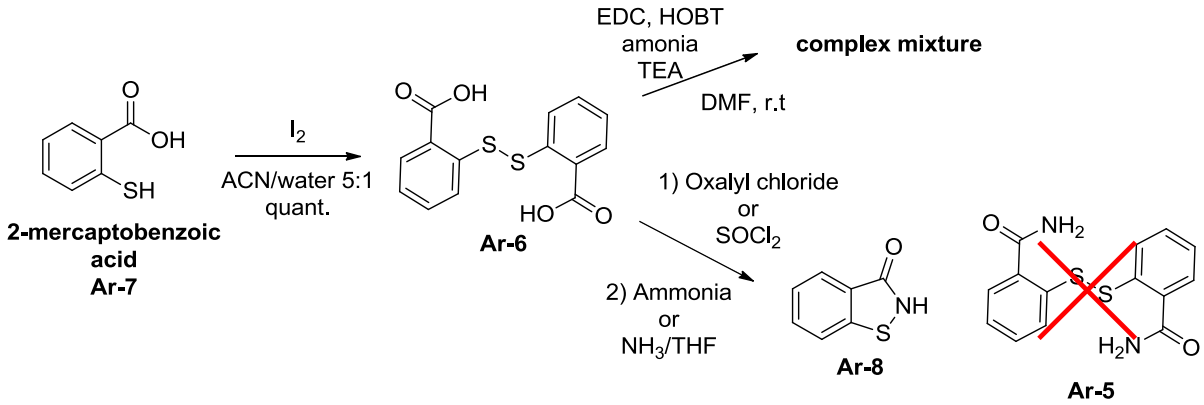

Scheme 3.7: *First synthetic strategy for 2-mercaptobenzamide* ***Ar-1d*** *obtaining*

Amide formation through intermediate acyl chloride was an alternative strategy (**Scheme 3.7**), although several reported procedures both with thionyl chloride or oxalyl chloride were followed[29-32], but all attempts to obtain 2,2'-disulfanediyldibenamide (**Ar-5**) were unsuccessful (**Table 3.5**). The analysis of the obtained product by ^{1}H-NMR spectra showed 4 aromatic protons, however, evidence of NH_2 and SH functionalities were not clear (**Figure 3.24**). HRMS showed unexpected mass: 152 corresponding to hypothetic "$[½M]^+$" what was completely unexpected. IR spectrum showed an intense peak around 1640 cm^{-1} which could agree with C=O of amide formation but NH_2 presence was not clear.

Entry	Conditions	Ar-5 formation	Ar-8 formation
1	EDC, HOBT, NH_3, TEA DMF, r.t.	Complex mixture	
2	1) Oxalyl chloride, DMF, r.t. 2) NH_3 conc. aq.	Obtaining of starting **Ar-6**	
3	1) Thionyl chloride, 7ºC, on 2) NH_3 conc. in THF	n.d.	quantitative
4	1) Oxalyl chloride, DMF and THF, r.t. 2) NH_4Cl, TEA, DCM, r.t.	n.d.	Detected but not isolated

Table 3.5: *summary of conditions tested to synthesized* ***Ar-5***

Bibliographic research pointed us to the possible formation of the cyclic benzothiazolone byproduct **Ar-8**[33,34]. Our hypothesis was disulfide bond breaking forming the sulfenyl chloride intermediate **Ar-9** and *in-situ* cyclization when ammonia was present in reaction medium (**Scheme 3.8**) to lead to **Ar-8**. As this product was commercially available at reasonable prices, it was used to compare it with the product obtained in our reactions, confirming the same structure although NH signal at ^{1}H-NMR spectrums of our products was not clearly observed (**Figure 3.24**).

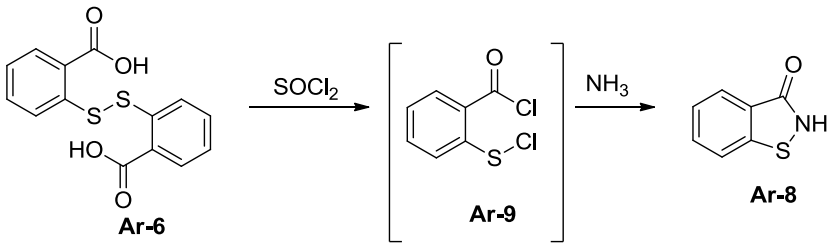

Scheme 3.8: *Hypothetic mechanism of benzothiazolone* ***Ar-8*** *formation*

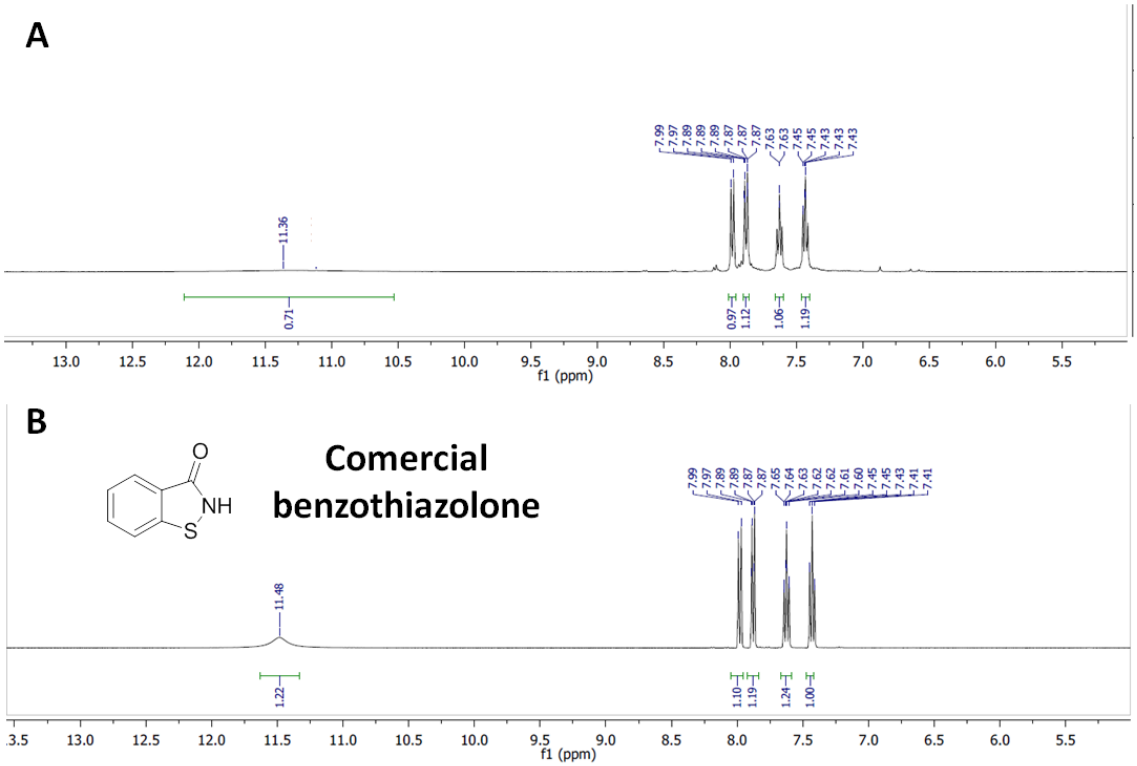

Figure 3.24: *H-NMR comparison of A) one of obtained solids throw chloride intermediate reactions and B) commercial benzothiazolone which is hypothetically form in our reactions*

At this point, an alternative strategy was undertaken using **Ar-8** as starting material to obtain desired **Ar-1d**. It was described in chemical literature that S-N bond could be broken under reductive conditions using $NaBH_4$[35-37]. Hence, when **Ar-8** was treated under reducing conditions, the desired compound **Ar-1d** was obtained in moderate yield (55%) (**Scheme 3.9**). It is worthy to mention that this product was easily oxidized to **Ar-8** (also obtained as reaction by-product in low yield, 23%) even with atmospheric oxygen (**Scheme 3.9**).

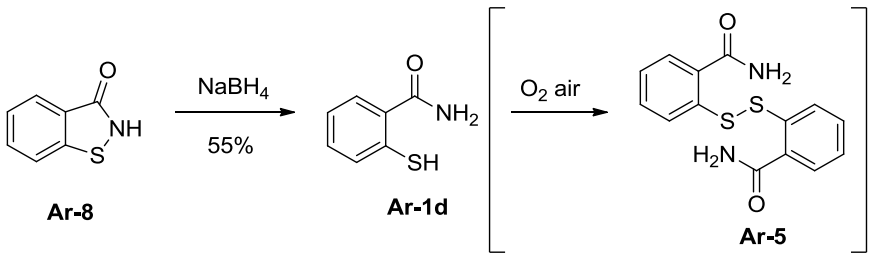

Scheme 3.9: *2-mercaptobenzamide obtention and product oxidation*

To conclude, the desired compound **Ar-1d** was obtained in moderated yield in one step from **Ar-8**. Our initial strategy via the diamide **Ar-5** and diacid **Ar-6** was unsuccessful due to formation of cyclic **Ar-8** as main reaction product.

3.2.2.2. Arylthiol incorporation to ceramide skeleton

Once having all thiophenol derivatives **Ar-1** the synthesis of desired 1-phenylthioceramide derivatives was attempted. *N*-acylaziridine **G** was reacted under same conditions used by Anna Alcaide in her doctoral thesis in order to obtain desired intermediates **II-1** (results are summarized in **Table 6**). The preparation of **II-1d** worked with high yields (**Table 3.6**, *Entry 4*) comparable to that of **II-1a**. Notably, when the reaction was done using freshly prepared 2-mercaptobenzamide **Ar-1d**, the reaction gave better yields, although product handling was complicated due the low solubility of the products. In the case of methyl ester derivative **II-1b**, the reaction took place with moderate yield (**Table 3.6**, *Entry 2*), but when the reaction was done with 2-mercaptobenzoic acid (**Ar-1c**), the desired compound could not be isolated from the reaction crude, in spite of TLC control showed a new product formation. It is worth mentioning the amphiphilic character of this product, having long hydrophobic chains and an ionizable polar group such as the 2-alkylthiobenzoic acid moiety. This was difficulting **II-1c** handling and purification to the extent that a new route was proposed.. Taking this into account, it was thought to use methyl-ester analogue **I-1b** as synthetic precursor, from which the acid **I -1c** could be successfully obtained after ester hydrolysis.

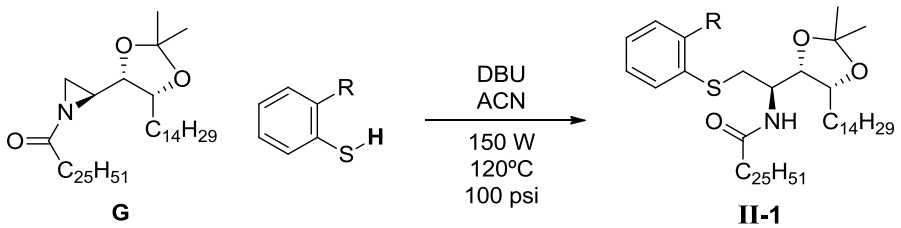

G **II-1**

R = a) CH_2OH, b) COOMe, c) COOH, d) $CONH_2$

Entry	Thiophenol	Time	Yield	Product number
1	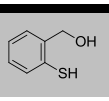	90 min	74%	**II-1a**
2	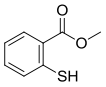	75 min	42%	**II-1b**
3	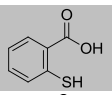	60 min	-	**II-1c**
4	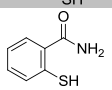	180 min	82%	**II-1d**

Table 3.6: *Summary of reaction conditions of acyl-aziridine **H** ring opening reaction to obtain 1-phenylthioceramide derivatives*

A final acetal deprotection step under acid conditions is required to obtain the final compounds **I-1**. Taking into account the purification problems of this kind of compounds, some volatile acids that could be removed under reduced pressure were screened in order to perform the reaction, avoiding further chromatographic separations of reagents. The test reactions were carried out using **II-1a** as model; results are summarized in **Table 3.7**. Initially, following procedures described in literature[38] TFA was attempted. This acid is widely used in acetal deprotection reactions with good yields and was used as our first candidate (*Entry 1 and 2*). Hence, different TFA conditions were tested and complex crudes were obtained showing mixtures of products. Attempted column chromatography purifications were unsuccessful. Other conditions were tried, using concentrated HCl aq. as acid, initially starting product was solved in DCM/MeOH and a complex mixture was obtained too (*Entry 3*). Finally reaction was repeated using HCl/dioxane and with this reagent the reaction worked smoothly to give a pure product after solvent evaporation. Surprisingly, the ^{1}H-NMR spectra was not in concordance with the expected one, showing aliphatic signals for protons 1H, 1'H, 2H, 3H and 4H with different shifts as those ones described in Dr. Alcaide's thesis. We hypothesized that the product obtained was a different product. Bibliography research revealed a possible explanation for this undesired product. I. F. Hermans and co-workers[39] describe a N→O acyl migration process under acidic conditions in αGalCer (**2**) and similar signal displacements were observed in our product (**Scheme 3.10**).

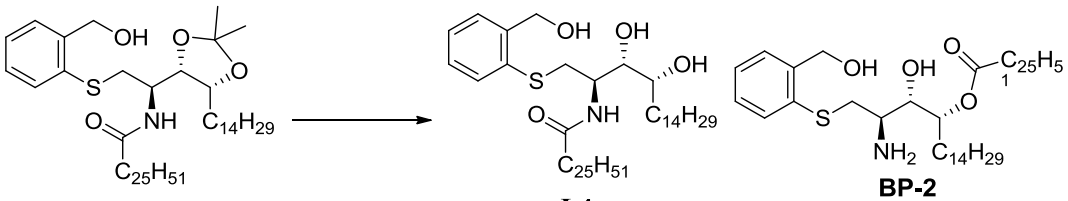

Entry	Acid	Solvents	Time	I-1a	BP-2
1	TFA	-	2h	Complex mixture of products	
2	TFA	DCM	2h	Complex mixture of products	
3	HCl	DCM/MeOH 5:2	2h	Complex mixture of products	
4	HCl	Dioxane/DCM	o.n.	Not detected	88% of **BP-2**

Table 3.7: *Summary of conditions with volatile acids used to achieve final acetal removal*

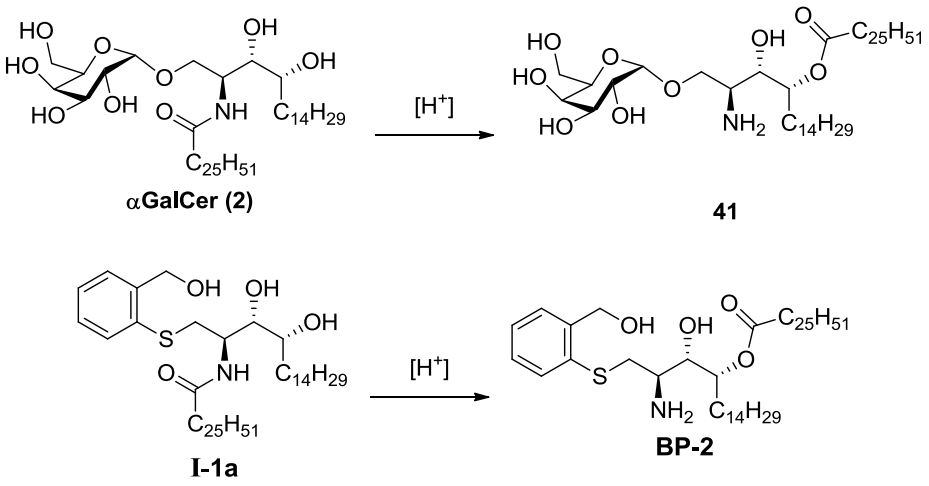

Scheme 3.10: *Hypothetic byproduct form under strong acid conditions*

In light of these findings and to minimize this side reaction, a softer acid should be used and removed from reaction medium before solvent evaporation to avoid crude concentration under acid conditions. To that purpose, Camphorsulfonic acid (CSA) was the selected one and neutralization with basic resin (such as IRA-400) was strategically used for acid removal. Different ratios of solvents, reaction concentration, temperature and reaction time were tested (**Table 3.8**).

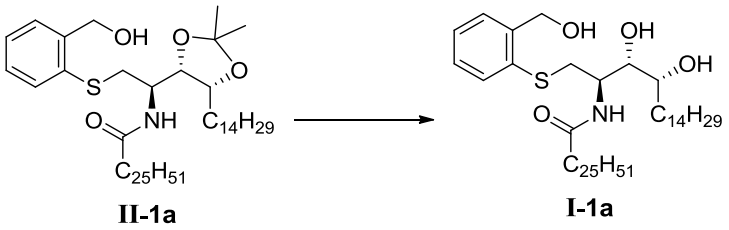

Entry	Acid	DCM/MeOH	[C]	Time	Temp	I-1a
1	CSA	DCM/MeOH 5:2	0,03M	o.n.	r.t.	33%
2	CSA	DCM/MeOH 1:1	0,01M	o.n.	r.t.	67%
3	CSA	DCM/MeOH 1:1	0,015M	o.n.	35ºC	40%

Table 3.8: *Summary of soft acid conditions of final acetal removal; all reactions were followed by basic resin IRA-400 treatment before solvent removal.*

In our hands, the best conditions were CSA in DCM/MeOH 1:1 at room temperature overnight, acid removal with basic resin IRA-400 and column purification (*Entry 2*); these conditions were then considered as general optimal methodology.

Bearing in mind all the expertise acquired from the previous experiments, the preparation of final products was carried out following the established general procedure in good to excellent yields (**Scheme 3.11**). It should be noted that **I-1b** was obtained with 67% yield after *flash* chromatography on Silica Gel purification while **I-1d** was obtained with 87% yield after product precipitation in DCM/MeOH 1,2:1. Remarkably, both products needed to be heated up to 30ºC to be totally solved in the

reaction mixture, they were allowed to reach room temperature and further stirred overnight to avoid acyl-migration or product degradation.

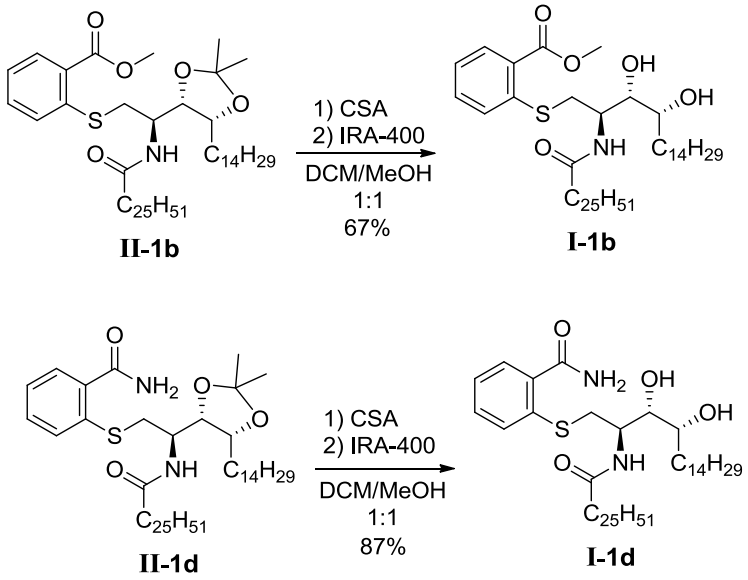

Scheme 3.11: *final deprotection to obtain target compounds* ***I-1b*** *and* ***I-1d***

Once methyl-ester derivative **I-1b** was obtained, ester hydrolysis under basic conditions (NaOH in THF/MeOH 5:1) gave desired acid **I-1c** in excellent yield (95%) (**Scheme 3.12**).

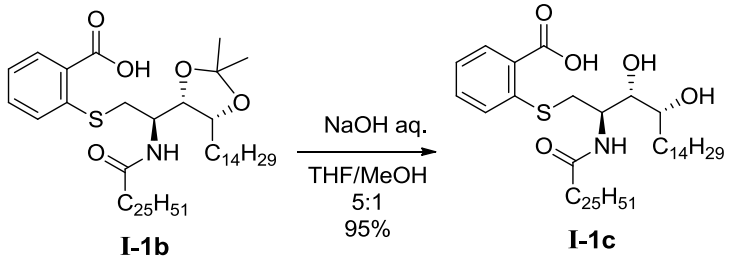

Scheme 3.12: *obtaining of final compound* ***I-1c*** *after ester hydrolysis of* ***I-1b***

In conclusion, the four target compounds were obtained. Compounds **I-1a**, **I-1b** and **I-1d** were obtained following acyl-aziridine **G** ring opening reaction strategy and subsequent acetal removal (**Scheme 3.5**) under acid conditions with 50%, 28% and 71% of overall yields. Finally, the acid derivative **I-1c** was obtained from basic hydrolysis of its methyl ester precursor in 27% of overall yield. Some other considerations were drawn from all this experiments. In general, these products were difficult to manipulate as aqueous/organic extractions were experimentally difficult. Moreover, the purification by *flash* chromatography on Silica Gel led to low product recovery even when the reaction crudes showed a main product. The final acetal deprotection was a delicate reaction and should be carried out under careful attention to avoid N→O acyl migration.

3.2.3. Synthesis of Aryloxyceramide derivatives (I-2)

The second synthetic objective of this thesis comprises a series of isosteric analogues of our initial *hit* compound in which sulfur was replaced by oxygen (compounds **I-2a** to **I-2d**, **Figure 3.25**).

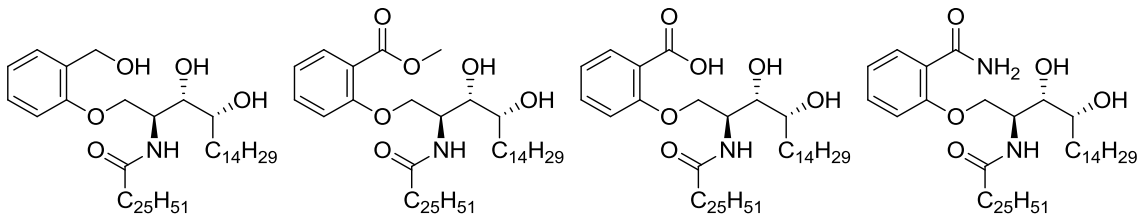

I-2a **I-2b** **I-2c** **I-2d**

Figure 3.25: *structures of phenol-like derivatives*

To attempt this synthesis, phenolic derivatives were tried to be implemented in the acylaziridine **G** strategy that proved successful with phenylthio-derivatives **I-1**. Therefore, the same methodology using microwave assisted reaction was our initial choice (**Scheme 3.13)**.

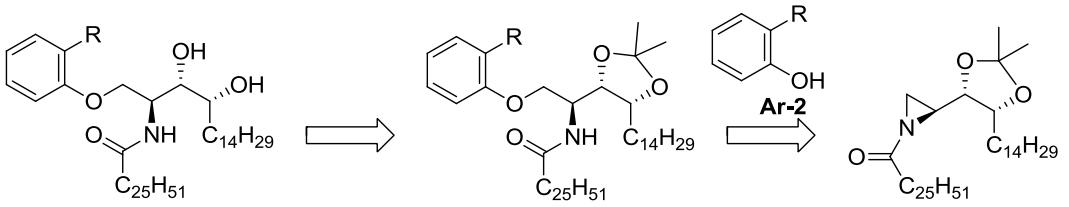

I-2 **II-2** **G**

R= CH_2OH, COOMe, COOH, $CONH_2$

Scheme 3.13: *Retrosynthesis of Aryloxy analogues type* ***I-1***

The aryloxyceramide synthesis was first tested with methyl-ester derivative **I-2b** (**Scheme 3.14** summarizes tested conditions) to obtain the ceramide derivative **II-2b**. All attempts to reproduce in the oxygen series the microwave assisted conditions of thiophenol reactions were unsuccessful. After 120 min the starting aziridine remained and no signals of new product formation were observed, reflecting the lower nucleophilicity of the phenolic- compounds (**Ar-2**) in front of thiophenolic ones (**Ar-1**).

Other strategies were explored following literature procedures. Exploring both aziridine ring opening with phenols and epoxides (as similar moieties), some papers agreed in Lewis Acid catalysis to favor phenol nucleophilic attack[40,41]. Comparing options found in literature, $BF_3{\cdot}Et_2O$ was estimated to be our best option as it was immediately available and reported as good catalyst[42] with a wide range of alcohols and showed moderate yields with phenol under microwave conditions. Following reported conditions, using acyl-aziridine **G** in DCM, with methyl salicylate and $BF_3{\cdot}Et_2O$ under microwave irradiation ad 75 W at room temperature gave a unique product after 5 min, showing complete reaction of the aziridine. However, the isolated product

was not the expected phenolic ether, since no H-aromatic signals appeared when analyzed by ^{1}H-NMR. MS and NMR data suggested an intramolecular reaction to form a 5-member ring resulting oxazoline **BP-3** (**Scheme 3.14**) as a single product.

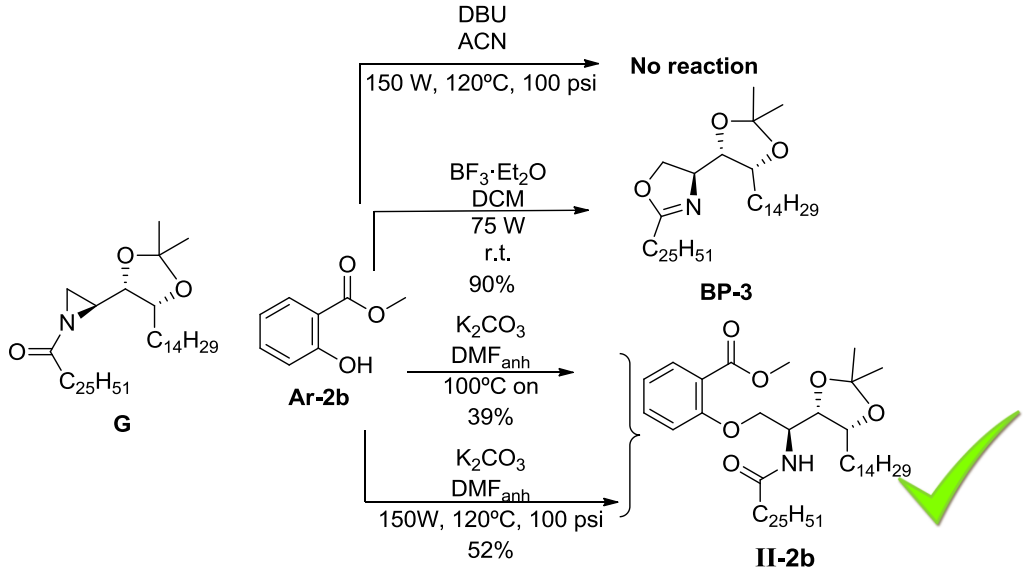

Scheme 3.14: *Synthesis of* ***I-2b*** *via acyl-aziridine* ***G*** *ring opening reaction*

In light of these results, the choice of an appropriate base seemed critical to increase aryl-OH nucleophilicity. More conventional conditions were tested using potassium carbonate as a base in anhydrous DMF at 100ºC. After 4 days reaction was stopped and analyzed showing promising results, desired product **II-2b** was obtained after *flash* chromatography on silica gel in moderate yield (39%). A reaction optimization was explored using similar reaction conditions under microwave irradiation (150 W, 120ºC and 100 psi). The desired product **II-2b** was obtained with slight yield improvement (52%) (**Scheme 3.14**).

Following the best conditions, salicylamide derivative **II-2d** was our subsequent target (**Scheme 3.15**). Acyl-aziridine **G** was mixed with salicylamide **Ar-2d** and potassium carbonate under inert atmosphere and solved in anhydrous DMF, sealed and irradiate at 150 W, 120º and 100 psi. Surprisingly, after 3 hours no starting aziridine was observed however the isolated product was the oxazoline **BP-3** instead of desired arylether **II-2d**. Again, poor nucleophilicity of hydroxyl was thought to be the main reason of reaction failure. It was decided to employ a stronger base under thermal conditions to allow a better control of the reaction progress. The acyl-aziridine **G** was mixed with salicylamide **Ar-2d** and sodium hydride under inert atmosphere with anhydrous DMF as solvent and the reaction was heated to 85ºC overnight. After final purification, the desired ether **II-2d** was obtained in moderate yield (38%) (**Scheme 3.15**).

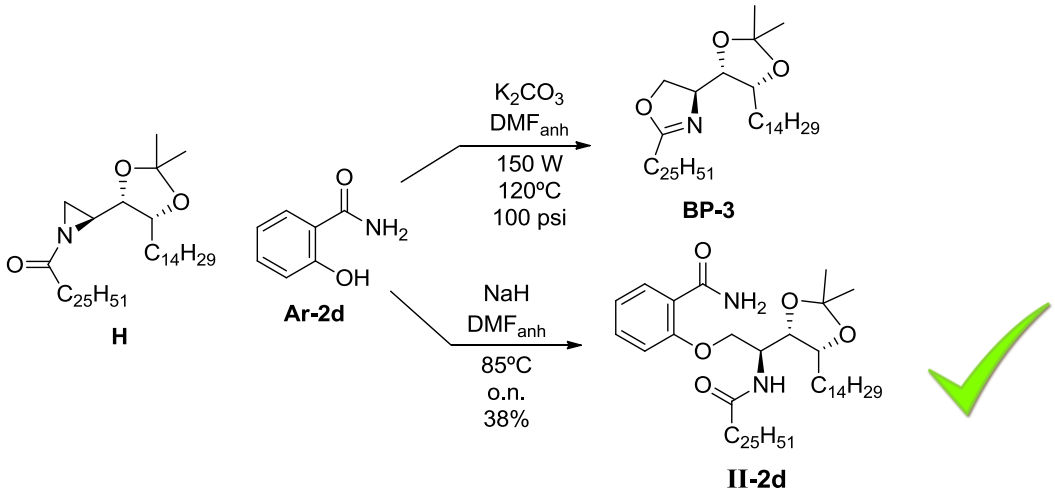

Scheme 3.15: *Synthesis of* ***II-2b***

An experimental observation was made during the purification of **II-2d** by column chromatography, the solutions of this compound showed blue fluorescence when illuminated with a UV lamp[43]. This property was general to all aryloxyceramide derivatives bearing a carbonyl group (**b**, **c** and **d**).

In parallel to that of **II-2b**, the synthesis of the 2-hydroxymethylphenoxy derivative **II-2a** (**Scheme 3.16**) was also undertaken. When the microwave conditions combined with NaH in DMF were used with acylaziridine **G** and 2-(hydroxyphenyl)methanol (**Ar-2a**) the final compound **II-2a** was obtained after chromatographic purification in low yield (20%). This result could not be confirmed in subsequent attempts to obtain a second lot of **II-2a** under apparent identical conditions, indicating a narrow margin of reproducibility. Thermal conditions were also tested although no reaction progress was observed (**Scheme 3.16**).

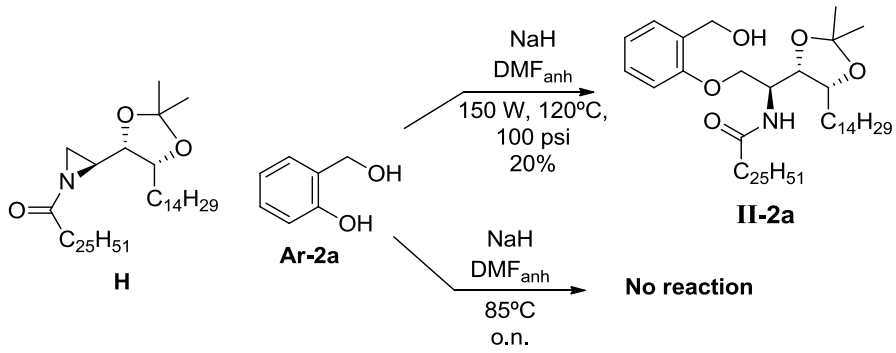

Scheme 3.16: *Synthesis of* ***II-2a***

At this point and bearing in mind the possibility of expanding our family of aromatic ethers, it became clear that the poor and somewhat capricious reactivity of acylaziridine **G** would be a serious drawback for medicinal chemistry optimization of these compounds. This was even more evident if aromatic moieties are non-commercial high value compounds. Therefore, we decided to explore a new strategy,

based on nosylaziridine **H**, which was previously used in our group in the synthesis of aminocyclitol phytosphingosine[6,19,20] derivatives (**Scheme 3.17**). A higher reactivity toward nucleophiles could be expected from the *N*-sulfonyl group at the expense of elongating the synthetic sequence. Our plan involved nosylaziridine **H** reaction with the phenol derivatives **Ar-2** in basic media to give type **III** intermediates. Nosyl-group removal would give amines **IV**, which could be acylated to give desired *O,O*-diprotected intermediate **II-2**.

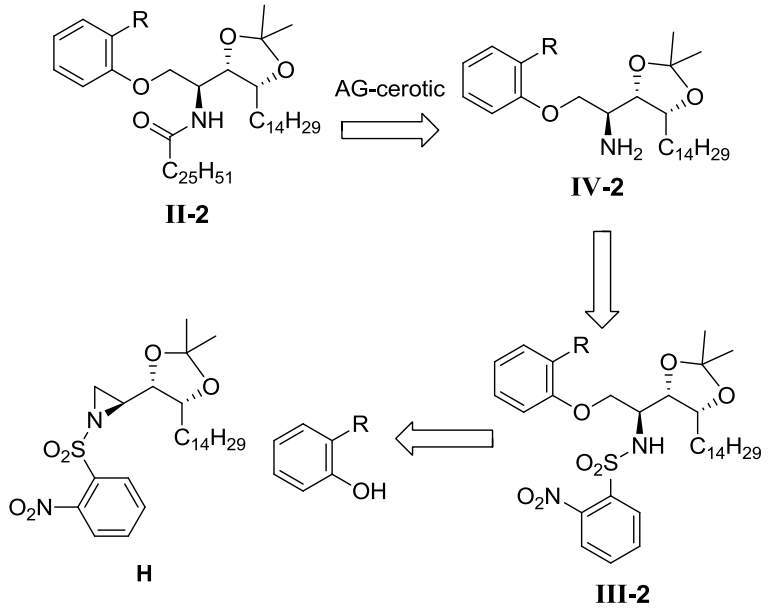

Scheme 3.17: *General retrosynthetic scheme of the nosylaziridine **H** route; *AG= activating group*

Although this new strategy involved more synthetic steps it had several benefits. In addition to the expected higher reactivity of the aziridine, the free amine intermediates **IV** increase synthetic versatility since could be acylated with any desired acyl chain, opening a wide range of opportunities to diversify the compound library.

So, this new synthetic route was initially tested to obtain **II-2a** (**Scheme 3.18**). Nosylaziridine **H** was reacted with 2-(hydroxyphenyl)methanol (**Ar-2a**) and cesium carbonate in ACN at 85ºC for 4 hours. Final purification yield 89% of desired compound **III-2a**. The *N*-nosyl group was removed with thiophenol and cesium carbonate in ACN at room temperature overnight, to give the desired amine **IV-2a** in good yield (82%) after purification. The obtention of *O,O*-diprotected phenolic ceramide derivative was subjected to the acylation step, in order to avoid free hydroxyl acylation, a selective reaction was carried out using cerotic acid, EDC and HOBT in AcOEt at room temperature with a small amount of DMF to solubilize the reagents. A Final purification yielded the desired compound **II-2a** in moderate yield (40%) (**Scheme 3.18**).

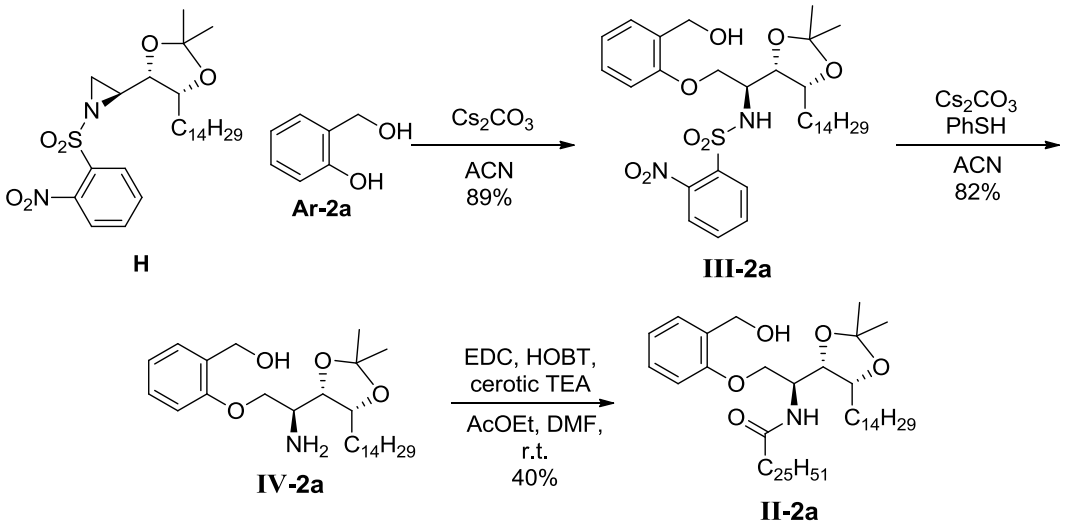

Scheme 3.17: *General retrosynthetic scheme of nosyl-aziridine **H** route; *AG= activating group*

This strategy seemed to be effective to incorporate phenol derivatives to the aromatic sphingolipids, even if they are not good nucleophiles. Furthermore, another advantage was that reaction crude purity after aziridine ring opening reaction was excellent, and could be used into next step without purification.

To test the efficacy and generality of the nosylaziridine **H** route, the methyl salicylate and salicylamide analogues were next attempted as a proof of the new synthetic concept. In this way, nosylaziridine **H** was mixed with phenol derivatives and cesium carbonate in ACN and heated at 85ºC for 4 hours until total aziridine reaction. Next the reaction mixture was allowed to reach room temperature, and a second batch of cesium carbonate and thiophenol were added and reaction was stirred overnight to directly remove the *N*-nosyl activating group. The free amine intermediates of type **IV-2** were obtained in excellent yields after two steps (86% for methyl salicylate and 95% for salicylamide) confirming the advantages of this approach(**Table 3.9**). These results confirm this strategy as a reliable and versatile alternative to the acylaziridine **G** route, opening new opportunities to expand the derivative scope.

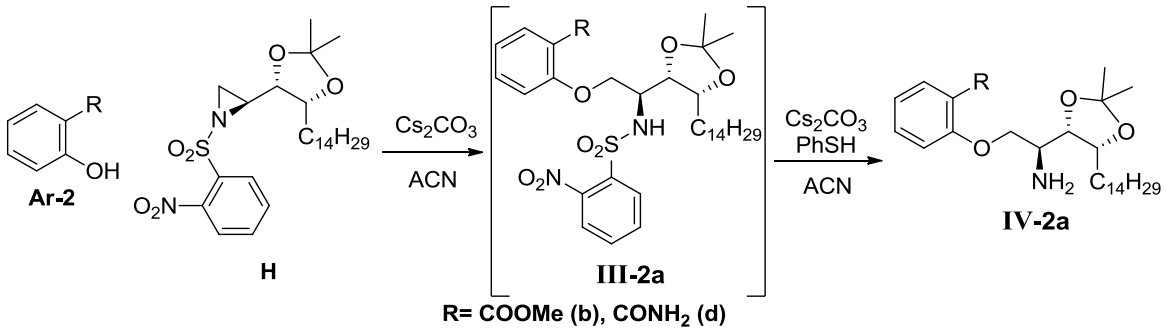

Entry	Ar-2	R	% overall
1	**Ar-2b**	COOMe	86
2	**Ar-2d**	$CONH_2$	95

Table 3.9: *Summary of nosyl-aziridine **H** ring opening and nosyl-group removal reactions with **Ar-2**.*

Once intermediates **II-2a**, **II-2b**, **II-2d** were obtained, final acetal removal was carried out using the previously established procedure. Thereby, intermediates **II-2** were mixed with CSA in $CHCl_3$/MeOH 1,2:1 to improve the poor solubility in DCM. Reactions were heated at 30ºC until no starting material remained. Reaction crudes were neutralized using basic resin IRA-400 and filtrated. Final compounds **I-2a** and **I-2b** were obtained in moderated yields (55% and 69% respectively) after purification by *flash* chromatography on silica gel. Final compound **I-2d** was isolated pure after filtration and solvent removal without further purification in quantitative yield (**Table 3.10**).

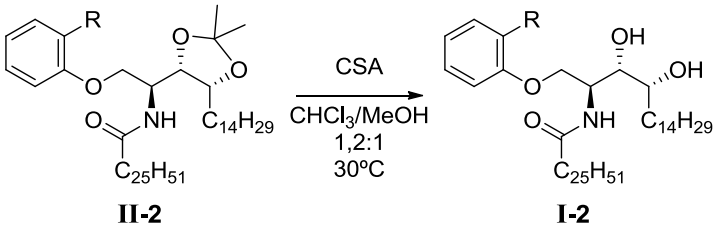

Entry	Initial product	Time	Final product	Yield (%)
1	**II-2a**	**o.n.**	**I-2a**	55%
2	**II-2b**	**2h 30ºC + r.t. o.n.**	**I-2b**	69%
3	**II-2d**	**4h**	**I-2d**	Quant.

Table 3.10: *Summary of final deprotection reactions to obtain target compounds **I-2** (phenol derivatives)*

Finally, the acid derivative **I-2c** was obtained from methyl ester precursor **I-2b** in THF/MeOH 5:1 and aqueous NaOH 2M in good yield (76%) (**Scheme 3.18**).

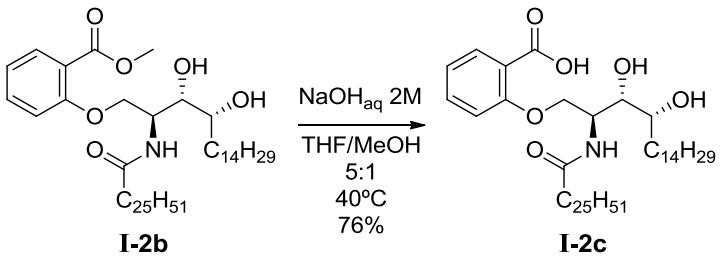

Scheme 3.18: *Hydrolysis of methyl-ester* ***I-2b*** *to acid* ***I-2c***

In summary, the desired compounds **II-2b**, **II-2b** and **II-2d** were achieved in moderate yields (36%, 38 and 27% respectively), the hydroxymethyl analogue **II-2a** was obtained with moderate yield in both strategies (11% via acyl-aziridine **G** and 16% via nosyl-aziridine **H**). It is worthy to mention that the ceramide derivatives were experimentally demanding, in particular on in liquid-liquid extractions using water; complex interphases were formed complicating product handling, for that reason it was better to purify reaction crudes directly after solvent removal. On the other hand, a new methodology was set up with excellent yields via nosyl-aziridine **H**, this strategy appeared more effective and reliable to integrate poor nucleophilic substrates, as well as facilitating the diversity of acyl chains in the final products.

3.2.4. Synthesis of Arylaminoceramide derivatives (I-3)

We next focused in the synthesis of some aniline-derivatives **I-3**. In light of good results obtained in the nosylaziridine **H** route with phenols, this strategy was chosen to synthesize this family (**Scheme 3.19**).

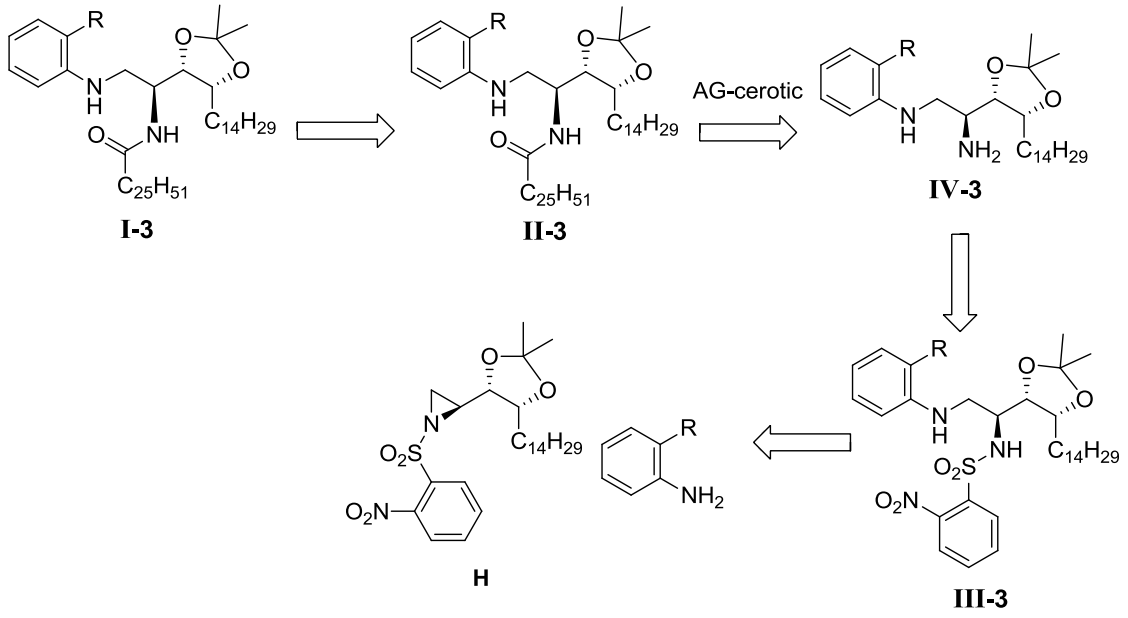

Scheme 3.19: *General retrosynthetic scheme of nosyl-aziridine* ***H*** *route to obtain aniline-derivatives* ***I-3****;*
**AG= activating group*

The first attempt was carried out with 2-(aminophenyl)methanol (**Ar-3a**) (**Scheme 3.20**). Nosyl-aziridine **H** was mixed with **Ar-3a** in ACN without base, reaction was heated at 85ºC 4 hours. Crude purification yield desired compound **III-3a** in good yield (84%). Freshly obtained intermediate **III-3a** was deprotected with cesium carbonate and thiophenol in ACN at room temperature overnight. After final purification desired free amine intermediate **IV-3a** was obtained with moderate-good yield (62%). Overall yield after two steps was 52%.

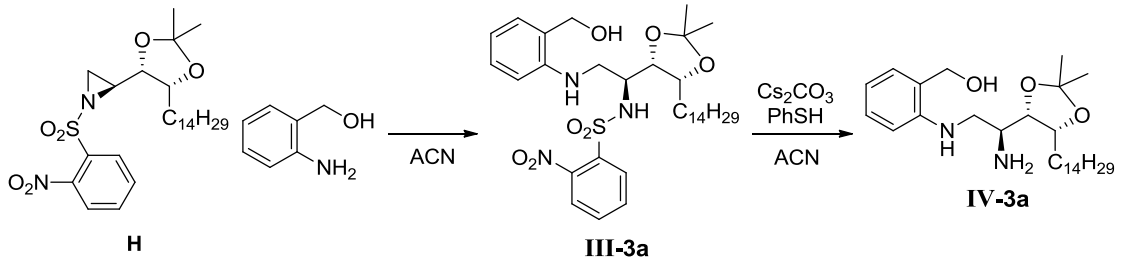

Scheme 3.20: *Synthesis of intermediate **IV-3a** via nosylaziridine **J** ring opening reaction*

A second strategy was also tested in which intermediate **III-3a** was not isolated. Thus, one-pot strategy was carried out, nosylaziridine **H** reacted under same conditions until total consumption, after cooling to room temperature, cesium carbonate and thiophenol were added and the reaction was stirred overnight. After final purification, the desired free amine intermediate **IV-3a** was achieved with excellent yield after two steps (84%) (**Table 3.11**). Yield improvement was achieved avoiding as much as possible column purification, as these products had low recovery when purified on silica gel. In is worthy to point out special instability of this intermediates in long term solution and especially sensitive to acid traces. During NMR characterization in $CDCl_3$, one of these intermediates completely degraded.

In light of this excellent result, the other arylamino derivatives were obtained following one-pot strategy (**Table 3.11**). In this way, from nosylaziridine **H** and methyl 2-aminobenzoate (**Ar-3b**) or 2-aminobenzamide (**Ar-3d**), **IV-3b** (85%) and **IV-3d** (92%) were respectively prepared (**Table 3.11**).

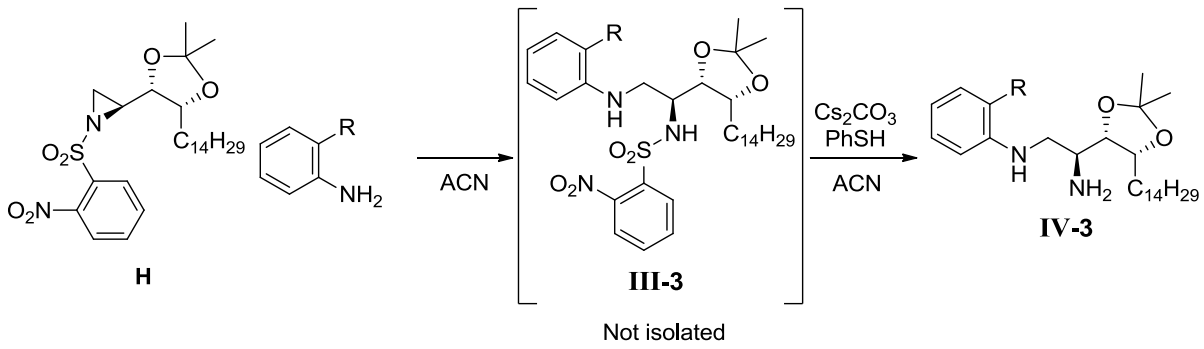

Aniline	Step 1 conditions	Step 2 conditions	Yield
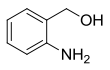	ACN at 0,1 M 85ºC 4 hours	Cesium Carbonate 4eq. Thiophenol 3 eq. ACN at 0,1 M r.t.; o.n.	84%
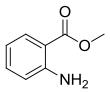	ACN at 0,1 M 85ºC 4 hours	Cesium Carbonate 4eq. Thiophenol 3 eq. ACN at 0,1 M r.t.; o.n.	85%
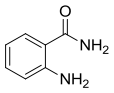	ACN at 0,1 M 85ºC 4 hours	Cesium Carbonate 4eq. Thiophenol 3 eq. ACN at 0,1 M r.t.; o.n.	92%

Table 3.11: *Summary of intermediates* ***IV-3*** *via nosylaziridine* ***H*** *ring opening and nosyl-removal one-pot strategy*

With the amine intermediates **IV-3** in hand, the primary amine acylation was attempted. Bearing in mind the precedent problems encountered in liquid-liquid extraction of this type of lipidic compounds, we considered acylation strategies avoiding the extractive reaction work-up using water. For ester and amide derivatives, as no side *O*-acylation could occur, a classical acylation using acid chloride were used. For the 2-hydroxymethyl derivative an amino selective activating agent was chosen: NHS derivative of cerotic acid. As it can be observed in **Table 3.12**, the results for the acylation step were from moderated to good after product isolation by column chromatography.

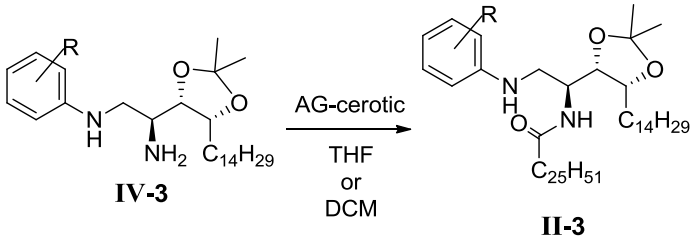

R= CH_2OH, COOMe, $CONH_2$
AG= Cl or NHS

Starting intermediate	Acylation agent	Solvent and reaction conditions	Yield
IV-3a	NHS-cerotic	TEA 3 eq, THF_{anh} at 0,06 M; 50ºC, o.n.	75%
IV-3b	Cl-cerotic	TEA 1,5 eq, DCM_{anh} at 0,08 M; 50ºC, o.n.	50%
IV-3d	Cl-cerotic	TEA 1,5 eq, DCM_{anh} at 0,07 M; 50ºC, o.n.	75%

Table 3.12: *Summary of intermediates* ***II-3*** *obtaining after acylation reactions*

It is worth mentioning that reaction crude before purification ^{1}H-NMR spectra showed clean spectrum with good to excellent conversion of reactions, however yields after purifications never reached such good results. As it was mentioned before, *Flash* chromatography on Silica Gel of the compounds with these long lipid chains lead to low recovery. In the phenol and thiophenol series a similar behavior was observed.

The final compounds **I-3** were achieved following the general procedure with CSA as it was previously described (**Table 3.13**). These acetal cleavage reactions worked properly for compounds **I-3b** and **I-3d** with 87% yield for first one after column purification and 50% for the second one after product precipitation after adding small amount of water.

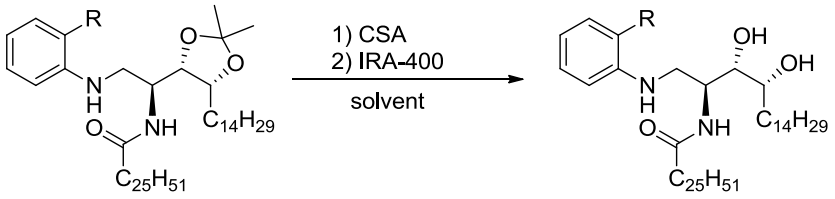

II-3 **I-3**

Entry	Starting product	R	Solvent	conditions	Final product	Yield (%)
1	**II-3a**	CH_2OH	$CHCl_3$/MeOH	3h 30ºC	**I-3a-Me**	51%
2	**II-3a**	CH_2OH	Dioxane/water 10:1	r.t. , o.n.	**I-3a**	11%
3	**II-3b**	COOMe	$CHCl_3$/MeOH	11h 30ºC	**I-3b**	87%
4	**II-3d**	$CONH_2$	$CHCl_3$/MeOH	4h 30ºC	**I-3d**	50%

Table 3.13: *Summary of final deprotection results of aniline derivatives* ***I-3***

Surprisingly, an unexpected product was obtained when **II-3a** was reacted under general conditions. In this case, reaction mixture was heated at 30ºC and stirred 3 hours until total disappearing of starting material. After the usual work-up and purification a white solid was obtained (51%). The ^{1}H-NMR spectra was compatible with the desired compound however with an extra singlet consistent with the presence of a methoxy group. MS data confirm it corresponded to the methylated derivative **I-3a-Me**.

As it was observed with other precursors, the position 2 of aniline derivatives was especially unstable when it was substituted by a hydroxymethyl group, compound degradation were detected during nosyl-group removal, and the products in solution lead to progressive deterioration . In this case, the compound reactivity was revealed by integration of a methoxy substituent in the main product during acetal removal, presumably coming from the MeOH solvent used (**Scheme 3.21**). Similar reactions are well precedented in literature, involving a *o*-quinone methide imines as intermediates[44], which have been used in self-immolative linkers[45] and cycloaddition

reactions starting from 2-hydroxyalkylanilines under acidic catalysis[46,47], similar to the conditions here employed.

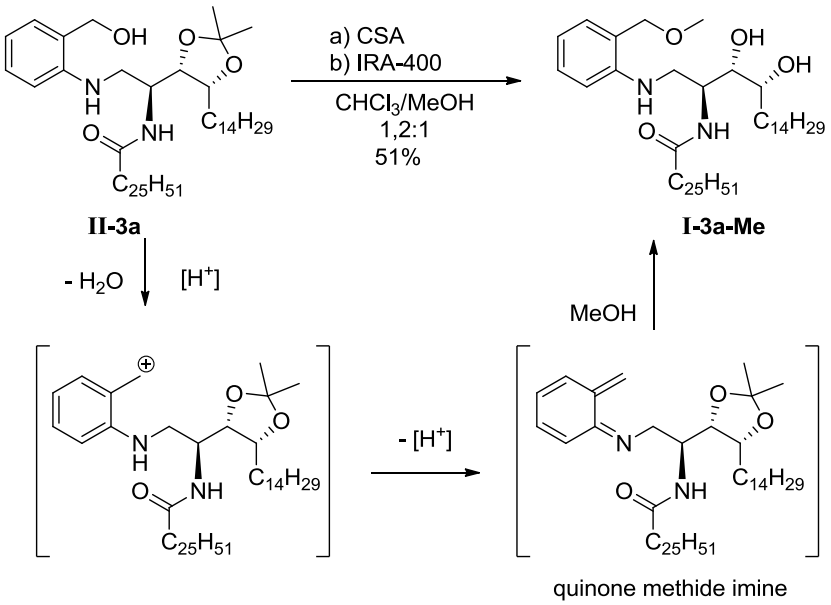

Scheme 3.21: *Hypothetic mechanism of byproduct* ***I-3a-Me*** *formation*

To avoid the formation of byproduct **I-3a-Me**, a similar procedure was followed using CSA and Dioxane/water 10:1 as solvents instead of $CHCl_3$/MeOH. Reaction was stirred at room temperature overnight and stopped by neutralization with basic resin IRA-400. The final purification give desired compound **I-3a** in low yield (11%).

Finally, the synthesis of the acid derivative **I-3c** was tackled from its ester precursor **I-3b**. Similar reaction conditions to those proved successful in preceding aromatic acids were used. Although the product was detected by HPLC-MS, all attempts to purify this product form its precursor and other reaction impurities were ineffective (**Scheme 3.22**).

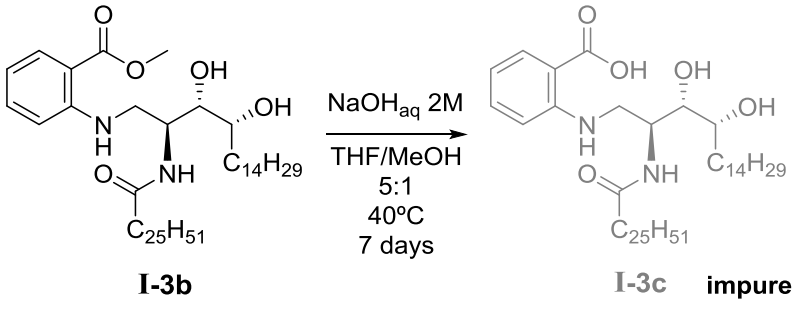

Scheme 3.22: *hydrolysis of methyl-ester* ***I-3b*** *to obtain target acid* ***I-3c***

Concluding, aniline derivatives **I-3a**, **I-3b** and **I-3d** were obtained in low to moderate yield after 3 steps (7%, 37% and 35% respectively) (**Figure 3.26**). When the hydroxymethyl intermediate **II-3a** was treated under general conditions for acetal removal, a methylated byproduct **I-3a-Me** was obtained, again showing high sensitive

of this product, especially under acidic conditions. Unfortunately, acid compound **I-3c** could not be isolated in pure state, although its formation was confirmed by HPLC-MS. This family confirmed the versatility of nosylaziridine **H** route to incorporate poor nucleophilic reagents.

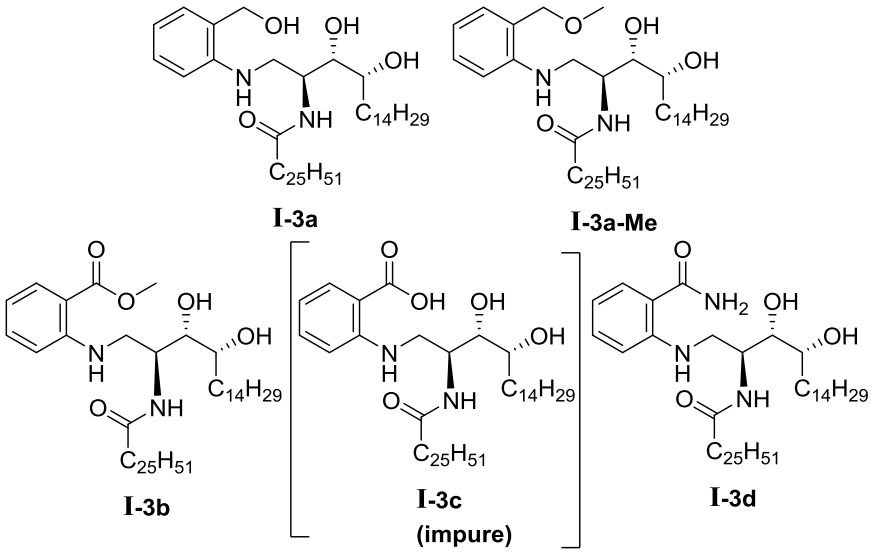

Figure 3.26: *Target aniline-ceramide derivatives* ***I-3***

3.2.5. Synthesis of 2-*O*-linked-pyridineceramide derivatives (I-4)

As it was mentioned at the beginning of this chapter, phenyl ring replacement by pyridine was considered of interest in order to modify physicochemical properties of compounds, specially related to polarity increase or water solubility improvement. In this sense, target compounds **I-4a** to **I-4d** were designed (**Figure 3.27**).

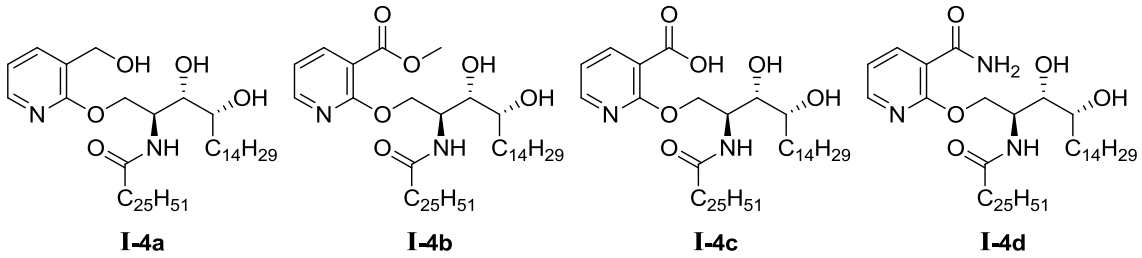

Figure 3.27: *Target 2-o-linked-pyridine-ceramide derivatives* ***I-4***

A new synthetic strategy was planned for this kind of compounds (**Scheme 3.23**) involving the azido-alcohol **D** , an intermediate in the sphingoaziridine synthetic route, as nucleophile to attack the electrophilic 2-halopyridine ring via aromatic nucleophilic substitution. This would lead to new azido-pyridine intermediates **V**, which could be reduced to free amine intermediate type **IV**, which after *N*-acylation and acetal deprotection would afford the target compounds **I-4**.

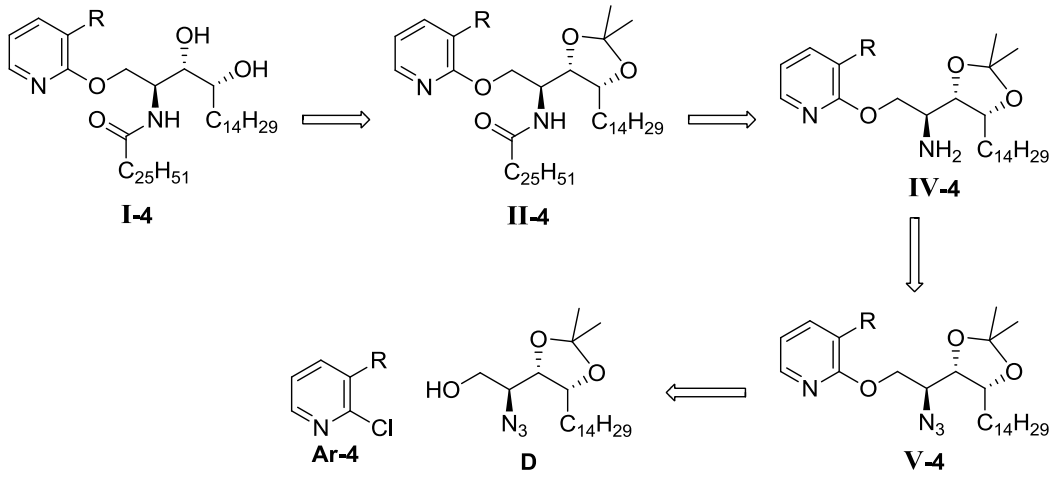

Scheme 3.23: *Retrosynthetic route for 2-O-linked-pyridine-ceramide derivatives* ***I-4*** *obtaining*

The first attempts were carried out with the readily available 2-chloronicotinamide **Ar-4d** (**Scheme 3.24**) to obtain azido-pyridine derivative **V-4d**. Initially, a small scale reaction was tested using 1 eq. of **Ar-4d**, 1 eq. of sodium hydride as base in anhydrous DMF at 85ºC. Final purification yield 22% of the desired product. Although the yield was not optimal, this could be improved when the reaction scale was increased, indicating a possible effect of adventitious moisture in the reaction. In this attempt, 1,1 eq of **Ar-4d**, 2 eq of sodium hydride instead of 1 eq. used in previous reaction, reaction was slightly more concentrated (from 0,08 to 0,13M) in anhydrous DMF. Reaction was faster and after overnight no starting azido-alcohol **D** remained. After work-up, ^{1}H-NMR showed a unique product and excellent purity.

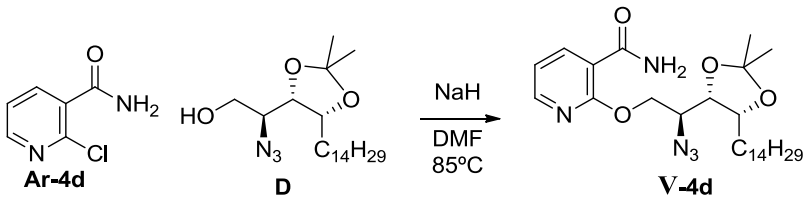

Scheme 3.24: *First azido-pyridine intermediate type* ***V*** *obtained via aromatic nucleophilic substitution of 2-chloronicotinamide* ***Ar-4d*** *by azido-alcohol* ***D***

To face the hydroxymethyl derivative synthesis, 2-chloro-3-pyridinealdehyde **Ar-4a'** was chosen as precursor to avoid hydroxyl competitive deprotonation and possible side-reactions. Initial attempts to synthesize aldehyde-pyridine-azido intermediate **V-4a'** were carried out using same conditions previously established for the benzamide preparation (**Table 3.**14, *Entry 1*) without success. Different reaction conditions were tested, but unsuccessful results were obtained with this strategy. Base screening was done and finally lithium tert-butoxide was the only one the best one (**Table 3.14**). Surprisingly, directly aldehyde reduction *in situ* was observed during this reaction, as the hydroxymethyl-azido derivative **V-4a** was isolated after column purification.

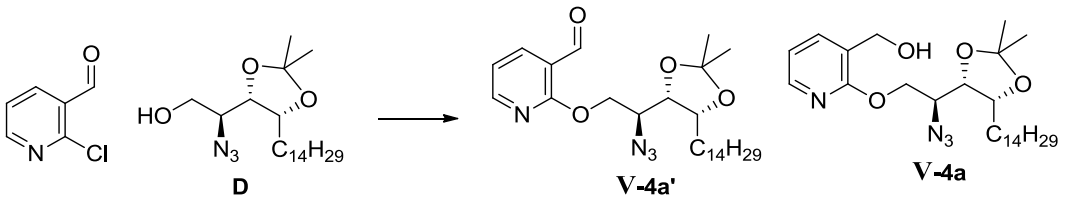

Entry	Conditions	% V-4a'	% V-4a
1	NaH, DMF 0,1M, 85ºC o.n.	Complex mixture	
2	Cs2CO3, cat., NaH, DMF 0,1M, 85ºC o.n.	Complex mixture	
3	Li^{t}BuO, DMF 0,1M, 85ºC o.n.	10	10
4	Li^{t}BuO, DMF 0,1M, 85ºC weekend	Not detected	17

Table 3.14: *Summary of reactions carried out to obtain intermediate* ***V-4a'*** *and direct obtaining of* ***V-4a***

In parallel to this reaction, methyl-ester derivative **V-4b** synthesis was faced (**Table 3.15**). Although similar conditions were tested, in this case best results (70%) were obtained with NaH with similar conditions as amide-derivative **V-4d** (**Table 3.15**, *Entry 5*). It is worth mentioning that high purity of azido-alcohol **D** is needed to carry out this reactions, as presence of traces of TBDPS derived products(tolerated for aziridine route) coming from its deprotection are negative influencing the reaction progress.

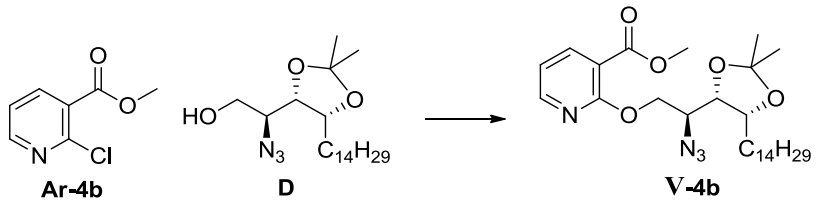

Entry	Conditions	% V-4b	Comments
1	Cs_2CO_3, cat., NaH, DMF 0,1M, 85ºC o.n.	0	Complex mixture
2	NaH, DMF 0,1M, 85ºC o.n.	62	Dirty crude
3	Li^{t}BuO, DMF 0,1M, 85ºC o.n.	0	Product degradation
4	Li^{t}BuO, DMF 0,1M, 85ºC weekend	0	Product degradation
5	NaH, DMF 0,1M, 50ºC o.n.	70	Clean crude, column purification

Table 3.15: *Summary of reactions carried out to obtain intermediate* ***V-4b***

Once all azido intermediates **V** were obtained, the azide reduction to amide was examined. Again, the amide derivative was used to set up properly the reaction conditions. In order to obtain free amino intermediate **IV-4d** and avoid column purification after liquid-liquid extractions, which were always experimentally troublesome and notably reduced product yields, we thought that hydrogenation with Pd catalysis could be an attractive strategy, as reaction treatment simply involved filtration and solvent evaporation (**Table 3.16**). A small scale test was carried out using Pd/C catalyst and THF/MeOH 1:1 as solvents, common conditions in our lab for similar reactions. Reaction was left overnight and TLC did not show starting material, reaction was filtrated off and concentrated in vacuum. Surprisingly, the 1H-NMR spectra showed a mixture of products without aromatic signals (**Figure 3.28**).

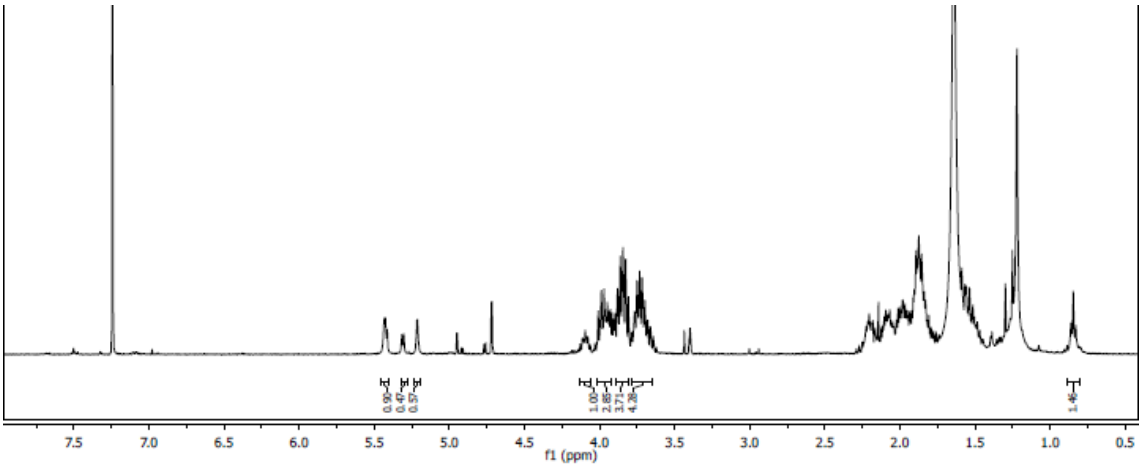

Figure 3.28: *1H-NMR spectrum of first azido-reduction reaction crude after filtration*

Our hypothesis was that the pyridine ring was reduced under the hydrogenation conditions. Several conditions were tested and reaction progress was temporally monitored instead of leaving it to run overnight (**Table 3.16**). When reaction was carried out in MeOH/THF 1:1 either with Pd/C or $Pd(OH)_2/C$ a complex mixture was observed by TLC control at 1h, showing the formation of pyridine-reduction by-product (*Entries 2 and 3*). Gratifyingly, with AcOEt as solvent (*Entry 4*) the reaction rate decreased, and the starting product remained after 1 hour and a new product was formed - without evidence of formation of over-reduced byproducts. After 4 hours the reaction was complete and the desired intermediate **IV-4d** was obtained in quantitative yield.

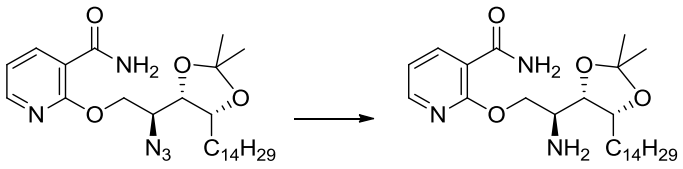

V-4d **IV-4d**

Entry	Conditions	Time	% IV-4d	Comments
1	Pd/C cat. MeOH/THF 1:1	o.n.	Not detected	Pyridine reduction observed by ^{1}H-NMR
2	Pd/C cat. MeOH/THF 1:1	1h	Not detected (TLC)	By-product formation
3	$Pd(OH)_2/C$ cat. MeOH/THF 1:1	1h	Not detected (TLC)	By-product formation
4	Pd/C cat. AcOEt	4h	Quant.	No side-reaction observed

Table 3.16: *Summary of reactions carried out to obtain intermediate* ***IV-4b***

The following reactions were carried out using these conditions (**Table 3.17**) giving amine **IV-4a** from precursor **V-4a** in quantitative yield, while methyl-ester intermediate **IV-4b** was obtained from its azido precursor **V-4b** in good yield (78%).

V-4 **IV-4**

Entry	Starting product	Conditions	% IV-4
1	**V-4a**	Pd/C cat. AcOEt, 4h	Quant. (**IV-4a**)
2	**V-4b**	Pd/C cat. AcOEt, 4h	78% (**IV-4b**)

Table 3.17: *Summary of reactions carried out to obtain other two intermediates* ***IV-4***

The acylation of intermediates **IV-4** to obtain *O,O*-diprotected-ceramide intermediates **II-4** were examined under specific conditions of each compound. As it is indicated in **Table 3.18**, the three desired compounds were obtained in moderate yield after column chromatography purification. In the cases of hydroxymethyl derivative **II-4a** and the amide derivative **II-4d**, good reaction conversion and clean crude reaction were obtained but, again, the product recovery after column purification was low, reducing the isolated yields.

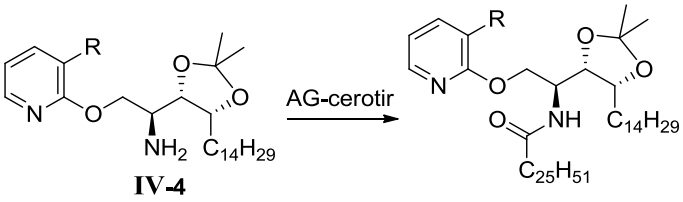

IV-4 **II-4**

Entry	Starting product	Conditions	% II-4
1	**IV-4a**	NHS-cerotic, TEA DCM 50ºC, o.n.	55% (**II-4a**)
2	**IV-4b**	Cl-cerotic, TEA THF, 50ºC, o.n.	52% (**II-4b**)
3	**IV-4d**	NHS-cerotic, TEA THF, 50ºC, o.n.	37% (**II-4d**)

Table 3.18: *Summary of acylation reactions to obtain intermediates* ***II-4****; AG=activating group*

The final compounds **I-4** were obtained using the acetal deprotection established conditions in moderate yields (**Table 3.19**). The hydroxymethyl derivative **I-4a** required purification by *flash* chromatography on silica gel, again decreasing reaction yield (39%). Methyl-ester derivative **I-4b** was obtained as pure solid after reaction filtration in moderate yield (67%). Amide derivative **I-4d** was similarly obtained in moderate yield (48%). This product precipitated after reaction neutralization with basic resin; any attempt to dissolve the product was unsuccessful so it was filtrated off together with resin and manually separated from it.

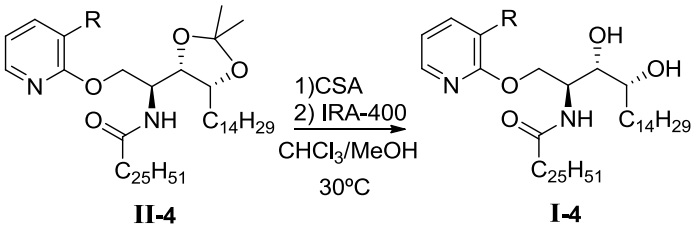

II-4 **I-4**

Entry	Starting product	Time	Reaction treatment	% II-4
1	**II-4a**	3h	Column purif.	39% (**I-4a**)
2	**II-4b**	3,5h	Filtration	67% (**I-4b**)
3	**II-4d**	1h	Precipitation	48% (**I-4d**)

Table 3.19: *Summary of final deprotection to reach target compounds* ***I-4***

Finally, the acid derivative **I-4c** was obtained by ester hydrolysis in THF/MeOH and NaOH 1M at 50ºC overnight. A white solid appeared which was filtrated off, suspended in MeOH and neutralized with concentrated TFA added dropwise until neutral pH. Again a white precipitated appear which was filtrated and dried in vacuum to yield (51%) of desired compound **I-4c**. This product had extremely low solubility and its characterization was difficult to complete (**Scheme 3.25**).

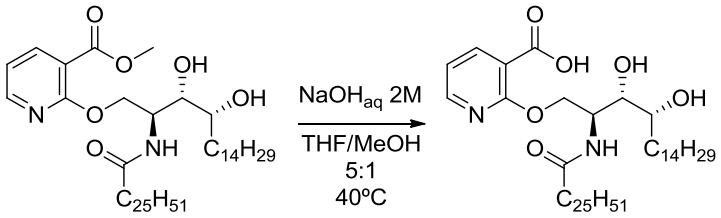

I-4b **I-4c**

Scheme 3.25: *hydrolysis of methyl-ester* ***I-4b*** *to obtain target acid* ***I-4c***

To conclude, all four target compounds **I-4** were synthesized with moderate yields. A new synthetic route allowed incorporating pyridine moieties with diverse results depending on the chloropyridine reactivity. The purity of azido-alcohol **D** was playing an important role in reaction progress. We solved the problems in the azide reduction step, which should be carried out under careful attention to minimize pyridine ring reduction. The acylation and final deprotection steps worked acceptably under the general procedures established during present doctoral thesis.

3.2.6. Synthesis of 2-*S*-linked-pyridineceramide derivatives (I-5)

Finally, the last collection of target compounds considered comprised the 2-*S*-linked-pyridines **I-5** (**Figure 3.29**).

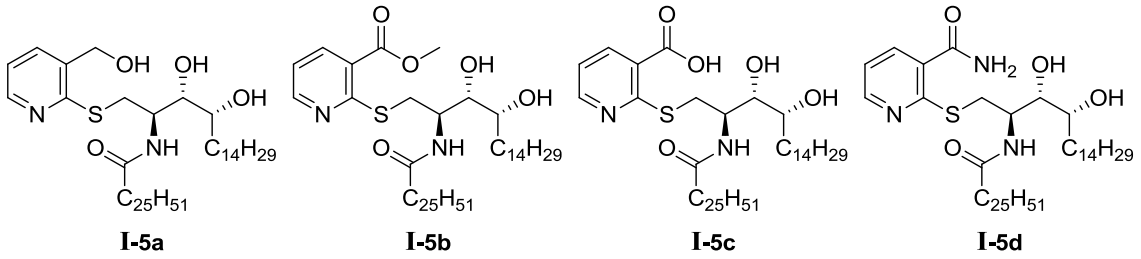

Figure 3.29: *chemical structure of target 2-S-linked-pyridine derivatives* ***I-5***

The synthesis of this family was planned in analogy of the previously oxygen bridged pyridines **I-4**. As a nucleophilic sulfur derivative of phytosphingosine was needed (**Scheme 3.26**), taking advantage of mesylazido intermediate **E** as a precursor of aziridine synthesis, incorporating sulfur atom at that stage was our strategy to obtain acetylated thio-azido intermediate **J** (see the synthesis at section 3.2.1). From intermediate **J**, the free thiol **K** could be obtained and subsequent reaction with 2-chloropyridines **Ar-4** would give azido intermediates **V-5**. Following steps would follow the preceding synthesis of the 2-alkoxypyridines: azide reduction to amine, acylation and final acetal removal would hit to desired final compounds **I-5**.

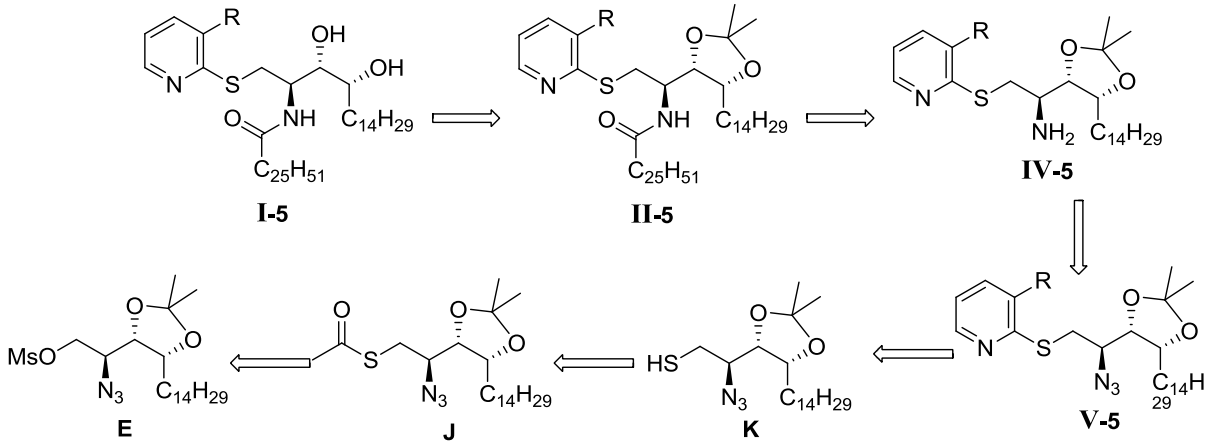

Scheme 3.26: *Retrosynthetic route for 2-S-linked-pyridine-ceramide derivatives* ***I-5*** *obtaining*

Aware of possible chemical incompatibility of a thiol and an azide in the same molecule, we checked literature to look for precedents of this type of compounds. We were encouraged by some reported compounds bearing both moieties[48-51], which prompted us to isolate thio-azide intermediate **K**. Unfortunately, this first strategy involving the isolation of intermediate **K** from the reaction mixture was unsuccessful.. Alternatively, it was thought that the free thiol could be directly generated *in-situ* and allowed to react with the 2-chloropyridine (**Table 3.20**). After extensive experimentation, acetyl-thio intermediate **J** reaction with chloropyridine **Ar-4d** in degassed DMF with cesium carbonate were the only conditions in which the desired product was obtained in low isolated yield (30%).

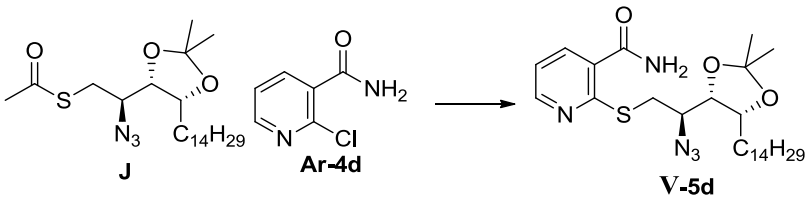

Entry	Reaction conditions	% V-5d	Comments
1	NaOH 0,2M; $MeOH_{degassed}$, 40ºC on	Not detected	No reaction
2	TEA; $MeOH_{degassed}$, 40ºC on	Not detected	Complex mixture
3	Cs_2CO_3; $DMF_{degassed}$, H_2O, 85ºC on	30%	Complex crude

Table 3.20: *Summary of tested conditions to reach target compound* ***V-5d***

Based in these findings, the reactions of 2-hydroxymethyl and 2-methoxycarbonyl chloropyridines **Ar-4a** and **Ar-4b** were carried out under same conditions (**Scheme 3.27**). In the case of methyl-ester derivative **V-5b** was obtained with low yield (11%), however the hydroxymethyl derivative **V-5a** was not detected in the crude mixture.

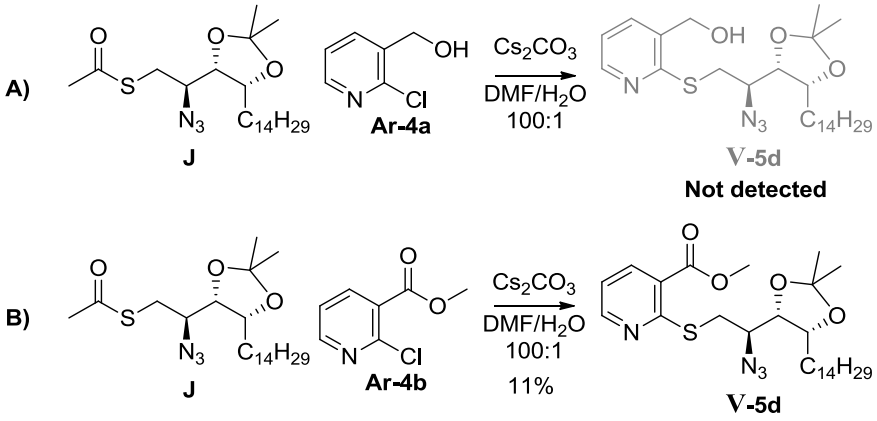

Scheme 3.27: *2-S-linked-pyridine derivatives* ***I-5*** *by aromatic nucleophilic substitution*

In light of complexity of these reactions, it was thought to invert reactivity, used 2-thiopyridines as nucleophiles to displace mesylate group onto intermediate **E** (**Scheme 3.28**). Unfortunately, the desired thiopyridines were not commercially available, so at this point, it was decided to postpone the synthesis until the first biological results of the aromatic ceramides were supporting the interest in this series.

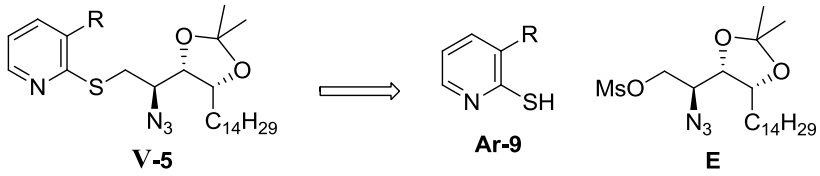

R= CH_2OH (a), COOMe (b), COOH (c), $CONH_2$ (d)

Scheme 3.28: *Retrosynthetic route for 2-S-linked-pyridine derivatives* ***I-5*** *obtaining by mesylate displacement*

In conclusion, chloropyridine reaction with the 1-thiolate derivative of phytosphingosine was attempted, with diverse results depending on the pyridine used.

In any case, *in-situ S*-deacetylation and nucleophilic substitution was the only strategy that minimally worked. Their synthesis will be attained in subsequent future studies after biological data in the obtained compounds confirm their potential bioactivity

3.2.7. Summary of results and final remarks

The desired key intermediates azido-alcohol **D**, acylaziridine **G**, nosylaziridine **H** and acetylthiosphingosine **J** were obtained with excellent yields starting from commercial phytosphingosine hydrochloride.

Non-commercially available 2-mercaptobenzmide (**Ar-1d**) was obtained by benzothiazolone **Ar-8** reduction in moderate yield (55%).

The aryl-ceramide families designed at the beginning of the present doctoral thesis comprise five scaffolds, four out of these five families were synthesized in low to moderate overall yields. Phenylthio, phenyloxy, phenylamino and 2-*O*-linked-pyridine derivatives targets were reached while only 2-*S*-linked-pyridine derivatives are pending. Three different synthetic strategies were followed: azylaziridine **H** ring opening reaction, nosylaziridine **G** ring opening reaction or the aromatic nucleophilic substitution of 2-chloropyridines.

The final acetal removal showed problematic side-reaction when strong acids were used, prompting N→O acyl migration and byproduct formation. A general methodology was set up to minimize this side-reaction.

Those compounds bearing a carbonyl group as substituent (COOMe – **b**, COOH – **c** and $CONH_2$ – **d**) showed fluorescent properties under blue light.

The nosylaziridine route showed an excellent reactivity as a phytosphingosine moiety to incorporate poor nucleophilic aromatic scaffolds, such as aniline derivatives. This methodology was used to synthesize around 50 new compounds for library extension in order to broaden the chemical diversity of our family and further protect these new compounds under a patent.

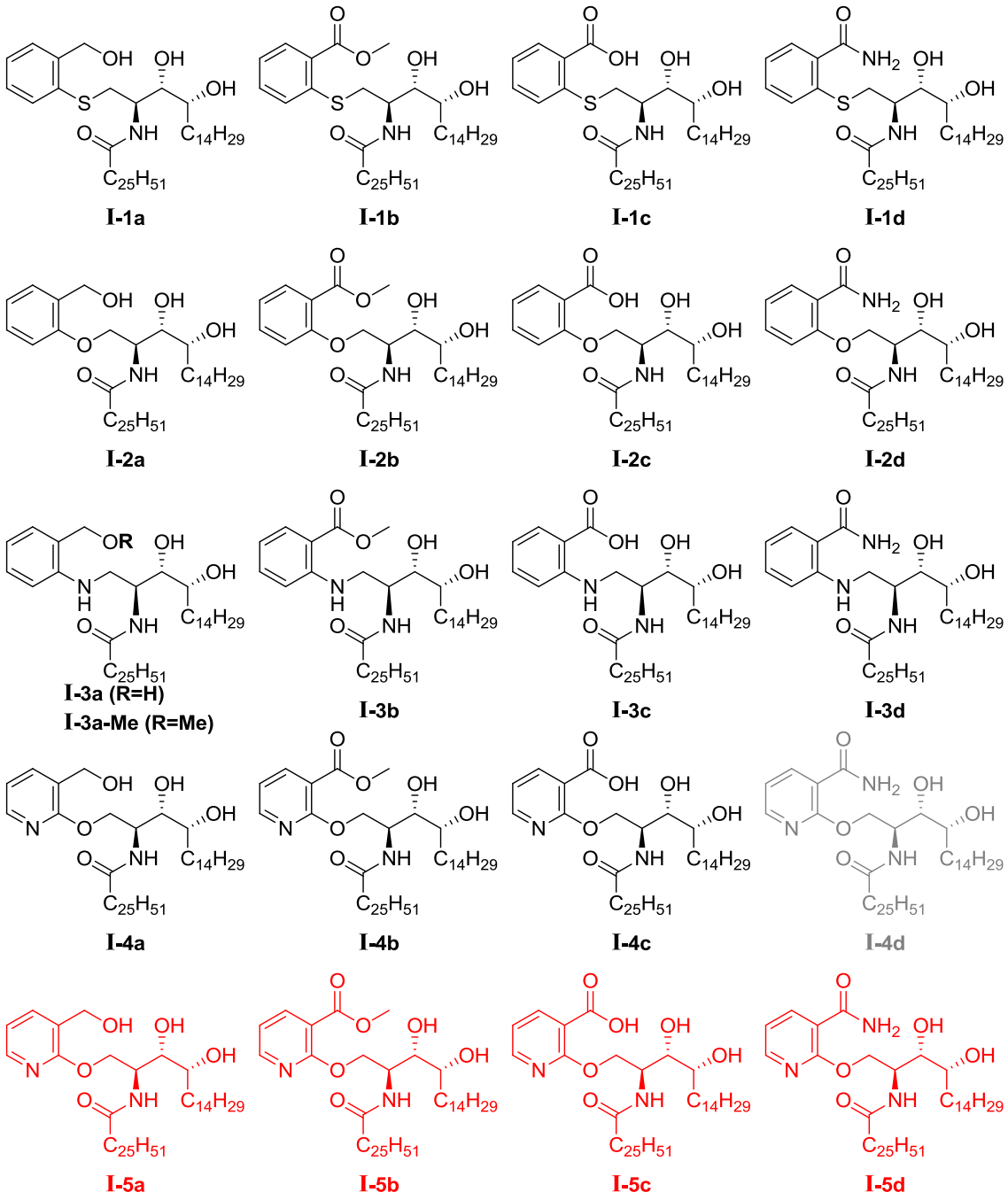

Figure 3.30: *Summary of compounds obtained*

3.3. CHAPTER 3: Biological activity of the new aromatic-ceramide family as NKT cell activators

The immunological versatility of NKT cells makes them an attractive therapeutic target. Their implication in early Immune System response confers them a promising position to modulate the treatment of a wide range of disorders from autoimmune disease[52] to cancer[53,54], among others[55-59]. Some decades ago, a natural compound isolated from a sponge, agelasphin, was identified as NKT activator and KRN7000, its synthetic analogue, resulted in a powerful antigen of these cells: it is known as αGalCer (**2**). Upon NKT activation with this glycolipid, a huge release of cytokines is triggered, without discrimination between the pro-inflammatory (T_H1) and the anti-inflammatory (T_H2) ones. As it was mentioned in the Introduction, a large number of compounds have been synthesized and evaluated as NKT activators, looking for an improved antigen, with higher selectivity and better potency control. However, deciphering the key interactions has not been trivial, as some compounds presented opposite effects when were evaluated in human and mice cells, as was the cases of α-C-GalCer (**21**)[60,61] or α-S-GalCer (**22**)[62,63] (**Table 3.21**).

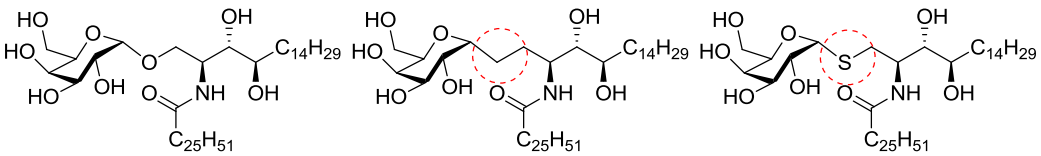

αGalCer (2) α-C-GalCer (21) α-S-GalCer (22)

Compound	% IFN-γ (T_H1)	% IL-4 (T_H2)	Ratio IFN-γ/IL-4	Specie
2 – αGalCer	100	100	1	m
	100	100	1	h
21	89,2	7,8	11,6	m
	0	0	Inactive	h
22	0	0	Inactive	m
	53,3	53,8	0,99	h

Table 3.21: *Summary of activities of analogues with glycosidic bond modifications **21** and **22***

Apart from its controversial bioactivity, αGalCer (**2**) showed other drawbacks that minimized its potential as immunotherapeutic agent. It is a very powerful NKT cell activator, which induces an unresponsiveness NKT cell state in mice after NKT cell activation. This extremely powerful bioactivity can be illustrated by the fact that administration of 1 or 2 micrograms (just a few nmol) of this compound to a mouse are enough to induce a very strong cytokine response. Related to its chemical structure, αGalCer (**2**) structure comprises several functionalities that can be potentially recognized and degraded by glycolipid metabolism enzymes (such as the glycosidic bond or the fatty acid amide bond); on the other hand, its chemical synthesis is difficult to be accomplished, especially the alpha-glycosidic bond to a sphingolipid. All

together, exploring chemical space of new antigens is a hot topic and its potential biological activity is an attractive research project.

As it was already mentioned, our *"hit"* **I-1a** was tested as *i*NKT cell activator during a pre-doctoral stage of Anna Alcaide in Dirk Elewaut Laboratory in Belgium, being the most active compound (**Figure 3.31**) of the tested series

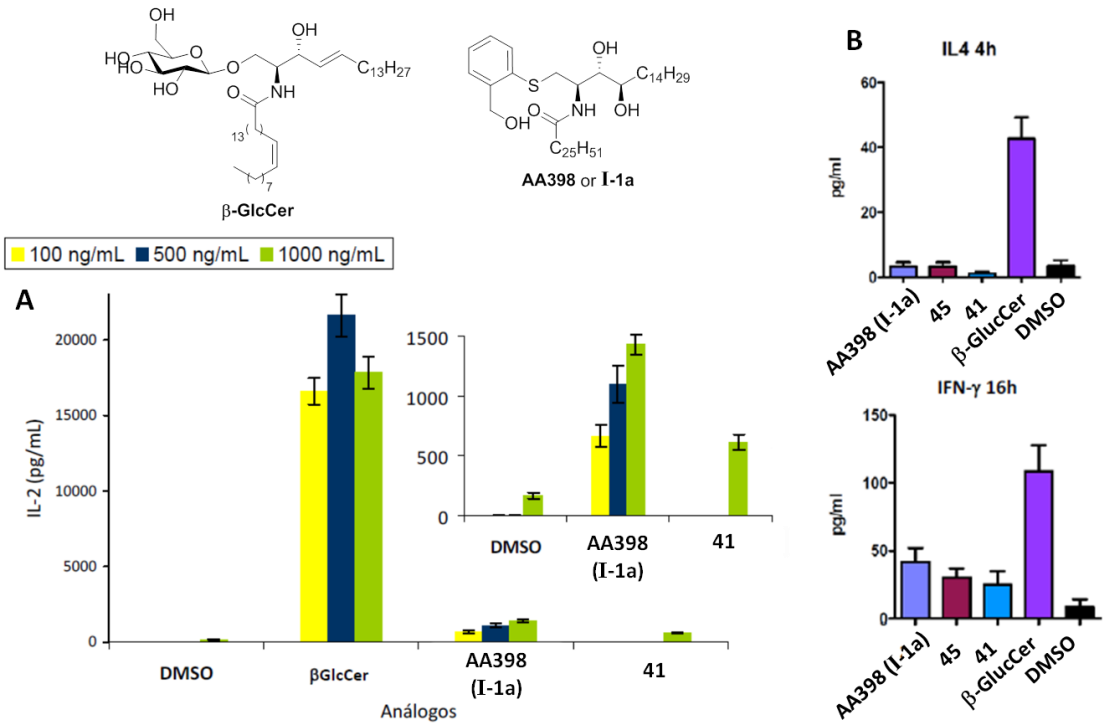

Figure 3.31: *Summary of biological activity of* ***I-1a****; A) in vitro experiments with mice cells; B) in vivo experiments with Balb mice*

In these preliminary studies, initial *in vitro* experiments measuring IL-2 production (a representative pro-inflammatory cytokine commonly used as value of NKT cell stimulation) were carried out showing **I-1a** as best candidate among the collection tested. This analogue showed a dose-response activity at concentrated test although its activity was considerably lower than the standard compounds including β-GlcCer, a compound with much lower activity than αGalCer that was believed to be the NKT endogenous ligand at the time these experiments were performed[64]. To further assess compound immune profile T_H1/T_H2, *in vivo* experiments in Balb mice were conduct in which representative IFN-γ and IL-4 (T_H1 and T_H2 respectively); these experiments showed a clear T_H1 profile as **I-1a** induced around half of INF-γ as standard (in this case β-GlcCer was used) while nearly no IL-4 production was observed. Despite its lower potency, its unprecedented structure conferred to this compound a high interest as NKT cell activator candidate for medicinal chemistry optimization. During the course of present doctoral thesis, this compound was also tested as human-NKT cell activator showing encouraging and promising potency, comparable to the NKT standard

activator αGalCer (**2**) (**Figure 3.32**). This experiment was carried out at Dr. Carme Roura Laboratory, a molecular immunology group at Universitat Autònoma de Barcelona; compound activity was measured by TNF-α cell secretion, again as a representative pro-inflammatory cytokine and NKT cell activator value.

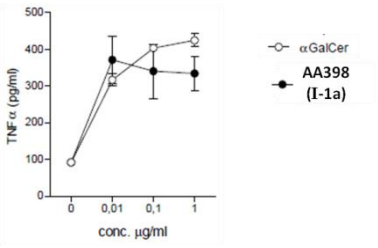

Figure 3.32: *Comparison of human NKT cell activation with αGalCer (**2**) and **I-1a***

These results increase notably the interest of this new family of derivatives, now not only because of their structure but also because of its promising activity in human cell experiments.

The main objective of this thesis is the synthesis of **I-1a** analogues and their biological evaluation as NKT cell activators. We are interested in decipher if the biological activity is specific for just one compound or it can be extended to other similar structures, which could open the possibility of obtaining structurally unprecedented and groundbreaking NKT stimulators, never explored before. Towards this end, testing our compounds as NKT cells activators was crucial to build our SAR. During the last period of the present doctoral thesis, two collaborations were set up with different groups to perform biological experiments to evaluate our compounds activity. These involved the group of Javier Briones in the Servei d'Hematologia de l'Hospital de Sant Pau; this group reported promising results using αGalCer (**2**) as vaccine adjuvant for B cell lymphoma treatment, reaching 100% of survival against first exposure to disease, and 80% of survival after to a second tumor inoculation[54]. The collaboration with the group of Carme Roura in the Unitat d'Immunologia, the Universitat Autònoma de Barcelona involves compound testing in human NKT cells. This group has a research program in the cooperative role of NKT cell with Regulatory T cell in the control of autoimmune diseases with special emphasis on type I diabetes.

At the time these collaborations were established, a small group of 8 compounds was selected for a preliminary screening trying to establish a Structure-Activity in this minimal set (**Figure 3.33**). Compound stock solutions were prepared in DMSO at 0,5 mg/mL instead of more commonly used 1 mg/mL due to the limited product solubility of the aromatic ceramides. The DMSO stock solutions were after diluted with PBS to the desired test concentrations.

This minimal set of compounds took into account different aspects. The experiments included αGalCer (**2**) as reference standard, and our "*hit*" compound **I-1a.** The modification of the hydroxymethyl group in **I-1a** to increase interactions with TCR

residues, lead us to introduce a carbonyl moiety as H-acceptor containing groups, To further assess our hypothesis, the ester and amide analogues, **I-1b** and **I-1d,** respectively, were selected. Sulfur replacement by oxygen leads to family of compounds **I-2;** among them, three analogues were selected (**I-2a**, **I-2b** and **I-2d**), whereby the relation of substituents and the linking atom could be studied. Finally, in order to introduce one compound of the phenylamino-ceramide family **I-3** and oxy-pyridine-ceramide family **I-4** and considering instability problems showed by hydroxymethyl derivative **I-3a**, led us to select the amide analogues, allowing a comparison of the same C2-carboxamido substituent in all four families (**Figure 3.33**).

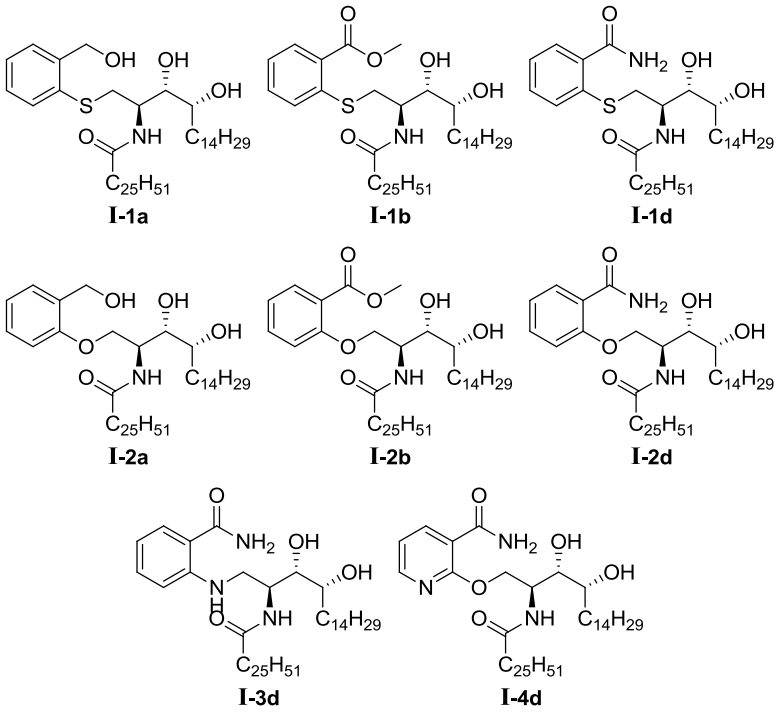

Figure 3.33: *Selected compounds for biological evaluation*

As it was explained in Introduction, the most common cytokines measured to determine a NKT response profile of glycolipid antigens are IFN-γ as representative T_H1 response and IL-4 for T_H2 response. For this reason, these cytokine were selected to be measured, so further comparison with other reported compounds could be established. Standard commercial sandwich ELISA analyses were done to detect cytokines in cell culture supernatants, this technique consist of trapping the substance to be detected by means of selective antibodies (**Figure 3.34**).

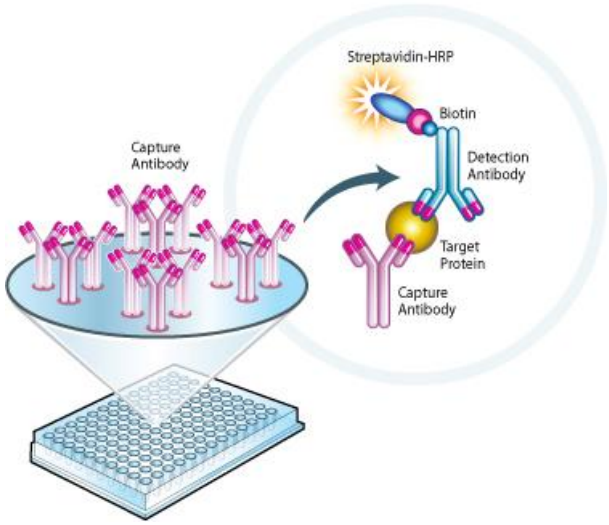

Figure 3.34: *Schematic image of Sandwich ELISA cytokine detection. Well-plate is coated with capture antibodies previous to problem solution addition. Once target analyte is trapped by capture antibody, second marked antibody is added which will detect first antibody-target complex. Finally, conjugation of Biotin with Streptavidint-HRP will generate fluorescent response when OPD or similar substance is added.*

3.3.1. Aromatic-ceramide analogues as mouse NKT cell activators

These experiments were carried out by Laura Escribà at Javier Briones' Laboratory, at Sant Pau Hospital.

In vitro evaluation in mice cells was carried out at Dr. Javier Briones Lab at Hospital de Sant Pau. For the experiment design two concentrations should be selected, taking into account preceding results obtained by Anna Alcaide in her thesis in which **I-1a** showed around 10% of αGalCer (**2**) activity at 1 µg/mL in terms of IL-2 production, 1 µg/mL and 5 µg/mL were selected to ensure a measurable response of all compounds if were less active than our *"hit"* compound. Splenocytes were isolated from bone marrow of Balb mice, co-cultured with 1 or 5 µg/mL of each compound and 100 ng/mL of αGalCer (**2**) used as positive control. After 4 days, supernatants were collected and cytokines were measured by ELISA experiments. Surprisingly, measurements of cultures treated with 5 µg/mL of compound did not show cytokine production. Taking advantage of fluorescent properties of some of the tested compounds, the cell cultures were examined at the microscope under blue filter, and extensive cell death was observed. Unfortunately, the images were not recorded and are not available to be included here. Remarkably, the experiments performed at 1 µg/mL gave promising results; all compounds induced IFN-γ production at similar levels of αGalCer (**2**) (although at a dose 10-fold higher) and no IL-4 production could be observed (**Figure 3.35**).

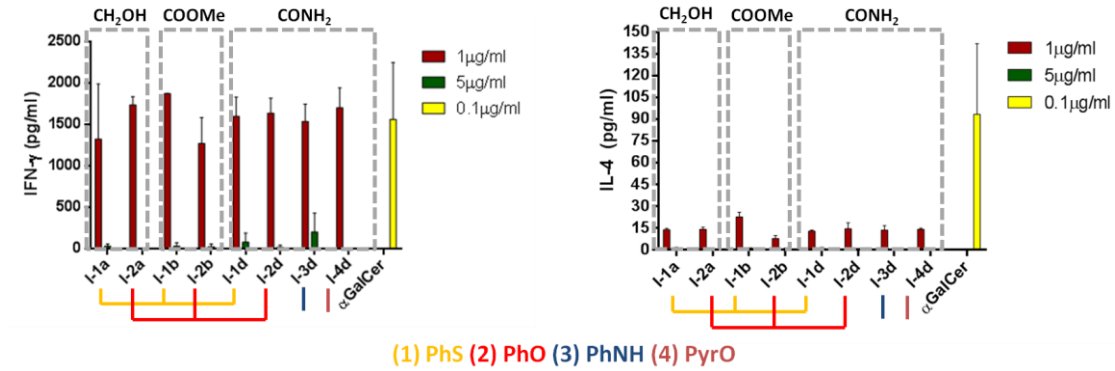

Figure 3.35: *In vitro cytokine production of new aromatic-ceramide analogue at different concentrations*

In general, all compounds showed a similar activity profile and comparable cytokine induction levels. Due to the reduced number of replicates no significant differences could be established, especially in compound of **I-1a** that shows a high standard deviation that precludes any definite conclusion. To note that the levels of all tested compounds are in the same range of activity.. All together, the replacement of the sulfur atom linker by oxygen or nitrogen atoms seemed to not disturb the potent activity. A similar proposal can be made from the modification of 2-hydroxymethyl group by ring substituents having a carbonyl group. Phenol ring replacement by pyridine does not reveal a big influence in IFN-γ production, at least at this preliminary testing level.

Surprisingly and in contrast to previously obtained results by Anna Alcaide (in which **I-1a** showed poor NKT cell activation), our new compounds were able to stimulate NKT cells producing similar levels of INF-γ than αGalCer (**2**) at 10-fold more concentrated. On the other hand, our compounds showed IL-4 production at same level as vehicle, meaning that no IL-4 was produced by the aromatic ceramide compounds at 1 μg/mL presence, in contrast to αGalCer (**2**) that induced a high production of IL-4 at 100 ng/mL .

Although being preliminary experiments carried out at only two concentrations, this promising polarizing activity of our compounds conferred them a highly interesting value as NKT cell activators candidates. On the other hand the toxicity at the higher concentration could indicate a high potency of the compounds, which could induce an overactivation of the NKT cells, or toxicity related to the presence of the aryl group in the ceramides. An accurate biological characterization will be necessary to guarantee product safety. The dose response curves would give us deeper information to establish differences between compounds and establish a better comparison to αGalCer (**2**).

In conclusion, it seems that all the compounds included in the set of 8 aromatic ceramide tested induced a potent INF-γ cytokine production at low concentrations (similar to that obtained with 10 times less αGalCer). In contrast, under the same

conditions the aromatic compounds showed much lower IL-4 production than αGalCer, suggesting a T_H1 bias. At higher concentrations, a toxic effect on cells was observed.

3.3.2. Aromatic-ceramide analogues as human *i*NKT cell activators

These experiments were carried out by Lorena Usero and Roser Borràs at Carme Roura's Laboratory, at Universitat Autònoma de Barcelona.

Bearing in mind the promising preliminary results obtained and the toxicity warning at high concentration from *in vitro* stimulation of mice splenocytes, a similar group of compounds was tested as human *i*NKT cell activators. For this experiment, 7 aromatic-ceramide compounds were tested together with αGalCer (**2**) and HS161 (**39**), an aminocyclitol-ceramide analogue from our first structural library of compounds. This compound was selected for its high T_H1 polarizing activity in order to compare its results with our aromatic-ceramide family. Taking into account previous experiments carried out with **I-1a** measuring TNFα production and its promising results, in this case same and lower concentration were selected (10 ng/mL and 1 μg/mL). Moreover, *i*NKT cells were isolated from the blood of human donors and expanded with established protocol in Roura's laboratory. CD1d transfected C1R cells were used as presenting cells, C1R is a mutated B cell line widely used in immunology as transfection recipient. PBMCs were used as feeder cells to confer an appropriate cell culture environment.

C1R-$CD1d^+$ (C1Rd) cells were pre-incubated 1h at 37ºC with desired concentration of each compound following of 15 min irradiation at 45Gy. Then, C1Rd cells expressing each compound were co-cultivated at 37ºC in presence of isolated *i*NKT and PBMCs as feeder cells. PHA-L and αCD3CD28 beads were used as positive controls. Supernatants were collected at 48h and analyzed by ELISA (**Figure 3.36**). In general, ELISA data showed that all tested compounds were *i*NKT cell activators, meaning that this new family of compounds could be considered as promising for searching for new structures NKT activator analogues. In general, compounds showed slightly less INF-γ production than αGalCer (**2**) at both tested concentrations but production of IL-4 was markedly lower than that of αGalCer in all cases. It is necessary to remark that in these experiments al the compounds were tested at the same concentrations as αGalCer. In contrast with results obtained with mice cells, where our compounds showed a nearly total cytokine production polarization bias towards INF-γ, IL-4 production in human cells was higher than vehicle but far from the high levels of IL-4 produced by αGalCer.

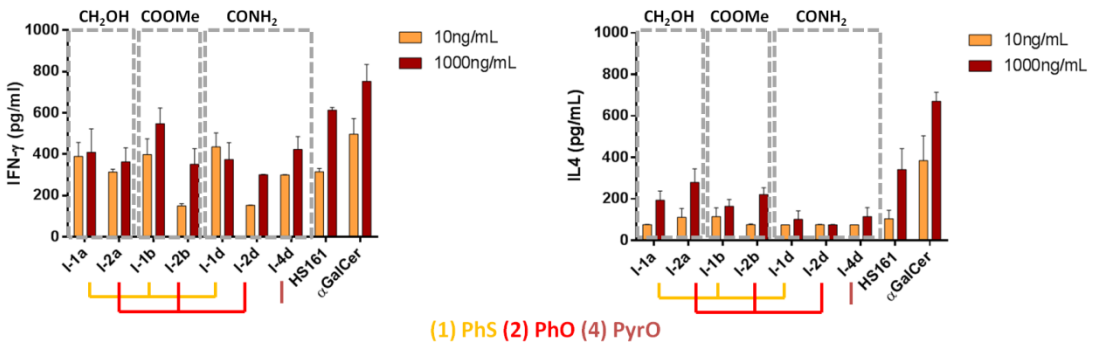

Figure 3.36: *in vitro stimulation of human iNKT with new aromatic-ceramide analogues*

In detail, all three phenylthio-derivatives (**I-1a**, **I-1b** and **I-1d**) showed promising IFN-γ production, even at the low dose tested (10 ng/mL) with comparable levels to those induced by αGalCer (**2**), although somewhat lower, around 80% in average (**Table 3.22**). At the high dose tested αGalCer (**2**) produced considerably higher amount of this cytokine while our compounds showed around 50% in case of hydroxymethyl **I-1a** and amide **I-1d** while the methyl ester derivative **I-1b** showed the higher production among the aromatic derivatives (around 70%). The aminocyclitol derivative **39** showed a strong potency at high dose while markedly decreased at the low one. Moving to IL-4 analysis, at both concentrations aromatic-ceramide derivatives showed low production of this cytokine compared to αGalCer (**2**), between 2 to 5 times less of this cytokine; in this sense, the aminocyclitol derivative HS161 induced IL-4 at similar levels to that obtained with the aromatic compounds at low dose, while IL-4 production was more pronounced at the higher concentration. All together, the phenylthio family showed promising T_H1 biased response at low dose, with around 80% or IFN-γ production versus only 20-30% of IL-4 production compare to αGalCer (**2**) (**Table 3.22**). A similar trend was obtained with the non-glycosidic aminocyclitol HS161 (**39**) although it seems to be less selective than the aromatic ceramides. At higher dose considerably less IFN-γ than αGalCer (**2**) was produced (around 50%) while similar decrease of IL-4 was observed (around 20%).

Contrary to the previous results with mice cells, in human cells phenoxy derivatives showed lower cytokine production compared to sulfur analogues in all three cases (hydroxymethyl **I-2a**, methyl-ester **I-2b** and amide **I-2d**). Again, a T_H1 biased response was observed for all three compounds, however considerably IFN-γ production was observed at low dose (around 30% compared to αGalCer (**2**)) for ester and amide analogues (**I-2b** and **I-2d**). The hydroxymethyl analogue **I-2a** showed the best response for this *O*-linked family, as it was able to produce the most amount of IFN-γ comparable to our *S*-linked "*hit*" compound **I-1a**. In this way, aryloxy compounds maintained the same polarizing response towards T_H1 although in a less pronounced manner (**Figure 3.26** and **Table 3.22**).

Finally, the oxy-pyridine-amide derivative **I-4d** showed similar cytokine production as its arylthio analogue and, surprisingly, higher potency than its *O*-linked analogue. Hence, **I-4d** showed low production of IL-4 compared to αGalCer (**2**) (around 20%) while decrease of IFN-γ was not so marked (around 60%) at both concentrations (**Figure 3.26** and **Table 3.22**).

All together, in human cells, hydroxymethyl compounds **I-1a** and **I-2a** were the most potent together with thiophenol-amide **I-2d**. These compounds showed similar levels of IFN-γ at both concentrations so it was uncertain if their potency would be maintained at lower dose and, maybe, be comparable or even higher to that of αGalCer (**2**) or, by contrast, would notably decrease and then, still being less potent than αGalCer (**2**). Methyl ester derivative showed opposite effects, while sulfur derivative **I-1b** showed increased potency compared to its hydroxymethyl analogue **I-1a**, whereas the oxygen derivative **I-2b** showed considerably decreased potency compared to its analogue **I-2a** (and so compared with its sulfur analogue **I-1b**). About the amide derivatives, the *S*-linked analogue **I-1d** showed the best results followed by oxy-pyridine **I-4d**, while *O*-linked derivative **I-2d** showed the lowest potency.

Although the maximum levels of INF-γ production compared to αGalCer (**2**) were not reached by our compounds, at 10 ng/mL it was similar to αGalCer (**2**) response and together with considerably lower production of IL-4 at this concentration, our compounds could be considered as T_H1 polarizing antigens for NKT cells (**Table 3.22**). INF-γ/IL-4 ratios in all cases were higher than αGalCer (**2**) both in relative and absolute values.

	10 ng/mL				1000 nm/mL			
	% INF-γ	% IL-4	Rel. ratio	Abs. ratio	% INF-γ	% IL-4	Rel. ratio	Abs. ratio
I-1a	78,4	19,8	3,9	5,1	54,4	28,9	1,9	2,1
I-2a	63,1	29,0	2,2	2,8	48,2	41,7	1,2	1,3
I-1b	80,2	29,7	2,7	3,5	72,7	24,6	2,9	3,3
I-2b	30,1	19,9	1,5	1,9	46,7	33,0	1,4	1,6
I-1d	87,6	19,3	4,5	5,9	49,7	15,1	3,3	3,7
I-2d	30,7	19,8	1,6	2,0	40,1	11,3	3,5	3,9
I-4d	60,3	19,3	3,1	4,0	56,2	17,0	3,3	3,7
HS161 **(39)**	63,4	27,3	2,3	3,0	81,5	50,9	1,6	1,8
αGalCer (**2**)	100	100	1	1,2	100	100	1	1,1

Table 3.22: *Summary of cytokine results compared to αGalCer (**2**). Rel.= relative; Abs.= absolute*

All together, these results confirm a promising activity among all tested compounds with clear T_H1 bias response. Further studies are needed to establish the products biological responses and confirm our preliminary results.

In light of these results, our initial computational studies in which no significant differences were observed among disubstituted analogues were in line of recently

obtained biological data. To put some light on promising activity of our compounds with human *i*NKT cells, it was planned to study some of tested compounds in a human-CD1d-humanTCR system with computational tools. Considering that rigid protein studies were not the most appropriate methodology to study this system, new MD simulations were launch considering crystal structure of human proteins (hCD1d-αGalCer-hTCR, PDB code: 2OP6[65]). For these studies, both hydroxymethyl derivatives **I-1a** and **I-2a** were selected together with reported ligands with different known response: αGalCer (**2**) as reference compounds, our HS161 (**39**) and HS44 (**38**) as TH1 polarizing compounds, OCH (**5**) as TH2 biased ligand and 2'H-α-GalCer (**23**) and α-C-GalCer (**21**) as inactive compounds. Simulations were currently under process.

Finally, it is worthy to highlight that a recent collaboration has been established with a biotech company, to which a small collection of our compounds have been sent to further study their properties. Experiments were ongoing at the time of this thesis was written and are not concluded.

3.3.3. Summary of results and final remarks

The first preliminary *in vitro* experiments with aromatic ceramides in mice cells showed a potent response with total polarizing activity as pro-inflammatory (T_H1, INF-γ) antigens. These results require additional studies, including dose-response curves to confirm product potency and to a proper comparison with αGalCer (**2**). In addition, the possible toxicity of the products at high concentrations needs to be clearly established.

In vitro experiments on purified human NKT cell stimulation with aromatic ceramides confirm a similar tendency to that obtained in mice cells. However, in human cells it could be detected a slight production of anti-inflammatory cytokines (T_H2, IL-4). Our compounds showed comparable potency (80% of IFN-γ production in best cases) to αGalCer (**2**) at low dose (10 ng/mL) while marked decrease of IL-4 production (around 20% to that produced with αGalCer in most cases). These results conferred to our new aromatic-ceramide family a high interest as promising new candidates to be explored.

It is worth to mention the low level of chemical functionality of the aromatic replacement of the sugar analogues, only one ring substituent at "*polar-head*" being enough to induce similar response to that of glycolipid antigens. The future exploration of other substituents, ring types and positional isomers or a combination of these structural factors could help to improve not only physicochemical properties but also a finely modulate the biological activity (**Figure 3.37**). Structural studies of the new family with CD1d and TCR proteins are also of interest to define the molecular determinants of the interactions and how these correlate with the biological activity. These data can also help to validate the computational studies in the ternary system.

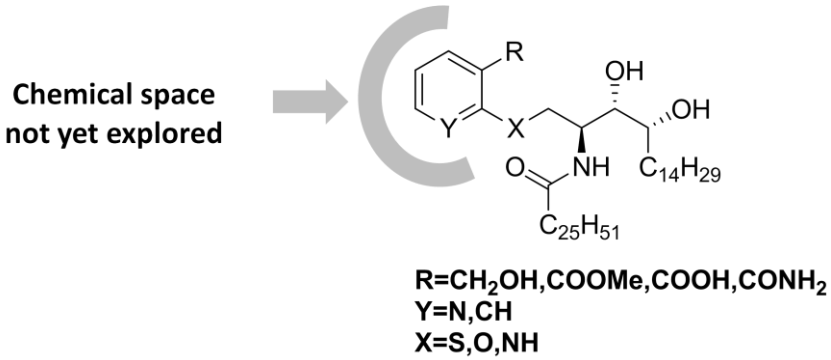

Figure 3.37: *Illustrative image of ring positions not yet substituted and potentially able to be explored*

BIBLIOGRAPHYC REFERENCES

1. Hénon, E., Dauchez, M., Haudrechy, A. & Banchet, A. Molecular dynamics simulation study on the interaction of KRN 7000 and three analogues with human CD1d. *Tetrahedron* **64**, 9480-9489 (2008).
2. Nadas, J., Li, C. & Wang, P.G. Computational Structure Activity Relationship Studies on the CD1d/Glycolipid/TCR Complex Using AMBER and AUTODOCK. *Journal of Chemical Information and Modeling* **49**, 410-423 (2009).
3. Laurent, X., Renault, N., Farce, A., Chavatte, P. & Henon, E. Relationships between Th1 or Th2 iNKT cell activity and structures of CD1d-antigen complexes: meta-analysis of CD1d-glycolipids dynamics simulations. *PLoS Comput Biol* **10**, e1003902 (2014).
4. Kerzerho, J.*, et al.* Structural and Functional Characterization of a Novel Nonglycosidic Type I NKT Agonist with Immunomodulatory Properties. *The Journal of Immunology* **188**, 2254 (2012).
5. Aspeslagh, S.*, et al.* Galactose-modified iNKT cell agonists stabilized by an induced fit of CD1d prevent tumour metastasis. *EMBO J* **30**, 2294-2305 (2011).
6. Harrak, Y.*, et al.* Aminocyclitol-Substituted Phytoceramides and their Effects on iNKT Cell Stimulation. *ChemMedChem* **4**, 1608-1613 (2009).
7. Chang, Y.J.*, et al.* Potent immune-modulating and anticancer effects of NKT cell stimulatory glycolipids. *Proc Natl Acad Sci U S A* **104**, 10299-10304 (2007).
8. Xing, G.W.*, et al.* Synthesis and human NKT cell stimulating properties of 3-O-sulfo-alpha/beta-galactosylceramides. *Bioorg Med Chem* **13**, 2907-2916 (2005).
9. Xia, C.*, et al.* The roles of 3' and 4' hydroxy groups in alpha-galactosylceramide stimulation of invariant natural killer T cells. *ChemMedChem* **4**, 1810-1815 (2009).
10. Zhang, W.*, et al.* Introduction of aromatic group on 4'-OH of alpha-GalCer manipulated NKT cell cytokine production. *Bioorg Med Chem* **19**, 2767-2776 (2011).
11. Glide, version 6.4; Schrödinger, LLC, New York, NY, 2014.
12. Schrödinger Suite 2014 Update 3, Schrödinger, LLC: New York, NY, 2014.
13. Aspeslagh, S.*, et al.* Enhanced TCR footprint by a novel glycolipid increases NKT-dependent tumor protection. *J Immunol* **191**, 2916-2925 (2013).
14. Schrödinger Suite 2014 Induced Fit Docking protocol; Glide, Schrödinger, LLC, New York, NY, 2014; Prime, Schrödinger, LLC, New York, NY, 2014.
15. Desmond Molecular Dynamics System, D. E. Shaw Research, New York, NY, 2014. Maestro-Desmond Interoperability Tools, Schrödinger, New York, NY, 2014.
16. Mori, K. & Tashiro, T. Sphingolipids and glycosphingolipids - their syntheses and bioactivities. *Heterocycles* **83**, 951-1003 (2011).
17. Akimoto, K., Natori, T. & Morita, M. Synthesis and stereochemistry of agelasphin-9b. *Tetrahedron Letters* **34**, 5593-5596 (1993).
18. Morita, M.*, et al.* Structure-activity relationship of alpha-galactosylceramides against B16-bearing mice. *J Med Chem* **38**, 2176-2187 (1995).
19. Harrak, Y., Barra, C.M., Delgado, A., Castaño, A.R. & Llebaria, A. Galacto-Configured Aminocyclitol Phytoceramides Are Potent in Vivo Invariant Natural

Killer T Cell Stimulators. *Journal of the American Chemical Society* **133**, 12079-12084 (2011).

20. Harrak, Y., Llebaria, A. & Delgado, A. A Practical Access to 1,2-Diaminophytosphingolipids. *European Journal of Organic Chemistry* **2008**, 4647-4654 (2008).
21. Alcaide, A. & Llebaria, A. Aziridine ring opening for the synthesis of sphingolipid analogues: inhibitors of sphingolipid-metabolizing enzymes. *J Org Chem* **79**, 2993-3029 (2014).
22. Alcaide, A. & Llebaria, A. Synthesis of 1-thio-phytosphingolipid analogs by microwave promoted reactions of thiols and aziridine derivatives. *Tetrahedron Letters* **53**, 2137-2139 (2012).
23. van den Berg, R.J.B.H.N.*, et al.* An Efficient Synthesis of the Natural Tetrahydrofuran Pachastrissamine Starting from d-ribo-Phytosphingosine. *The Journal of Organic Chemistry* **71**, 836-839 (2006).
24. Kim, S., Lee, S., Lee, T., Ko, H. & Kim, D. Efficient Synthesis of d-erythro-Sphingosine and d-erythro-Azidosphingosine from d-ribo-Phytosphingosine via a Cyclic Sulfate Intermediate. *The Journal of Organic Chemistry* **71**, 8661-8664 (2006).
25. Chen, W.-S.*, et al.* Synthesis of ganglioside Hp-s1. *RSC Advances* **4**, 47752-47761 (2014).
26. Alcaide, A. A modular approach to sphingolipi analogs mediated by aziridines: synthesis and biological studies. *Doctoral Thesis, University of Barcelona* (2012).
27. Lee, T., Lee, S., Kwak, Y.S., Kim, D. & Kim, S. Synthesis of pachastrissamine from phytosphingosine: a comparison of cyclic sulfate vs an epoxide intermediate in cyclization. *Org Lett* **9**, 429-432 (2007).
28. Zeynizadeh, B. & Zeynizadeh, B. Oxidative coupling of thiols to disulfides with iodine in wet acetonitrile. *Journal of Chemical Research* **2002**, 564-566 (2002).
29. Liu, C.*, et al.* Leonurine-cysteine analog conjugates as a new class of multifunctional anti-myocardial ischemia agent. *European Journal of Medicinal Chemistry* **46**, 3996-4009 (2011).
30. Eshghi, H., Seyedi, S.M. & Sandarooss, R. Synthesis of novel disulfide-bridged dilactam crown ethers. *Chinese Chemical Letters* **18**, 1439-1442 (2007).
31. Neamati, N.*, et al.* Metal-Dependent Inhibition of HIV-1 Integrase. *Journal of Medicinal Chemistry* **45**, 5661-5670 (2002).
32. Sengar, R.S., Miller, J.J. & Basu, P. Design, syntheses, and characterization of dioxo-molybdenum(vi) complexes with thiolate ligands: effects of intraligand NH[three dots, centered]S hydrogen bonding. *Dalton Transactions*, 2569-2577 (2008).
33. 1,2-Benzisothiazol-3(2H)-one [MAK Value Documentation, 1991]. in *The MAK-Collection for Occupational Health and Safety*.
34. Frerot, E., Bagnoud, A. & Cicchetti, E. Quantification of Hydrogen Sulfide and Methanethiol and the Study of Their Scavenging by Biocides of the Isothiazolone Family. *ChemPlusChem* **79**, 77-82 (2013).
35. Chen, F.-J., Liao, G., Li, X., Wu, J. & Shi, B.-F. Cu(II)-Mediated C–S/N–S Bond Formation via C–H Activation: Access to Benzoisothiazolones Using Elemental Sulfur. *Organic Letters* **16**, 5644-5647 (2014).

36. Sarma, B.K. & Mugesh, G. Redox Regulation of Protein Tyrosine Phosphatase 1B (PTP1B): A Biomimetic Study on the Unexpected Formation of a Sulfenyl Amide Intermediate. *Journal of the American Chemical Society* **129**, 8872-8881 (2007).
37. Voltrova, S., Hidasova, D., Genzer, J. & Srogl, J. Metallothionein-inspired prototype of molecular pincer. *Chemical Communications* **47**, 8067-8069 (2011).
38. Jervis, P.J*., et al.* Design, Synthesis, and Functional Activity of Labeled CD1d Glycolipid Agonists. *Bioconjugate Chemistry* **24**, 586-594 (2013).
39. Anderson, R.J*., et al.* A self-adjuvanting vaccine induces cytotoxic T lymphocytes that suppress allergy. *Nat Chem Biol* **10**, 943-949 (2014).
40. Llaveria, J., Espinoza, A., Negrón, G., Isabel Matheu, M. & Castillón, S. Efficient and regioselective ring-opening of arylaziridines with alcohols, thiols, amines and N-heteroaromatic compounds using sulphated zirconia. *Tetrahedron Letters* **53**, 2525-2529 (2012).
41. Lu, H.-f*., et al.* An efficient catalyst for ring opening of epoxides with phenol and thiophenol under solvent-free conditions. *Tetrahedron* **69**, 11174-11184 (2013).
42. Bhanu Prasad, B.A., Sanghi, R. & Singh, V.K. Studies on ring cleavage of aziridines with hydroxyl compounds. *Tetrahedron* **58**, 7355-7363 (2002).
43. Culf, A.S*., et al.* A spectroscopic study of substituted anthranilic acids as sensitive environmental probes for detecting cancer cells. *Bioorganic & Medicinal Chemistry* **24**, 929-937 (2016).
44. Wojciechowski, K. Aza-ortho-xylylenes in Organic Synthesis. *European Journal of Organic Chemistry* **2001**, 3587-3605 (2001).
45. Roth, M.E., Green, O., Gnaim, S. & Shabat, D. Dendritic, Oligomeric, and Polymeric Self-Immolative Molecular Amplification. *Chemical Reviews* **116**, 1309-1352 (2016).
46. Kretzschmar, M., Hodík, T. & Schneider, C. Brønsted Acid Catalyzed Addition of Enamides to ortho-Quinone Methide Imines—An Efficient and Highly Enantioselective Synthesis of Chiral Tetrahydroacridines. *Angewandte Chemie International Edition* **55**, 9788-9792 (2016).
47. Kretzschmar, M., Hofmann, F., Moock, D. & Schneider, C. Intramolecular Aza-Diels–Alder Reactions of ortho-Quinone Methide Imines: Rapid, Catalytic, and Enantioselective Assembly of Benzannulated Quinolizidines. *Angewandte Chemie International Edition* **57**, 4774-4778 (2018).
48. Bandyopadhyay, S. & Bong, D. Synthesis of Trifunctional Phosphatidylserine Probes for Identification of Lipid-Binding Proteins. *European Journal of Organic Chemistry* **2011**, 751-758 (2010).
49. Riedrich, M., Harkal, S. & Arndt, H.D. Peptide-Embedded Heterocycles by Mild Single and Multiple Aza-Wittig Ring Closures. *Angewandte Chemie International Edition* **46**, 2701-2703 (2007).
50. Marcaurelle, L.A. & Bertozzi, C.R. Chemoselective Elaboration of O-Linked Glycopeptide Mimetics by Alkylation of 3-ThioGalNAc. *Journal of the American Chemical Society* **123**, 1587-1595 (2001).
51. Wang, B., Huang, P.-H., Chen, C.-S. & Forsyth, C.J. Total Syntheses of the Histone Deacetylase Inhibitors Largazole and 2-epi-Largazole: Application of N-Heterocyclic Carbene Mediated Acylations in Complex Molecule Synthesis. *The Journal of Organic Chemistry* **76**, 1140-1150 (2011).

52. Simoni, Y., Diana, J., Ghazarian, L., Beaudoin, L. & Lehuen, A. Therapeutic manipulation of natural killer (NK) T cells in autoimmunity: are we close to reality? *Clin Exp Immunol* **171**, 8-19 (2013).
53. Nair, S. & Dhodapkar, M.V. Natural Killer T Cells in Cancer Immunotherapy. *Front Immunol* **8**, 1178 (2017).
54. Escribà-Garcia, L., Alvarez-Fernández, C., Tellez-Gabriel, M., Sierra, J. & Briones, J. Dendritic cells combined with tumor cells and α-galactosylceramide induce a potent, therapeutic and NK-cell dependent antitumor immunity in B cell lymphoma. *Journal of Translational Medicine* **15**, 115 (2017).
55. Fletcher, M.T. & Baxter, A.G. Clinical application of NKT cell biology in type I (autoimmune) diabetes mellitus. *Immunol Cell Biol* **87**, 315-323 (2009).
56. Matangkasombut, P., Pichavant, M., Dekruyff, R.H. & Umetsu, D.T. Natural killer T cells and the regulation of asthma. *Mucosal Immunol* **2**, 383-392 (2009).
57. O'Keeffe, J., Podbielska, M. & Hogan, E.L. Invariant natural killer T cells and their ligands: focus on multiple sclerosis. *Immunology* **145**, 468-475 (2015).
58. Slauenwhite, D. & Johnston, B. Regulation of NKT Cell Localization in Homeostasis and Infection. *Front Immunol* **6**, 255 (2015).
59. Van Kaer, L., Wu, L. & Parekh, V.V. Natural killer T cells in multiple sclerosis and its animal model, experimental autoimmune encephalomyelitis. *Immunology* **146**, 1-10 (2015).
60. Fujii, S*., et al.* Glycolipid alpha-C-galactosylceramide is a distinct inducer of dendritic cell function during innate and adaptive immune responses of mice. *Proc Natl Acad Sci U S A* **103**, 11252-11257 (2006).
61. Li, X., Chen, G., Garcia-Navarro, R., Franck, R.W. & Tsuji, M. Identification of C-glycoside analogues that display a potent biological activity against murine and human invariant natural killer T cells. *Immunology* **127**, 216-225 (2009).
62. Blauvelt, M.L*., et al.* Alpha-S-GalCer: synthesis and evaluation for iNKT cell stimulation. *Bioorg Med Chem Lett* **18**, 6374-6376 (2008).
63. Hogan, A.E*., et al.* Activation of human invariant natural killer T cells with a thioglycoside analogue of alpha-galactosylceramide. *Clin Immunol* **140**, 196-207 (2011).
64. Brennan, P.J*., et al.* Invariant natural killer T cells recognize lipid self antigen induced by microbial danger signals. *Nat Immunol* **12**, 1202-1211 (2011).
65. Borg, N.A*., et al.* CD1d-lipid-antigen recognition by the semi-invariant NKT T-cell receptor. *Nature* **448**, 44-49 (2007).

4. GENERAL CONCLUSIONS

4.1. General Conclusions

This thesis had three main objectives corresponding to the three chapters of this manuscript: Bearing in mind all considerations mentioned above, the main general goal of this thesis was:

The design (*Chapter 1*), synthesis (*Chapter 2*) and biological evaluation (*Chapter 3*) of new aromatic-ceramide derivatives mimicking alpha-galactosylceramide as NKT cell activators.

In Chapter 1, it was initially aimed to develop a computational docking model based on virtual library of ligands; this model should be able to select or purpose new aromatic-ceramide candidates as NKT cell activators. After all, results obtained in Chapter 1 led us to conclude that:

- Rigid docking tools (Molecular Docking and Induced Fit Docking - IFD) were used to study the binding mode in CD1d-Ag-TCR complex of the virtual aromatic ceramide ligand library. Methodologies based in rigid docking tools were limited by the high complexity of the ternary system studied and the huge number of degrees of freedom of the ligands.
- Truncated ligands at the lipid chains were considered to undergo ligand docking studies with simplified computational charges. After 10 iterative jobs, the calculations did not reach fully concluding results due to the diversity of binding modes adopted for most of ligands examined. However, disubstituted ligands showed good regularity in interactions with some of the key aminoacids described in literature to be essential for antigen interaction with the CD1d-TCR proteins. In contrast, trisubstituted aromatic ceramides had more random results and are less conclusives. IFD simulation of 10 selected truncated ligands did not end up with a clear computational ligand prioritization.
- To further assess ligand impact on ternary complex structure, Molecular Dynamic simulations of the 10 selected compounds were analyzed, pointing to lower H-Bond capacity of trisubstituted aromatic ligands to interact with essential residues while disubstituted aromatic ligands were able to reach sustained interactions patterns all along, maintaining mostly all reported interactions.
- As general conclusion, an operative computational docking model was not reached as this technique resulted not appropriated to analyze the system CD1d-Ag-TCR with a high level of complexity. However, complementary computational studies considering increased protein flexibility ended up with a clear tendency favoring disubstituted aromatic ligands over trisubstituted ones among the virtual library, this indicating disubstituted aromatics as the best candidates to be synthesized.

4. GENERAL CONCLUSIONS

In Chapter 2 it is described the synthesis of a small family of aromatic-ceramide derivatives. The family design was based on preceding computational results and biological tests of our "*hit*" compound **I-1a**; considering only one extra substituent on the ring a part from ceramide skeleton, 5 subfamilies were proposed (phenylthio – **1**, phenyloxy – **2**, phenylamino – **3**, 2-*O*-linked-pyridines – **4** and 2-*S*-linked-pyridines – **5**) with the same 4 substituents at C-2, considering the results of ligands studied under computational experiments (CH_2OH – **a**, COOMe – **b**, COOH – **c** and $CONH_2$ – **d**).

- The obtention of phenylthioceramide (**I-1**) and phenyloxyceramide (**I-2**) derivatives were accomplished following the acylaziridine **G** ring opening reaction strategy and subsequent acetal removal. 2-(Hydroxymethyl) **I-1a**, 2-(methoxycarbonyl) **I-1b**, 2-(carbamoyl) **I-1d**, 2-(Hydroxymethyl) **I-2a**, 2-(methoxycarbonyl) **I-2b**, 2-(carbamoyl) **I-2d** were obtained in moderate yields after two steps. Finally, 2-(carboxyl) derivatives **I-1c** and **I-2c** were obtained from basic hydrolysis of its methyl ester precursor in moderate yield. 2-(Hydroxymethyl)phenoxy-ceramide (**I-2a**) was obtained in moderate to good yield when was synthesized via nosylaziridine **H**.

- Nosylaziridine **H** methodology was set up with excellent yields to incorporate substrates with poor nucleophilicity. Although the synthetic route was two steps longer than that involving acylaziridines, the key step of aromatic scaffold incorporation to the sphingoid chain proceed with excellent yields and the final overall yields were comparable or even better than the acylaziridine. At the same time, this strategy opened new possibilities to easily diversify *N*-acyl chains if desired.

- Aniline-like derivatives synthesis was planned following nosylazirdine **H** ring opening reactions. 2-(Hydroxymethyl) **I-3a**, 2-(methoxycarbonyl) **I-3b** and 2-(carbamoyl) **I-3d** were obtained with moderate to good yield after 4 steps. When hydroxymethyl intermediate **II-3a** was treated under general conditions for acetal removal, a methylated byproduct **I-3a-Me** was obtained. Unfortunately, the acid **I-3c** could not be isolated pure although its formation was confirmed by HPLC-MS.

- The obtention of *O*-linked-pyridine compounds was accomplished via aromatic nucleophilic substitution of 2-chloropyridines with azido-alcohol **D**. 2-(Hydroxymethyl) **I-4a**, 2-(methoxycarbonyl) **I-4b**, 2-(carbamoyl) **I-4d** and 2-(carboxyl) **I-4c** were synthesized in moderate to good yields after 4 steps.

- *S*-linked-pyridine derivatives **I-5** were planned to be synthesized via aromatic nucleophilic substitution of 2-chloropyridines with azidothiol intermediate **K**. This compound could not be isolated, but was generated from its *S*-acetyl precursor. *In situ* deacetylation and pyridine chlorine substitution was explored

with moderate yields in case of 2-chloronicotinamide, in low yield in case of methyl 2-chloronicotinatate while no reaction was observed with 2-hydroxymethyl analogue. Due to low yields in product formation and the complex reactivity of the precursors, the synthesis of this family was not further explored.

The biological activity of aromatic ceramides as NKT cell activators is covered in Chapter 3. This new family of αGalCer (**2**) mimetics was analyzed as NKT cell activators in both mice splenotyces and human NKT cells. In all cases, the response in immune cell profiles of the antigens was studied measuring the production of representative cytokines (INF-γ as T_H1 and IL-4 as T_H2).

- *In vitro* experiments were carried out using splenocytes from bone marrow of Balb mice that contain a population of dendritic cells acting as antigen presenting cells. These experiments showed a total polarization towards T_H1 (INF-γ) response, as no IL-4 cytokine (T_H2) production was observed when cells were cultured with our compounds. Compounds **I-1a**, **I-1b**, **I-1d**, **I-2a**, **I-2b**, **I-2d**, **I-3d**, **I-4d** were tested.
- *In vitro* experiments on purified human NKT cells using transfected C1R cells (a B cell line commonly used as cell recipient in immunology) showed the same T_H1 polarization profile although with a slightly less selective response. At low dose (10 ng/mL), our compounds showed 80% of INF-γ production versus 20% of IL-4 when compared to those obtained with the standard NKT cell antigen compound αGalCer (**2**). Compounds **I-1a**, **I-1b**, **I-1d**, **I-2a**, **I-2b**, **I-2d**, **I-4d** were tested together with one of our best aminicyclitols - HS161 (**39**).
- These results confirm that our new family of aromatic-ceramide analogues of αGalCer (**2**) is able to stimulate NKT cells and polarize cell response towards T_H1 profile both in mice and human cell *in vitro* experiments at low concentrations.

4. GENERAL CONCLUSIONS

5. EXPERIMENTAL PART

5.1. Synthetic chemistry and characterization

5.1.1. Materials and Methods

Chemicals and solvents

All chemicals and solvents were obtained from commercial sources and used without purification, except solvents used in moisture-sensitive reactions which were treated prior to use with *PureSolv-EN*™ system, degassed under inert gases and dried by standard methods.

Reaction monitoring and purification

When possible, reactions were monitored by thin layer chromatography (TLC) on silica gel (60F, 0.2 mm, ALUGRAM Sil G/UV_{254} *Macherey-Nagel*) by visualization under 254 and/or 365 lamp. Compounds without chromophores were visualized using ethanolic solution of phosphomolybdic acid.

When purification was required, *flash* column chromatography on silica-gel 60 (*Panreac*, 40-63 microns RE) was used.

Nuclear Magnetic Resonance (NMR)

Compound characterization by Nuclear Magnetic Resonance (NMR) spectroscopy was performed with *Variant-Mercury 400 MHz* spectrometer or *Bruker-AVANCEIII-HD 500 MHz* spectrometer equipped with a z-gradient (65.7 G/ cm) inverse TCI cryoprobe. Chemical shifts δ are reported in parts per million (ppm) using residual non-deuterated solvent signal as reference (Chloroform-*d* δ=7.26 ppm (^{1}H), δ=77.16 ppm (^{13}C); DMSO-d_6 δ=2.50 ppm (^{1}H), δ=39.51 ppm (^{13}C), Methanol-d_4 δ=4.87 ppm, δ=3.31 ppm (^{1}H), δ=49.3 ppm (^{13}C)). The following abbreviations were used to designate multiplicities: s=singlet, d=doublet, t=triplet, q=quartet, m=multiplet, q=quintuplet, br=broad, dd=double-doublet, ddd=double-double-doublet. Coupling constant (*J*) was expressed in Hz.

Infrared Spectra (IR)

IR spectra were registered in chloroform solution and recorded with *Thermo Nicolet Avatar 360 FT-IR* Spectrometer.

Melting Point (mp)

Melting points were measured with *Melting Point B-545 (Büchi)*, ramp 0.5 ºC/min with digital temperature measurement.

Specific rotation ($[\alpha]_D$)

$[\alpha]_D$ values were measured in microaperture mode with a *Perkin-Elmer 341* polarimeter with Na/NaI lamp (589 nm) and 1dm of length cell (1 mL of capacity). [α]D are expressed in degrees and calculated as *c* x 100 / (*d* x *m*) where *c* is the concentration of the sample (in g/100 mL), *d* is the optical way (in dm) and *m* is the measured value (mean of 10 measurements).

High-resolution mass spectra (HRMS)

High-resolution mass spectra (HRMS) were analyzed by FIA (flux injected analysis) with Ultrahigh-Performance Liquid Chromatography (UPLC) *Aquity (Waters)* coupled to LCT Premier Orthogonal Accelerated Time of Flight Mass Spectrometer (TOF) (*Waters*). Data from mass spectra were analyzed by electrospray ionization in positive and negative mode. Spectra were scanned between 50 and 1500 Da with values every 0.2 seconds and peaks are given m/z. Data was acquired with MassLynx software version 4.1 (*Waters*). These analyses were performed by the mass spectrometry service of IQAC-CSIC.

Final compound purity

Purity of final compounds used in biological assays was determined by High-Performance Liquid Chromatography (HPLC) on a *2695 Alliance HPLC (Waters)* coupled to a photodiode array detector (*PDA) 2996 (Waters)* and *PL-ELS-1000* detector (Polymer Laboratories). Chromatographic method using Hexane – isoPropanol gradient was used, purity was measured based on ELS response. For all samples 10 µL were injected to *Zorbax Rx-Sil Analytical column 4.6x150 mm and 5 µm from Agilent* provided with *Zorbax Rx-Sil 4.6x12.5 mm and 5 µm* guard column.

Chromatographic gradient: Hexane - isoPropanol gradient. Constant flow at 1 mL/min

Time (min)	Hexane (%)	isoPropanol (%)
0	99	1
15	70	30
20	70	30
22	1	99
30	1	99

Table 5.1: *Chromatographic conditions*

Microwave reactions

Reactions under microwave irradiation were carried out in a *CEM Discover Focused™* Microwave reactor. The instrument consists in a continuous focused microwave power delivery system with operator selectable power output from 0-300 W. Reactions were performed in glass vessels of 10 mL sealed with septum. The temperature of the

content of the vessel was monitored using an IR sensor and the indicated temperature corresponds to the maximal temperature reached during each experiment. The content of the vessels are stirred by means of rotating magnetic plate located below the floor of the microwave cavity and a Teflon coated magnetic stir bar in the vessel. The specified time corresponds to the total irradiation time. Efficient cooling is accomplished by means of pressurized air during entire experiment.

5.1.2. Synthesis and characterization

Compounds previously described in literature are described only with H^1-NMR.

Compound nomenclature was extracted from ChemDraw software from CambridgeSoft

5.1.2.1. Synthesis of key intermediates of phytosphingosine derivatives or acyl analogues:

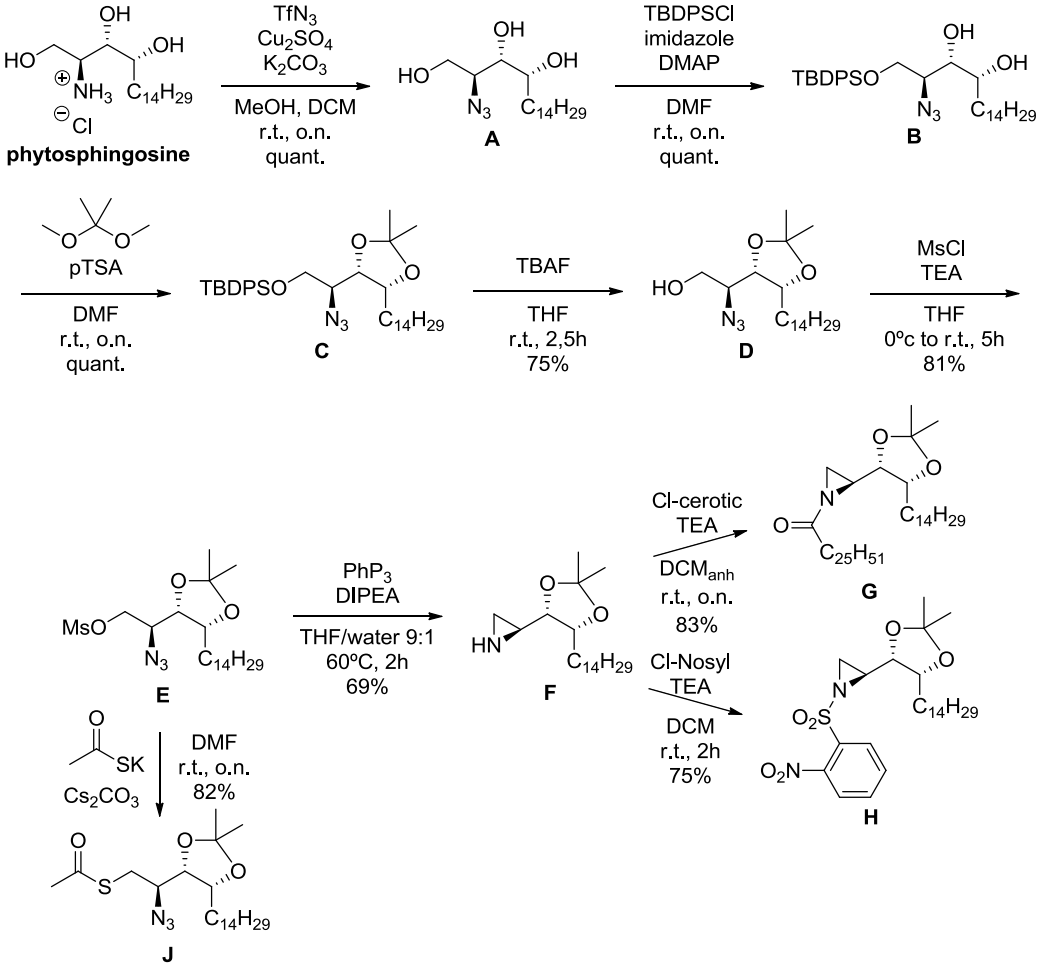

Scheme 5.1: *Synthesis of aziridine derivatives **G** and **H** from phytosphingosine hydrochloride*

Starting key intermediates of phytosphingosine derivatives were obtained using well-known procedures in our group[1-3], although some steps were optimized during this doctoral thesis.

5. EXPERIMENTAL PART

(2S,3S,4R)-2-azidooctadecane-1,3,4-triol (A)[4]

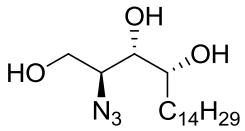

Triflic Anhydride (Tf_2O) (1.9 eq.) was added carefully dropwise to a solution of NaN_3 (10 eq.) in Water/DCM (1:1.7) and at 0ºC, the mixture was stirred 3 hours reaching room temperature to generate in situ the reactive TfN_3 (0.45 M). Organic layer of previous mixture was diluted with DCM to 0.2 M and then it was carefully added onto a previously prepared solution of phytosphingosine hydrochloride (1 eq.) in MeOH/Water (1.2:1) at 0.6 M with K_2CO_3 (1.55 eq.) and $CuSO_4$ (0.01 eq.) resulting in a white suspension into a greenish blue solution. Resulting mixture was stirred overnight or until no starting phytosphingosine was observed by TLC.

Initial procedure: Next day, solvents are removed under reduced pressure and the resulting white solid is resuspended into cool MeOH/water (1.2:1) solution, the precipitated is filtered and dried in vacuum to yield 2.6 g (quantitative yield) of a white solid. *This procedure leads to a difficult filtration due to plate stopping and mixture solvent removal.*

Improved procedure: Next day, reaction is transferred to a separator funnel to obtain the organic layer. Aqueous layer is washed only once with DCM/MeOH (1:1) mixture, organic layers were combined and concentrated under reduced pressure to obtain a white solid (3.6 g, quantitative yield).

Product was used directly into next step without purification. NMR spectra agreed with literature[4] in both cases. ^{1}H NMR (400 MHz, Methanol-d_4) δ 3.92 (dd, *J* = 11.6, 3.3 Hz, 1H), 3.75 (dd, *J* = 11.6, 8.0 Hz, 1H), 3.59 (ddd, *J* = 8.0, 4.6, 3.3 Hz, 1H), 3.55 – 3.48 (m, 2H), 1.72 – 1.62 (m, 1H), 1.58-1.47 (m, 1H), 1.43 - 1.22 (m, 24H), 0.90 (t, *J* = 7.5, 6.9 Hz, 3H).

(2S,3S,4R)-2-azido-1-((tert-butyldiphenylsilyl)oxy)octadecane-3,4-diol (B)[5]

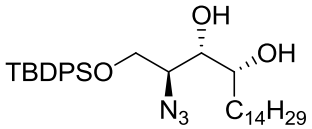

TBDPS-Cl (3.28 mL, 12.79 mmol) and solid Imidazole (1.45 g, 21.31 mmol) were added to a solution of azido-triol **A** (3.66 g, 10.65 mmol) in 25 mL of anhydrous DMF (0.5 M) under inter atmosphere. Reaction was stirred at room temperature overnight and stopped by dilution with 50 mL of AcOEt. The organic layer was washed three times with brine, dried with $MgSO_4$, filtered and concentrated in vacuum to yield 6.7 g (quantitative yield) of yellowish-brown oil, which was used directly into next step without purification. ^{1}H NMR spectrum agreed with bibliography[5]. ^{1}H NMR (400 MHz,

Chloroform-*d*) δ 7.73 – 7.67 (m, 4H), 7.50 – 7.35 (m, 6H), 4.03 (dd, *J* = 10.9, 4.2 Hz, 1H), 3.91 (dd, *J* = 11.0, 5.7 Hz, 1H), 3.71 – 3.64 (m, 2H), 3.61 – 3.54 (m, 1H), 1.59 – 1.51 (m, 2H), 1.31 – 1.23 (m, 24H), 1.08 (s, 9H), 0.88 (t, *J* = 10.5 Hz, 3H).

((S)-2-azido-2-((4S,5R)-2,2-dimethyl-5-tetradecyl-1,3-dioxolan-4-yl)ethoxy)(tert-butyl)diphenylsilane (C)[6]

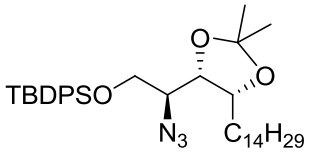

pTSA (0.6 g, 0.31 mmol) and 2,2-dimethoxypropane (10.73 mL, 87 mmol) were added to a solution of protected azido-diol **B** (5.2 g, 9 mmol) in 11 mL of DCM. The reaction mixture was stirred at room temperature overnight. The reaction was stopped by neutralization with TEA, and then it was diluted with DCM and organic layer was washed with brine. Aqueous phase was wash once with more DCM, combined with the other organic phase, dried with $MgSO_4$, filtered and concentrated in vacuum to yield 5.65 g (quantitative yield) of pale oil. Product was used directly into next step without purification. NMR spectra agreed with literature[6]. ^{1}H NMR (400 MHz, Chloroform-*d*) δ 7.71 (ddt, *J* = 9.6, 6.2, 1.6 Hz, 4H), 7.46 – 7.34 (m, 6H), 4.12 (ddd, *J* = 9.0, 5.6, 3.1 Hz, 1H), 4.02 (dd, *J* = 10.8, 2.6 Hz, 1H), 3.93 (dd, *J* = 9.7, 5.5 Hz, 1H), 3.83 (dd, *J* = 10.8, 7.0 Hz, 1H), 3.41 (ddd, *J* = 9.7, 7.1, 2.6 Hz, 1H), 1.61 – 1.46 (m, 2H), 1.41 - 1.19 (m, 30H), 1.07 (s, 9H), 0.87 (t, *J* = 7.5 Hz, 3H).

(S)-2-azido-2-((4S,5R)-2,2-dimethyl-5-tetradecyl-1,3-dioxolan-4-yl)ethanol (D)[6]

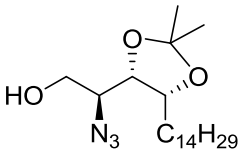

TBAF (1M in THF, 15.43 mL, 15.43 mmol) was added to a solution of azide **C** (4.8 g, 7.7 mmol) in 147 mL of THF under inert atmosphere. The reaction mixture was stirred at room temperature until no starting material remained (approx. 2.5 h). The solvent was removed under reduced pressure and the residue obtained was re-dissolved in 60 mL of DCM and washed with brine (3x50 mL), dried with $MgSO_4$, filtered and concentrated in vacuum. The crude was purified by *flash* chromatography on silica gel using gradient of Hexane/AcOEt from 0 to 30% to yield 2.2 g (75%) of desired compound as colorless oil. NMR spectra agreed with literature[6]. ^{1}H NMR (400 MHz, Chloroform-*d*) δ 4.17 (dt, *J* = 9.2, 4.4 Hz, 1H), 4.01 – 3.93 (m, 2H), 3.88 – 3.82 (m, 1H), 3.46 (ddd, *J* = 9.6, 5.6, 4.1 Hz, 1H), 1.62 – 1.50 (m, 2H), 1.42 (s, 3H), 1.39 - 1.20 (m, 27H), 0.87 (t, *J* = 6.4 Hz, 3H).

5. EXPERIMENTAL PART

((S)-2-azido-2-((4S,5R)-2,2-dimethyl-5-tetradecyl-1,3-dioxolan-4-yl)ethoxy)(tert-butyl)diphenylsilane (E)[2]

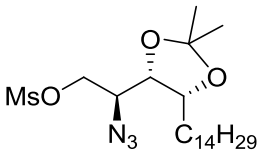

TEA (1.6 mL, 11.58 mmol) and methanesulfonyl chloride (0.67 µL, 8.65 mmol) were added to a solution of *O,O*-protected azido-alcohol **D** (2.2 g, 5.8 mmol) in anhydrous THF at 0ºC and the resulting mixture was stirred 10 min. at 0ºC and 5h at room temperature. Solvents were removed under reduced pressure; TEA salts were precipitated in diethyl ether and filtered off. The filtrate was concentrated in vacuum to yield 2.18 g (81%) of desired compound as pale oil. Product was used into next step without further purification[2]. ^{1}H NMR (400 MHz, Chloroform-*d*) δ 4.66 (dd, *J* = 10.8, 2.6 Hz, 1H), 4.30 (dd, *J* = 10.8, 7.7 Hz, 1H), 4.23 – 4.16 (m, 1H), 3.85 (dd, *J* = 9.3, 5.5 Hz, 1H), 3.71 (ddd, *J* = 9.3, 7.7, 2.6 Hz, 1H), 3.08 (s, 3H), 1.66 – 1.51 (m, 2H), 1.42 (s, 3H), 1.39 – 1.21 (m, 27H), 0.88 (t, *J* = 6.5 Hz, 3H).

(S)-2-((4S,5R)-2,2-dimethyl-5-tetradecyl-1,3-dioxolan-4-yl)aziridine (F)[2]

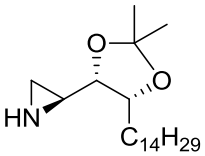

DIPEA (0.76 µL, 4.39 mmol) and triphenylphosphine (0.85 g, 3.25 mmol) were added to a solution of mesylate **E** (1g, 2.17 mmol) in 16 mL of a mixture THF/water (9:1). Reaction mixture was further stirred at 60ºC 2 hours. Solvents were removed under reduced pressure and resulting crude was solved in AcOEt and washed with brine, aqueous layer was washed with more AcOEt; the combined organic layers were dried with $MgSO_4$, filtered and concentrated in vacuum. Crude was purified by *flash* chromatography on silica gel using isocratic conditions of Hexane/AcOEt 7:3 to yield 513 mg (69%) of desired compound as colorless oil[2]. Product should be used into next step soon to avoid aziridine degradation. ^{1}H NMR (400 MHz, Chloroform-*d*) δ 4.20 (dt, *J* = 8.3, 5.9 Hz, 1H), 3.56 (t, *J* = 6.8 Hz, 1H), 2.08 (ddd, *J* = 7.6, 5.7, 3.4 Hz, 1H), 1.85 (d, *J* = 5.7 Hz, 1H), 1.73 – 1.65 (m, 2H), 1.57 (d, *J* = 3.4 Hz, 1H), 1.47 (s, 3H), 1.46 – 1.15 (m, 27H), 0.88 (t, *J* = 7.3 Hz, 3H).

(*S*)-2-((4*S*,5*R*)-2,2-dimethyl-5-tetradecyl-1,3-dioxolan-4-yl)-1-hexacosanoylaziridine (G)[1,7]

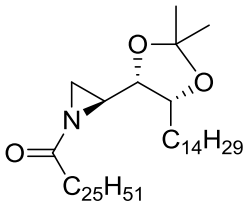

Cerotic acid (720 mg, 1.8 mmol) was solved in thionyl chloride (4.5 mL, 62 mmol) and heated to reflux for 2 hours. Excess of thionyl chloride was removed under reduced pressure and coevaporated with toluene to yield Cl-cerotic 752 mg (quantitative yield) of pale brown solid, with was directly used as reagent. In a separate flask, TEA (0.4 mL, 2.87 mmol) was added to a solution of aziridine **F** (513 mg, 1.5 mmol) in 20 mL of anhydrous DCM, the resulting mixture was cooled to -10 ºC. Freshly prepared Cl-cerotic was solved in 15 mL of anhydrous DCM and carefully added to aziridine solution. Reaction was further stirred and allowed to reach room temperature overnight. Solvent was removed under reduced pressure and resulting crude was purified by *flash* chromatography on silica gel using gradient of Hexane/AcOEt from 2 to 5% to yield 903 mg (83%) of desired compound as white solid[7]. ^{1}H NMR (400 MHz, Chloroform-*d*) δ 4.20 (dt, *J* = 8.6, 5.5 Hz, 1H), 3.78 (dd, *J* = 6.9, 5.9 Hz, 1H), 2.64 (ddd, *J* = 6.9, 5.9, 3.3 Hz, 1H), 2.48 – 2.30 (m, 2H), 2.28 (dd, *J* = 5.9, 1.1 Hz, 1H), 2.22 (dd, *J* = 3.3, 1.0 Hz, 1H), 1.87 – 1.70 (m, 2H), 1.67 – 1.58 (m, 2H), 1.46 (s, 3H), 1.37 – 1.22 (m, 71H), 0.88 (t, *J* = 6.7 Hz, 6H).

(S)-2-((4S,5R)-2,2-dimethyl-5-tetradecyl-1,3-dioxolan-4-yl)-1-((2-nitrophenyl)sulfonyl)aziridine (H)[2]

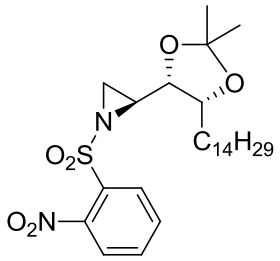

TEA and 0.94 mL, 6.7 mmol) and 2-nitrobenzene-1-sulfonyl chloride (1.19 g, 5.37 mmol) were added to a solution of aziridine **F** (1.5 g, 4.47 mmol) in 75 mL of DCM. Reaction was stirred at room temperature 2 hours. Solvents were removed under reduced pressure and crude was purified by *flash* chromatography son silica gel using isocratic conditions of Hexane/AcOEt 85:15 to yield 1.76 g (75%) of desired compound as white solid. ^{1}H-NMR spectra agreed with literature[2]. ^{1}H NMR (400 MHz, Chloroform-*d*) δ 8.26 – 8.16 (m, 1H), 7.81 – 7.68 (m, 3H), 4.21 (dt, *J* = 7.6, 6.1 Hz, 1H), 3.95 (t, *J* = 5.9 Hz, 1H), 3.17 (ddd, *J* = 7.1, 5.9, 4.7 Hz, 1H), 2.92 (d, *J* = 0.6 Hz, 1H), 2.52 (d, *J* = 4.7 Hz, 1H), 1.70 – 1.59 (m, 2H), 1.45 (s, 3H), 0.42 - 1.16 (m, 27H), 0.88 (t, J = 6.7 Hz, 3H).

S-((R)-2-azido-2-((4S,5R)-2,2-dimethyl-5-tetradecyl-1,3-dioxolan-4-yl)ethyl) ethanethioate (J)

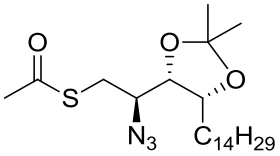

Mesyl intermediate **E** (1.3g, 2.85 mmol), cesium carbonate (0.464g, 1.42 mmol) and potassium thioacetate (0.651g, 5.7 mmol) were purged under inert atmosphere. Then all reagents were solved in anhydrous DMF (100 mL, 0.03M) to give a dark-green solution. The reaction flask was covered with aluminum foil and the reaction mixture was further stirred at room temperature overnight. Solvent was removed under reduced pressure and the resulting crude was resuspended in 100 mL of AcOEt, washed with saturated aqueous $NaHCO_3$ (2x100mL) and once with brine. The organic layer was dried with $MgSO_4$, filtered and concentrated in vacuum to give a pale brown oil which was purified by *flash* chromatography on silica gel using a gradient of Hexane/AcOEt from 20 to 100% to yield 1.03g (82%) of desired compound as pale oil. $[\alpha]^{25}_{D}$ -30.77 (*c*= 1; $CHCl_3$); IR ($CHCl_3$) *v* = 2922, 2853, 2117, 1699, 1464, 1370, 1246, 1220, 1132, , 1064cm^{-1}; ^{1}H NMR (400 MHz, Chloroform-*d*) δ 4.18 – 4.10 (m, 1H), 3.80 (dd, *J* = 8.8, 5.5 Hz, 1H), 3.60 (dd, *J* = 14.1, 3.1 Hz, 1H), 3.52 (td, *J* = 8.8, 3.1 Hz, 1H), 2.94 (dd, *J* = 14.1, 8.7 Hz, 1H), 2.37 (s, 3H), 1.60 – 1.53 (m, 2H), 1.46 (s, 3H), 1.42 – 1.18 (m, 27H), 0.86 (t, *J* = 6.7 Hz, 3H); ^{13}C NMR (101 MHz, Chloroform-*d*) δ 195.01, 108.60, 78.23, 77.90, 60.89, 32.41, 32.08, 30.72, 29.85, 29.83, 29.81, 29.79, 29.75, 29.73, 29.67, 29.51, 29.39, 28.11, 26.80, 25.73, 22.85, 14.28; HRMS calculated for $C_{23}H_{44}NO_3S$: 414.3042 $[M\text{-}N_2+H]^+$, found: 414.2990

(2R,3S,4S)-4-azido-2-tetradecyltetrahydrofuran-3-ol (BP-1)[8]

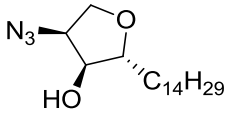

BP-1 was obtained as by-product formation from mesylate intermediate **E** when was stored for long time in frozen without purification. ^{1}H-NMR was in concordance with literature[8]. ^{1}H NMR (400 MHz, Chloroform-*d*) δ 4.14 (dd, *J* = 9.8, 5.9 Hz, 1H), 4.05 (td, *J* = 5.8, 4.6 Hz, 1H), 3.90 (q, *J* = 6.3 Hz, 1H), 3.81 (dd, *J* = 9.7, 4.6 Hz, 1H), 3.61 (ddd, *J* = 7.7, 6.4, 4.8 Hz, 1H), 2.05 (d, *J* = 7.5 Hz, 1H), 1.68 – 1.57 (m, 2H), 1.37 – 1.23 (m, 24H), 0.96 – 0.82 (m, 3H).

5.1.2.2. Synthesis of 2-mercaptobenzamide (Ar-1d)

First strategy via di-amide formation:

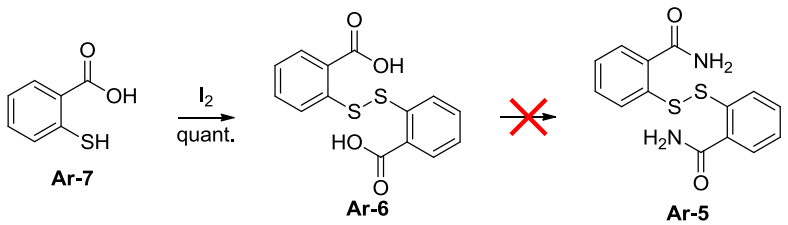

Scheme 5.2: *synthetic route of first strategy to obtain 2-mercaptobenzamide* ***Ar-1d***

2-((3-carboxyphenyl)disulfanyl)benzoic acid[9] (Ar-6)

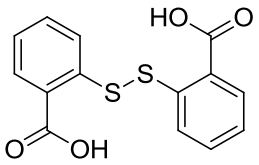

Iodine (412mg, 1.62 mmol) was added to a solution of 2-mercaptobenzoic acid (**Ar-7**) (500mg, 3.24 mmol) in 4 mL of ACN/water 5:1 to give yellowish brown solution with a white suspension. The reaction was stopped by adding 10 mL of 1% aqueous sodium thiosulfate until reaction mixture turns almost white. Conc. aq. HCl was added dropwise until acidic pH (0-2) and a white precipitate appeared, which was filtered off and dry in vacuum to yield 500 mg of title compound **Ar-6** (quantitative yield). ^{1}H NMR spectra agreed with literature[10]. ^{1}H NMR (400 MHz, DMSO-d_6) δ 13.55 (s, 2H), 8.03 (dd, *J* = 8.2, 2.5 Hz, 2H), 7.62 (dd, *J* = 8.2, 1.1 Hz, 2H), 7.56 (ddd, *J* = 8.3, 7.1, 1.5 Hz, 2H), 7.34 (ddd, *J* = 7.7, 7.1, 1.3 Hz, 2H).

Unsuccessful attempts to obtain 2-((3-carbamoylphenyl)disulfanyl)benzamide (Ar-5)

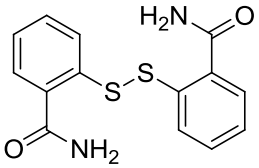

First attempt: EDC (37.5 mg, 0.196 mmol), HOBT (30 mg, 0.196 mmol) and TEA (45 µL, 0.326 mmol) were added to a solution of diacid **Ar-6** (20 mg, 0.065 mmol) in 2 mL of DMF, finally conc. aq. NH_3 (4.24 µL, 0.196 mmol) was added to the previous mixture and the reaction was stirred 3 days at room temperature. The reaction was stopped adding 10 mL of AcOEt, followed by washing with saturated aqueous $NaHCO_3$ (3x10 mL) and once with brine. The organic layer was dried with $MgSO_4$, filtered and concentrated in vacuum. The resulting crude was purified by *flash* chromatography on silica gel using DCM/AcOEt from 0 to 80%. Complex mixtures were obtained and the desired product could not be detected among the separated chromatography fractions.

Second attempt: To a stirred solution of diacid **Ar-6** (50 mg, 0.163 mmol) in 7.5 mL of anhydrous DMF in an ice bath oxalyl chloride (0.5 mL, 5.71 mmol) was carefully added. The resulting mixture was allowed to reach room temperature and further stirred overnight. When no starting material remained, conc. aq. ammonia (0.235 mL, 3.26 mmol) was added to the previous mixture and further stirred at room temperature. Next day, TLC control showed reaction progression to starting di-acid **Ar-6**. Reaction was discarded.

Third attempt: Diacid **Ar-6** (1g, 3.26 mmol) in 9 mL of thionyl chloride was heated at 75ºC overnight. The following day, excess of thionyl chloride was removed under reduced pressure and coevaporated with toluene to give a yellow-brown solid which was used directly without further purification. In a separated 3 neck flask, gaseous ammonia was dissolved in 40 mL THF at -78ºC with a gas stream until saturation. A batch of freshly obtained di-chloride was solved in 20 mL of anhydrous THF and carefully added onto previous ammonia solution. Solvents were removed under reduced pressure to yield 1.46 g of unique product with TEA salts. The ^{1}H-NMR spectra of the crude did not show expected signals. No further attempts to purify product from the solid salts were carried out. Spectral data of obtained solid was in agreement with the cyclic-byproduct[11,12] **Ar-8**: ^{1}H NMR (400 MHz, DMSO-d6) δ 7.98 (d, *J* = 8.2 Hz, 1H), 7.88 (dt, *J* = 7.9, 1.0 Hz, 1H), 7.63 (d, *J* = 1.2 Hz, 0H), 7.43 (t, *J* =7.4 Hz, 1H) – in agreement with commercial compound except that NH proton was not observed; HRMS calculated for C_7H_6NOS : 152.0170 $[M+H]^+$, found: 152.0160.

Fourth attempt: To a mixture of diacid **Ar-6** (500mg, 1.632 mmol) and 0.168 mL of DMF in THF (4.2 mL), oxalyl chloride (1.5 mL, 17.14 mmol) was slowly added at 0ºC. The reaction mixture was gradually warmed to room temperature and further stirred for 3h. The solvent was removed under reduced pressure to afford corresponding di-chloride as yellow solid in quantitative yield which was used without further purifications. The obtained crude solid was solved in anhydrous DCM (7.5 mL) and ammonium chloride (262 mg, 4.89 mmol) and TEA (1.364 mL, 9.8 mmol) were added. The reaction mixture was further stirred at room temperature. After several days, TLC controls showed only evidence of byproduct **Ar-8** formation. The reaction was discarded.

Second strategy via benzoisothiazolone Ar-8 reduction:

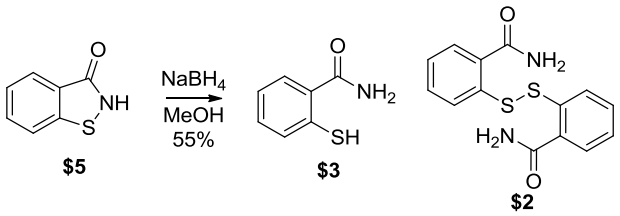

Scheme 5.3: *synthetic route of second strategy to obtain 2-mercaptobenzamide* ***Ar-1d***

2-mercaptobenzamide (Ar-1d)[13-16]

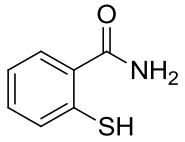

A solution of benzo[d]isothiazol-3(2H)-one (1.19 g, 7.84 mmol) in degassed MeOH at 0ºC under inert atmosphere was carefully added onto a solution of sodium borohydride (2.5 g, 66.7 mmol) in 20 mL degassed MeOH also at 0ºC; the resulting mixture was stirred at room temperature for 3 days. The reaction was stopped by acidification with 25 mL of aqueous HCl 1N, after stirring 30 min, the solvents were removed under reduced pressure and the resulting solid was re-suspended in more aqueous HCl 1N and stirred for 1 hour, a white precipitate appeared, which was filtered, washed with HCl 1N and water and dried in vacuum to yield 656.2 mg (55%) of the desired compound **Ar-1d** as a white solid[13]. ^{1}H NMR (400 MHz, DMSO-d_6) δ 7.92 (s, 1H), 7.57 (dd, *J* = 7.7, 1.5 Hz, 1H), 7.45 (s, 1H), 7.40 (dd, *J* = 7.9, 1.2 Hz, 1H), 7.28 (td, *J* = 7.6, 1.5 Hz, 1H), 7.15 (td, *J* = 7.5, 1.3 Hz, 1H), 5.47 (s, 1H). HRMS calculated for C_7H_6NOS: 152.0170 $[M-H]^-$, found: 152.0164.

2-((3-carbamoylphenyl)disulfanyl)benzamide (Ar-5)[17]

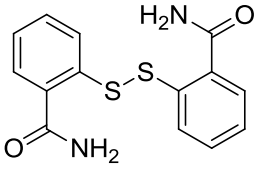

Diamide **Ar-5** was obtained as a by-product during 2-mercaptobenzamide **Ar-1d** obtaining reaction. Filtrate was separated and kept in fridge. Next day a white precipitated appeared, which was filtered off and dried in vacuum to yield 270.5 mg (23 %) of a white solid. H-NMR was in accordance with that one described[17] for compound **Ar-5**. ^{1}H NMR (400 MHz, DMSO-d_6) δ 8.12 (s, 0H), 7.72 (d, *J* = 6.7 Hz, 1H), 7.62 (d, *J* = 8.1 Hz, 2H), 7.44 (t, *J* = 7.8 Hz, 1H), 7.28 (t, *J* = 7.5 Hz, 1H).

5.1.2.3. Synthesis of new aromatic-ceramide derivatives and their intermediates

This section is organized by intermediate type from less complex ones to final compounds. In **Figure 5.1** is summarized the key nomenclature of compounds based on final compound structures.

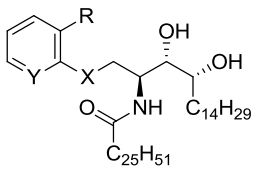

I-1a

R = CH_2OH, CHO, COOMe, COOH, $CONH_2$
X= S, O, NH
Y= CH_2, N

Roman Numeral: Intermediate level

Numbers: aromatic ring and linking atom
1= PhS
2= PhO
3= PhNH
4= PyrO
5= PyrS

Small letter: Substituent type as indicated (R)
a= CH_2OH
a'= CHO
b= COOMe
c= COOH
d= $COONH_2$

Figure 5.1: *Legend of new compounds nomenclature based on final compound structure*

All compounds were obtained following the general procedures described otherwise indicated.

Synthesis of intermediates type III: Nosyl-protected aromatic-phytosphingosines.

General Procedure 1: Nosyl-aziridine ring opening reaction with phenol-derivatives or aniline-derivatives.

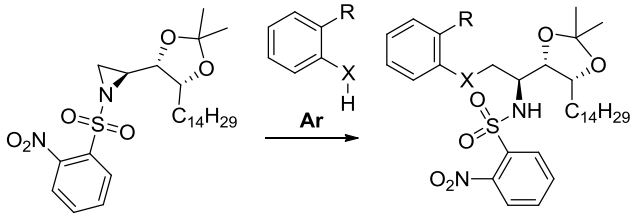

H **III**

R = CH_2OH, COOMe, COOH, $CONH_2$
X= O, NH

General scheme of ***General Procedure 1*** *to obtain intermediate type* ***III***

Nosyl-intermediate **H** was solved in ACN at 0.1M and the corresponding phenol or aniline (1.2 eq) was added followed by Cs_2CO_3 (1.5 eq) addition (only with phenols). The resulting mixture was stirred 4 hours at 85ºC until no starting material remained. The reaction mixture was diluted with AcOEt and water (10 mL each), the organic phase was separated and washed with brine, dried with $MgSO_4$, filtered and concentrated under reduced pressure. If needed, the resulting crude was purified by *flash* chromatography on silica gel using Hexane/AcOEt mixtures as mobile phase.

N-((S)-1-((4S,5R)-2,2-dimethyl-5-tetradecyl-1,3-dioxolan-4-yl)-2-(2-(hydroxymethyl)phenoxy)ethyl)-2-nitrobenzenesulfonamide (III-2a)

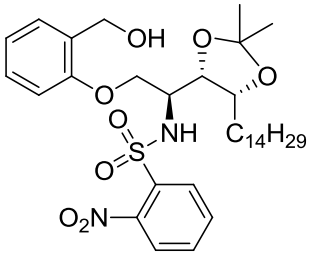

Compound **III-2a** was synthesized following **general procedure 1**, starting from nosyl-aziridine **H** (75 mg, 0.143 mmol), 2-(hydroxymethyl)phenol **(Ar-2a**) (21.3 mg, 0.172 mmol) and Cesium Carbonate (69.9 mg, 0.214 mmol). The resulting crude was purified using isocratic conditions of Hexane/AcOEt 7:3 to yield 82.3 mg (89%) of the desired compound as colorless oil. $[\alpha]^{25}_{D}$ +32.74 (*c*= 1; $CHCl_3$); IR ($CHCl_3$) *v* = 2922, 2853, 1542, 1454, 1352, 1242, 1168, 1059 cm^{-1}; ^1H NMR (400 MHz, Chloroform-*d*) δ 8.14 (dd, *J* = 6.4, 2.2 Hz, 1H), 7.75 (dd, *J* = 6.9, 2.2 Hz, 1H), 7.69 – 7.61 (m, 2H), 7.23 (dd, *J* = 7.4, 1.7 Hz, 1H), 7.10 (td, *J* = 7.8, 1.8 Hz, 1H), 6.90 (td, *J* = 7.4, 1.0 Hz, 1H), 6.47 (dd, *J* = 8.2, 1.0 Hz, 1H), 6.27 (d, *J* = 9.7 Hz, 1H), 4.64 (d, *J* = 12.4 Hz, 1H), 4.58 (d, *J* = 12.4 Hz, 1H), 4.27 – 4.15 (m, 3H), 4.07 – 3.98 (m, 1H), 3.93 (dd, *J* = 9.8, 2.9 Hz, 1H), 1.71 – 1.45 (m, 2H), 1.41 (s, 3H), 1.32 (s, 3H) 1.29 – 1.23 (m, 24H), 0.88 (t, *J* = 6.6 Hz, 3H); ^{13}C NMR (101 MHz, Chloroform-*d*) δ 156.37, 147.41, 135.53, 133.42, 132.99, 129.99, 129.64, 129.41, 128.92, 125.44, 121.42, 111.88, 108.30, 77.67, 76.03, 67.58, 61.47, 54.00, 31.90, 29.68, 29.64, 29.58, 29.57, 29.50, 29.34, 29.13, 27.86, 26.58, 25.44, 22.67, 14.10. HRMS calculated for $C_{34}H_{52}N_2O_8SNa$: 671.3342 $[M+Na]^+$, found: 671.3361.

N-((S)-1-((4S,5R)-2,2-dimethyl-5-tetradecyl-1,3-dioxolan-4-yl)-2-((2-(hydroxymethyl)phenyl)amino)ethyl)-2-nitrobenzenesulfonamide (III-3a)

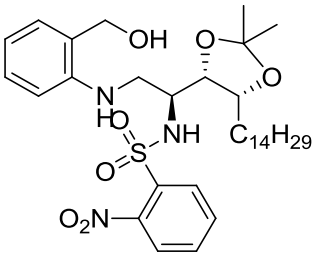

Compound **III-3a** was synthesized following **general procedure 1**, starting from nosyl-aziridine **H** (100 mg, 0.19 mmol) and 2-(aminophenyl)methanol **(Ar-3a**) (28.2 mg, 0.23 mmol). The resulting crude was purified using isocratic conditions of Hexane/AcOEt 7:3 to yield 104 mg (84%) of the desired compound as colorless oil. ^1H NMR (400 MHz, Chloroform-*d*) δ 8.11 (dd, *J* = 7.4, 1.9 Hz, 1H), 7.76 (dd, *J* = 7.0, 2.3 Hz, 1H), 7.69 – 7.59 (m, 2H), 7.03 (td, *J* = 9.4, 1.7 Hz, 1H), 6.98 (dd, *J* = 7.4, 1.6 Hz, 1H), 6.62 (td, *J* = 7.4, 1.1 Hz, 1H), 6.40 (dd, *J* = 8.1, 1.0 Hz, 1H), 6.07 (d, *J* = 9.2 Hz, 1H), 4.52 (s, 2H), 4.21 – 4.11 (m, 2H), 3.95 – 3.87 (m, 1H), 3.37 (dd, *J* = 13.5, 5.1 Hz, 1H), 3.26 – 3.19 (m, 1H), 1.65 –

1.58 (m, 1H), 1.44 (s, 3H), 1.32 - 1.22 (m, 27H), 0.87 (t, *J* = 7.0, 6.0 Hz, 3H); ^{13}C NMR (101 MHz, Chloroform-*d*) δ 147.56, 147.12, 135.50, 133.46, 133.18, 130.27, 130.23, 129.44, 129.27, 125.83, 125.18, 117.38, 110.93, 108.49, 77.98, 77.70, 64.56, 53.57, 44.13, 32.07, 29.85, 29.81, 29.75, 29.73, 29.68, 29.64, 29.50, 27.72, 26.59, 25.55, 22.83, 14.26. *No further characterization data could be obtained due to progressive sample degradation during NMR analysis.*

Synthesis of intermediates type V: *O*-linked-pyridine azido-phytosphingosines.

General Procedure 2: Nucleophilic substitution of Chloro-pyridines by azido-alcohol derivative **D** of phytosphingosine.

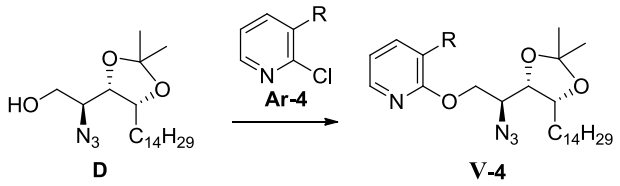

*General scheme of **General Procedure 2** to obtain intermediate type **V-4***

Azido-alcohol **D** was solved in anhydrous DMF at 0.1M under inert atmosphere and further stirred 15 min. Following addition of NaH (1.5 eq) or tBuOLi (2.2 eq) and the chloropyridine (1.1 to 1.3 eq). The resulting mixture was heated at 50ºC until no starting material remained. The reaction crude was diluted with AcOEt and water, the organic phase was separated and washed with brine, dried with $MgSO_4$, filtered and concentrated under reduced pressure. The crude residue was purified by *flash* chromatography on silica gel using Hexane/AcOEt as mobile phase.

2-((*S*)-2-azido-2-((4*S*,5*R*)-2,2-dimethyl-5-tetradecyl-1,3-dioxolan-4-yl)ethoxy)nicotinaldehyde (V-4a')

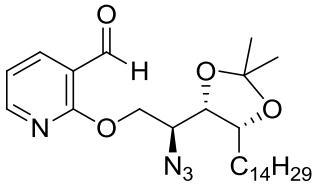

Intermediate **V-4a'** was obtained following **general procedure 2**, using azido-alcohol **D** as starting material (50 mg, 0.13 mmol), lithium tert-butoxide (22.96 mg, 0.29 mmol) and 2- chloronicotinaldehyde (**Ar-4a'**)(24 mg, 0.17 mmol) in 1.3 mL of anhydrous DMF over night. Subsequent purification using isocratic conditions of Hexane/AcOEt 4:1 yield 6.4 mg (10%) of desired compound **V-4a'** as a colorless oil and 7 mg (11%) of reduced aldehyde intermediate **V-4a** as colorless oil. $[\alpha]^{25}_{D}$ +10.96 (*c*= 0.5; $CHCl_3$); IR ($CHCl_3$) *v* = 2922, 2853, 2097, 1694, 1587, 1433, 1254, 1220, 1062 cm^{-1}; ^{1}H NMR (400 MHz, Chloroform-*d*) δ 10.41 (d, *J* = 0.8 Hz, 1H), 8.36 (dd, *J* = 4.9, 2.1 Hz, 1H), 8.14 (dd, *J* = 7.5, 2.1 Hz, 1H), 7.05 (ddd, *J* = 7.5, 4.9, 0.8 Hz, 1H), 5.00 (dd, *J* = 11.4, 2.6 Hz, 1H), 4.54

(dd, *J* = 11.4, 8.0 Hz, 1H), 4.20 (ddd, *J* = 9.4, 5.5, 3.8 Hz, 1H), 3.98 (dd, *J* = 9.4, 5.5 Hz, 1H), 3.86 (ddd, *J* = 9.4, 8.0, 2.6 Hz, 1H), 1.67 – 1.52 (m, 2H), 1.45 (s, 3H), 1.33 (s, 3H), 1.30 - 1.20 (m, 24H), 0.86 (t, *J* = 6.8 Hz, 3H); ^{13}C NMR (101 MHz, Chloroform-*d*) δ 188.86, 163.65, 152.83, 137.98, 119.13, 118.14, 108.68, 77.98, 76.01, 67.87, 59.69, 32.08, 29.85, 29.81, 29.79, 29.75, 29.71, 29.52, 29.49, 28.26, 26.74, 25.77, 22.85, 14.28; HRMS calculated for $C_{27}H_{45}N_4O_4$: 489.3441 $[M+H]^+$, found: 489.3451.

(2-((*S*)-2-azido-2-((4*S*,5*R*)-2,2-dimethyl-5-tetradecyl-1,3-dioxolan-4-yl)ethoxy)pyridin-3-yl)methanol (V-4a)

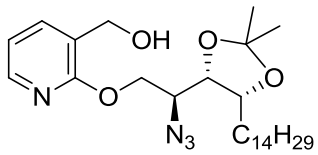

Compound **V-4a**: $[\alpha]^{25}_D$ +16.84 (*c*= 0.5; $CHCl_3$); IR ($CHCl_3$) *v* = 3435, 2923, 2853, 2098, 1592, 1433, 1250, 1221, 1062 cm^{-1}; ^{1}H NMR (400 MHz, Chloroform-*d*) δ 8.09 (dd, *J* = 5.1, 1.9 Hz, 1H), 7.65 (dd, *J* = 7.2, 1.9 Hz, 1H), 6.94 (dd, *J* = 7.2, 5.0 Hz, 1H), 4.92 (dd, *J* = 11.3, 2.9 Hz, 1H), 4.70 (dd, *J* = 6.2, 2.7 Hz, 2H), 4.47 (dd, *J* = 11.3, 7.6 Hz, 1H), 4.20 (ddd, *J* = 9.4, 5.5, 3.9 Hz, 1H), 4.00 (dd, *J* = 9.4, 5.5 Hz, 1H), 3.84 (ddd, *J* = 9.8, 7.6, 2.9 Hz, 1H), 1.70 – 1.59 (m, 2H), 1.46 (s, 3H), 1.45 -1.20 (m, 27H), 0.88 (t, *J* = 6.7 Hz, 3H); ^{13}C NMR (101 MHz, Chloroform-*d*) δ 160.60, 145.91, 137.09, 123.69, 117.72, 108.71, 67.11, 60.82, 59.65, 32.08, 29.85, 29.81, 29.79, 29.76, 29.71, 29.52, 28.23, 26.69, 25.79, 22.85, 14.28; HRMS calculated for $C_{27}H_{47}N_4O_4$: 491,3597 $[M+H]^+$, found: 491,3575.

Methyl 2-((*S*)-2-azido-2-((4*S*,5*R*)-2,2-dimethyl-5-tetradecyl-1,3-dioxolan-4-yl)ethoxy)nicotinate (V-4b)

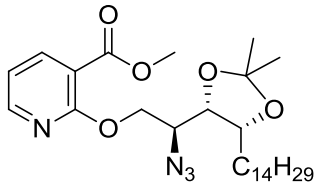

Compound **V-4b** was synthesized according to **general procedure 2**, using azido-alcohol **D** (97 mg, 0.25 mmol), sodium hydride (15.7 mg, 0.38 mmol) as a base and methyl 2-chloronicotinate (**Ar-4b**) (43.1 µL, 0.33 mmol) in 2.5 mL of anhydrous DMF overnight. The reaction crude was purified using isocratic conditions of Hexane/AcOEt 6:1 to yield 91.9 mg (70%) of the desired compound as a colorless oil. $[\alpha]^{25}_D$ +5.03 (*c*= 0.9; $CHCl_3$); IR ($CHCl_3$) *v* = 2923, 2853, 2099, 1739, 1716, 1589, 1578, 1432 1369, 1318, 1261, 1130, 1064 cm^{-1}; ^{1}H NMR (400 MHz, Chloroform-*d*) δ 8.29 (dd, *J* = 4.9, 2.0 Hz, 1H), 8.18 (dd, *J* = 7.5, 2.0 Hz, 1H), 6.98 (dd, *J* = 7.5, 4.9 Hz, 1H), 4.91 (dd, *J* = 11.4, 2.5 Hz, 1H), 4.50 (dd, *J* = 11.4, 7.8 Hz, 1H), 4.20 (ddd, *J* = 9.4, 5.5, 3.7 Hz, 1H), 4.05 (dd, *J* = 9.5, 5.5 Hz, 1H), 3.90 (s, 3H), 3.81 (ddd, *J* = 9.8, 7.8, 2.5 Hz, 1H), 1.68 – 1.53 (m, 2H), 1.44 (s, 3H), 1.42 -1.19 (m, 27H), 0.87 (t, *J* = 6.7 Hz, 3H); ^{13}C NMR (101 MHz,

Chloroform-*d*) δ 165.69, 161.44, 150.69, 141.66, 117.02, 114.46, 108.53, 77.97, 75.99, 67.69, 59.56, 52.54, 32.06, 29.83, 29.82, 29.79, 29.78, 29.74, 29.69, 29.54, 29.49, 28.28, 26.69, 25.80, 22.83, 14.25; HRMS calculated for $C_{28}H_{47}N_4O_5$: 519.3546 $[M+H]^+$, found: 519.3540.

2-((*S*)-2-azido-2-((4*S*,5*R*)-2,2-dimethyl-5-tetradecyl-1,3-dioxolan-4-yl)ethoxy)nicotinamide

(V-4d)

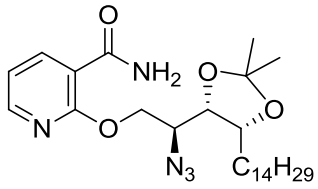

Compound **V-4d** was synthesized following **general procedure 2**, using azido-alcohol **D** (150 mg, 0.39 mmol), sodium hydride (36.9 mg, 0.92 mmol) as a base and 2-chloronicotinamide (**Ar-4d**) (67.5 mg, 0.431 mmol) in 3 mL of anhydrous DMF overnight. No purification was needed after liquid-liquid extractions. 187 mg (95%) of desired product were obtained as colorless oil. $[\alpha]^{25}_D$ -2.52 (*c*= 0.46; $CHCl_3$); IR ($CHCl_3$) *v* = 3371, 3190, 2918, 2850, 1644, 1541, 1468 , 1047 cm^{-1}; ^1H NMR (400 MHz, Chloroform-*d*) δ 8.53 (dd, *J* = 7.6, 2.0 Hz, 1H), 8.29 (dd, *J* = 4.8, 2.0 Hz, 1H), 7.72 (s, 1H), 7.10 (dd, *J* = 7.6, 4.8 Hz, 1H), 5.89 (s, 1H), 5.05 (dd, *J* = 11.6, 3.2 Hz, 1H), 4.60 (dd, *J* = 11.6, 7.0 Hz, 1H), 4.22 (ddd, *J* = 9.3, 5.5, 3.9 Hz, 1H), 4.00 (dd, *J* = 9.1, 5.5 Hz, 1H), 3.87 (ddd, *J* = 9.0, 7.0, 3.2 Hz, 1H), 1.71 – 1.50 (m, 2H), 1.48 (s, 3H), 1.42 – 1.19 (m, 27H), 0.88 (t, *J* = 6.6 Hz, 3H); ^{13}C NMR (101 MHz, Chloroform-*d*) δ 165.50, 160.06, 150.17, 142.40, 118.47, 115.73, 108.79, 77.91, 76.50, 66.82, 59.68, 32.08, 29.85, 29.83, 29.80, 29.77, 29.74, 29.69, 29.51, 29.46, 28.16, 26.75, 25.73, 22.84, 14.27; HRMS calculated for $C_{27}H_{46}N_5O_4$: 504.3550 $[M+H]^+$, found: 504.3547.

Attempts to obtain *S*-linked-pyridine azido-phytosphingosine intermediates V-5

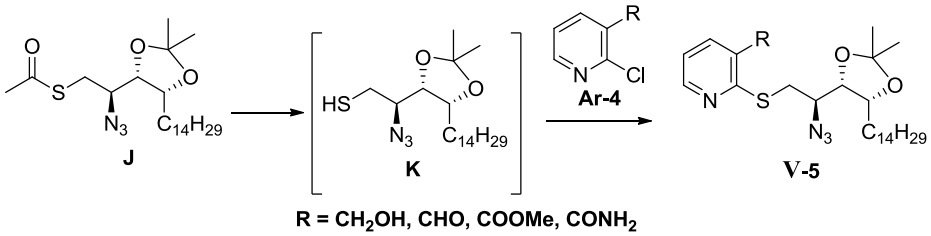

*General scheme of intermediate type **V-5** obtaining*

I) Deacetylation step, azido-thiol **K** isolation: Sodium methoxide 0.5 M in MeOH (3 µL, 1.5 µmol) was added to a solution of **J** (13.5 mg, 0.031 mmol) in 0.5 mL of dried MeOH (0.06M) under inert atmosphere, reaction was stirred at room temperature overnight. Reaction crude showed a complex mixture when analyzed by TLC. Any attempt to

purify the crude was unsuccessful. After chromatography, no pure product was isolated, the collected fractions contained mixtures of products not identified.

II) Acetyl removal and *in situ* reaction with chloropyridine **Ar-4d**:

First attempt: Acetyl-thio intermediate **J** (65.9 mg, 0.149 mmol) and chloropyridine **Ar-4d** (25.7 mg, 0.164 mmol) were solved in 1 mL of NaOH 0.2 M in degassed MeOH. Reaction was stirred at 40ºC two days but no reaction progress was observed. The starting material was recovered after column purification.

Second attempt: To a solution of intermediate **J** (27.3 mg, 0.062 mmol) and chloropyridine **Ar-4d** (19.4 mg, 0.124 mmol) in 1 mL of degassed MeOH, TEA (9.5 µL, 0.068 mmol) was added and reaction was stirred at 40ºC overnight. Reaction was diluted in 10 mL of AcOEt and washed with aq. sat. $NaHCO_3$ (10 mLx3) and once with 10 mL of brine, organic layer was dried with $MgSO_4$, filtered and concentrated in vacuum. ^{1}H-NMR showed a complex mixture which was not purified.

Third attempt: Intermediate **J** (28.2 mg, 0.064 mmol) and chloropyridine **Ar-4d** (20 mg, 0.128 mmol) under inert atmosphere were solved in 1 mL of degassed DMF with 10% of water and heated at 85ºC. Once room temperature was reached, cesium carbonate (22.9 mg, 0.07 mmol) was added and reaction was covered with aluminum foil and further stirred at 85ºC overnight. Following day reaction was diluted with 110 mL of AcOEt, washed with aq. sat. $NaHCO_3$ (10 mLx3) and once with 10 mL of brine, organic layer was dried with $MgSO_4$, filtered and concentrated in vacuum to afore 30 mg of yellow oil. Crude was purified by *flash* chromatography on silica gel using isocratic conditions of Hexane/AcOEt 1:1 to give 10 mg (30%) of desired compound **V-5d** as pale oil.

2-(((R)-2-azido-2-((4S,5R)-2,2-dimethyl-5-tetradecyl-1,3-dioxolan-4-yl)ethyl)thio)nicotinamide (V-5d)

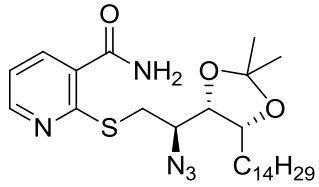

^{1}H NMR (400 MHz, Chloroform-*d*) δ 8.50 (dd, *J* = 4.8, 1.8 Hz, 1H), 7.93 (dd, *J* = 7.7, 1.8 Hz, 1H), 7.11 (dd, *J* = 7.7, 4.8 Hz, 1H), 6.16 (broad d, *J* = 184.4 Hz, 2H), 4.18 (dt, *J* = 9.6, 5.0 Hz, 1H), 4.12 (dd, *J* = 14.3, 3.1 Hz, 1H), 3.92 (dd, *J* = 8.6, 5.5 Hz, 1H), 3.76 (td, *J* = 8.9, 3.2 Hz, 1H), 3.21 (dd, *J* = 14.2, 9.0 Hz, 1H), 1.67 – 1.58 (m, 2H), 1.54 (s, 3H), 1.42 – 1.18 (m, 27H), 0.88 (t, *J* = 6.7 Hz, 3H); ^{13}C NMR (101 MHz, cdcl$_3$) δ 168.00, 156.31, 150.83, 137.22, 128.79, 119.49, 108.54, 78.59, 78.05, 60.99, 33.54, 32.08, 29.84, 29.81, 29.79, 29.76, 29.74, 29.69, 29.51, 29.38, 28.02, 26.95, 25.77, 22.85, 14.27; HRMS calculated for $C_{27}H_{46}N_5O_3S$: 520.3321 $[M+H]^+$, found: 520.3311.

III) Acetyl removal and *in situ* reaction with chloropyridines **Ar-4a** and **Ar-4b**:

(2-(((R)-2-azido-2-((4S,5R)-2,2-dimethyl-5-tetradecyl-1,3-dioxolan-4-yl)ethyl)thio)pyridin-3-yl)methanol (V-5a)

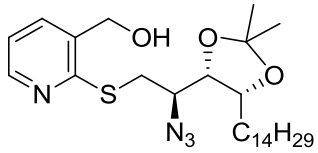

To a solution of intermediate **J** (102 mg, 0.233 mmol) and chloropyridine **Ar-4a** (66.8 mg, 0.465 mmol) in 3.5 mL of degassed DMF with 10% of water at 85ºC, cesium carbonate (83 mg, 0.256 mmol) was added; reaction mixture was covered with aluminum foil and further stirred at 85ºC overnight. Following day reaction was diluted with AcOEt and washed with aq. sat. $NaHCO_3$ (x3) and once with brine, organic layer was dried with $MgSO_4$, filtered and concentrated in vacuum. Spectral data of obtained crude showed complex mixture of signals. Column purification did not give any pure fraction and desired product was not detected among any of collected samples.

methyl 2-(((R)-2-azido-2-((4S,5R)-2,2-dimethyl-5-tetradecyl-1,3-dioxolan-4-yl)ethyl)thio)nicotinate (V-5b)

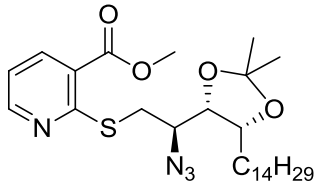

To a solution of intermediate **J** (102.4 mg, 0.232 mmol) and chloropyridine **Ar-4b** (80 mg, 0.464 mmol) in 3.5 mL of degassed DMF with 10% of water at 85ºC, cesium carbonate (83 mg, 0.256 mmol) was added; reaction mixture was covered with aluminum foil and further stirred at 85ºC overnight. Following day reaction was diluted with AcOEt and washed with aq. sat. $NaHCO_3$ (x3) and once with brine, organic layer was dried with $MgSO_4$, filtered and concentrated in vacuum. Column purification using isocratic conditions of Hexane/AcOEt 95:5 yield 14.2 mg (11%) desired product with traces of TBDPS. ^{1}H NMR (400 MHz, Chloroform-*d*) δ 8.54 (dd, *J* = 4.7, 1.9 Hz, 1H), 8.23 (dd, *J* = 7.8, 1.9 Hz, 1H), 7.08 (dd, *J* = 7.8, 4.7 Hz, 1H), 4.19 (dt, *J* = 8.6, 5.2 Hz, 1H), 4.04 (dd, *J* = 14.2, 3.2 Hz, 1H), 3.99 – 3.89 (m, 4H), 3.77 (td, *J* = 8.8, 3.2 Hz, 1H), 3.17 (dd, *J* = 14.2, 9.0 Hz, 1H), 1.68 – 1.58 (m, 2H), 1.55 (s, 3H), 1.45 – 1.16 (m, 27H), 0.88 (t, *J* = 6.8 Hz, 3H); HRMS calculated for $C_{28}H_{47}N_4O_4S$: 535.3318 $[M+H]^+$, found: 535.3301.

Synthesis of intermediates type IV: aromatic-phytosphingosines.

General Procedure 3[2]: One-pot reaction of Nosyl-aziridine **H** ring opening reaction followed by Nosyl-group removal.

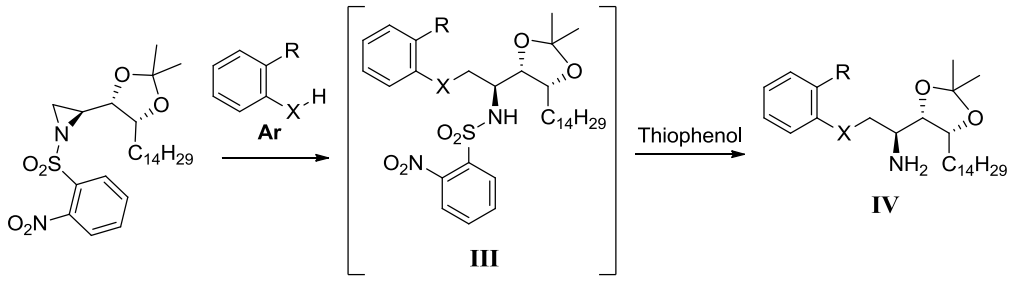

*General scheme of **General Procedure 3** to obtain intermediate type **IV***

Nosyl-intermediate **G** was solved in ACN at 0.1M and corresponding phenol or aniline (1.2 eq) was added followed by Cs_2CO_3 (1.5 eq) addition (if needed). Resulting mixture was stirred at 85ºC until no starting material remained. The reaction crude was checked by TLC or NMR and they were used directly into next step without any other treatment. Reaction was allowed to reach room temperature and thiophenol (3 eq) and Cs_2CO_3 (4 eq) were added to the corresponding solution of nosyl-intermediate **III** in ACN at 0.1M. The resulting mixture was stirred at room temperature overnight. The reaction mixture was diluted with AcOEt (10 mL) and water (10 mL), the organic layer was separated and washed with saturated aqueous NaCl (10 mL and dried with $MgSO_4$, filtered and concentrated under reduced pressure. Resulting crude was purified by *flash* chromatography on silica gel.

General Procedure 4[2]: Nosyl-group removal.

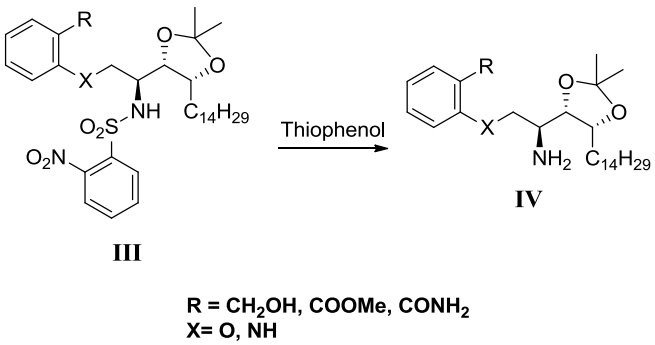

*General scheme of **General Procedure 4** to obtain intermediate type **IV***

Thiophenol (3 eq) and Cs_2CO_3 (4 eq) were added to the corresponding solution of nosyl-intermediate **III** in ACN at 0.1M and the resulting mixture was stirred at room temperature overnight. The reaction crude was diluted with AcOEt (10 mL) and water (10 mL), the organic layer was separated and washed with saturated aqueous NaCl (10

mL); the organic layer was dried with $MgSO_4$, filtered and concentrated under reduced pressure. Resulting crude was purified by *flash* chromatography on silica gel.

General Procedure 5: Azide reduction.

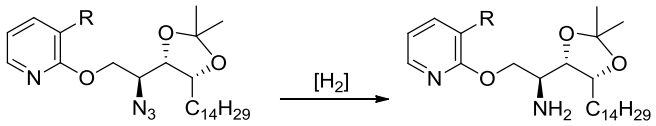

V **IV**

R = CH_2OH, COOMe, $CONH_2$

*General scheme of **General Procedure 5** to obtain intermediate type **IV***

Azido-intermediate **IV** was solved in AcOEt at 0.02M. Pd/C was added to the preceding solution and the resulting mixture was stirred in a sealed tube under 1 atm of H_2 until no starting material remained. Reaction mixture was filtered on Celite® and concentrated in vacuum to yield the title compounds which were used directly into next step without further purification.

(2-((S)-2-amino-2-((4S,5R)-2,2-dimethyl-5-tetradecyl-1,3-dioxolan-4-yl)ethoxy)phenyl)methanol (IV-2a)

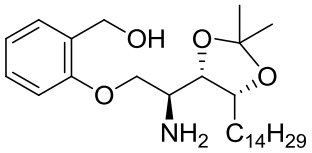

Compound **IV-2a** was synthesized according to **general procedure 4**, using **III-2a** (34 mg, 0.052 mmol), cesium carbonate (54.5 mg, 0.17 mmol) and thiophenol (22 µL, 0.21 mmol) solved in 0.8 mL of ACN. Reaction was purified using isocratic conditions of Hexane/AcOEt 2:8 to yield 20 mg (82%) of colorless oil. $[\alpha]^{25}_D$ -1.94 (*c*= 1; $CHCl_3$); IR ($CHCl_3$) *v* = 3298, 2922, 2853, 2360, 1492, 1454, 1370, 1242, 1047 cm^{-1}; ^1H NMR (400 MHz, Chloroform-*d*) δ 7.29 – 7.24 (m, 4H), 6.97 – 6.91 (m, 2H), 4.71 (d, *J* = 12.3 Hz, 1H), 4.63 (d, *J* = 12.3 Hz, 1H), 4.30 (dd, *J* = 9.6, 3.1 Hz, 1H), 4.24 – 4.18 (m, 1H), 4.06 – 3.97 (m, 2H), 3.32 – 3.19 (m, 1H), 2.24 (s, 3H), 1.58 (t, *J* = 4.3 Hz, 4H), 1.43 (s, 3H), 1.33 (s, 3H), 1.30 – 1.22 (m, 24H), 0.88 (t, *J* = 6.7 Hz, 3H); ^{13}C NMR (101 MHz, Chloroform-*d*) δ 157.34, 130.31, 129.50, 129.27, 121.40, 112.81, 108.39, 79.23, 77.84, 71.49, 62.14, 50.68, 32.08, 29.85, 29.82, 29.77, 29.75, 29.52, 28.24, 26.53, 25.89, 22.85, 14.28; HRMS calculated for $C_{28}H_{50}N_1O_4$: 464.3740 $[M+H]^+$, found: 464.3740.

methyl 2-((S)-2-amino-2-((4S,5R)-2,2-dimethyl-5-tetradecyl-1,3-dioxolan-4-yl)ethoxy)benzoate (IV-2b)

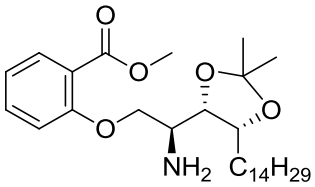

Compound **IV-2b** was synthesized according **general procedure 3** starting from nosylaziridine **H** (54.8 mg, 0.104 mmol), cesium carbonate (37.4 mg, 0.115 mmol) and methyl 2-hydroxybenzoate (**Ar-2b**) (15 µL, 0.115 mmol) in 1 mL of ACN. When no starting aziridine **H** was observed by TLC, mixture was cooled to room temperature and thiophenol (43 µL, 0.42 mmol) and cesium carbonate (68.1 mg, 0.21 mmol) were added as indicated above. Reaction crude was purified using isocratic conditions of DCM/AcOEt 8:2 to yield 44.4 mg (86% after two steps) of the desired compound as colorless oil. $[\alpha]^{25}_{D}$ +2.13 (*c*= 1; $CHCl_3$); IR ($CHCl_3$) *v* = 2922, 2852, 1726, 1600, 1491, 1450, 1376, 1244, 1083 cm^{-1}; ^{1}H NMR (400 MHz, Chloroform-*d*) δ 7.83 (dd, *J* = 7.8, 1.8 Hz, 1H), 7.46 (ddd, *J* = 8.8, 7.4, 1.8 Hz, 1H), 7.03 – 6.95 (m, 2H), 4.27 (dd, *J* = 8.9, 2.9 Hz, 1H), 4.22 (dt, *J* = 8.6, 4.3 Hz, 1H), 4.07 – 3.99 (m, 2H), 3.88 (s, 3H), 3.27 (ddd, *J* = 9.4, 6.7, 2.9 Hz, 1H), 1.65 – 1.52 (m, 2H), 1.43 (s, 3H), 1.38 – 1.22 (m, 27H), 0.88 (d, *J* = 6.3 Hz, 3H); ^{13}C NMR (101 MHz, Chloroform-*d*) δ 207.06, 166.56, 159.00, 133.82, 131.98, 120.48, 119.98, 113.71, 108.09, 78.91, 78.09, 77.16, 72.15, 52.03, 50.40, 32.07, 31.07, 29.93, 29.84, 29.81, 29.77, 29.51, 28.52, 26.43, 26.08, 22.84, 14.27; HRMS calculated for $C_{29}H_{50}N_1O_4$: 492.3689 $[M+H]^+$, found: 492.3290.

2-((S)-2-amino-2-((4S,5R)-2,2-dimethyl-5-tetradecyl-1,3-dioxolan-4-yl)ethoxy)benzamide (IV-2d)

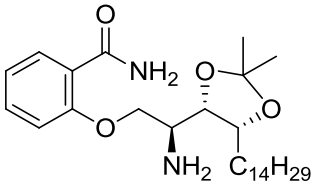

Compound **IV-2d** was synthesized according **general procedure 3**, starting from nosylaziridine **H** (50 mg, 0.095 mmol), cesium carbonate (34.2 mg, 0.105 mmol) and 2-hydroxybenzamide (**Ar-2d**) (14.4 mg, 0.105 mmol) in 1 mL of ACN. When no aziridine **H** was observed by TLC, the reaction mixture was cooled to room temperature and thiophenol (39 µL, 0.38 mmol) and cesium carbonate (62.1 mg, 0.19 mmol) were added as indicated above. The reaction crude was purified using isocratic conditions of DCM/AcOEt 5:95 to yield 43 mg (95% after two steps) of colorless oil. $[\alpha]^{25}_{D}$ +4.16 (*c*= 1; $CHCl_3$); IR ($CHCl_3$) *v* = 3467, 3310, 3191, 2922, 2853, 1650, 1695, 1454, 1378, 1232, 1217, 1167, 1047 cm^{-1}; ^{1}H NMR (400 MHz, Chloroform-*d*) δ 8.16 (dd, *J* = 7.8, 1.9 Hz,

1H), 8.04 (s, 1H), 7.45 (ddd, *J* = 8.9, 7.4, 1.9 Hz, 1H), 7.08 (td, *J* = 7.6, 1.0 Hz, 1H), 7.02 (dd, *J* = 8.4, 1.0 Hz, 1H), 5.86 (s, 1H), 4.34 (dd, *J* = 9.4, 3.5 Hz, 1H), 4.26 – 4.19 (m, 1H), 4.10 (dd, *J* = 9.4, 6.5 Hz, 1H), 3.96 (dd, *J* = 8.8, 5.6 Hz, 1H), 3.31 (ddd, *J* = 9.5, 6.5, 3.5 Hz, 1H), 1.62 – 1.53 (m, 4H), 1.43 (s, 3H), 1.37 – 1.19 (m, 25H), 0.88 (t, *J* = 6.8 Hz, 3H); ^{13}C NMR (101 MHz, Chloroform-*d*) δ 167.34, 157.32, 133.34, 132.57, 121.72, 121.62, 113.04, 108.44, 79.75, 77.90, 72.69, 50.37, 32.07, 29.92, 29.84, 29.80, 29.75, 29.51, 28.40, 26.42, 25.99, 22.84, 14.27; HRMS calculated for $C_{28}H_{49}N_2O_4$: 477.3692 $[M+H]^+$, found: 477.3692.

(2-(((*S*)-2-amino-2-((4*S*,5*R*)-2,2-dimethyl-5-tetradecyl-1,3-dioxolan-4-yl)ethyl)amino)phenyl)methanol (IV-3a)

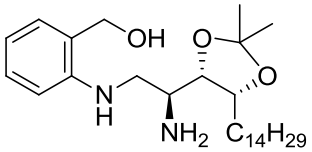

First attempt: Compound **IV-3a** was initially synthesized following **general procedure 4** starting from preceding intermediate **III-3a** (75 mg, 0.116 mmol), cesium carbonate (11.3 mg, 0.35 mmol) and thiophenol (48 µL, 0.46 mmol). The reaction crude was purified using a gradient of DCM/MeOH from 0 to 5% to yield 33mg (62 %) of the desired compound as colorless oil (52% after two steps).

Second attempt: Compound **IV-3a** was synthesized following **general procedure 3**. Starting from nosyl-aziridine **H** (50 mg, 0.095 mmol) and 2-(aminophenyl)methanol (**Ar-3a**) (14.1 mg, 0.114 mmol) solved in 1 mL of ACN. After total starting aziridine consumption, mixture was allowed to reach room temperature. To the previous mixture, cesium carbonate (93 mg, 0.29 mmol) and thiophenol (39 µL, 0.38 mmol) were added. Final purification using isocratic conditions of DCM/MeOH 95:5 yield 37 mg (84% after two steps) of desired product as colorless oil. $[\alpha]^{25}_D$ +4.02 (*c*= 1; $CHCl_3$); IR ($CHCl_3$) *v* = 3371, 2923, 2853, 1607, 1586, 1518, 1462, 1378, 1247, 121, 1165, 1052 cm^{-1}; ^{1}H NMR (400 MHz, Chloroform-*d*) δ 7.22 (td, *J* = 7.8, 1.7 Hz, 1H), 7.07 (dd, *J* = 7.3, 1.6 Hz, 1H), 6.77 (dd, *J* = 8.2, 1.1 Hz, 1H), 6.68 (dd, *J* = 7.3, 1.1 Hz, 1H), 4.66 (dd, *J* = 14.9, 11.9 Hz, 2H), 4.21 – 4.08 (m, 1H), 3.87 (dd, *J* = 8.2, 5.6 Hz, 1H), 3.54 (dd, *J* = 12.2, 2.7 Hz, 1H), 3.17 – 3.00 (m, 2H), 1.54 (dt, *J* = 13.4, 4.1 Hz, 2H), 1.46 (s, 3H), 1.40 – 1.17 (m, 27H), 0.88 (t, *J* = 7.1 Hz, 3H); ^{13}C NMR (101 MHz, Chloroform-*d*) δ 147.80, 129.76, 129.36, 125.06, 116.88, 111.38, 108.26, 80.95, 78.04, 64.70, 50.03, 48.23, 32.07, 30.05, 29.84, 29.82, 29.81, 29.76, 29.75, 29.51, 28.46, 26.34, 26.08, 22.84, 14.27; HRMS calculated for $C_{28}H_{51}N_2O_3$: 463.3900 $[M+H]^+$, found: 463.3898.

Methyl 2-(((*S*)-2-amino-2-((4*S*,5*R*)-2,2-dimethyl-5-tetradecyl-1,3-dioxolan-4-yl)ethyl)amino)benzoate (IV-3b)

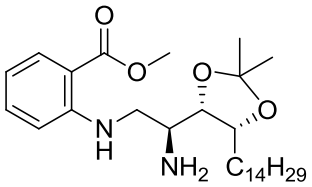

Compound **IV-3b** was synthesized following **general procedures 3**. Starting from nosyl-aziridine **H** (102 mg, 0.195 mmol) and methyl 2-aminobenzoate (**Ar-3b**) (30 µL, 0.233 mmol) solved in 2 mL of ACN. Cesium carbonate (196 mg, 0.603 mmol) and Thiophenol (83 µL, 0.804 mmol) were added in second step. Final purification using gradient of DCM/MeOH from 0 to 1.5% yielded 81 mg (85% after two steps) of the desired product as a colorless oil. $[\alpha]^{25}_{D}$ +29.31 (*c*= 0.51; $CHCl_3$); IR ($CHCl_3$) *v* = 3358, 2922, 2853, 2358, 1683, 1607, 1581, 1456, 1378, 1258, 1234, 1064 cm^{-1}; ^1H NMR (400 MHz, Chloroform-*d*) δ 8.02 (t, *J* = 4.9 Hz, 1H), 7.90 (dd, *J* = 8.0, 1.7 Hz, 1H), 7.35 (ddd, *J* = 8.7, 7.0, 1.7 Hz, 1H), 6.80 (dd, *J* = 8.6, 1.0 Hz, 1H), 6.59 (ddd, *J* = 8.1, 7.0, 1.1 Hz, 1H), 4.17 (dd, *J* = 8.1, 5.4 Hz, 1H), 3.92 – 3.84 (m, 4H), 3.66 – 3.58 (m, 1H), 3.18 – 3.08 (m, 2H), 1.59 – 1.50 (m, 2H), 1.46 (s, 3H), 1.40 – 1.19 (m, 27H), 0.88 (t, *J* = 4.8, 3.9 Hz, 3H); ^{13}C NMR (101 MHz, Chloroform-*d*) δ 169.12, 151.45, 134.58, 131.62, 114.56, 111.56, 110.09, 108.04, 80.41, 77.92, 51.46, 50.06, 47.35, 31.89, 29.87, 29.66, 29.63, 29.58, 29.56, 29.33, 28.39, 26.12, 25.95, 22.66, 14.09; HRMS calculated for $C_{29}H_{51}N_2O_4$: 491.3849 $[M+H]^+$, found: 491.3857.

2-(((*S*)-2-amino-2-((4*S*,5*R*)-2,2-dimethyl-5-tetradecyl-1,3-dioxolan-4-yl)ethyl)amino)benzamide (IV-3d)

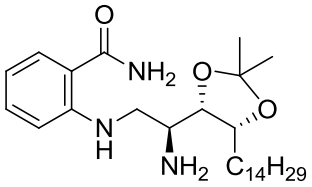

Compound **IV-3d** was initially synthesized following **general procedures 3**, starting from nosylaziridine **H** (104.9 mg, 0.2 mmol) and 2-aminobenzamide (33 mg, 0.24 mmol) in 2 mL of ACN. Cesium carbonate (204 mg, 0.626 mmol) and thiophenol (86 µL, 0.835 mmol) were added in the second step. Final purification using gradient of DCM/MeOH from 0 to 4% yielded 88 mg (92% after two steps) of the desired product as colorless oil. $[\alpha]^{25}_{D}$ +31.34 (*c*= 0.5; $CHCl_3$); IR ($CHCl_3$) *v* = 3402, 3353, 3189, 2918, 2850, 1638, 1615, 1607, 1509, 1467, 1397, 1216, 1064 cm^{-1}; ^1H NMR (400 MHz, Chloroform-*d*) δ 8.06 (d, *J* = 6.6 Hz, 1H), 7.38 (dd, *J* = 7.9, 1.5 Hz, 1H), 7.32 (ddd, *J* = 8.6, 7.1, 1.6 Hz, 1H), 6.83 (dd, *J* = 8.5, 1.0 Hz, 1H), 6.59 (dd, *J* = 8.0, 1.1 Hz, 1H), 5.70 (s, 2H), 4.17 (dt, *J* = 7.7, 5.7 Hz, 1H), 3.88 (dd, *J* = 8.7, 5.5 Hz, 1H), 3.65 – 3.54 (m, 1H), 3.20 – 3.06 (m, 2H), 1.61 – 1.49 (m, 2H), 1.46 (s, 3H), 1.35 (s, 3H), 1.25 (m, 24H), 0.88 (t, *J* =

6.8 Hz, 3H); ^{13}C NMR (101 MHz, $CDCl_3$) δ 172.23, 150.84, 133.72, 128.45, 114.77, 113.34, 112.44, 108.19, 80.44, 78.14, 50.17, 47.69, 32.08, 30.05, 29.84, 29.81, 29.77, 29.51, 28.58, 26.30, 26.13, 22.84, 14.28; HRMS calculated for $C_{28}H_{50}N_3O_3$: 476.3852 $[M+H]^+$, found: 476.3848.

(2-((*S*)-2-amino-2-((4*S*,5*R*)-2,2-dimethyl-5-tetradecyl-1,3-dioxolan-4-yl)ethoxy)pyridin-3-yl)methanol (IV-4a)

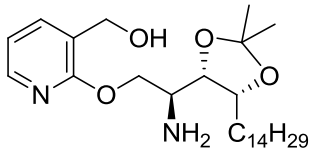

Compound **IV-4a** was obtained according to **general procedure 5** using intermediate **V-4a** (16 mg, 0.033 mmol) as starting material. After crude filtration and concentration, 16 mg (quant. yield) of the desired compound as a colorless oil was obtained. The residue was pure enough to go to the following step without purification. $[\alpha]^{25}_D$ +4.07 (*c*= 1; $CHCl_3$); IR ($CHCl_3$) *v* = 3363, 2922, 2853, 1594, 1432, 1399, 1248, 1219, 1048 cm^{-1}; ^{1}H NMR (400 MHz, Chloroform-*d*) δ 8.09 (dd, *J* = 5.1, 1.9 Hz, 1H), 7.56 (dd, *J* = 7.2, 1.9 Hz, 1H), 6.89 (dd, *J* = 7.1, 5.1 Hz, 1H), 4.70 – 4.58 (m, 3H), 4.32 (dd, *J* = 10.8, 6.6 Hz, 1H), 4.25 – 4.14 (m, 1H), 3.99 (dd, *J* = 8.6, 5.6 Hz, 1H), 3.25 (ddd, *J* = 8.6, 6.6, 3.8 Hz, 1H), 1.62 – 1.56 (m, 2H), 1.44 (s, 3H), 1.38 – 1.21 (m, 27H), 0.88 (t, *J* = 6.9 Hz, 3H); ^{13}C NMR (101 MHz, $cdcl_3$) δ 161.84, 146.20, 137.16, 124.10, 117.34, 108.36, 80.05, 78.08, 69.50, 61.41, 50.22, 32.08, 29.85, 29.82, 29.78, 29.75, 29.52, 28.29, 26.44, 26.01, 22.85, 14.28.; HRMS calculated for $C_{27}H_{49}N_2O_4$: 465.3692 $[M+H]^+$, found: 465.3694.

Methyl 2-((S)-2-amino-2-((4S,5R)-2,2-dimethyl-5-tetradecyl-1,3-dioxolan-4-yl)ethoxy)nicotinate (IV-4b)

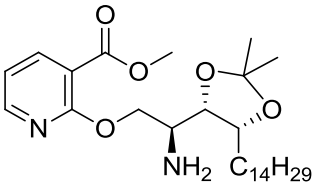

Compound **IV-4b** was obtained according to **general procedure 5** using intermediate **V-4b** (90 mg, 0.174 mmol) as starting material. After crude filtration and concentration, 67 mg (78%) of the desired compound as a colorless oil was obtained. This residue was pure enough to go to the following step without purification. $[\alpha]^{25}_D$ +34.32 (*c*= 1; $CHCl_3$); IR ($CHCl_3$) *v* = 3350, 2923, 2853, 1695, 1586, 1511, 1438, 1379, 1295, 1246, 1133, 1055 cm^{-1}; ^{1}H NMR (400 MHz, Chloroform-*d*) δ 8.30 (dd, *J* = 4.9, 2.0 Hz, 1H), 8.18 (dd, *J* = 7.5, 2.0 Hz, 1H), 6.95 (dd, *J* = 7.5, 4.9 Hz, 1H), 4.67 (dd, *J* = 10.5, 2.9 Hz, 1H), 4.34 (dd, *J* = 10.5, 6.8 Hz, 1H), 4.25 – 4.17 (m, 1H), 4.03 (dd, *J* = 9.1, 5.5 Hz, 1H), 3.90 (s, 3H), 3.27 (ddd, *J* = 9.5, 6.8, 2.9 Hz, 1H), 1.68 – 1.55 (m, 2H), 1.43 (s, 3H),

1.42-1.21 (m, 27H), 0.88 (t, *J* = 6.8 Hz, 3H); ^{13}C NMR (101 MHz, cdcl$_3$) δ 165.28, 162.30, 150.93, 141.27, 116.44, 113.79, 107.89, 78.92, 77.94, 70.03, 52.13, 49.94, 31.89, 29.75, 29.70, 29.66, 29.64, 29.62, 29.60, 29.33, 28.30, 26.28, 25.90, 22.66, 14.09; HRMS calculated for $C_{28}H_{49}N_2O_5$: 493.3641 $[M+H]^+$, found: 493.3622.

2-((*S*)-2-amino-2-((4*S*,5*R*)-2,2-dimethyl-5-tetradecyl-1,3-dioxolan-4-yl)ethoxy)nicotinamide (IV-4d)

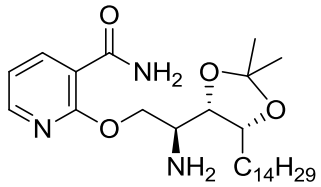

First attempt: Intermediate **V-4b** (20 mg, 0.04 mmol) in a reaction tube was dissolved in 1 mL of THF/MeOH 1:1, a small quantity of Pd/C was added, the tube was sealed under H_2 (1 atm) and stirred overnight. Next day, TLC control did not show starting material, however the desired product could not be observed by ^{1}H-NMR. Further purification using gradient of Hexane/AcOEt from 6:4 to 3:7 did not result in the isolation of any defined product. The major component of the mixtures did not show aromatic signals by ^{1}H-NMR.

Reaction Conditions screening: Three different conditions were monitored using 10mg (0.02 mmol) of starting intermediate **V-4b**.

I) The same conditions as above: after 1 hour, no starting intermediate was observed, however product degradation to an identified mixture of non-aromatic compounds was also observed.

II) Using Pd(OH)/C as a catalyst in THF/MeOH 1:1. After 1 hour, no starting intermediate was observed, however, product degradation to an identified mixture of non-aromatic compounds was observed by ^{1}H-NMR.

III) Pd/C in AcOEt as solvent: after 4 hours, the pure desired product was observed.

These conditions were set as general procedure 5 for future similar reactions.
Compound **IV-4d** was obtained according to **general procedure 5** using intermediate **V-4d** (127 mg, 0.253 mmol) as starting material in AcOEt. After crude filtration and concentration, 107 mg (88%) of desired compound as a colorless oil was obtained. The residue was pure enough to go to the following step without purification. A fraction of this residue (35 mg) was purified by flash chromatography in silica gel, giving a high purity compound (10 mg, 29%) as colorless oil. $[\alpha]^{25}_D$ +12.42 (*c*= 0.53; $CHCl_3$); IR ($CHCl_3$) *v* = 3463, 3341, 2922, 2853, 2359, 2342, 1672, 1585, 1462, 1429, 1378, 1235, 1059 cm^{-1}; ^{1}H NMR (400 MHz, Chloroform-*d*) δ 8.49 (dd, *J* = 7.6, 2.1 Hz, 1H), 8.28 (dd, *J* = 4.8, 2.0 Hz, 1H), 8.11 (s, 1H), 7.06 (dd, *J* = 7.6, 4.9 Hz, 1H), 5.76 (s, 1H), 4.74 (dd, *J* = 10.9, 4.2 Hz,

1H), 4.48 (dd, *J* = 10.9, 6.3 Hz, 1H), 4.22 (dt, *J* = 9.8, 5.6 Hz, 1H), 3.97 (dd, *J* = 8.7, 5.6 Hz, 1H), 3.31 (ddd, *J* = 8.7, 6.3, 4.2 Hz, 1H), 1.63 – 1.57 (m, 2H), 1.44 (s, 3H), 1.33 (s, 3H), 1.39-1.20 (m, 24H), 0.88 (t, *J* = 6.3 Hz, 3H);^{13}C NMR (101 MHz, cdcl$_3$) δ 165.86, 160.87, 150.22, 142.10, 118.02, 115.76, 114.06, 108.43, 80.35, 78.08, 77.36, 70.37, 50.06, 32.08, 29.87, 29.85, 29.81, 29.77, 29.52, 28.37, 26.39, 26.06, 22.85, 14.28; HRMS calculated for $C_{27}H_{48}N_3O_4$: 478.3645 $[M+H]^+$, found: 478.3646.

Synthesis of intermediates type II: *O,O*-diprotected aromatic-ceramides.

General Procedure 6: Acyl-aziridine ring opening reaction under microwave irradiation.

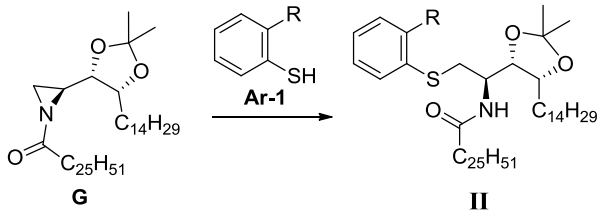

*General scheme of **General Procedure 6** to obtain intermediate type **II***

To a 0.1M solution of acylaziridine **G** and thiophenol (**Ar-1**) (1.3 eq) in ACN under inert atmosphere in a microwave glass tube, was added DBU (1.2 eq). The tube was sealed and irradiated at 150W, 120 ºC and 100 psi until no starting aziridine **G** was observed by TLC. The solvent was removed under reduced pressure and the crude was purified by *flash* chromatography on silica gel.

Via acylation strategies:

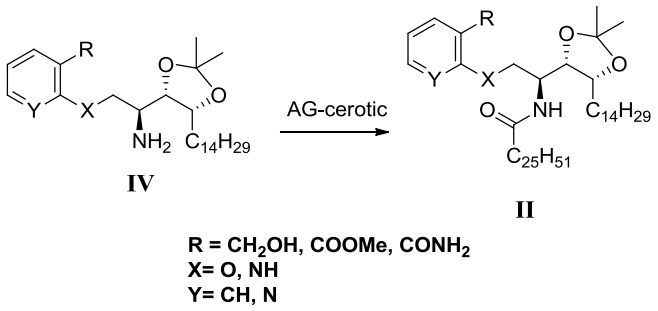

*General scheme of **General Procedures 7 and 8** to obtain intermediate type **II***

General Procedure 7: Acylation reaction with NHS-cerotic derivative.

Amine intermediate **IV** (1 eq) and freshly prepared NHS-cerotic ester (1.5 eq) were dissolved in anhydrous THF (0.05-0.06 M), TEA (3 eq) was added and the reaction was heated at 50ºC overnight or until no starting amine was observed. Solvents were removed under reduced pressure and crudes were purified by flash Chromatography on silica gel using DCM/MeOH.

General Procedure 8: Acylation reaction with Cl-cerotic derivative.

Amine intermediate **IV** (1 eq) and freshly prepared Cl-cerotic (1.2 eq) were dissolved in anhydrous DCM or THF (0.07-0.08 M), TEA (1.5 eq) was added and the reaction was heated at 50ºC overnight or until no starting amine was observed. Solvents were removed under reduced pressure and crudes were purified by flash Chromatography on silica gel using DCM/MeOH or Hexane/AcOEt.

_N_-((_R_)-1-((4_S_,5_R_)-2,2-dimethyl-5-tetradecyl-1,3-dioxolan-4-yl)-2-((2-(hydroxymethyl)phenyl)thio)ethyl)hexacosanamide (II-1a)[7]

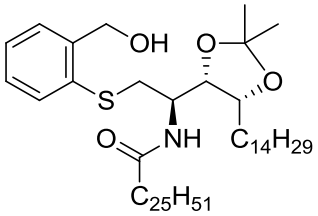

Compound **II-1a** was synthesized according to **general procedure 6**, from acylaziridine **G** (180.7 mg, 0.252 mmol), 2-mercaptobenzylalcohol (**Ar-1a**) (45.9 mg, 0.327 mmol) and DBU (41 µL, 0.277 mmol) in 2.3 mL of ACN. After 90 min reaction was completed. The reaction crude was purified using gradient of Hexane/AcOEt 8:2 to yield 159 mg (74%) of desired product as a white solid. ^{1}H-NMR was in concordance with previously reported[7]. 1H NMR (400 MHz, Chloroform-d) δ 7.54 – 7.49 (m, 1H), 7.42 (td, J = 5.9, 2.3 Hz, 1H), 7.30 – 7.22 (m, 2H), 5.86 (d, J = 9.2 Hz, 1H), 4.97 (d, J = 12.3 Hz, 1H), 4.66 (d, J = 12.3 Hz, 1H), 4.26 – 4.17 (m, 1H), 4.15 (t, J = 6.3 Hz, 1H), 4.10 – 4.04 (m, 1H), 3.30 (dd, J = 14.3, 3.0 Hz, 1H), 3.09 (dd, J = 14.3, 7.0 Hz, 1H), 1.92 (ddd, J = 8.0, 6.8, 4.3 Hz, 2H), 1.56 – 1.44 (m, 2H), 1.43 (s, 3H), 1.35 – 1.15 (m, 73H), 0.88 (t, J = 7.3, 6.6 Hz, 6H).

Methyl 2-(((_R_)-2-((4_S_,5_R_)-2,2-dimethyl-5-tetradecyl-1,3-dioxolan-4-yl)-2-hexacosanamidoethyl)thio)benzoate (II-1b)

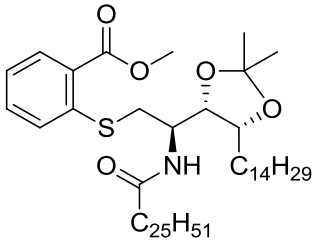

Compound **II-1b** was synthesized according to **general procedure 6**, from acylaziridine **G** (76.7 mg, 0.107 mmol), methyl 2-mercaptobenzoate (**Ar-1b**) (20 µL, 0.145 mmol) and DBU (26 µL, 0.171 mmol) in 1 mL of ACN. After 75 min. reaction was completed. The reaction crude was purified using gradient of Hexane/AcOEt from 0 to 15% to yield 40.2 mg (43%) of desired product as a white solid. $[\alpha]^{25}_{D}$ +13.54 (*c*= 0.5; $CHCl_3$); IR ($CHCl_3$) *v* =3289, 2916, 2849, 1715, 1653, 1544, 1469, 1247 cm^{-1}; ^{1}H NMR (400 MHz, Chloroform-*d*) δ 7.75 (dd, *J* = 7.8, 1.3 Hz, 1H), 7.50 (d, *J* = 7.9 Hz, 1H), 7.47 – 7.38 (m,

1H), 7.20 (d, *J* = 7.1 Hz, 1H), 6.17 (d, *J* = 8.8 Hz, 1H), 4.33 (dd, *J* = 8.5, 4.1 Hz, 1H), 4.27 (dd, *J* = 8.3, 5.6 Hz, 1H), 4.15 – 4.07 (m, 1H), 3.94 (s, 3H), 3.36 (dd, *J* = 13.6, 4.7 Hz, 1H), 3.27 (dd, *J* = 13.6, 3.5 Hz, 1H), 1.97 – 1.81 (m, 2H), 1.56 – 1.36 (m, 7H), 1.36-1.12 (m, 71H), 0.88 (t, *J* = 6.8 Hz, 6H); ^{13}C NMR (101 MHz, Chloroform-*d*) δ 172.80, 168.37, 139.06, 132.21, 131.18, 130.20, 130.15, 125.65, 108.22, 77.90, 76.94, 52.56, 48.31, 36.73, 36.65, 32.09, 29.86, 29.82, 29.78, 29.77, 29.71, 29.67, 29.53, 29.43, 29.31, 28.13, 26.69, 25.81, 25.58, 22.85, 14.28; HRMS calculated for $C_{55}H_{100}NO_5S$: 886.7322 $[M+H]^+$, found: 886.7299; mp: 107.4-107.5 ºC.

2-(((*R*)-2-((4*S*,5*R*)-2,2-dimethyl-5-tetradecyl-1,3-dioxolan-4-yl)-2-hexacosanamidoethyl)thio)benzamide (II-1d)

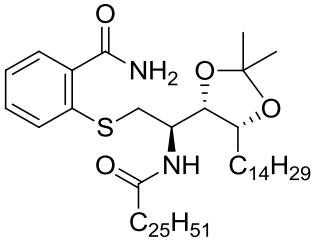

Compound **II-1d** was obtained following **general procedure 6** from acyl aziridine **G** (50 mg, 0.07 mmol), 2-mercaptobenzamide (**Ar-1d**) (12.8 mg, 0.084 mmol) and DBU (25 µL, 0.167 mmol) in 1 mL of ACN. After 180 min. reaction was completed. The desired product was precipitated in MeOH filtered and dried in vacuum to yield 50 mg (82%) of the desired compound as a white solid. $[\alpha]^{25}_{D}$ +6.70 (*c*= 0.47; $CHCl_3$); IR ($CHCl_3$) *v* =3365, 3296, 2917, 2850, 1646, 1539, 1469, 1219 cm^{-1}; ^{1}H NMR (400 MHz, Chloroform-*d*) δ 7.61 (dd, *J* = 8.3, 1.1 Hz, 1H), 7.45 – 7.34 (m, 2H), 7.29 (dd, *J* = 7.2, 1.3 Hz, 1H), 7.25 – 7.21 (m, 1H), 6.13 (s, 1H), 5.85 (s, 1H), 4.31 (dd, *J* = 9.3, 5.2 Hz, 1H), 4.25 (ddd, *J* = 9.2, 6.0, 3.0 Hz, 1H), 4.16 – 4.05 (m, 1H), 3.34 (dd, *J* = 14.4, 3.6 Hz, 1H), 3.25 (dd, *J* = 14.4, 3.0 Hz, 1H), 1.74 – 1.67 (m, 2H), 1.51 – 1.43 (m, 2H), 1.41 (s, 3H), 1.38 – 1.10 (m, 73H), 0.87 (d, *J* = 7.3 Hz, 6H); ^{13}C NMR (101 MHz, $cdcl_3$) δ 173.04, 172.34, 138.72, 135.10, 134.57, 131.12, 127.69, 127.10, 108.07, 77.36, 48.88, 48.78, 39.83, 36.05, 36.00, 32.08, 29.89, 29.87, 29.86, 29.83, 29.81, 29.79, 29.73, 29.70, 29.54, 29.52, 29.51, 29.44, 29.13, 28.27, 26.75, 25.98, 25.43, 22.85; HRMS calculated for $C_{54}H_{99}N_2O_4S$: 871.7326 $[M+H]^+$, found: 871.7297; mp: 109.9-110.7 ºC.

_N_-((_S_)-1-((4_S_,5_R_)-2,2-dimethyl-5-tetradecyl-1,3-dioxolan-4-yl)-2-(2-hydroxymethyl)phenoxy)ethyl)hexacosanamide (II-2a)

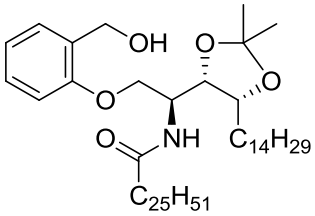

First attempt: Compound **II-2a** was synthesized following a modification of **general procedure 6 using NaH** instead of DBU. Acylaziridine **G** (40.3 mg, 0.056 mmol), 2-(hydroxyphenyl)methanol (**Ar-1a**) (**Ar-2a**) (8.7 mg, 0.070 mmol) and sodium hydride (4.2 mg, 0.105 mmol) in 1 mL of anhydrous DMF were reacted under MW irradiation. After 3 hours the reaction was completed, the crude was diluted with 2 mL of HCl 5M and further stirred 1 hour, then the mixture was extracted with 20 mL of AcOEt. The organic layer was washed with HCl 1N (3x20 mL) and once with brine, dried with $MgSO_4$, filtered and concentrated in vacuum. The residue was purified by *flash* chromatography on silica gel using gradient of Hexane/AcOEt from 0 to 20% to yield 10 mg (~20%) of impure desired product.

Second attempt: Thermal conditions were used instead of MW irradiation. Acylaziridine **G** (40 mg, 0.056 mmol), 2-(hydroxymethyl)phenol (**Ar-2a**) (13.83 mg, 0.111 mmol), and sodium hydride (2.67 mg, 0.111 mmol) were dissolved in 1 mL of anhydrous DMF under inert atmosphere and stirred at 85ºC. No reaction progress was observed after several days by TLC and the reaction was discarded without further manipulation.

Third attempt: Compound **II-2a** was synthesized following acylation strategy from intermediate **IV-2a**. Intermediate **IV-2a** (35.6 mg, 0.077 mmol) and TEA (32 µL, 0.23 mmol) were dissolved in AcOEt. Then, cerotic acid (34.8 mg, 0.09 mmol), HOBT (18.3 mg, 0.12 mmol) and EDC (22.4 mg, 0.018 mmol) were added to this solution and the reaction mixture was stirred at room temperature overnight. Next day, 0.5 mL of DMF were added and the reaction was further stirred 1 day. The reaction was stopped by dilution with 25 mL of AcOEt, washed with saturated aqueous $NaHCO_3$ (3x25 mL) and once with brine. The organic layer was dried with $MgSO_4$, filtered and concentrated in vacuum. The crude residue was purified by *flash* chromatography on silica gel using a gradient of Hexane/AcOEt from 10 to 50% to yield 26 mg (40%) of desired compound as white solid.

$[\alpha]^{25}_D$ +12.74 (*c*= 0.5; $CHCl_3$); IR ($CHCl_3$) *v* = 3317, 2917, 2850, 1652, 1456 cm^{-1}; ^1H NMR (400 MHz, Chloroform-*d*) δ 7.30 – 7.26 (m, 1H), 7.26 – 7.22 (m, 1H), 6.94 (t, *J* = 7.4 Hz, 1H), 6.87 (d, *J* = 8.1 Hz, 1H), 6.01 (d, *J* = 9.5 Hz, 1H), 4.69 (d, *J* = 12.2 Hz, 1H), 4.62 (d, *J* = 12.2 Hz, 1H), 4.46 (tt, *J* = 8.6, 3.6 Hz, 1H), 4.25 – 4.13 (m, 4H), 2.13 (t, *J* = 7.6 Hz, 2H),

1.65 – 1.56 (m, 4H), 1.44 (s, 3H), 1.38 – 1.16 (m, 71H), 0.88 (t, *J* = 6.7 Hz, 6H); ^{13}C NMR (101 MHz, Chloroform-*d*) δ 173.04, 157.39, 129.76, 129.71, 129.54, 121.32, 112.42, 108.49, 77.94, 76.91, 62.38, 48.46, 37.04, 32.09, 29.88, 29.86, 29.83, 29.81, 29.79, 29.76, 29.71, 29.67, 29.54, 29.52, 29.47, 29.09, 27.97, 26.85, 25.83, 25.66, 22.85, 14.28; ; HRMS calculated for $C_{54}H_{99}NO_5Na$: 864.7421 $[M+Na]^+$, found: 864.7410; mp: 97.7-97.8 ºC.

Methyl 2-((*S*)-2-((4*S*,5*R*)-2,2-dimethyl-5-tetradecyl-1,3-dioxolan-4-yl)-2-hexacosanamidoethoxy)benzoate (II-2b)

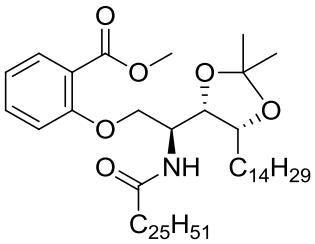

First attempt: According to **general procedure 6**, acylaziridine **G** (52.2 mg, 0.073 mmol), methyl 2-hydroxybenzoate (**Ar-1b**) (11 µL, 0.087 mmol) and DBU (15 µL, 0.102 mmol) were reacted under MW irradiation. After 120 min. no reaction progress was observed.

Second attempt: Aziridine opening reaction using $BF_3{\cdot}Et_2O$ as Lewis acid as described in literature[18] was assayed. Acylaziridine **G** (50 mg, 0.07 mmol), methyl 2-hydroxybenzoate (**Ar-1b**) (11 µL, 0.087 mmol) and Boron trifluoride etherate (0.88 µL, 7 µmol) were mixed under inert atmosphere. All reagents were solved in 1 mL of DCM and irradiated at 75 W at room temperature in a MW reactor. After 5 min. no starting material remained. The crude was purified by *flash* chromatography on silica gel using gradient of Hexane/AcOEt from 0 to 20% to yield 45 mg of a compound (90%). MS and NMR data agreed with cyclic byproduct of ceramide **BP-3** (see product spectral data above).

Third attempt: Acylaziridine **G** (49.3 mg, 0.069 mmol), potassium carbonate (9.5 mg, 0.07 mmol) and methyl 2-hydroxybenzoate (**Ar-1b**) (13 µL, 0.103 mmol) were mixed under inert atmosphere, dissolved in 1 mL of anhydrous DMF and the reaction flask was sealed and stirred. The following day, 4 µL (0.03 mmol) of methyl 2-hydroxybenzoante (**Ar-1b**) were added and mixture was heated at 100ºC. After 4 days the reaction was stopped adding 20 mL of AcOEt, and washing with saturated aqueous $NaHCO_3$ (3x20 mL). After phase separation, the organic layer was dried with $MgSO_4$, filtered and concentrated in vacuum. The crude was purified by *flash* chromatography on silica gel using gradient of Hexane/AcOEt from 0 to 30% to yield 23 mg (39%) of desired compound **II-2b**.

Fourth attempt: Compound **II-2b** was synthesized from acylaziridine **G** (50 mg, 0.07 mmol), potassium carbonate (19.2 mg, 0.14 mmol) and methyl 2-hydroxybenzoate (14 µL, 0.104 mmol) in 1mL of anhydrous DMF under inert atmosphere under microwave irradiation. After 4 hours the reaction was not complete, so the stirred mixture was left at 100ºC overnight. The evaporation crude was purified by *flash* chromatography on silica gel using a gradient of Hexane/AcOEt from 0 to 20 % to yield 31.3 mg (52%) of the desired compound as a white solid.

$[\alpha]^{25}_{D}$ +26.16 (*c*= 0.55; $CHCl_3$); IR ($CHCl_3$) *v* =3277, 2915, 2848, 1732, 1710, 1650, 1554, 1493, 1469, 1380, 1305, 1241, 1083 cm^{-1}; ^1H NMR (400 MHz, Chloroform-*d*) δ 7.81 (dd, *J* = 7.8, 1.8 Hz, 1H), 7.46 (ddd, *J* = 8.8, 7.5, 1.8 Hz, 1H), 7.12 (d, *J* = 9.6 Hz, 1H), 7.02 – 6.92 (m, 2H), 4.61 (dd, *J* = 9.0, 1.3 Hz, 1H), 4.46 – 4.33 (m, 1H), 4.26 (dd, *J* = 10.0, 5.3 Hz, 1H), 4.20 – 4.11 (m, 1H), 3.93 – 3.86 (m, 4H), 2.14 (td, *J* = 7.3, 2.3 Hz, 2H), 1.57 (s, 4H), 1.44 (s, 3H), 1.37 – 1.12 (m, 71H), 0.88 (t, *J* = 6.7 Hz, 6H); ^{13}C NMR (101 MHz, $cdcl_3$) δ 173.06, 166.51, 159.70, 134.16, 131.67, 120.79, 119.72, 114.88, 108.05, 78.14, 77.36, 75.70, 70.05, 52.08, 47.83, 37.06, 32.10, 32.08, 29.89, 29.86, 29.84, 29.82, 29.74, 29.65, 29.54, 29.52, 29.41, 28.89, 28.52, 26.77, 26.01, 25.87, 22.85, 14.28; HRMS calculated for $C_{55}H_{100}NO_6$: 870.7551 $[M+H]^+$, found: 870.7516; mp: 86.9-96.4 ºC.

(S)-4-((4S,5R)-2,2-dimethyl-5-tetradecyl-1,3-dioxolan-4-yl)-2-pentacosyl-4,5-dihydrooxazole (BP-3)

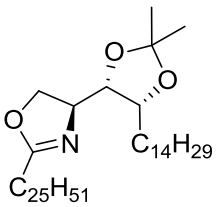

^1H NMR (400 MHz, Chloroform-*d*) δ 4.26 – 4.16 (m, 3H), 4.13 (t, *J* = 7.5 Hz, 1H), 4.02 (t, *J* = 6.4 Hz, 1H), 2.27 (t, *J* = 7.7 Hz, 2H), 1.68 – 1.56 (m, 4H), 1.42 (s, 3H), 1.41 – 1.17 (m, 71H), 0.88 (t, *J* = 6.7 Hz, 6H); ^{13}C NMR (101 MHz, $cdcl_3$) δ 169.52, 107.83, 79.81, 77.73, 69.74, 66.21, 32.09, 29.86, 29.82, 29.78, 29.66, 29.52, 29.43, 29.33, 28.33, 27.85, 26.73, 26.28, 25.53, 22.85, 14.28; HRMS calculated for $C_{47}H_{92}NO_3$: 718.7077 $[M+H]^+$, found: 718.7097.

2-((*S*)-2-((4*S*,5*R*)-2,2-dimethyl-5-tetradecyl-1,3-dioxolan-4-yl)-2-hexacosanamidoethoxy)benzamide (II-2d)

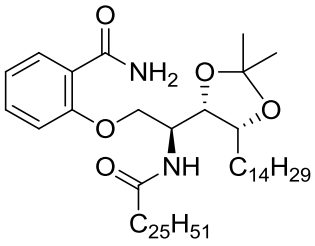

First attempt: Acylaziridine **G** (54 mg, 0.075 mmol), 2-hydroxybenzamide (**Ar-1d**) (12.4 mg, 0.09 mmol) and potassium carbonate (20.8 mg, 0.15 mmol) were mixed in 1 mL of anhydrous DMF under inert atmosphere. The reaction was irradiated at 150 W, 120ºC and 100 psi, after 3 hours no starting aziridine was observed. The reaction was diluted in 20 mL of AcOEt, washed with saturated aqueous $NaHCO_3$ (3x20 mL) and once with brine, dried with $MgSO_4$, filtered and concentrated in vacuum. The crude residue was purified by *flash* chromatography on silica gel using a gradient of Hexane/AcOEt from 0 to 10% to yield 30 mg (56%) of a compound with spectral data in agreement with the cyclic by-product **BP-3**. No evidence of formation of the desired product was detected.

Second attempt: Compound **II-2d** was synthesized from acyl-aziridine **G** (50 mg, 0.07 mmol), 2-hydroxybenzamide (**Ar-1d**) (20 mg, 0.146 mmol) and sodium hydride (11 mg, 0.275 mmol) in 1 mL of anhydrous DMF under inert atmosphere. The reaction mixture was heated at 85ºC overnight. Reaction was stopped by adding 5 mL of AcOEt, washing with saturated aqueous $NaHCO_3$ (2x10 mL) and once with brine. The organic phase was dried with $MgSO_4$, filtered and concentrated in vacuum. The crude residue was purified by *flash* chromatography on silica gel using a gradient of Hexane/AcOEt from 10 to 50% to yield 22.7 mg (38%) of desired compound as white waxy solid. $[\alpha]^{25}_{D}$ +1.84 (*c*= 0.51; $CHCl_3$); IR ($CHCl_3$) *v* =3377, 3290, 3185, 2917, 2849, 1649, 1543, 1469, 1379, 1246, 1218, 1048 cm^{-1}; ^1H NMR (400 MHz, Chloroform-*d*) δ 8.14 (dd, *J* = 7.8, 1.7 Hz, 1H), 7.62 (s, 1H), 7.47 – 7.41 (m, 1H), 7.07 (t, *J* = 7.5 Hz, 1H), 6.93 (d, *J* = 8.4 Hz, 1H), 5.91 (d, *J* = 9.6 Hz, 1H), 5.69 (s, 1H), 4.63 – 4.47 (m, 1H), 4.31 (dd, *J* = 9.6, 2.6 Hz, 1H), 4.21 (t, *J* = 7.7 Hz, 1H), 4.16 – 4.07 (m, 2H), 2.16 (t, *J* = 7.6 Hz, 2H), 1.63 – 1.52 (m, 4H), 1.47 (s, 3H), 1.40 – 1.15 (m, 71H), 0.88 (t, *J* = 6.8 Hz, 6H); ^{13}C NMR (101 MHz, Chloroform-*d*) δ 173.23, 167.15, 157.18, 133.29, 132.52, 121.73, 121.62, 112.50, 108.63, 77.91, 77.81, 77.48, 77.36, 77.16, 76.84, 70.05, 48.60, 37.01, 32.09, 29.88, 29.86, 29.82, 29.79, 29.75, 29.72, 29.67, 29.52, 29.44, 29.21, 27.70, 26.91, 25.81, 25.49, 22.85, 14.28; HRMS calculated for $C_{54}H_{99}N_2O_5$: 855.7554 $[M+H]^+$, found: 855.7594.

N-((*S*)-1-((4*S*,5*R*)-2,2-dimethyl-5-tetradecyl-1,3-dioxolan-4-yl)-2-((2-(hydroxymethyl)phenyl)amino)ethyl)hexacosanamide (II-3a)

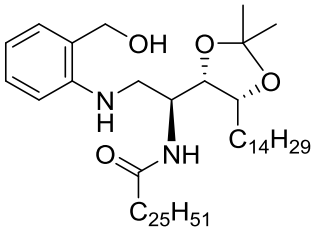

Compound **II-3a** was synthesized following **general procedure 7** from intermediate amine **IV-3a** (33 mg, 0.071 mmol), NHS-cerotic (52.8 mg, 0.107 mmol) and TEA (30 µL, 0.214 mmol) in 1.2 mL of anhydrous THF. Reaction was purified using isocratic conditions of DCM/MeOH 99:1 to yield 45 mg (75%) of the desired compound as white solid. $[\alpha]^{25}_{D}$ +6,34 (*c*= 0.8; $CHCl_3$); IR ($CHCl_3$) *v* = 3125, 2917, 2850, 1639, 1610, 1588, 1519, 1468, 1379, 1247, 1220 cm^{-1}; ^{1}H NMR (400 MHz, Chloroform-*d*) δ 7.19 (td, *J* = 7.8, 1.6 Hz, 1H), 7.07 (dd, *J* = 7.4, 1.6 Hz, 1H), 6.74 – 6.59 (m, 2H), 5.65 (d, *J* = 9.2 Hz, 1H), 4.67 (d, *J* = 12.2 Hz, 1H), 4.60 (d, *J* = 12.2 Hz, 1H), 4.39 – 4.26 (m, 1H), 4.21 – 4.12 (m, 1H), 4.10 (t, *J* = 6.2 Hz, 1H), 3.51 (dd, *J* = 12.9, 3.2 Hz, 1H), 3.28 (dd, *J* = 12.9, 7.5 Hz, 1H), 2.07 (t, *J* = 7.6 Hz, 2H), 1.61 – 1.47 (m, 7H), 1.42 – 1.15 (m, 71H), 0.88 (t, *J* = 6.7 Hz, 6H); ^{13}C NMR (101 MHz, $cdcl_3$) δ 173.79, 147.73, 129.61, 129.51, 124.73, 116.83, 110.71, 108.48, 78.56, 77.88, 64.46, 49.63, 45.89, 37.00, 32.09, 29.88, 29.86, 29.83, 29.82, 29.77, 29.73, 29.68, 29.66, 29.52, 29.46, 29.42, 27.65, 26.85, 25.70, 25.57, 22.85, 14.28; HRMS calculated for $C_{54}H_{101}N_2O_4$: 841.7761 $[M+H]^+$, found: 841.7756; mp: 85.1-95.8 ºC.

Methyl 2-(((*S*)-2-((4*S*,5*R*)-2,2-dimethyl-5-tetradecyl-1,3-dioxolan-4-yl)-2-hexacosanamidoethyl)amino)benzoate (II-3b)

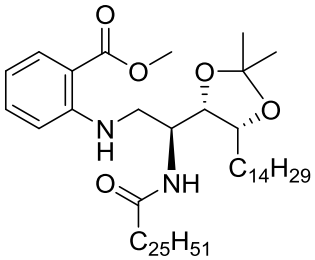

Compound **II-3b** was synthesized following **general procedure 8** from intermediate amine **IV-3b** (40 mg, 0.082 mmol), Cl-cerotic (40.6 mg, 0.098 mmol) and TEA (17 µL, 0.122 mmol) in 1 mL of anhydrous DCM. Crude purification using a gradient of DCM/MeOH from 0 to 1% yielded 35.5 mg (50%) of the desired compound as a white solid. $[\alpha]^{25}_{D}$ +31.28 (*c*= 0.5; $CHCl_3$); IR ($CHCl_3$) *v* = 3308, 2917, 2859, 1689, 1648, 1578, 1550, 1519, 1470, 1367, 1235, 1220, 1060 cm^{-1}; ^{1}H NMR (400 MHz, Chloroform-*d*) δ 7.92 – 7.81 (m, 2H), 7.37 – 7.27 (m, 1H), 6.79 (d, *J* = 8.5 Hz, 1H), 6.58 (t, *J* = 7.4, 7.0 Hz, 1H), 5.52 (d, *J* = 9.2 Hz, 1H), 4.30 (tt, *J* = 10.0, 5.1 Hz, 1H), 4.16 – 4.06 (m, 2H), 3.85 (s, 3H), 3.62 – 3.52 (m, 1H), 3.50 – 3.41 (m, 1H), 2.12 (td, *J* = 7.4, 3.7 Hz, 2H), 1.54 – 1.47

(m, 5H), 1.39 – 1.14 (m, 73H), 0.88 (t, *J* = 6.7 Hz, 6H); ^{13}C NMR (101 MHz, cdcl$_3$) δ 172.67, 168.91, 151.49, 134.53, 131.67, 114.88, 111.47, 110.37, 109.99, 108.25, 77.69, 51.49, 48.67, 36.89, 31.90, 29.67, 29.55, 29.33, 27.77, 26.49, 25.58, 22.66, 14.09; HRMS calculated for $C_{55}H_{101}N_2O_5$: 869.7711 $[M+H]^+$, found: 869.7703; mp: 116.3-130.3 ºC.

2-(((*S*)-2-((4*S*,5*R*)-2,2-dimethyl-5-tetradecyl-1,3-dioxolan-4-yl)-2-hexacosanamidoethyl)amino)benzamide (II-3d)

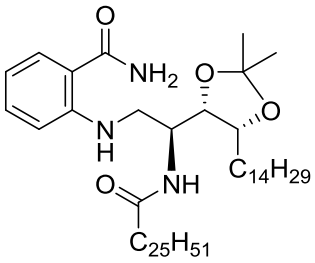

Compound **II-3d** was synthesized according **general procedure 8** from amine intermediate **IV-3d** (35 mg, 0.074 mmol), Cl-cerotic (36.7 mg, 0.088 mmol) and TEA (15 µL, 0.11 mmol) in 1 mL of anhydrous DCM. The crude purification using a isocratic conditions of DCM/MeOH 98:2 yielded 47 mg (75%) of the desired compound as a white waxy solid. $[\alpha]^{25}_D$ +28.81 (*c*= 0.52; $CHCl_3$); IR ($CHCl_3$) *v* = 3377, 3305, 3209, 2917, 2850, 1649, 1617, 1578, 1519, 1469, 1378, 1246, 1219, 1070 cm^{-1}; ^{1}H NMR (400 MHz, Chloroform-*d*) δ 7.87 (s, 1H), 7.36 (d, *J* = 6.6 Hz, 1H), 7.30 (d, *J* = 8.2 Hz, 1H), 6.83 (d, *J* = 8.5 Hz, 1H), 6.58 (t, *J* = 7.5 Hz, 1H), 5.74 (s, 1H), 5.64 (d, *J* = 9.2 Hz, 1H), 4.35 – 4.22 (m, 1H), 4.17 – 4.04 (m, 2H), 3.54 (d, *J* = 13.6 Hz, 1H), 3.46 (dd, *J* = 13.7, 4.7 Hz, 1H), 2.21 – 2.01 (m, 2H), 1.53 – 1.43 (m, 5H), 1.37 – 1.11 (m, 73H), 0.88 (t, *J* = 6.7 Hz, 6H); ^{13}C NMR (101 MHz, cdcl$_3$) δ 172.70, 171.20, 150.78, 133.53, 128.23, 114.92, 113.34, 112.41, 108.21, 77.71, 77.29, 48.66, 43.71, 36.86, 31.90, 29.69, 29.67, 29.64, 29.63, 29.60, 29.57, 29.51, 29.49, 29.37, 29.33, 29.27, 27.87, 27.87, 26.43, 26.43, 25.58, 22.66, 14.09; HRMS calculated for $C_{54}H_{100}N_3O_4$: 854.7714 $[M+H]^+$, found: 854.7728.

N-((*S*)-1-((4*S*,5*R*)-2,2-dimethyl-5-tetradecyl-1,3-dioxolan-4-yl)-2-((3-(hydroxymethyl)pyridin-2-yl)oxy)ethyl)hexacosanamide (II-4a)

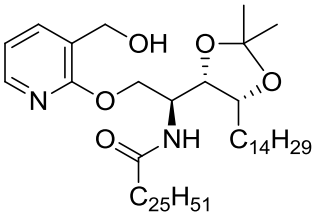

Compound **II-4a** was synthesized according to **general procedure 7** from amine intermediate **IV-4a** (16 mg, 0.034 mmol), NHS-cerotic (25.5 mg, 0.052 mmol) and TEA (14 µL, 0.103 mmol) in 0.5 mL of anhydrous DCM. Final purification using a isocratic conditions of DCM/MeOH 99:1 yielded 16 mg (55%) of desired compound as a white

solid. ^{1}H NMR (400 MHz, Chloroform-*d*) δ 8.04 (dd, *J* = 5.1, 1.9 Hz, 1H), 7.52 (dd, *J* = 7.2, 1.9 Hz, 1H), 6.85 (dd, *J* = 7.1, 5.0 Hz, 1H), 5.85 (d, *J* = 8.9 Hz, 1H), 4.62 (dd, *J* = 10.5, 2.5 Hz, 1H), 4.56 (dd, *J* = 13.1, 3.9 Hz, 2H), 4.51 – 4.40 (m, 2H), 4.21 – 4.08 (m, 2H), 2.08 (t, *J* = 7.6 Hz, 2H), 1.71 – 1.52 (m, 4H), 1.45 (s, 3H), 1.37 – 1.12 (m, 71H), 0.86 (t, *J* = 7.2 Hz, 6H); ^{13}C NMR (101 MHz, Chloroform-*d*) δ 173.43, 161.73, 146.10, 137.85, 123.85, 117.31, 108.56, 78.16, 77.90, 66.63, 61.24, 48.94, 37.11, 33.60, 32.09, 29.88, 29.86, 29.83, 29.82, 29.80, 29.74, 29.66, 29.61, 29.52, 29.42, 29.22, 27.53, 26.90, 25.75, 25.53, 24.91, 22.85, 14.28; HRMS calculated for $C_{53}H_{99}N_2O_5$: 843.7554 $[M+H]^+$, found: 843.7535.

Methyl 2-((*S*)-2-((4*S*,5*R*)-2,2-dimethyl-5-tetradecyl-1,3-dioxolan-4-yl)-2-hexacosanamidoethoxy)nicotinate (II-4b)

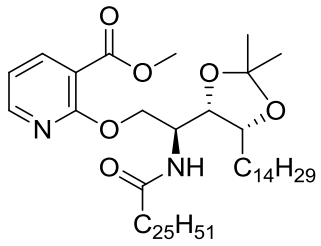

Compound **II-4d** was synthesized according to **general procedure 8** from amine intermediate **IV-4d** (45.5 mg, 0.092 mmol), Cl-cerotic (57.5 mg, 0.14 mmol) and TEA (39 µL, 0.28 mmol) in 1.5 mL of anhydrous THF. Final purification using a gradient of Hexane/AcOEt from 10 to 50% yielded 42.2 mg (52%) of desired product. $[\alpha]^{25}_{D}$ +14.27 (*c*= 1; $CHCl_3$); IR ($CHCl_3$) *v* = 3280, 2918, 2848, 1706, 1650, 1591, 1554, 1468, 1443, 1324, 1272, 1239, 1165, 1135, 1064 cm^{-1}; ^{1}H NMR (400 MHz, Chloroform-*d*) δ 8.30 (dd, *J* = 4.9, 2.0 Hz, 1H), 8.16 (dd, *J* = 7.6, 2.0 Hz, 1H), 6.95 (dd, *J* = 7.6, 4.9 Hz, 1H), 6.50 (d, *J* = 9.5 Hz, 1H), 4.74 (dd, *J* = 10.4, 2.1 Hz, 1H), 4.50 – 4.33 (m, 2H), 4.23 (dd, *J* = 9.1, 5.4 Hz, 1H), 4.16 (dt, *J* = 9.5, 2.4 Hz, 1H), 3.90 (s, 3H), 2.14 (t, *J* = 7.5 Hz, 2H), 1.69 – 1.50 (m, 4H), 1.43 (s, 3H), 1.36-1.12 (m, 71H), 0.88 (t, *J* = 6.6 Hz, 6H); ^{13}C NMR (101 MHz, $cdcl_3$) δ 172.49, 165.01, 162.50, 151.23, 141.00, 116.69, 113.57, 107.88, 77.94, 76.17, 67.02, 52.10, 47.43, 36.94, 31.91, 31.89, 29.69, 29.67, 29.65, 29.62, 29.57, 29.47, 29.34, 29.33, 29.21, 28.71, 28.09, 26.69, 25.72, 25.64, 22.66, 14.08; HRMS calculated for $C_{54}H_{99}N_2O_6$: 871.7503 $[M+H]^+$, found: 871.7488; mp: 91.3-91.5 ºC.

2-((*S*)-2-((4*S*,5*R*)-2,2-dimethyl-5-tetradecyl-1,3-dioxolan-4-yl)-2-hexacosanamidoethoxy)nicotinamide (II-4d)

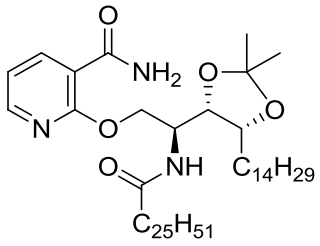

Compound **II-4d** was synthesized according to **general procedure 7** from amine intermediate **IV-4d** (74.6 mg, 0.156 mmol), NHS-cerotic (93 mg, 0.187 mmol) and TEA (76 µL, 0.547 mmol) in 2.6 mL of anhydrous THF. Final purification using a isocratic conditions of Hexane/AcOEt 7:3 yielded 50 mg (37%) of the desired compound as a white solid. $[\alpha]^{25}_{D}$ -2.54 (*c*= 0.5; $CHCl_3$); IR ($CHCl_3$) *v* = 3291, 2918, 2850, 1685, 1626, 1586, 1559, 1468, 1434 cm^{-1}; ^1H NMR (400 MHz, Chloroform-*d*) δ 8.51 (dd, *J* = 7.5, 2.0 Hz, 1H), 8.25 (dd, *J* = 4.9, 2.0 Hz, 1H), 7.88 (s, 1H), 7.05 (dd, *J* = 7.6, 4.9 Hz, 1H), 5.78 (s, 1H), 5.71 (d, *J* = 9.5 Hz, 1H), 4.70 (dd, *J* = 11.1, 2.7 Hz, 1H), 4.62 (dd, *J* = 9.2, 6.3 Hz, 1H), 4.44 (dd, *J* = 11.1, 8.9 Hz, 1H), 4.26 – 4.15 (m, 1H), 4.12 (t, *J* = 6.1 Hz, 1H), 2.14 (t, *J* = 7.9 Hz, 2H), 1.75 – 1.57 (m, 4H), 1.50 (s, 3H), 1.43 – 1.16 (m, 71H), 0.88 (t, *J* = 6.7 Hz, 6H); ^{13}C NMR (101 MHz, cdcl$_3$) δ 173.38, 165.44, 160.69, 150.04, 142.25, 118.05, 115.75, 108.77, 78.50, 77.79, 68.23, 48.62, 37.09, 34.10, 32.08, 29.88, 29.86, 29.82, 29.76, 29.72, 29.67, 29.52, 29.41, 29.32, 27.47, 26.89, 25.77, 25.52, 25.09, 22.85, 14.28; HRMS calculated for $C_{54}H_{98}N_3O_7$: 900.7402 $[M+HCOO]^-$, found: 900.7432; 103.2-103.6 ºC.

Synthesis of final compounds type I: aromatic-ceramide analogues of αGalCer (2).

The final compounds were obtained after acetal removal under mild acidic conditions. Careful attention should be paid at this step to avoid N→O acyl migration or product degradation.

General Procedure 9: Acetal removal under mild acidic conditions.

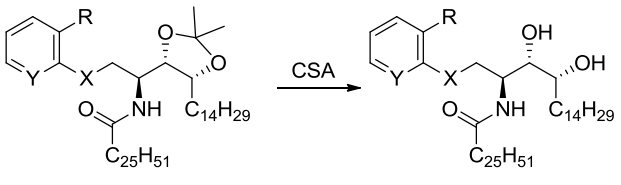

II **I**

R = CH_2OH, COOMe, $CONH_2$
Y= CH, N
X= S, O, NH

*General scheme of **General Procedure 9** to obtain final products **I***

CSA (2 to 4 eq) was added to a solution of the corresponding intermediate type **II** in $CHCl_3$/MeOH (1.2:1) mixture at 0.015M, and the resulting mixture was stirred at 30ºC until no starting material remained. Precipitated products were isolated by filtration in vacuum; otherwise the reaction mixture was neutralized using acidic resin IRA-400 (purchased by Sigma-Aldrich), filtered and concentrated in vacuum. In some cases, final compounds were purified by *flash* chromatography on silica gel.

General Procedure 10: Methylester hydrolysis under basic conditions.

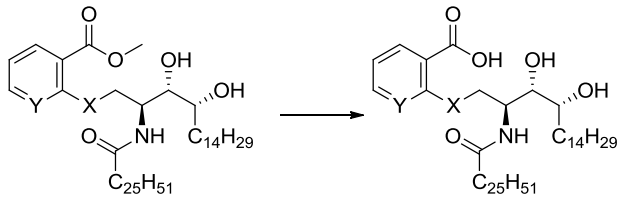

*General scheme of **General Procedure 10** to obtain final products **I-c***

NaOH 2M aq. (5 eq) was added to a solution of desired methyl ester **I-b** in THF/MeOH (5:1) at 0.01M, the resulting solution was stirred at 40-50ºC until no starting material remained. The mixture was neutralized with acid resin Amberlite A-15 until neutral pH, filtered and concentrated in vacuum to give desired compound.

***N*-((2*R*,3*S*,4*R*)-3,4-dihydroxy-1-((2-(hydroxymethyl)phenyl)thio)octadecan-2-yl)hexacosanamide (I-1a)[7]**

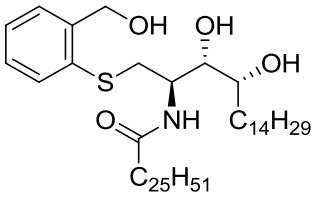

Screening of acetal removal conditions:

I) *O,O*-diprotected precursor **II-1a** (10mg, 0.012 mmol) was dissolved in 1 mL of conc. TFA and the reaction was stirred 1 hour at room temperature. After solvent removal, ^{1}H-NMR showed a complex mixture of products were the desired ceramide product was not detected.

II) To a solution of **II-1a** (43.5 mg, 0.051 mmol) in 4 mL of DCM (0.013M), TFA (4 mL, 52 mmol) was added and reaction was stirred at room temperature 2 hours. A complex mixture was obtained and purification by *flash* chromatography on silica gel did not give any defined fraction. The reaction was discarded.

III) To a solution of **II-1a** (23 mg, 0.027 mmol) in 2 mL of DCM/MeOH 1:1 (0.013M), concentrated HCl aq. (2 drops – approx. 20 µL, 0.24 mmol) was added and the reaction was stirred at room temperature for 2 hours. A complex mixture of products was obtained and attempted purification by *flash* chromatography on silica gel did not give any pure fraction. The reaction was discarded.

IV) To a solution of *O,O*-diprotected precursor **II-1a** (19mg, 0.022 mmol) in 2 mL of DCM/Dioxane 1:1 HCl 4M in dioxane was added (2 drops – approx. 20 µL, 0.08 mmol), resulting mixture was stirred at room temperature overnight. Next day solvents were removed under reduced pressure to yield 16 mg (88%) of pure product. Spectral data was in concordance with full N→O acyl migrated by-product **BP-2**.

(2R,3S,4R)-2-amino-3-hydroxy-1-((2-(hydroxymethyl)phenyl)thio)octadecan-4-yl hexacosanoate (BP-2)

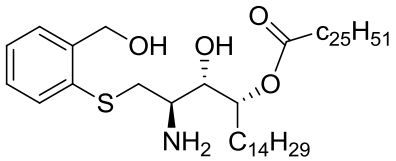

^{1}H NMR (400 MHz, Methanol-d_4) δ 7.13 – 7.10 (m, 1H), 7.02 (dd, *J* = 5.7, 3.4 Hz, 1H), 6.96 – 6.91 (m, 2H), 4.56 (d, *J* = 11.8 Hz, 1H), 4.53 – 4.45 (m, 1H), 4.14 (d, *J* = 11.9 Hz, 1H), 3.44 (dd, *J* = 9.3, 1.9 Hz, 1H), 3.06 – 2.98 (m, 1H), 2.69 – 2.56 (m, 2H), 1.70 – 1.53 (m, 2H), 1.44 – 1.34 (m, 1H), 1.15 – 1.05 (m, 3H), 0.95 – 0.81 (m, 68H), 0.49 (t, *J* = 6.7 Hz, 6H); ^{13}C NMR (101 MHz, cd$_3$od) δ 173.11, 143.04, 133.94, 130.12, 129.05, 128.47, 72.06, 70.79, 66.82, 62.91, 50.67, 33.94, 31.74, 31.73, 29.50, 29.46, 29.44, 29.42, 29.32, 29.17, 29.15, 29.14, 29.11, 28.89, 24.65, 22.45, 22.43, 13.51, 13.49; ; HRMS calculated for $C_{51}H_{96}NO_4S$: 818.7060 $[M+H]^+$, found: 818.7108.

V) CSA (6.5 mg, 0.028 mmol) was added to a solution of **II-1a** (12 mg, 0.014 mmol) in 0.45 mL of DCM/MeOH (5:2) (0.033M), resulting a suspension that was stirred at room temperature overnight. Next day DCM was added until total solution and the crude was neutralized with basic resin IRA-400 until neutral pH and further stirred 1 hour, crude was filtered and concentrated in vacuum. The residue was purified by *flash* chromatography on silica gel using gradient of Hexane/AcOEt from 4:1 to 1:4 to yield 3.8 mg (33%) of desired compound.

VI) CSA (12,99 mg, 0.056 mmol) was added to a solution of **II-1a** (24 mg, 0.028 mmol) in 2 mL of DCM/MeOH (1:1) (0.015M), the resulting suspension was stirred at 35ºC overnight. Next day the crude was neutralized with basic resin IRA-400 and further stirred 1 hour, the mixture was filtered and concentrated in vacuum. The residue was purified by *flash* chromatography on silica gel using isocratic conditions of Hexane/AcOEt 3:2 to yield 9.16 mg (40%) of the desired compound.

VII) Solid CSA (11 mg, 0.047 mmol) was added to a 0.01M solution of **II-1a** (10.5mg, 0.014 mmol) in 1.2 mL of DCM/MeOH (1:1). The resulting solution was stirred at room temperature overnight. Next day the mixture was neutralized with basic resin IRA-400 until neutral pH and further stirred 1 hour, crude was filtered and concentrated in vacuum. The residue was purified by *flash* chromatography on silica gel using isocratic conditions of Hexane/AcOEt 1:1 to yield 6.7 mg (67%) of desired compound as white solid. NMR was in concordance with previously described[7]. **These conditions are referred as General Procedure 9.** ^{1}H NMR (400 MHz, Chloroform-*d*) δ 7.41 – 7.38 (m, 1H), 7.32 (dd, *J* = 6.9, 2.3 Hz, 1H), 7.18 – 7.11 (m, 2H), 7.06 (d, *J* = 8.7 Hz, 1H), 4.75 (d, *J* = 12.4 Hz, 1H), 4.59 (d, *J* = 12.4 Hz, 1H), 4.07 – 3.99 (m, 1H), 3.50 (dd, *J* = 6.1, 5.0 Hz, 1H), 3.41 – 3.32 (m, 1H), 3.23 (dd, *J* = 13.9, 3.5 Hz, 1H), 3.06 (dd, *J* = 13.8, 8.5 Hz, 1H), 1.90 (t, *J* = 7.6 Hz, 2H), 1.48 – 1.36 (m, 4H), 1.21-1.12 (m, 68H), 0.78 (t, *J* = 7.1 Hz, 6H).

Methyl 2-(((2*R*,3*S*,4*R*)-2-hexacosanamido-3,4-dihydroxyoctadecyl)thio)benzoate (I-1b)

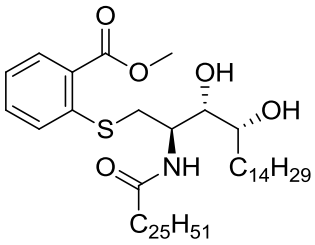

Compound **I-1b** was obtained following **general procedure 9** from *O,O*-diprotected precursor **II-1b** (35 mg, 0.04 mmol) in 2.5 mL of $CHCl_3$/MeOH (1.2:1) and CSA (18.34 mg, 0.08 mmol). Final purification using isocratic conditions of DCM/MeOH 98:2 yielded 17 mg (51%) of desired compound as a white waxy solid. $[\alpha]^{25}_{D}$ -2.58 (*c*= 0.5; $CHCl_3$/MeOH 9:1); IR ($CHCl_3$) *v* = 3323, 2918, 2850, 1712, 1642, 1561, 1468, 1434, 1278, 1450, 1064 cm^{-1}; ^{1}H NMR (in $CDCl_3$/MeOD-*d*4 9:1) ^{1}H NMR (in $CDCl_3$/MeOD-*d*4 9:1) (400 MHz, Chloroform-d) δ 7.81 (dd, J = 7.9, 1.5 Hz, 1H), 7.41 (ddd, J = 14.3, 7.6, 1.5 Hz, 2H), 7.15 – 7.07 (m, 1H), 4.21 – 4.11 (m, 1H), 3.83 (s, 3H), 3.56 (dd, J = 6.5, 4.3 Hz, 1H), 3.46 (ddd, J = 9.1, 6.5, 2.6 Hz, 1H), 3.26 (d, J = 3.9 Hz, 1H), 3.17 (dd, J = 13.4, 8.7 Hz, 1H), 2.04 (t, J = 7.6 Hz, 2H), 1.58 (dd, J = 14.6, 8.3 Hz, 2H), 1.27 – 1.16 (m, 70H), 0.79 (d, J = 7.0 Hz, 6H); ^{13}C NMR (in $CDCl_3$/MeOD-*d*4 9:1) (101 MHz, Chloroform-*d*) δ 174.85, 140.30, 132.54, 130.99, 128.51, 127.30, 124.55, 75.73, 72.50, 52.18, 50.79, 36.48, 33.17, 32.49, 31.92, 29.73, 29.70, 29.69, 29.64, 29.50, 29.35, 29.27, 25.79, 25.69, 22.67, 14.04; HRMS calculated for $C_{52}H_{96}NO_5S$: 846.7009 $[M+H]^+$, found: 846.6979.

2-(((2*R*,3*S*,4*R*)-2-hexacosanamido-3,4-dihydroxyoctadecyl)thio)benzoic acid (I-1c)

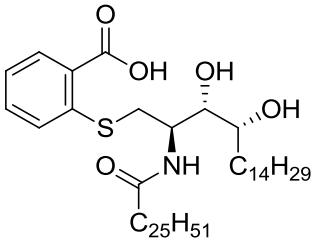

Compound **I-1c** was obtained from methyl ester **I-1b** (12.8 mg, 0.015 mmol) solved in THF/MeOH 5:1 according **general procedure 10** using aqueous NaOH 2M (5eq) at 40ºC during 1 hour. After neutralization with acid resin Amberlite A-15 and filtration, 12 mg (95%) of the desired compound were as a white solid. $[\alpha]^{25}_{D}$ -6.93 (*c*= 0.46; $CHCl_3$/MeOH 9:1); IR ($CHCl_3$/MeOH 9:1) *v* = 3291, 2918, 2850, 1646, 1548, 1467, 1378, 1249, 1060 cm^{-1}; ^1H NMR (500 MHz, Chloroform-*d*) δ 8.08 – 7.98 (m, 1H), 7.68 (d, *J* = 8.1 Hz, 1H), 7.41 (d, *J* = 8.1 Hz, 1H), 7.32 – 7.27 (m, 1H), 7.12 (t, *J* = 7.5 Hz, 1H), 4.23 – 4.16 (m, 1H), 3.64 – 3.60 (m, 1H), 3.51 – 3.45 (m, 1H), 3.23 – 3.16 (m, 2H), 1.97 – 1.88 (m, 2H), 1.58 – 1.48 (m, 2H), 1.47 – 1.35 (m, 2H), 1.31-0.97 (m, 68H), 0.80 (t, *J* = 6.9 Hz, 6H); ^{13}C NMR (126 MHz, Chloroform-*d*) 174.5, 137.1, 131.6, 130.3, 130.1, 126.1; ^{13}C NMR (126 MHz, $CDCl_3$) δ 174.36-174.45, 136.99, 131.61, 130.29, 130.07, 126.08, 75.86, 72.82, 70.75, 51.45, 36.79, 34.79, 32.97, 32.39, 31.65, 30.35, 30.17, 30.11, 28.64, 28.43, 27.86, 26.42, 26.25, 26.05, 23.03, 14.50; HRMS calculated for $C_{51}H_{92}NO_5S$: 830.6696 $[M-H]^-$, found: 830.6719. ***This compound showed unstable in long-term solution state.***

2-(((2R,3S,4R)-2-hexacosanamido-3,4-dihydroxyoctadecyl)thio)benzamide (I-1d)

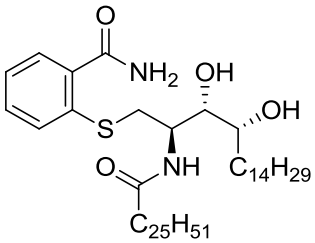

Compound **I-1d** was synthesized according to **general procedure 9** from *O,O*-diprotected precursor **II-1d** (30 mg, 0.034 mmol) and CSA (16 mg, 0.07 mmol) in 2.3 mL of $CHCl_3$/MeOH (1.2:1). After neutralization, filtration and concentration in vacuum, the final compound was obtained by precipitation in DCM/MeOH 1.2:1 ***at room temperature (not higher than 20ºC)***, 25 mg (87%) of the desired compound was obtained as a white solid. $[\alpha]^{25}_{D}$ -2.52 (*c*= 0.46; $CHCl_3$/MeOH 9:1); IR ($CHCl_3$/MeOH 9:1) *v* = 3371, 3191, 2919, 2850, 1644, 1542, 1468, 1419, 1047 cm^{-1}; ^1H NMR (in $CDCl_3$/MeOD-*d*4 9:1) (400 MHz, Chloroform-*d*) δ 7.48 (d, *J* = 7.9 Hz, 1H), 7.37 (d, *J* = 7.5 Hz, 1H), 7.30 (t, *J* = 7.7 Hz, 1H), 7.19 (t, *J* = 7.5 Hz, 1H), 4.05 – 3.99 (m, 1H), 3.57 (t, *J* = 5.6 Hz, 1H), 3.44 (dd, *J* = 11.0, 4.4 Hz, 1H), 3.24 (dd, *J* = 14.1, 3.3 Hz, 1H), 3.14 (dd, *J* = 14.0, 7.6 Hz, 1H), 1.82 (p, *J* = 7.1 Hz, 2H), 1.47 – 1.40 (m, 3H), 1.20 – 1.13 (m, 69H), 0.80

(t, *J* = 6.7 Hz, 6H); ^{13}C NMR (101 MHz, Chloroform-d) δ 174.70, 174.57, 137.65, 133.63, 132.54, 130.60, 127.56, 126.80, 75.08, 72.08, 51.11, 31.79, 29.59, 29.57, 29.52, 29.23, 22.55, 13.92; HRMS calculated for $C_{51}H_{95}N_2O_4S$: 831.7013 $[M+H]^+$, found: 831.6981; mp: 143.0-143.5 ºC

_N_-((2_S_,3_S_,4_R_)-3,4-dihydroxy-1-(2-(hydroxymethyl)phenoxy)octadecan-2-yl)hexacosanamide (I-2a)

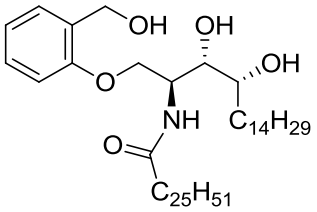

Compound **I-2a** was obtained according to **general procedure 9** from *O,O*-diprotected precursor **II-2a** (26 mg, 0.031 mmol) and CSA (16 mg, 0.07 mmol) in 2.3 mL of $CHCl_3$/MeOH (1.2:1). Final purification using Hexane/AcOEt from 50 to 100% yielded 13.5 mg (55%) of the desired compound as white solid. $[\alpha]^{25}_D$ +15.62 (*c*= 0.53; $CHCl_3$/MeOH 9:1); IR ($CHCl_3$)*v* = 3294, 2918, 2850, 1635, 1539, 1495, 1468, 1456, 1246 cm^{-1}; ^{1}H NMR (400 MHz, Chloroform-*d*) δ 7.23 (d, *J* = 8.7 Hz, 1H), 7.18 (dd, *J* = 7.4, 1.7 Hz, 1H), 7.02 (d, *J* = 8.9 Hz, 1H), 6.90 (d, *J* = 7.4 Hz, 1H), 6.86 (d, *J* = 8.6 Hz, 1H), 4.66 (d, *J* = 11.8 Hz, 1H), 4.52 (d, *J* = 11.8 Hz, 1H), 4.39 (q, *J* = 3.8 Hz, 1H), 4.32 (dd, *J* = 9.6, 3.8 Hz, 1H), 4.16 (dd, *J* = 9.6, 3.4 Hz, 1H), 3.65 (t, *J* = 5.7 Hz, 1H), 3.58 (td, *J* = 6.1, 3.0 Hz, 1H), 2.17 (t, *J* = 7.7 Hz, 2H), 1.70 – 1.44 (m, 4H), 1.32 – 1.12 (m, 68H), 0.85 (t, *J* = 6.7 Hz, 6H); ^{13}C NMR (101 MHz, Chloroform-*d*) δ 174.10, 157.22, 129.93, 129.73, 128.72, 121.03, 111.81, 74.89, 72.84, 67.80, 61.99, 49.84, 36.73, 32.98, 32.01, 29.79, 25.92, 25.85, 22.78, 14.19; HRMS calculated for $C_{51}H_{96}NO_5$: 802.7289 $[M+H]^+$, found: 802.7275; mp: 97.0-97.5 ºC.

Methyl 2-(((2_S_,3_S_,4_R_)-2-hexacosanamido-3,4-dihydroxyoctadecyl)oxy)benzoate (I-2b)

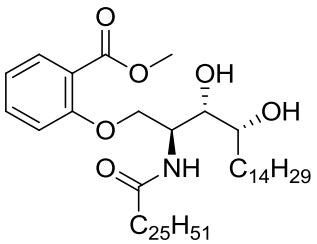

Compound **I-2b** was obtained according to **general procedure 9** from *O,O*-diprotected precursor **II-2b** (26 mg, 0.03 mmol) and CSA (13.9 mg, 0.06 mmol) in 2.2 mL of $CHCl_3$/MeOH (1.2:1). Final purification using DCM/MeOH 2% yielded 21 mg of slightly impure desired compound as white solid. Second purification was done using the same conditions, except that the product was loaded adsorbed in silica onto the column to yield 17 mg (69%) of desired product as a waxy solid. $[\alpha]^{25}_D$ +40.67 (*c*= 0.5;

$CHCl_3$/MeOH 9:1); IR ($CHCl_3$)*v* = 3322, 2917, 2850, 1714, 1645, 1541, 1493, 1467, 1250. 1088 cm^{-1}; ^1H NMR (in $CDCl_3$/MeOD-*d*4 9:1) (400 MHz, Chloroform-*d*) δ 7.84 (dd, *J* = 7.9, 1.8 Hz, 1H), 7.44 (td, *J* = 7.9, 1.8 Hz, 1H), 6.94 (dd, *J* = 8.2, 5.1 Hz, 2H), 4.43 – 4.37 (m, 2H), 4.16 – 4.11 (m, 1H), 3.81 (s, 3H), 3.53 – 3.44 (m, 2H), 2.15 (t, *J* = 7.6 Hz, 2H), 1.83 – 1.64 (m, 1H), 1.53 (t, *J* = 7.3 Hz, 2H), 1.21 – 1.11 (m, 69H), 0.80 (t, *J* = 6.8 Hz, 6H).^{13}C NMR (in $CDCl_3$/MeOD-*d*4 9:1) (101 MHz, Chloroform-*d*) δ 174.14, 166.46, 158.75, 134.66, 132.15, 120.85, 118.25, 113.04, 75.14, 72.75, 68.84, 52.13, 49.74, 49.53, 49.32, 49.10, 48.94, 48.89, 48.68, 48.46, 36.62, 33.61, 31.91, 29.70, 29.69, 29.65, 29.62, 29.48, 29.35, 29.33, 29.23, 25.74, 25.63, 22.67, 14.04; HRMS calculated for $C_{52}H_{96}NO_6$: 830.7238 $[M+H]^+$, found: 830.7231.

2-(((2*S*,3*S*,4*R*)-2-hexacosanamido-3,4-dihydroxyoctadecyl)oxy)benzoic acid (I-2c)

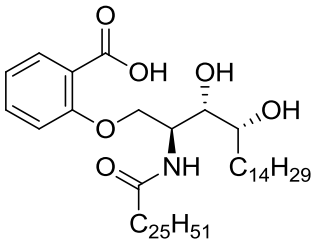

Compound **I-2c** was obtained according **general procedure 10** from preceding methyl ester **I-2b** (8 mg, 8 µmol) and aqueous NaOH 2M (5eq) solved in THF/MeOH 5:1 at 40ºC during 1.5 hours. A white precipitated appeared, which was removed by filtration. The solid was suspended in $CHCL_3$/MeOH 9:1, and both suspended solid and the filtrate were neutralized with Amberlite A-15 until neutral to slightly acid pH (7-6) and stirred 1 hour, removed by filtration and concentrated in vacuum to yield 6 mg from the resuspended solid and 3 mg from filtrated (76%) of white solids. Both compounds showed same spectral data in concordance with desired compound. $[\alpha]^{25}_D$ +21.82 (*c*= 0.5; $CHCl_3$/MeOH 9:1); IR ($CHCl_3$)*v* = 3306, 2918, 2850, 1719, 1645, 1602, 1541, 1467, 1243 cm^{-1}; ^1H NMR (400 MHz, Chloroform-*d*) δ 7.91 (dd, *J* = 7.8, 2.0 Hz, 1H), 7.43 (t, *J* = 7.9 Hz, 1H), 7.03 – 6.86 (m, 2H), 4.47 – 4.32 (m, 2H), 4.17 (dd, *J* = 9.3, 2.6 Hz, 1H), 3.49 (ddd, *J* = 15.3, 8.8, 5.9 Hz, 2H), 2.14 (t, *J* = 7.6 Hz, 2H), 1.57 – 1.42 (m, 4H), 1.37-1.00 (m, 68H), 0.80 (t, *J* = 6.7 Hz, 6H); ^{13}C NMR (101 MHz, $cdcl_3$) δ 174.13, 167.96, 158.58, 134.63, 132.78, 121.02, 118.20, 112.69, 75.30, 72.61, 68.80, 36.56, 33.55, 31.92, 29.75, 29.71, 29.69, 29.67, 29.65, 29.51, 29.36, 29.26, 25.76, 25.62, 22.68, 14.05; HRMS calculated for $C_{51}H_{92}NO_6$: 814.6625 $[M-H]^-$, found: 814.6933.

2-(((2*S*,3*S*,4*R*)-2-hexacosanamido-3,4-dihydroxyoctadecyl)oxy)benzamide (I-2d)

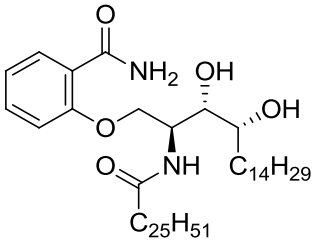

Compound **I-2d** was obtained according to **general procedure 9** from preceding *O,O*-diprotected precursor **II-2d** (17 mg, 0.02 mmol) and CSA (9.23 mg, 0.04 mmol) solved in 1.4 mL of $CHCl_3$/MeOH (1.2:1). After 4 hours reaction was completed. Reaction was neutralized with IRA-400, filtered and concentrated in vacuum to yield 17 mg (quant.) of the pure desired product as a white solid. $[\alpha]^{25}_D$ +15.85 (*c*= 0.33; $CHCl_3$/MeOH 9:1); IR ($CHCl_3$)*v* = 3450, 3297, 2918, 2850, 1729, 1655, 1629, 1565, 1466, 1234 cm^{-1}; ^1H NMR (in $CDCl_3$/MeOD-*d*4 9:1) (400 MHz, Chloroform-*d*) δ 7.97 (dd, *J* = 7.8, 1.8 Hz, 1H), 7.37 (ddd, *J* = 8.8, 7.4, 1.8 Hz, 1H), 6.97 (t, *J* = 7.5 Hz, 1H), 6.92 (d, *J* = 8.3 Hz, 1H), 4.46 (dt, *J* = 5.7, 3.7 Hz, 1H), 4.23 (qd, *J* = 9.7, 4.7 Hz, 2H), 3.59 – 3.49 (m, 2H), 2.12 (d, *J* = 7.2 Hz, 2H), 1.63 – 1.43 (m, 4H), 1.24 – 1.10 (m, 68H), 0.79 (t, *J* = 6.8 Hz, 6H); ^{13}C NMR (in $CDCl_3$/MeOD-*d*4 9:1) (101 MHz, Chloroform-*d*) δ 174.47, 174.07, 157.30, 133.53, 131.89, 121.15, 112.17, 74.83, 72.27, 68.08, 49.70, 36.54, 32.99, 31.90, 29.70, 29.67, 29.63, 29.50, 29.36, 29.34, 29.27, 25.77, 25.72, 22.66, 14.02; HRMS calculated for $C_{51}H_{95}N_2O_5$: 815.7241 $[M+H]^+$, found: 815.7238.

N-((2*S*,3*S*,4*R*)-3,4-dihydroxy-1-((2-(hydroxymethyl)phenyl)amino)octadecan-2-yl)hexacosanamide (I-3a-Me)

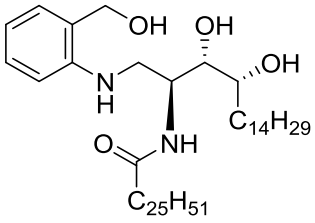

Following **general procedure 9,** form *O,O*-diprotected precursor **II-3a** (30 mg, 0.036 mmol) and CSA (16.6 mg, 0.071 mmol) in 2.55 mL of $CHCl_3$/MeOH (1.2:1). After 3 hours reaction was completed and neutralized with resin IRA-400 until neutral or slightly acid pH (7-6). Final purification with isocratic conditions of DCM/MeOH 98:2 yielded 15 mg (51%) of white waxy solid, which was in accordance with methylated compound **I-3a-Me**. $[\alpha]^{25}_D$ +9.64 (*c*= 0.5; $CHCl_3$/MeOH 9:1); IR ($CHCl_3$)*v* = 3368, 3291, 2918, 2850, 1729, 1634, 1609, 1516, 1467, 1089 cm^{-1}; ^1H NMR (400 MHz, Chloroform-*d*) δ 7.23 (dd, *J* = 7.8, 1.6 Hz, 1H), 7.07 (dd, *J* = 7.4, 1.5 Hz, 1H), 6.83 (d, *J* = 8.1 Hz, 1H), 6.73 (t, *J* = 7.4 Hz, 1H), 6.15 (d, *J* = 7.9 Hz, 1H), 4.44 (s, 2H), 4.37 – 4.23 (m, 1H), 3.70 – 3.59 (m, 2H), 3.46 (qd, *J* = 13.1, 5.9 Hz, 2H), 3.32 (s, 3H), 2.18 (t, *J* = 7.7 Hz, 2H), 1.56 – 1.41 (m, 4H), 1.34 – 1.16 (m, 68H), 0.88 (t, *J* = 6.7 Hz, 6H); ^{13}C NMR (101 MHz, cdcl$_3$) δ 173.92, 146.88,

130.14, 129.79, 122.61, 117.76, 111.58, 73.89, 73.10, 57.49, 51.10, 43.54, 36.76, 33.49, 31.90, 29.68, 29.33, 25.80, 25.66, 22.66, 14.09; HRMS calculated for $C_{52}H_{99}N_2O_4$: 815.7605 $[M+H]^+$, found: 815.7641.

N-((2*S*,3*S*,4*R*)-3,4-dihydroxy-1-((2-(hydroxymethyl)phenyl)amino)octadecan-2-yl)hexacosanamide (I-3a)

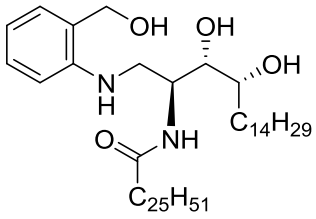

Compound **I-3a** was obtained from preceding *O,O*-diprotected precursor **II-3a** (20 mg, 0.024 mmol) in dioxane/water (10:1) and CSA (12.32 mg, 0.053 mmol). Reaction was stirred at room temperature overnight, followed by basic resin IRA-400 addition until basic pH, filtered and concentrated in vacuum. The residue was purified by *flash* chromatography on silica gel using isocratic conditions of Hexane /AcOEt 1:1 to yield 2.16 mg (11%) of the desired compound as white waxy solid. $[\alpha]^{25}_D$ +5.0 (*c*= 0.2; $CHCl_3$); IR ($CHCl_3$/MeOH 9:1)*v* = 3297, 2918, 2850, 1643, 1518, 1466, 1081 cm^{-1}; ^1H NMR (500 MHz, Chloroform-*d*) δ 7.23 (t, *J* = 7.7 Hz, 1H), 7.07 (dd, *J* = 7.3, 1.6 Hz, 1H), 6.83 (d, *J* = 8.1 Hz, 1H), 6.73 (t, *J* = 7.3 Hz, 1H), 6.22 (d, *J* = 8.0 Hz, 1H), 4.65 (s, 2H), 4.33 (dd, *J* = 9.3, 3.6 Hz, 1H), 3.73 – 3.64 (m, 2H), 3.52 (dd, *J* = 13.0, 5.3 Hz, 1H), 3.45 (dd, *J* = 12.9, 6.3 Hz, 1H), 2.17 (t, *J* = 6.8 Hz, 2H), 1.70 – 1.56 (m, 2H), 1.38 – 1.10 (m, 70H), 0.88 (t, *J* = 6.9 Hz, 6H); ^{13}C NMR (126 MHz, $CDCl_3$) δ 174.84, 147.33, 130.36, 129.94, 125.93, 118.54, 112.41, 76.58, 73.70, 65.10, 51.80, 44.64, 37.44, 37.84, 35.59, 35.46, 35.10, 34.90, 34.15, 32.55, 32.12, 31.93, 30.79, 30.35, 29.96, 29.31, 28.72, 28.14, 26.26, 24.99, 23.35, 21.66, 16.34, 14.72; HRMS calculated for $C_{51}H_{97}N_2O_4$: 801.7448 $[M+H]^+$, found: 801.7454.

Methyl 2-(((2*S*,3*S*,4*R*)-2-hexacosanamido-3,4-dihydroxyoctadecyl)amino)benzoate (I-3b)

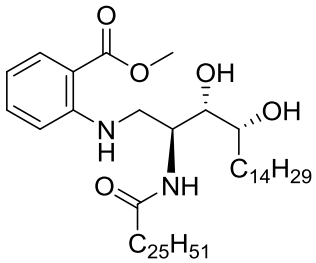

Compound **I-3b** was obtained according to **general procedure 9** from preceding *O,O*-diprotected precursor **II-3b** (30 mg, 0.035 mmol) and CSA (16.03 mg, 0.07 mmol) in 2.3 mL of $CHCl_3$/MeOH (1:1), after 11 h the reaction was completed. Final purification using DCM/AcOEt from 10 to 50% yielded 25 mg (87%) of desired compound as a

white solid. $[\alpha]^{25}_{D}$ +19.05 (*c*= 0.59; $CHCl_3$/MeOH 9:1); IR ($CHCl_3$/MeOH 9:1)*v* = 3335, 2917, 2849, 1689, 1642, 1578, 1541, 1518, 1468, 1238, 1164, 1113, 1077 cm^{-1}; ^1H NMR (in $CDCl_3$/MeOD-*d*4 9:1) (400 MHz, Chloroform-*d*) δ 7.88 (dd, *J* = 8.0, 1.7 Hz, 1H), 7.36 (ddd, *J* = 8.6, 7.1, 1.7 Hz, 1H), 6.89 (d, *J* = 8.5 Hz, 1H), 6.74 – 6.70 (m, 1H), 6.66 (t, *J* = 7.6 Hz, 1H), 4.26 (dt, *J* = 7.3, 4.4 Hz, 1H), 3.83 (s, 3H), 3.65 – 3.48 (m, 4H), 2.16 (t, *J* = 7.6 Hz, 2H), 1.69 – 1.46 (m, 4H), 1.32 – 1.12 (m, 68H), 0.85 (t, *J* = 7.2 Hz, 6H); ^{13}C NMR (in $CDCl_3$/MeOD-*d*4 9:1) (101 MHz, cdcl$_3$) δ 174.78, 169.06, 149.92, 135.01, 131.83, 116.56, 112.96, 111.44, 75.62, 72.84, 51.81, 50.78, 50.78, 50.31, 50.10, 49.89, 49.67, 49.46, 49.25, 49.03, 36.77, 33.37, 32.02, 29.82, 29.79, 29.75, 29.59, 29.49, 29.45, 29.38, 25.91, 25.79, 22.78, 14.19; HRMS calculated for $C_{52}H_{97}N_2O_5$: 829.7398 $[M+H]^+$, found: 829.7416; mp: 115.7-127.1 ºC.

2-(((2*S*,3*S*,4*R*)-2-hexacosanamido-3,4-dihydroxyoctadecyl)amino)benzoic acid (I-3c)

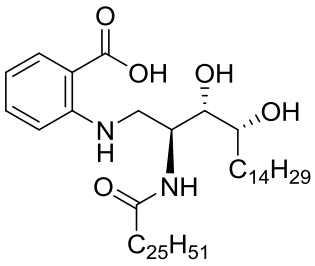

Compound **I-3c** was obtained according **general procedure 10** from methyl ester **I-3b** (8 mg, 8.65 µmol) dissolved in THF/MeOH 5:1 and aqueous NaOH 2M (5eq) at 40ºC during 7 days. TLC control showed a complex mixture which was purified by *flash* chromatography on silica gel to yield 2 impure fractions. The desired compound was detected by HPLC-MS-FIA but it was not possible to be isolated. HPLC-MS calculated for $C_{51}H_{95}N_2O_5$: 815.724 $[M+H]^+$, found: 815.679.

2-(((2*S*,3*S*,4*R*)-2-hexacosanamido-3,4-dihydroxyoctadecyl)amino)benzamide (I-3d)

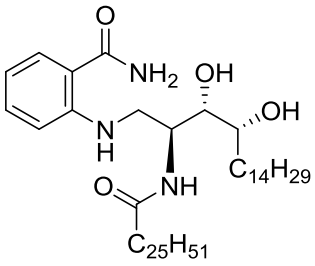

Compound **I-3d** was obtained according to **general procedure 9** from *O,O*-diprotected precursor **II-3d** (42 mg, 0.049 mmol) and CSA (22.84 mg, 0.098 mmol) in 2.6 mL of $CHCl_3$/MeOH (1:1), after 4 h the reaction was completed. The reaction mixture was neutralized with basic resin IRA-400, after that a white precipitate appeared when small amount of water was added. The solid was filtered and dried in vacuum to yield 20 mg (50%) of the desired compound as a white solid. $[\alpha]^{25}_{D}$ +21.36 (*c*= 0.45; $CHCl_3$/MeOH 9:1); IR ($CHCl_3$/MeOH 9:1)*v* = 3338, 2918, 2850, 1635, 1519, 1467 cm^{-1};

^{1}H NMR (in $CDCl_3$/MeOD-*d*4 9:1) (500 MHz, Chloroform-*d*) δ 7.37 (d, *J* = 7.9 Hz, 1H), 7.31 – 7.24 (m, 1H), 6.84 (d, *J* = 8.4 Hz, 1H), 6.61 (d, *J* = 7.7 Hz, 1H), 4.19 (q, *J* = 5.0 Hz, 1H), 3.59 – 3.35 (m, 4H), 2.10 (t, *J* = 7.8 Hz, 2H), 1.64 – 1.41 (m, 4H), 1.37 – 1.02 (m, 68H), 0.80 (t, *J* = 6.8 Hz, 6H); ^{13}C NMR (in $CDCl_3$/MeOD-*d*4 9:1) (126 MHz, $CDCl_3$) δ 171.89, 174.10, 147.94, 134.45, 129.42, 127.76, 117.09, 114.12, 77.16, 76.17, 73.33, 51.10, 44.01, 37.32, 33.92, 33.87, 33.85, 32.70, 31.98, 30.42, 30.19, 27.57, 26.53, 26.63, 23.41, 21.96, 14.82, 13.22; HRMS calculated for $C_{51}H_{96}N_3O_4$: 814.7401 $[M+H]^+$, found: 814.7396; mp: 134.0-134.1 ºC

N-((2*S*,3*S*,4*R*)-3,4-dihydroxy-1-((3-(hydroxymethyl)pyridin-2-yl)oxy)octadecan-2-yl)hexacosanamide (I-4a)

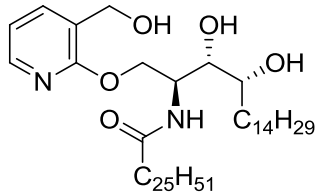

Compound **I-4a** was obtained according to **general procedure 9** from preceding *O,O*-diprotected precursor **II-4a** (13 mg, 0.015 mmol) in 1.1 mL of $CHCl_3$/MeOH (1:1) and CSA (10.74 mg, 0.046 mmol), after 3 hours reaction was completed. Reaction was neutralized until slightly acid pH (6-5), filtered and concentrated in vacuum. Final purification using isocratic mixture of DCM/AcOEt 20% yielded 4.8 mg (39%) of the desired product as white solid and 3 mg of a fraction of impure product. $[\alpha]^{25}_{D}$ +18.17 (*c*= 0.47; $CHCl_3$/MeOH 9:1); IR ($CHCl_3$)*v* = 3278, 2918, 2850, 1637, 1559, 1467 cm^{-1}; ^{1}H NMR (400 MHz, Chloroform-*d*) δ 8.01 (dd, *J* = 5.1, 1.9 Hz, 1H), 7.58 (dd, *J* = 7.2, 1.9 Hz, 1H), 6.89 (dd, *J* = 7.2, 5.1 Hz, 1H), 6.72 (d, *J* = 8.8 Hz, 1H), 4.60 (d, *J* = 4.6 Hz, 2H), 4.56 (s, 2H), 4.42 (d, *J* = 4.7 Hz, 1H), 3.65 – 3.48 (m, 2H), 2.16 (d, *J* = 7.8 Hz, 2H), 1.73 – 1.48 (m, 4H), 1.36 – 1.14 (m, 68H), 0.85 (d, *J* = 7.1 Hz, 6H); ^{13}C NMR (101 MHz, cdcl$_3$) δ 173.96, 161.39, 145.36, 138.23, 123.99, 117.38, 74.77, 72.70, 65.92, 60.56, 50.67, 50.18, 49.96, 49.75, 49.54, 49.32, 36.76, 32.98, 31.88, 29.66, 29.62, 29.48, 29.32, 29.24, 25.82, 25.68, 22.65, 14.07; HRMS calculated for $C_{50}H_{95}N_2O_5$: 803.7241 $[M+H]^+$, found: 803.7225.

Methyl 2-(((2*S*,3*S*,4*R*)-2-hexacosanamido-3,4-dihydroxyoctadecyl)oxy)nicotinate (I-4b)

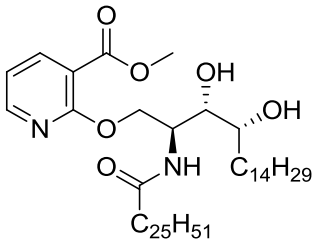

Compound **I-4b** was obtained according to **general procedure 9** from *O,O*-diprotected precursor **II-4b** (113.66 mg, 0.130 mmol) in 9.2 mL of DCM/MeOH (1:1) and CSA (67.6 mg, 0.291 mmol), after 4 h the reaction was completed and a white precipitated appeared, which was filtered off, washed with cool DCM/MeOH 1.2:1 and dried in vacuum to yield 72.5 mg (67%) of the desired product as a white solid. $[\alpha]^{25}_{D}$ +32.98 (*c*= 0.52; $CHCl_3$/MeOH 9:1); IR ($CHCl_3$) *v* = 3457, 3315, 2917, 1849, 1716, 1644, 1586, 1545, 1433, 1304, 1262, 1093 cm^{-1}; ^{1}H NMR (400 MHz, Chloroform-*d*) δ 8.31 (dd, *J* = 4.9, 2.0 Hz, 1H), 8.23 (dd, *J* = 7.6, 2.0 Hz, 1H), 6.98 (dd, *J* = 7.6, 4.9 Hz, 1H), 6.75 (d, *J* = 8.6 Hz, 1H), 4.69 (qd, *J* = 11.3, 3.0 Hz, 2H), 4.57 – 4.47 (m, 1H), 3.90 (s, 3H), 3.65 – 3.52 (m, 2H), 2.19 (t, *J* = 7.6 Hz, 2H), 1.63 – 1.38 (m, 4H), 1.37 – 1.16 (m, 68H), 0.86 (t, *J* = 6.8 Hz, 6H); ^{13}C NMR (101 MHz, cdcl$_3$) δ 172.88, 164.64, 161.21, 151.67, 141.67, 117.25, 112.95, 75.47, 73.15, 52.61, 49.02, 36.95, 33.77, 32.05, 29.83, 29.62, 29.49, 29.39, 25.84, 22.82, 14.24; HRMS calculated for $C_{51}H_{95}N_2O_6$: 831.7190 $[M+H]^+$, found: 831.1788; mp: 125.6-125.7 ºC

2-(((2*S*,3*S*,4*R*)-2-hexacosanamido-3,4-dihydroxyoctadecyl)oxy)nicotinic acid (I-4c)

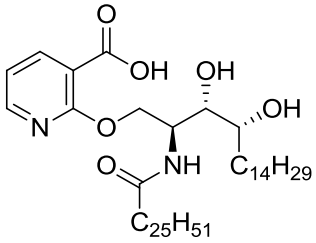

Compound **I-4c** was following **General Procedure 10** from preceding methyl-ester **II-4b** (56.4 mg, 0.068 mmol) and aqueous NaOH 2M (3eq) solved in 4.3 mL of THF/MeOH (5:1). The reaction mixture was stirred overnight at 50ºC. A white precipitated appeared which was filtered off, washed with THF/MeOH 4:1 and dried in vacuum. This solid was suspended in MeOH and neutralized dropwise with TFA until neutral pH. The solid was filtered, washed with MeOH and dried in vacuum to yield 28.4 mg (51%) of the desired compound as a white solid. ***This product was extremely insoluble in most common organic solvents.*** $[\alpha]^{25}_{D}$ not detected (low product solubility); IR ($CHCl_3$) *v* = 3297, 2916, 1848, 1632, 1587, 1468, 1438, 1298, 1243, 1098 ; ^{1}H NMR (in $CDCl_3$/MeOD-*d*4 9:1) (500 MHz, Chloroform-d) δ 7.96 – 7.84 (m, 2H), 6.72 (ddd, J = 7.1, 4.9, 1.8 Hz, 1H), 4.40 – 4.33 (m, 1H), 4.30 (d, J = 11.3 Hz, 1H), 4.21 – 4.16 (m, 1H), 3.41

(t, J = 7.9, 5.6 Hz, 1H), 3.33 (t, J = 8.0 Hz, 1H), 1.94 (t, J = 7.7 Hz, 2H), 1.51 – 1.22 (m, 4H), 1.08 – 0.94 (m, 68H), 0.62 (t, J = 6.7 Hz, 6H); ^{13}C NMR(in $CDCl_3$/MeOD-*d*4 9:1) (126 MHz, $CDCl_3$) δ 173.89, 168.90, 148.67, 140.28, 161.00, 116.67, 73.76, 71.71, 66.05, 49.02, 32.01, 31.43, 31.38, 29.24, 29.17, 28.75, 28.73, 25.33, 22.27, 22.15, 22.05, 13.31; HRMS calculated for $C_{50}H_{91}N_2O_6$: 815.6877 $[M-H]^-$, found: 815.6829; mp: 188.0-188.8 ºC

2-(((2*S*,3*S*,4*R*)-2-hexacosanamido-3,4-dihydroxyoctadecyl)oxy)nicotinamide (I-4d)

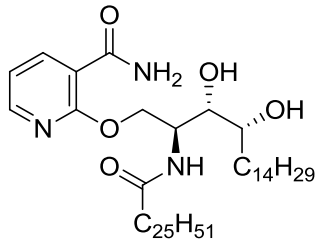

Compound **I-4d** was obtained according to **general procedure 9** from preceding *O,O*-diprotected precursor **II-4d** (40 mg, 0.047 mmol) in 3.2 mL of $CHCl_3$/MeOH (1.2:1) and CSA (21.7 mg, 0.093 mmol), after 3 h reaction was not completed, so 1 eq of CSA was added. After 1 hour, the reaction was neutralized and further stirred 1 hour until a white precipitate appeared which was filtered and manually separated from resin beads to yield 18.4 mg (48%) of the pure desired product as a white solid. $[\alpha]^{25}_D$ +4.97 (*c*= 0.3; $CHCl_3$/MeOH 9:1); IR ($CHCl_3$)*v* = 3446, 3284, 2917, 2849, 1661, 1630, 1585, 1542, 1467, 1436, 1233 cm^{-1}; ^{1}H NMR (in $CDCl_3$/MeOD-*d*4 9:1) (500 MHz, Chloroform-d) δ 8.38 (dt, J = 7.6, 2.1 Hz, 1H), 8.17 (dt, J = 4.7, 2.2 Hz, 1H), 7.00 (ddd, J = 7.5, 5.0, 2.3 Hz, 1H), 4.70 – 4.59 (m, 1H), 4.57 – 4.41 (m, 2H), 3.57 – 3.42 (m, 2H), 2.15 – 2.04 (m, 2H), 1.71 – 1.39 (m, 4H), 1.28 – 1.10 (m, 68H), 0.80 (td, J = 6.9, 2.4 Hz, 6H); ^{13}C NMR (in $CDCl_3$/MeOD-*d*4 9:1) (126 MHz, $CDCl_3$) δ 175.03, 166.64, 161.37, 150.38, 142.57, 118.33, 116.04, 75.55, 72.81, 67.38, 50.57, 37.25, 33.60, 32.52, 32.46, 30.29, 29.87, 29.83, 26.44, 26.35, 26.30, 23.28, 23.25, 14.64; HRMS calculated for $C_{51}H_{94}N_3O_7$: 860.7092 $[M+HCOO^-]^-$, found: 860.7081.

5.2. Biological evaluation as NKT cell activators

5.2.1. *In vitro* assays in murine cells

These experiments were carried out by Dr. Laura Escribà under Dr. Javier Briones supervision at *Laboratori d'Hematologia Oncològica i Transplantament (LHOT)* at Hospital de la Santa Creu i Sant Pau in Barcelona.

5.2.1.1. Mice of experiment

Balb/c mice were purchased from Charles River (France) and in house bred (in accordance with general recommendations for animal breeding and housing) at the Laboratory Animal Facility at Hospital de Santa Creu i Sant Pau (Barcelona), and maintained in controlled temperature atmosphere (range between 20-22ºC) with light cycle of 12h light/12h dark. All experiments were conducted according to the European Animal Care. Mice used for experiments were 7 weeks old.

5.2.1.2. Splenocytes obtaining and cell cultures

Splenocytes were isolated from spleen according to standard protocols. Whole splenocytes were cultured at $5x10^5$ cells/well in 96-well plate and stimulated with desired analogues under study at 1 µg/mL and 5 µg/mL during 4 days, in presence of IL-2 added at day 2 at 25 IU/mL according preceding methodology[19]. Cultures were maintained for 96 hours and cell supernatants were collected at each desired time. The levels of murine IFN-γ and IL-4 were measured by ELISA tests following manufacturer's instructions. αGalCer (**2**) was used as positive control at 100 ng/mL. Aromatic-ceramide compounds were resuspended in 100% of DMSO at concentration of 0.5 mg/mL and a use stock in PBS at 10 µg/mL was prepared. Compounds were heated at 60ºC and sonicated before being diluted in complete culture media to the final concentration. Less than 5% v:v of DMSO in cellular assay was present in our cultures, a concentration described not toxic for cells.

5.2.1.3. ELISA experiments: IFN-γ and IL-4 detection

Mouse IFN-γ and IL-4 ELISA MAX™Deluxe Sets purchased by BioLegend®.

Solutions used in ELISA measurement were prepared as following (quantities for one plate assay are indicated):

- Coating Buffer A: To prepare 12 mL of Coating Buffer A Solution, 2.4 mL of Coating Buffer A (5x) was solved in 9.6mL of deionized water.
- Capture antibody solution: 60 µL of Mouse INF-γ or IL4 ELISA MAX™ Capture Antibody (200x) was diluted in 11.94 mL of Coating Buffer A.
- Assay Diluent Solution: 12 mL from purchased Assay Diluent A (5x) were diluted in 48 mL of PBS.

- A) Standard Solution of Mouse IFN-γ at 1000 pg/mL: 1 mL of this solution was prepared by adding 8.3 µL of reconstituted standard stock solution (Mouse IFN-γ Standard stock at 120 ng/mL in PBS) to 991.7 µL of Assay Diluent Solution, a standard of 1000 pg/mL was obtained. Six two-fold serial dilutions were performed from the 1000 pg/mL with Assay Diluent Solution in separate wells and an extra Assay Diluent Solution well was used as zero standard (0 pg/mL).
- B) Standard Solution of Mouse IL4 at 125 pg/mL: 1 mL of this solution was prepared by making an initial dilution 1:10 from reconstituted standard stock solution (Mouse IL4 Standard stock at 90 ng/mL in PBS), adding 10 µL of this solution to 90 µL of Assay Diluent Solution. Then 13.9 µL of this solution were added to 986.1 µL of Assay Diluent Solution. Six two-fold serial dilutions were performed from the 125 pg/mL with Assay Diluent Solution in separate wells and an extra Assay Diluent Solution well was used as zero standard (0 pg/mL).
- Detection Antibody Solution: 60 µL of Mouse IFN-γ or IL4 ELISA MAX™ Detection Antibody (200x) was solved in 11.94 mL of Assay Diluent Solution.
- Stop Solution: Sulfuric acid solution at 2N in deionized water.
- Washing solution: 0.05% Tween-20 in PBS.
- Avidin-HRP solution: 12 µL of concentrated Avidin-HRP (1000x) were solved in 11.99 µL of Assay Diluent Solution.
- TMB Substrate Solution: equal volumes of Substrate Solution A and Substrate Solution B were mixed. This solution was prepared immediately prior to use.

ELISA Assay was carried out according to Standard protocol given by BioLegend. A MaxiSorp 96-well/plate was coated with 100 µL/well of Capture Antibody solution of desired cytokine, sealed and incubated overnight between 2 to 8ºC. Plate was washed 4 times with at least 300 µL of Wash Buffer per well, 200 µL of Assay Diluent A was added per well and plate was incubated again at room temperature 1 hour while shaking. Hereafter, plate was washed again similarly as before and samples and standards (100 µL/well) were added and plate was incubated 2 hours at room temperature with shaking. Subsequently, plate was washed 4 times as described above and 100 µL of Detection Antibody solution was added to each well, sealed and incubated at room temperature with shaking. Then, the plate was washed 4 times, 100 µL of Avidin-HRP solution were added and further incubated 30 min at room temperature with shaking. Plate was washed again 5 times and, for this final wash, each well was soaked with Wash Buffer for 30 seg to 1 min. Finally, 100 µL of freshly prepared Substrate Solution were added and further incubated in dark for 20 min, assay was stopped by adding 100 µL of Stop Solution to each well. Light absorption was measured at 450 nm within 15 min.

5.2.2. *In vitro* assays in purified human *i*NKT cells

These experiments were carried out by Dr. Lorena Usero and by Roser Borràs under Carme Roure-Mir supervision at *Laboratori d'Immunolgia Cel·lular* of *Institut de Biomedicina I Biotecnologia* at Universitat Autonoma de Barcelona.

5.2.2.1. Cells used as APC and NKT

C1R-CD1d$^+$ were used as APC. C1R-CD1d$^+$ consist on a transfected C1R cells with CD1d proteins while lacks surface HLA A and B antigens typical from human B-cell linage.

iNKT cells were isolated from peripheral blood lymphocytes samples using density gradient using Ficoll (Lymphoprep). iNKT cells were specifically isolated from the rest of lymphocytes using an Automacs system based on human Anti-iNKT Microbeads kit (Miltenyi Biotec). This kit is based on monoclonal antibodies anti- Vα24Jα18 able to generate two cell populations: those ones with Vα24Jα18$^+$ phenotype (iNKT-cells) and those ones without it (Vα24Jα18$^-$) corresponding to another cell population.

5.2.2.2. *In vitro* stimulation assay

For in vitro stimulation, three cell types were used: C1R-CD1d$^+$ cells as APC, PBMs as feeders and iNKT cells as "*reactive*" cells. C1R-CD1d$^+$ cells were incubated at 90000 cells/eppendorff and each analogue at different concentrations during 1 hour at 37ºC and then they were irradiated at 45 Gy. Equally, PBMs were also irradiated at 30 Gy. After that, C1R-CD1d$^+$ cells loading different analogues were plated at 30000 cells/well in 96-well plate together with PBMs at 40000 cells/well and co-cultured with purified iNKT at 10000 cells/well. αCD3/CD28 conjugated beads (Dynabeeds, Lite Technologies) were used as positive control of the assay. Assay medium used was IMDM (Iscove's Modified Dolbecco's Medium) complemented with 8% of human serum, L-Glutamine (2 mM), Penicillin (100 U/mL) and Streptomycin (100 μg/mL). At 24h and 48h supernatants were collected and stored in freezer until measured. αGalCer (**2**) was used as positive control at 100 ng/mL. Aromatic-ceramide compounds were resuspended in 100% of DMSO at concentration of 0.5 mg/mL and a use stock in PBS at 10 μg/mL was prepared. Compounds were heated at 37ºC and sonicated 10 min before being diluted in complete culture media to final concentration. Less than 5% of DMSO in cellular assay was present in our cultures, a concentration described not toxic for cells.

5.2.2.3. ELISA experiments: IFN-γ and IL-4 detection

Human IFN-γ and IL-4 ELISA CytoSet™ Sets purchased by Invitrogen®.

Solutions used in ELISA measurement were prepared as following (quantities for one plate assay are indicated):

- Coating Buffer A: PBS was used as Coating Buffer at pH 7.4.
- Capture antibody solution: 10 µL of Human INF-γ or IL4 ELISA CytoSet™ Capture Antibody was diluted in 9.990 mL of Coating Buffer A.
- Assay Diluent Solution: PBS with BSA and Tween 20 was used as Assay Buffer at neutral pH.
- A) Standard Solution of Mouse IFN-γ at 1000 pg/mL: 1 mL of this solution was prepared by adding 12 mL to reconstitute recombinant standard stock (Human IFN-γ Standard stock at 12 ng/Vial), a standard of 1000 pg/mL was obtained. Seven two-fold serial dilutions were performed from the 1000 pg/mL with Assay Diluent Solution in separate eppendorffs and an extra Assay Diluent Solution well was used as zero standard (0 pg/mL).
- B) Standard Solution of Mouse IL4 at 1000 pg/mL: 1 mL of this solution was prepared by adding 12 mL to reconstitute recombinant standard stock (Human IL4 Standard stock at 12 ng/Vial), a standard of 1000 pg/mL was obtained. Seven two-fold serial dilutions were performed from the 1000 pg/mL with Assay Diluent Solution in separate eppendorffs and an extra Assay Diluent Solution well was used as zero standard (0 pg/mL).
- Detection Antibody Solution (at 0.16 µg/mL): 4 µL of Human IFN-γ or IL4 ELISA CytoSet™ Detection Antibody (0.2 mg/mL) was solved in 4.996 mL of Assay Diluent Solution.
- Stop Solution: Sulfuric acid solution at 2N in deionized water.
- Washing Buffer solution: 0.05% Tween-20 and 0.04% EDTA in PBS at pH 7.4.
- Streptavidin-HRP solution: A) For IFN-γ detection: 4 µL of concentrated Avidin-HRP (0.25 mL) were solved in 9.996 µL of Assay Diluent Solution. B) For IL4 detection: 3 µL of concentrated Avidin-HRP (0.25 mL) were solved in 9.997 µL of Assay Diluent Solution.
- OPD Substrate Solution: both tables were solved in 20 mL of deionized water immediately prior to use (SigmaAldrich P9187).

ELISA Assay was carried out according to Standard protocol given by Invitrogen. A MaxiSorp 96-well/plate was coated with 100 µL/well of Capture Antibody solution of desired cytokine, sealed and incubated overnight between 2 to 8ºC. Plate was washed 4 times with at least 300 µL of Wash Buffer per well, 300 µL of Assay Diluent A was added per well and plate was incubated at room temperature 1 hour while shaking. Hereafter, extra liquid was removed and samples and standards (100 µL/well) were

added together with 50 µL/well of Detection Antibody Solution, plate was shacked and incubated at room temperature for 2 hours. Subsequently, plate was washed 4 times as described above and 100 µL of Avidin-HRP solution were added and further incubated 30 min at room temperature with shaking. Plate was washed again 5 times and, finally, 100 µL of freshly prepared OPD (o-Phenylenediamine dihydrochloride) Substrate Solution were added and further incubated in dark for 30 min, assay was stopped by adding 100 µL of Stop Solution to each well. Light absorption was measured at 450 nm within 30 min.

5.3. Computational studies of new aromatic-ceramide derivatives

All the computational work was carried out with the Schrödinger Suite 2014[20], through its graphical interface Maestro[21]. Coordinates of TCR-Ag-CD1d (PDB code 3RTQ)[22] were obtained from the Protein Data Bank[23] web site. Protein X-ray structures were prepared using the Protein Preparation Wizard[24] included in Maestro to remove solvent molecules and ions, adding hydrogens, setting protonation states and minimizing energies. Ligands were set up with the LigPrep module[25] included in Maestro to generate ionization states, ring conformations and geometry optimization previous to use. The program MacroModel[26], its default force field OPLS 2005 (a modified version of the OPLS-AA force field)[27] and GB/ SA water solvation conditions were used for all energy calculations. The program Glide[28] was used for the docking calculations using the default XP precision settings except for a setting of 100 000 poses per ligand for the initial phase of docking, a scoring window of 200 for keeping initial poses, and a limit of 800 poses per ligand for energy minimization. Selected ligands were submitted to the Induce Fit Docking Protocol[29] of the Schrödinger Suite, which takes in consideration protein residues flexibility around the ligand within a given distance (5 Å) from the bound ligands, in order to refine the geometries and scores of the docked poses. The same group of ligands was submitted under Molecular Dynamics simulations using Desmond software included in Schrödinger Suite at 20ns, considering explicit water at 300K under Periodic Boundary conditions (NPT ensemble) using OPLS_2005 force field[27]. Simulation systems for molecular dynamics were built using the System Builder of the Maestro-Desmond interface,[30] which automatically assigns parameters to all atom. Each CD1d-Ag-TCR complex was immersed in an orthorhombic box (sides at 10 Å of the closest solute atom) of TIP3P water with enough Cl^- anions to achieve neutrality (~35000 water molecules, ~106000 atoms in total). Systems were relaxed by minimization (initial steepest descent followed by LBFGS minimization), first with the solute restrained and then without restrains, until a gradient threshold of 0.1 kcal $mol^{-1}Å^{-1}$ was reached. Then, they were heated stepwise up to 300 K with short MD runs under periodic boundary conditions (PBC) (25 ps at 0.1, 10, 100 and 300 K), and equilibrated for 2 ns at the same temperature and 1.0 bar, in the NPT ensemble. Production MD simulations (20 ns, 2 fs timestep) were performed under the same conditions (PBC, NPT ensemble, 300 K and 1.0 bar) using the Nose-Hoover thermostat method[31,32] with a relaxation time of 1.0 ps and the Martyna-Tobias-Klein barostat method[33] with isotropic coupling and a relaxation time of 2 ps. Integration was carried out with the RESPA integrator[32] using time steps of 2.0, 2.0, and 6.0 fs for the bonded, short range and long range interactions, respectively. A cut-off of 9.0 Å was applied to van der Waals and short-range electrostatic interactions, while long-range electrostatic interactions were computed using the smooth particle mesh Ewald method with an Ewald tolerance of 10^{-9} [34,35]. Bond lengths to hydrogen

atoms were constrained using the Shake algorithm[36]. Coordinates were saved every 20 ps, hence 1000 snapshots were obtained from each MD run. The Simulation Event Analysis application included in the Desmond-Maestro interface was used to analyze the trajectories.

BIBLIOGRAPHIC REFERENCES:

1. Alcaide, A. & Llebaria, A. Synthesis of 1-thio-phytosphingolipid analogs by microwave promoted reactions of thiols and aziridine derivatives. *Tetrahedron Letters* **53**, 2137-2139 (2012).
2. Harrak, Y., Llebaria, A. & Delgado, A. A Practical Access to 1,2-Diaminophytosphingolipids. *European Journal of Organic Chemistry* **2008**, 4647-4654 (2008).
3. Alcaide, A. & Llebaria, A. Aziridine ring opening for the synthesis of sphingolipid analogues: inhibitors of sphingolipid-metabolizing enzymes. *J Org Chem* **79**, 2993-3029 (2014).
4. van den Berg, R.J.B.H.N.*, et al.* An Efficient Synthesis of the Natural Tetrahydrofuran Pachastrissamine Starting from d-ribo-Phytosphingosine. *The Journal of Organic Chemistry* **71**, 836-839 (2006).
5. Kim, S., Lee, S., Lee, T., Ko, H. & Kim, D. Efficient Synthesis of d-erythro-Sphingosine and d-erythro-Azidosphingosine from d-ribo-Phytosphingosine via a Cyclic Sulfate Intermediate. *The Journal of Organic Chemistry* **71**, 8661-8664 (2006).
6. Chen, W.-S.*, et al.* Synthesis of ganglioside Hp-s1. *RSC Advances* **4**, 47752-47761 (2014).
7. Alcaide, A. A modular approach to sphingolipi analogs mediated by aziridines: synthesis and biological studies. *Doctoral Thesis, University of Barcelona* (2012).
8. Lee, T., Lee, S., Kwak, Y.S., Kim, D. & Kim, S. Synthesis of pachastrissamine from phytosphingosine: a comparison of cyclic sulfate vs an epoxide intermediate in cyclization. *Org Lett* **9**, 429-432 (2007).
9. Zeynizadeh, B. Oxidative coupling of thiols to disulfides with iodine in wet acetonitrile. *J. Chem. Res., Synop.*, 564-566 (2002).
10. Sengar, R.S., Miller, J.J. & Basu, P. Design, syntheses, and characterization of dioxo-molybdenum(vi) complexes with thiolate ligands: effects of intraligand NH[three dots, centered]S hydrogen bonding. *Dalton Transactions*, 2569-2577 (2008).
11. Frerot, E., Bagnoud, A. & Cicchetti, E. Quantification of Hydrogen Sulfide and Methanethiol and the Study of Their Scavenging by Biocides of the Isothiazolone Family. *ChemPlusChem* **79**, 77-82 (2013).
12. 1,2-Benzisothiazol-3(2H)-one [MAK Value Documentation, 1991]. in *The MAK-Collection for Occupational Health and Safety*.
13. Yamamura, T., Tadokoro, M., Nakamura, N., Tanaka, K. & Asakura, K. Ni(II) Complexes of *N*,*N*'-Ethylenebis(*o*-mercaptobenzamide): A Quadridentate Thiolato Amide $\{S_2N_2\}$ Ligand. *Bulletin of the Chemical Society of Japan* **63**, 999-1004 (1990).
14. Chen, F.-J., Liao, G., Li, X., Wu, J. & Shi, B.-F. Cu(II)-Mediated C–S/N–S Bond Formation via C–H Activation: Access to Benzoisothiazolones Using Elemental Sulfur. *Organic Letters* **16**, 5644-5647 (2014).
15. Sarma, B.K. & Mugesh, G. Redox Regulation of Protein Tyrosine Phosphatase 1B (PTP1B): A Biomimetic Study on the Unexpected Formation of a Sulfenyl Amide Intermediate. *Journal of the American Chemical Society* **129**, 8872-8881 (2007).
16. Voltrova, S., Hidasova, D., Genzer, J. & Srogl, J. Metallothionein-inspired prototype of molecular pincer. *Chemical Communications* **47**, 8067-8069 (2011).
17. Pietka-Ottlik, M., Potaczek, P., Piasecki, E. & Mlochowski, J. Crucial Role of Selenium in the Virucidal Activity of Benzisoselenazol-3(2H)-ones and Related Diselenides. *Molecules* **15**(2010).
18. Bhanu Prasad, B.A., Sanghi, R. & Singh, V.K. Studies on ring cleavage of aziridines with hydroxyl compounds. *Tetrahedron* **58**, 7355-7363 (2002).

19. Harrak, Y., Barra, C.M., Delgado, A., Castaño, A.R. & Llebaria, A. Galacto-Configured Aminocyclitol Phytoceramides Are Potent in Vivo Invariant Natural Killer T Cell Stimulators. *Journal of the American Chemical Society* **133**, 12079-12084 (2011).
20. Schrödinger Suite 2014 Update 3, Schrödinger, LLC: New York, NY, 2014.
21. Maestro, version 9.9; Schrödinger, LLC, New York, NY, 2014.
22. Kerzerho, J.*, et al.* Structural and Functional Characterization of a Novel Nonglycosidic Type I NKT Agonist with Immunomodulatory Properties. *The Journal of Immunology* **188**, 2254 (2012).
23. Berman, H.M.*, et al.* The Protein Data Bank. *Nucleic Acids Research* **28**, 235-242 (2000).
24. Schrödinger Suite 2014 Protein Preparation Wizard; Epik, Schrödinger, LLC, New York, NY, 2014; Impact, Schrödinger, LLC, New York, NY, 2014; Prime, Schrödinger, LLC, New York, NY, 2014.
25. LigPrep, Schrödinger, LLC, New York, NY, 2014.
26. MacroModel, version 10.5; Schrödinger, LLC: New York, NY, 2014.
27. Banks Jay, L.*, et al.* Integrated Modeling Program, Applied Chemical Theory (IMPACT). *Journal of Computational Chemistry* **26**, 1752-1780 (2005).
28. Glide, version 6.4; Schrödinger, LLC, New York, NY, 2014.
29. Schrödinger Suite 2014 Induced Fit Docking protocol; Glide, Schrödinger, LLC, New York, NY, 2014; Prime, Schrödinger, LLC, New York, NY, 2014.
30. Schrödinger. Release 2016-1: Maestro-Desmond Interoperability Tools. (D. E. Shaw Research, New York, NY, 2016).
31. Evans, D.J. & Holian, B.L. The Nose–Hoover thermostat. *The Journal of Chemical Physics* **83**, 4069-4074 (1985).
32. Martyna, G.J., Klein, M.L. & Tuckerman, M. Nosé–Hoover chains: The canonical ensemble via continuous dynamics. *The Journal of Chemical Physics* **97**, 2635-2643 (1992).
33. Martyna, G.J., Tobias, D.J. & Klein, M.L. Constant pressure molecular dynamics algorithms. *The Journal of Chemical Physics* **101**, 4177-4189 (1994).
34. Darden, T., York, D. & Pedersen, L. Particle mesh Ewald: An N · log(N) method for Ewald sums in large systems. *The Journal of Chemical Physics* **98**, 10089-10092 (1993).
35. Essmann, U.*, et al.* A smooth particle mesh Ewald method. *The Journal of Chemical Physics* **103**, 8577-8593 (1995).
36. Kräutler, V., van Gunsteren, W.F. & Hünenberger, P.H. A fast SHAKE algorithm to solve distance constraint equations for small molecules in molecular dynamics simulations. *Journal of Computational Chemistry* **22**, 501-508 (2001).

5. EXPERIMENTAL PART

6. INDEX OF COMPOUNDS

6. INDEX OF COMPOUNDS

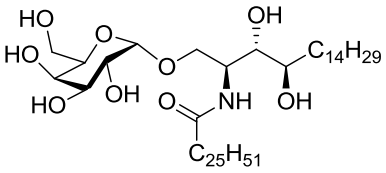

αGalCer (2)

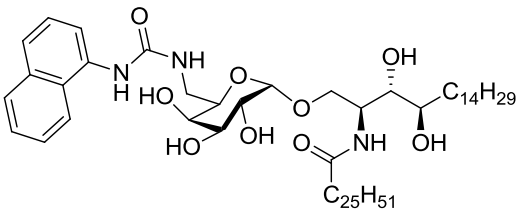

NU-α-GalCer (34)

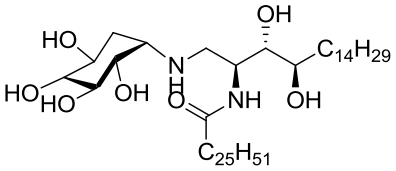

HS44 (38)

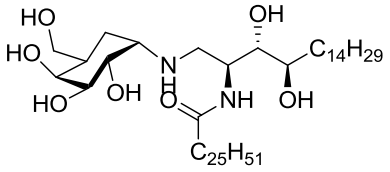

HS161 (39)

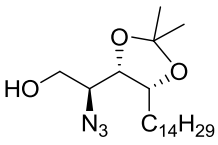

D

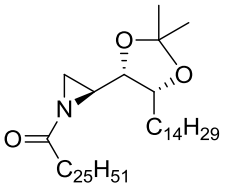

G

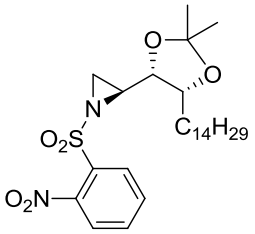

H

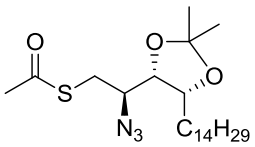

J

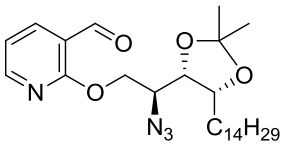

V-4a'

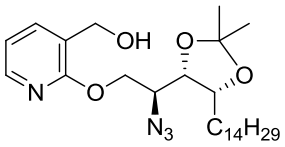

V-4a

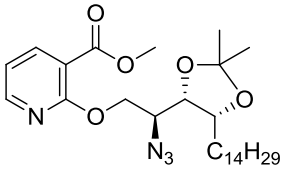

V-4b

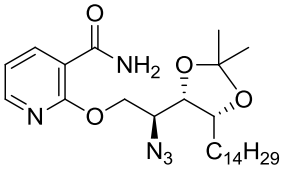

V-4d

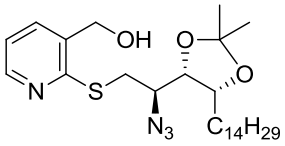

V-5a

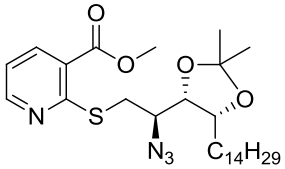

V-5b

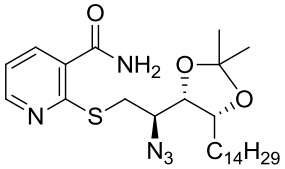

V-5d

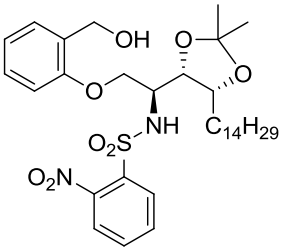

III-2a

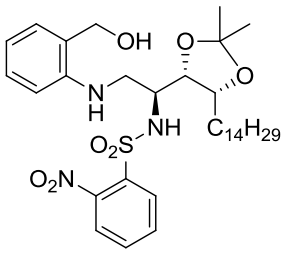

III-3a

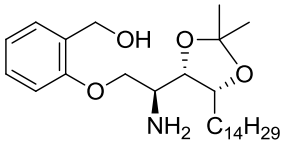

VI-2a

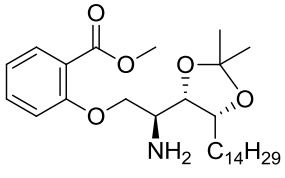

VI-2b

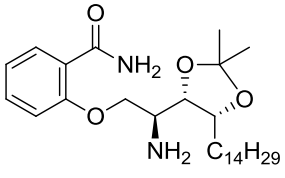

VI-2d

6. INDEX OF COMPOUNDS

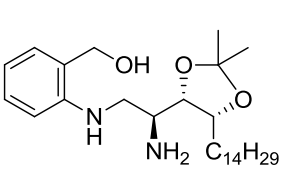

VI-3a

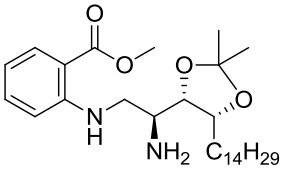

VI-3b

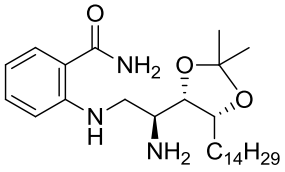

VI-3d

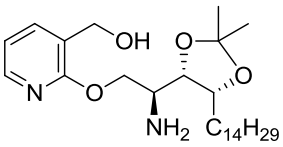

VI-4a

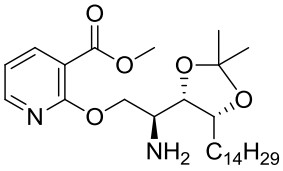

VI-4b

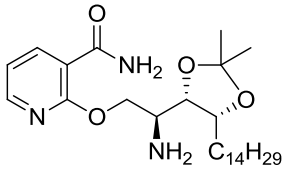

VI-4d

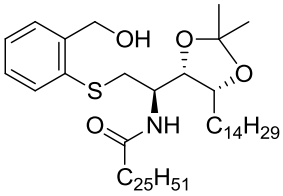

II-1a

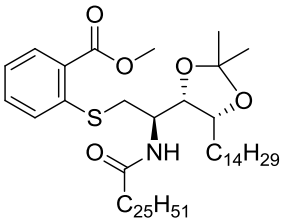

II-1b

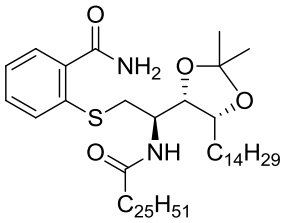

II-1d

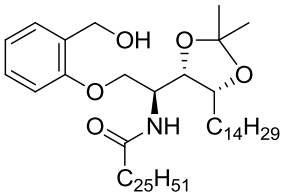

II-2a

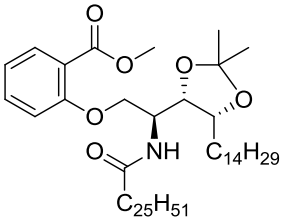

II-2b

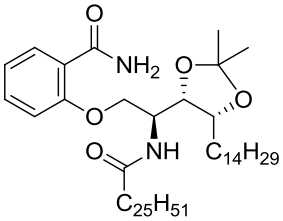

II-2d

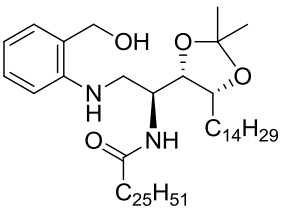

II-2a

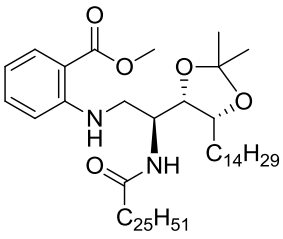

II-2b

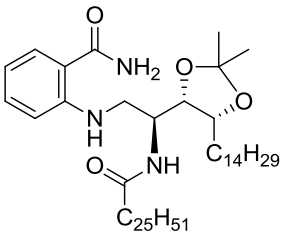

II-2d

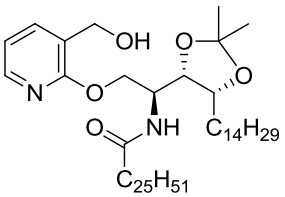

II-4a

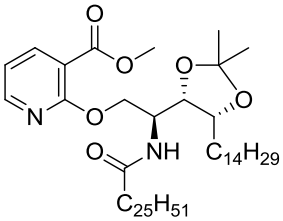

II-4b

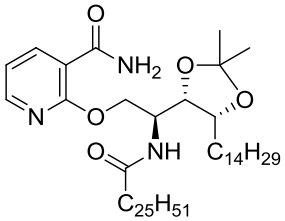

II-4d

6. INDEX OF COMPOUNDS

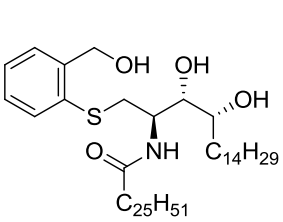

I-1a

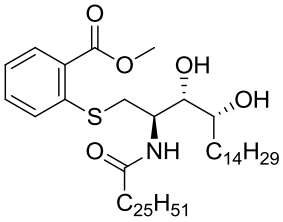

I-1b

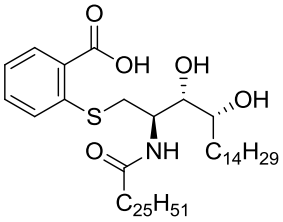

I-1c

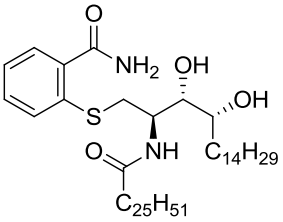

I-1d

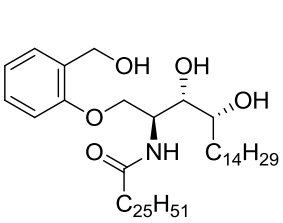

I-2a

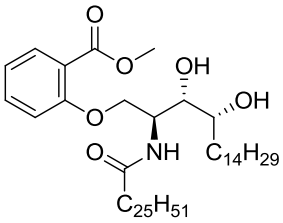

I-2b

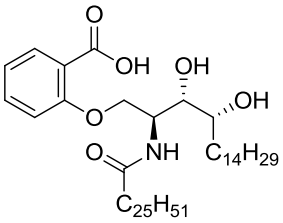

I-2c

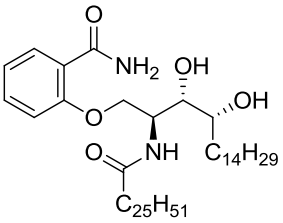

I-2d

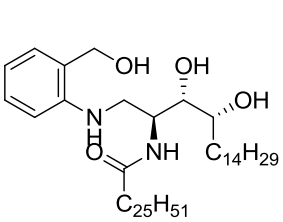

I-3a

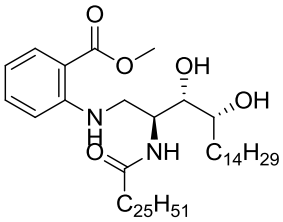

I-3b

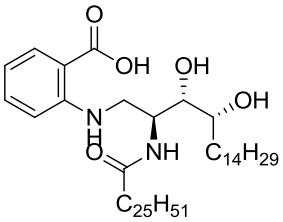

I-3c

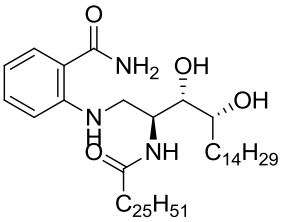

I-3d

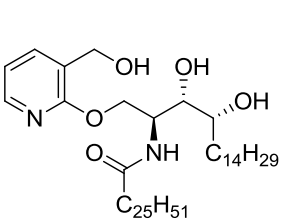

I-4a

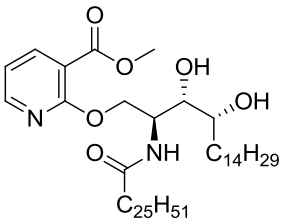

I-4b

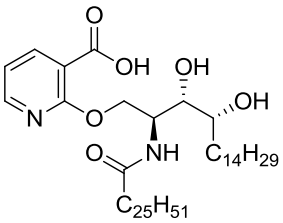

I-4c

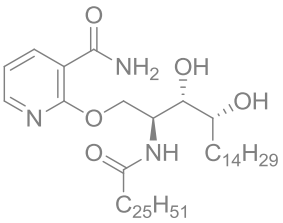

I-4d

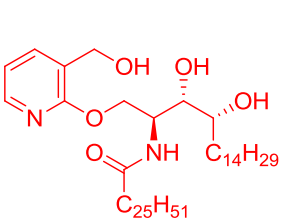

I-5a

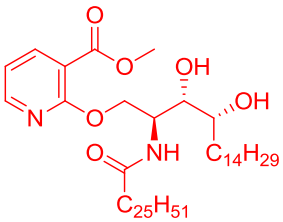

I-5b

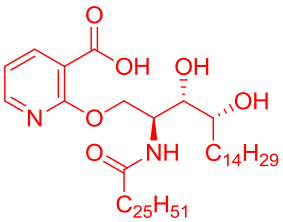

I-5c

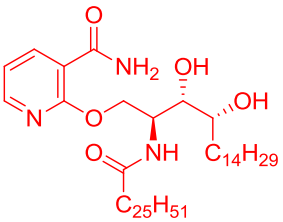

I-5d

6. INDEX OF COMPOUNDS